**Title**
The Phylogenomics and Macroevolutionary Dynamics of Australasian Diplodactyloid Geckos



**Author**
Skipwith, Phillip

**Publication Date**
2017

Peer reviewed|Thesis/dissertation

# The Phylogenomics and Macroevolutionary Dynamics of Australasian Diplodactyloid Geckos

By

Phillip L. Skipwith

A dissertation submitted in partial satisfaction of the

requirements for the degree of

Doctor of Philosophy

in

Integrative Biology

in the

Graduate Division

of the

University of California, Berkeley

Committee in charge:

Professor Jimmy A. McGuire, Chair
Professor Rauri C. Bowie
Professor Rosemary G. Gillespie

Summer 2017

The Phylogenomics and Macroevolutionary Dynamics of Australasian Diplodactyloid Geckos



by Phillip L. Skipwith

Abstract

The Phylogenomics and Macroevolutionary Dynamics of Australasian Diplodactyloid Geckos

by

Phillip L. Skipwith

Doctor of Philosophy in Integrative Biology

University of California, Berkeley

Professor Jimmy A. McGuire, Chair

Our planet supports a staggering array of biodiversity. A firm understanding of the species with which we share this planet requires researchers to develop a solid basis on which pertinent questions about biodiversity can addressed. My dissertation uses one group of speciose and ecologically diverse geckos to ask questions regarding evolutionary relationships, macroevolutionary patterns, adaptive radiation, and processes at the species level responsible for generating this diversity. I implement a number of cutting edge molecular and computational methods to demonstrate the importance of taking an integrative approach by incorporating both molecules and morphology.

Chapter 1: Molecular data has vast applications in exploring the evolutionary histories of organisms. Some groups, however, continually confound attempts at elucidating their relationships with conventional molecular methods. The advent of genomic sequencing has allowed researchers to gather vast amounts of sequence data to tackle troublesome phylogenetic questions. The diplodactyloid geckos endemic to Australasia are an extremely diverse of clade squamates with an array of ecologies and phenotypes. However, there exist a number of poorly resolved relationships and some studies recover well-supported groups which disagree across datasets. Here, we implement 4,268 ultraconserved element loci (UCEs) to address the phylogeny of the diplodactyloids. In comparison to previous studies, the UCEs resolved nearly every node, the exceptions being some at the base of the New Caledonian and core Australian diplodactylid clades. Our concatenated and coalescent phylogenies directly conflict with those from four previous studies, sometimes by as much as 45% of nodes, and received much higher support. Divergence time estimates were largely congruent previous estimates, though slightly older for some deeper nodes. Our findings demonstrate the importance of incorporating numerous independent loci in phylogenetic estimates.

Chapter 2: Adaptive radiations are notoriously difficult to define, particularly across broad taxonomic and temporal scales. However, most examples can be characterized by ecological differentiation. The diplodactyloid geckos exhibit a staggering array of ecologies accompanied by a morphological diversity that vastly exceeds that seen elsewhere in Gekkota. Using ecological data and ecomorphological measurements, we address how ecological differentiation has progressed in this clade as well as the prevalence of convergent evolution due to similar selective

pressures. Ancestral trait reconstruction methods find that diplodactyloids were ancestrally rupicolous. Hansen models find that arboreal forms have higher rates body size evolution than all other ecological categories. We also find that convergence is widespread within the diplodactyloids, though intraclade convergence was more common that interclade convergence. Furthermore, tests of phenotypic convergence reveal that convergence is most widespread in the insular diplodactylids. The phenomenon of adaptive radiation has been most well documented in groups like *Anolis* lizards and cichlid fishes, but diplodactyloids likely represent another example of exceptional morphological diversification in novel habitats.

Chapter 3: The generation of biodiversity has fascinated researchers for decades, particularly in the case of putative adaptive radiations. Speciation and extinction rates are subject to both biotic and abiotic forces, and both are notoriously difficult to estimate from molecular data without fossils. However, many methods have limited power to inform us of diversification trajectories. The diplodactyloids represent a unique opportunity to investigate rates of diversification and trait evolution. Examination of branch lengths and divergence times indicated that the insular forms, which were recent arrivals, had experienced bursts of diversification over the background rate for the whole clade. We used likelihood and Bayesian-based methods to infer diversification trajectories of diplodactyloids, implementing a phylogenomic estimate of more the 4,200 independent loci. Remarkably, most methods find that there is no rate heterogeneity in the diplodactyloid tree, but that the background rate of speciation is relatively high. In contrast to previous studies that have suggested a mass extinction event around the Eocene-Oligocene boundary (EOb), we find very little support for any such event. The weak signature of mass extinction we find vastly predates the EOb, dating back to the Campanian. Diplodactyloids demonstrate a complex pattern of trait evolution, with signatures of modularity in the rate of phenotypic diversification. Using Bayesian methods, we found that not all traits are evolving at the same rate for all clades. Rather, certain traits, namely those tied to substrate and diet experienced higher rates of diversification than others. While the insular clades possessed similar net diversification patterns to the rest of the diplodactyloids, they exhibited higher rates of trait evolution. A similar pattern is evident in clades that have transitioned to new substrates. These findings suggest that high rates of background diversification coupled with dispersal and environmental instability have facilitated phenotypic and ecological diversification in this clade.

Chapter 4: Australia has acted as an engine of biodiversity for a number of disparate clades, producing a wide diversity of species and ecologies seen nowhere else in the world. While the continent is typified by arid environs, a major epicenter of biodiversity is located in the ancient monsoonal tropics of the north. In this study, we investigate the phylogeographic patterns of the marbled velvet gecko (*Oedura marmorata*) in the Top End. Using mitochondrial (mtDNA) data and 4,268 UCEs, we find that there are eight well supported clades in this species complex. However, the UCEs vastly outperform the mtDNA in resolving the phylogenetic relationships between them as well provide context as to the geographic features that led to this diversity. Furthermore, we find signatures of potential hybrid speciation and Dobzhansky-Muller incompatibilities. From clustering analyses, it appears that several major rivers have played a large role in isolating lineages in the Top End. In conjunction with ancient formations such as the Arnhem Plateau and Carpentarian Gap, these rivers have allowed for the formation and maintenance of these lineages.

## TABLE OF CONTENTS

**ACKNOWLEDGEMENTS**

This six year undertaking would not have been possible if it were not for the support and involvement of countless people. Too many to thank on a single page. Firstly, I need to thank my parents, Caroline and Robert Skipwith. Neither of them had the education I have been so lucky have, but they've been behind me every step of the way. My mother supported my curious nature with books and occasional outings to the local park to catch snakes. She should have known that I'd end up being a herpetologist the day my father threw a toad in the bathtub when I was three. He will be missed, my father.

My time at Berkeley would not have been possible had it not been for my undergraduate advisors, Dan Hernandez and Ilene Eberly, and my Masters advisors, Aaron Bauer and Todd Jackman. I have the latter two to thank for my love geckos. While it was research that drew me to apply to Berkeley, it was the graduate student community which made me stay. From intellectual support to much needed friendship, this community is above and beyond anything I have seen at any other institution. Special thanks to Dana Lin, for always being there for me and putting up with my crazy. I would also not have made if it were not for my friends Ashley Poust, Whitney Reiner, Lucy Chang, Daniel Portik, Sean Reilly, Tesla Monson, Luke Bloch, Jesyka Melendez, Sarah Werning, Sarah Hykin, and Sonal Singhal. I would also like to thank the postdocs of the MVZ, Guin Wogan, Ammon Corl, and Raina Bell. I met Paul Oliver, a postdoc in Australia, at the 2012 World Congress of Herpetology, and it has been through continued collaboration that this project has matured into what it is today. My time in the field with him will always be memorable.

All of the vouchers and tissues used in my dissertation were generously loaned and I have the following institutions to thank: The Museum of Vertebrate Zoology (MVZ), California Academy of Science (CAS), Louisiana State University Museum (LSU), Museum and Art Gallery of the Northern Territory (NTM), Australian Museum (AM), Queensland Museum (QM), Western Australian Museum (WAM), South Australian Museum (SAM), Museum Victoria (NMV), Australian National Wildlife Collection (ANWC), Auckland Museum (AMNZ), and Te Papa Museum (TPM).

My dissertation committee has been invaluable in providing advice and making this project possible. I would especially like to thank Jim McGuire for his input on all of my project ideas, grant proposals, and postdoc applications. Thank you for having such an open-door policy and welcoming me into the MVZ community, Jim.

Lastly, I would like acknowledge my funding agencies: Sigma Xi, the Australian Research Council, Museum of Vertebrate Zoology, University of California, Berkeley, and the National Science Foundation (DEB: 1601806).

# Chapter 1

## DIPLODACTYLOID GECKO PHYLOGENETICS INFERRED FROM 4,200 ULTRACONSERVED ELEMENTS

### Introduction

The Australasian region offers a unique opportunity for biologists to investigate evolution in isolation and this is supported by a rich biota predominated by phylogenetically divergent and unique lineages. This region has acted as a refugium for some taxa such as marsupials (Mitchell *et al.*, 2014) to persist and diversify, and has also served as a center of origin for other major clades such as passerine birds (Moyle *et al.*, 2016). Despite its geographic isolation, Australasia has incredibly high levels of species diversity and endemicity for some lineages. Australia itself harbors more than 1,000 species of squamate reptile which are represented by a combination of old endemics and recent invaders from Asia (Oliver & Sanders, 2009; Vidal *et al.*, 2012; Lee *et al.*, 2016). Geckos represent a major component of the squamate fauna of Australia and its adjacent islands (~25% for Australia alone) and are of particular interest as this region harbors two major clades that have very different biogeographic histories. The first, the gekkonids, represent at least a dozen distantly related genera that have repeatedly invaded New Guinea, Australia, and the remainder of Oceania from Asia during the Cenozoic (Horner, 2005; Fujita *et al.*, 2010; Oliver *et al.*, 2010b; Heinicke *et al.*, 2011; Shea *et al.*, 2011; Doughty *et al.*, 2012; Flecks *et al.*, 2012; Sistrom *et al.*, 2012; Oliver *et al.*, 2014a; Skipwith & Oliver, 2014). However, the bulk of Australasian gecko diversity is represented by the diplodactyloids which are endemic to the region.

The Diplodactyloidea (referred to as the Pygopodomorpha or Pygopodoidea by Hedges and Vidal (2009) and Brennan and Oliver (2017)) is a diverse clade of ~213 species in 39 genera (Uetz *et al.*, 2017) delimited between three morphologically distinct families: the Diplodactylidae (~141 sp, 25 genera), Carphodactylidae (~29 sp, 7 genera), and Pygopodidae (~43 sp, 7 genera). These families are largely restricted to mainland Australia, although two diplodactylid clades containing nearly 60 species have independently colonized New Caledonia and New Zealand, respectively, and a single pygopodid is present in New Guinea (figure 1). The three diplodactyloid families are collectively sister the remaining four gekkotan families which constitute the Gekkonoidea (families: Gekkonidae, Phyllodactylidae, Sphaerodactylidae, and Eublepharidae). The split between gekkonoids and diplodactyloids dates back to the early to late-early Cretaceous and has been suggested to represent a west (gekkonoids) – east (diplodactyloids) Gondwanan divide between crown gekkotans (Feng *et al.*, 2007; Oliver & Sanders, 2009; Zheng & Wiens, 2016). Despite representing only ~12% of the ~1,700 species of geckos, diplodactyloids illustrate all of the morphological diversity seen within gekkotans globally. This clade contains some of the smallest ($\leq$ 40 mm SVL) as well as the largest extant and extinct gecko species ($\geq$ 280 mm SVL). In addition to body sizes that span more than an order of magnitude, this clade also possesses a wide array of limb and digit morphologies ranging from the carphodactylids lacking adhesive toepads, to the padded diplodactylids, to the near limbless pygopodids (limb reduction occurs nowhere else in Gekkota). Furthermore, toepad configurations vary widely within the Diplodactylidae, with some genera bearing large, spatulate pads while others bear reduced apical scansors. Lastly, ecomorphological diversity is extremely diverse within diplodactyloids with some taxa having small heads suited for dealing with small prey (*Lucasium/Diplodactylus* clade), other with large heads and hypertrophied caniform teeth (*Rhacodactylus auriculatus*), still others with enlarged reinforced skulls (*Nephrurus* and kin), and finally others with highly kinetic skulls

that facilitate handling slippery smooth—scaled vertebrate prey such as scincid lizards (*Lialis*). Caudal morphology also varies widely with ornamentation ranging from leaf mimics (*Phyllurus, Saltuarius*, and *Orraya*) to prehensile tails with adhesive distal lamellae (all New Caledonian and New Zealand genera) and tails with specialized glands capable of projecting sticky anti-predator substances (*Strophurus* and *Eurydactylodes*).

Given this diversity, diplodactyloids offer a unique opportunity to investigate how lineages diversify in isolation both in terms of species diversity and ecological diversity. These issues are best addressed with a well-resolved phylogeny. Given its morphologic breadth, Diplodactyloidea has been the subject numerous taxonomic and phylogenetic studies using morphology alone (Underwood, 1954, 1955; Kluge, 1976, 1983, 1987; Bauer, 1990). The results of these studies have been inconsistent with one another due to rampant homoplasy and, furthermore, have usually conflicted with the findings of recent molecular studies (Donnellan *et al.*, 1999; Chambers *et al.*, 2001; Hutchinson *et al.*, 2009; Oliver & Sanders, 2009; Oliver *et al.*, 2010a; Nielsen *et al.*, 2011; Oliver & Bauer, 2011; Bauer *et al.*, 2012; Oliver *et al.*, 2012; Garcia-Porta & Ord, 2013; Oliver *et al.*, 2014c; Skipwith *et al.*, 2014; Brennan *et al.*, 2016; Nielsen *et al.*, 2016; Oliver & Doughty, 2016; Skipwith *et al.*, 2016; Brennan & Oliver, 2017). Relationships between the three families have stabilized on diplodactylids being sister to the carphodactylids and pygopodids (Brennan & Oliver, 2017). However, the relationships of several clades remain problematic, namely the intergeneric relationships of the New Caledonian and core Australian diplodactylids, the placement of *Orraya* within the carphodactylids, and interrelationships between the pygopodid genera.

There is growing consensus that the diplodactyloids represent an old lineage of Gondwanan origin (Oliver & Sanders, 2009; Oliver *et al.*, 2014b). This stands in contrast to most other Australasian squamate lineages that appear to be relatively recent invaders from the northwest, having arrived in the late Paleogene or Neogene (Skinner *et al.*, 2011; Lee *et al.*, 2016). Most studies relying on molecular divergence dating have estimated that the diversification of crown diplodactyloids occurred during the late Cretaceous (85 – 65 mya) (Gamble *et al.*, 2008a; Gamble *et al.*, 2008b; Oliver & Sanders, 2009; Oliver *et al.*, 2010a; Nielsen *et al.*, 2011; Oliver & Bauer, 2011; Garcia-Porta & Ord, 2013; Doughty *et al.*, 2016; Nielsen *et al.*, 2016; Skipwith *et al.*, 2016). However, multispecies coalescent analyses by Skipwith *et al.* (2016) suggests that this clade may have originated as recently as the Paleocene (~ 63 mya). While the bulk of species diversity in this clade is restricted to mainland Australia, there have been at least three overwater dispersals to nearby islands in Oceania. Divergence dating places the crown ages for the New Caledonian and New Zealand diplodactylids in either the Oligocene or Miocene (Nielsen *et al.*, 2011; Skipwith *et al.*, 2016) while the pyogopodid *Lialis* dispersed to New Guinea much later in the Neogene (Hugall *et al.*, 2007; Garcia-Porta & Ord, 2013). While previous studies have yielded similar dates for the crown age divergence of the diplodactyloids, most studies have targeted individual clades and none have approached questions regarding topology and divergence time with more than a handful of markers (typically < 6 loci). As such, we address the phylogenetic relationships, divergence timing, and diversification history of Diplodactyloidea with a large, newly generated phylogenomic dataset.

Here, we present a revised phylogeny for the diplodactyloids implementing a large phylogenomic dataset of ~4,200 ultraconserved elements. Probes were designed to target orthologous loci from across Tetrapoda. We describe our library preparation protocol, target capture methodology, and the overall efficacy of our experiment below. Our new phylogenetic hypothesis incorporates sequence data from 160 described species, 10 candidate species, and all

but one genus of diplodactyloid, roughly 75% of the recognized diversity. In addition to traditional concatenation methods, we implemented summary multispecies coalescent analyses to infer the species tree from our ~4,200 loci. Lastly, we estimate divergence times within this clade using our UCE data and contrast our estimates with those recovered by smaller Sanger-based studies.

**Methods**

*Taxon Sampling*

We included 290 geckos in this study comprising 10 gekkonoid outgroup taxa and 280 diplodactyloid individuals. Of the diplodactyloids, 160 of the 213 described species and all but one genus was sampled (tables 1 and 2). We also included representatives from potentially undescribed species identified in previous studies (Nielsen *et al.*, 2011; Oliver *et al.*, 2012; Oliver *et al.*, 2014c; Skipwith *et al.*, 2016). For clades with sparser sampling relative to the number of described species (i.e.- pygopodids, *Diplodactylus*, *Crenadactylus*, etc.), we tried to included representatives that encompassed the deepest divergence within a given clade based on previous molecular studies (Jennings *et al.*, 2003; Oliver *et al.*, 2007b; Oliver *et al.*, 2007a; Doughty *et al.*, 2008; Oliver *et al.*, 2009; Oliver *et al.*, 2010a; Brennan *et al.*, 2016; Doughty *et al.*, 2016). This sampling strategy was implemented to ensure that divergence dating analyses inferred accurate crown ages for these clades.

*Genomic Library Preparation and Target Capture*

Genomic DNA was extracted using a modified guanidine-thiocyanate extraction method for fresh samples stored in RNAlater (Lawalata, unpublished). However, most of the tissues used in this study were of low quality, being either small or degraded. For these samples, we used a modified phenol-chloroform extraction protocol (Wogan, unpublished) wherein tissue lysates were exposed to a series of phenol and chloroform washes using phase-lock gel tubes (5Prime). After the final chloroform wash, the extractions were subjected to a bead cleanup using a 2x ratio of Sera-Mag magnetic beads (GE Healthcare) with 10% tween solution. This method proved to be vastly superior to the guanidine-thiocyanate method in terms of DNA yield, sometimes producing an order of magnitude more double-stranded DNA for problematic samples. DNA quantification for extractions and all ensuing PCR reactions was done with the high-sensitivity kit on a Qubit 2.0 fluorometer (Life Technologies). We followed a modified Meyer-Kircher library protocol (referred to as MK from herein) (Meyer & Kircher, 2010) using1,100 ng of double-stranded DNA diluted in 110 µl of EBT buffer (EB buffer with 0.05% tween solution). A number of extractions produced low yields (< 500 ng) and for these the entire sample was used. Library insert size was selected as specified for the UCE MYbaits kit (MYcroarray) with a target size range of 400-700 bp. Shearing was done on a Bioruptor UCD-200 (Diagenode) with the following setting: 30s on, 90s off on high for 7-9 cycles. Approximate insert size was determined by running sheared samples on a 1.5% agarose gel. We followed the MK protocol for blunt-end repair, adapter ligation, and adapter fill-in with slight modifications in reagent volumes. Blunt-end repair to adapter fill-in products were purified using a 1.8x Sera-Mag bead cleanup. The post-adapter fill-in indexing PCR step employed unique 7 bp P7 indexing oligos for each individual, with most samples requiring 12 cycles to achieve 15-35 ng/µl of product. Samples with very low extraction concentrations were subjected to 14-16 index PCR cycles. Indexing PCR products were cleaned using a 1.3x Sera-Mag bead cleanup and all samples went through three rounds of PCR.

The MYbaits UCE kit contains probes that are designed to capture targets from across the tetrapod phylogenetic tree (Crawford *et al.*, 2012; Faircloth *et al.*, 2012; McCormack *et al.*, 2012; McCormack *et al.*, 2013; Smith *et al.*, 2014). Thus, samples were not necessarily pooled by phylogenetic relatedness but rather indexing PCR DNA concentration as assessed by Qubit. Each pool contained 8-9 individuals for a total of 800 ng of DNA. Prior to hybridization each pool was dried in a heated vacuum centrifuge at 65º for 45 minutes before being rehydrated in 5 µl of water. Our target capture protocol followed the MYbaits guidelines with minor alterations to the reagent volume for the library mix. Instead of using the kit blocking oligos, we opted to use chicken COT-1 (replaces kit block #1) as well as P5 and P7 xGEN (Integrated DNA Technologies) blocking oligos (replaces kit block #3). We chose the xGEN blockers over the manufacturer's as previous studies have shown that they outperform other blocking oligos in preventing daisy-chaining (Portik *et al.*, 2016). Libraries were hybridized with the UCE probes for 24 hours at 65º C. After hybridization, libraries were purified with Dynabeads streptavidin beads (ThermoFisher Scientific) following the MYbaits bait wash protocol. Captured libraries were then amplified using the KAPA HiFi HotStart ReadyMix (KAPA Biosystems) for 16-17 cycles with the annealing time optimized for mid-sized targets (300-700 bp). Each library went through four rounds of post-capture amplification to ensure amplicon diversity before being eluted in 10 µl of EBT buffer. Capture efficiency was assessed with via qPCR of pre-capture and post-capture pools with custom primers targeting non-target exons and target UCEs. Post-capture concentration was determined with the Qubit high-sensitivity kit and target size was assessed on a Bioanalyzer 2100 DNA 1000 chip (Agilent Technologies). Post-capture libraries had an average size of 496 bp (range: 420-584 bp). Final post-capture libraries were pooled in equimolar amounts and sequenced on an Illumina HiSeq 4000 platform with 150 bp paired-end reads (Illumina).

*Data Assembly*

We used custom perl scripts to process UCE capture data from methods described in Singhal (2013), Bi *et al.* (2012), Bi *et al.* (2013), and (Portik *et al.*, 2016). Scripts for de novo target capture and assembly for phylogenomics are available via the github repository (https://github.com/CGRL-QB3-UCBerkeley/denovoTargetCapturePhylogenomics). Raw fastq reads were filtered using CUTADAPT (Martin, 2011) and TRIMMOMATIC v0.36 (Bolger *et al.*, 2014) with a trimming length cutoff of 50 bp, removing low quality reads and adapter sequences. The quality trimming threshold for TIMMOMATIC was set to 20. Bacterial contamination was removed from filtered raw reads by aligning individual sequences to the *Escherichia coli* genome with BOWTIE2 (Langmead & Salzberg, 2012).

1) 1-ScrubReads cleanPE -f *raw reads* -o *cleaned reads* -t Trimmomatic- -c *E. coli* genome.fasta -k 8 -h 50 -q 20 -l 150 -z

Duplicates and low complextity reads were removed during the filtering stage with a the custom scrubreads script. We used SPADES for de novo assembly of cleaned reads, a multi-kmer approach to deal with the likely increase in polymorphism that would accompany the high number of individuals and phylogenetic diversity used in this study (Bankevich *et al.*, 2012).

2) 2-GenerateAssembliesPhylo spades –reads *cleaned reads* –out *raw assemblies* –np *number of cores*

We used Blastn (evalue cutoff = 1e-10, similarity cutoff = 80) to compare SPAdes raw assemblies of each individual to the tetrapod UCE baits to identify assembled contigs that stemmed from UCE loci (Faircloth *et al.*, 2012). We also ran a self-Blastn (evalue cutoff =1e-20) to compare the contigs against themselves to mask any regions from a contig that matched other regions from other contigs. The resulting, non-redundant, UCE assemblies from each individual sample is used as a raw reference that includes targeted UCE and the flanking sequences (+/-500bp to targeted UCE region). Paired-end and merged cleaned reads from each individual were then aligned to the individual-specific assemblies using Novoalign (Li & Durbin, 2009) and we only retained reads that mapped uniquely to the reference. We used Picard (http://broadinstitute.github.io/picard/) to add read groups and GATK (McKenna *et al.*, 2010) to perform re-alignment around indels. We finally used SAMtools/BCFtools (Li & Durbin, 2009)q

3) 3-FindingTargets combineExon –t *target fasta* –a *raw assemblies* –m 0.98 –d 0.3 –p 80 –e 4

4) 4-TransExonCapPhylo contig –t 4 –a *fasta files* –f *bed files* –b *cleaned reads* –G *GATK* –P *Picard* –I 500 –M 0.6 –c 0 –r 150 –R "vertebrata metazoan"

Flanking regions for contigs were kept if they were within 500 bp of the target region to which they mapped (–f). Final contigs were aligned to their individual specific in-target assemblies using NOVOALIGN (Li & Durbin, 2009, http://www.novocraft.com/) while the Genome Analysis Toolkit (GATK) v3.6 and PICARD (McKenna *et al.*, 2010) were used for realignment. We kept both non-concordant and concordant reads (–c) and individual loci were discarded if 60% or more the sequences were composed of missing data (–M).

5) 4-TransExonCapPhylo alignment –e *final contigs* –b *list of library names* –a 1 –m 0.4 –n 0.3 –l 1 –h 99.5 –H 99.5 –z 0.4 –s *number samples*

Multi-individual alignments of each locus were generated with MAFFT v7 (Katoh & Standley, 2013) and trimmed with TRIMAL (Capella-Gutierrez *et al.*, 2009). Sites were treated as 'N's' if the read depth was lower than 5x or above 100,000x (–d, –D). REPEATMASKER was implemented to mask putatively repetitive elements agaisnt short repeats, using the vertebrate metazoan database (Smit *et al.*, 2015). We calculated read depth by trimming off loci that fell outside of the 1$^{st}$ and 99.5 percentiles while loci that fell outside the 99.5 percentile for heterozygosity were removed (–l, –h, –H). A locus was further discarded if the proportion of shared polymorphic sites exceeded 40% (–z). We then blasted our final set of UCEs against the *Anolis carolinensis* genome so that this species could be used to root the gekkotan tree.

*Sequence Capture Evaluation*

Capture efficiency was evaluated by calculating the average coverage (i.e. – sequencing depth) per site for the target and flanking regions for each locus based on aligment (BAM) generated using SAMtools and its "depth" function (Li & Durbin, 2009). We calculated sensitivity, the percentage of bases within a target sequence that are recovered in one or more reads, was assessed by comparing final assemblies to target UCE sequences We further tested for capture specificity by determining what percentage of cleaned reads mapped to target UCE sequences. This was determined by calculating what percentage of the cleaned data mapped to the reference UCE target

sequence for each sample. Coverage, sensitivity, and specificity were determined with custom Perl scripts.

The major appeal of using UCEs over other reduced representation sequence capture methods lies largely in the ability to capture large numbers of individuals for a larger number orthologous markers in a cost and time effective manor, without the necessity of marker design. However, UCEs themselves are largely invariable and potentially inappropriate for phylogenomic studies focusing on recently diverged taxa. With this in mind, we determined the efficacy of UCEs for taxa with deep and shallow divergences by estimating the proportion of missing sequence data, proportion of missing taxa, and proportion of parsimony informative sites for each locus. The relationship between locus length (bp) and the number of informative sites was determined with linear regression. Estimation of alignment completeness and number of informative sites was done with custom Python scripts (https://github.com/dportik).

*Phylogenetic Analyses*

This study took a multifaceted approach towards phylogenetic inference. PartitionFinder v2 was used to determine the appropriate model of substitution for each UCE locus and the optimal partitioning strategy for the concatenated alignment (Lanfear *et al.*, 2012). Akaike Information Criterion (AIC) and Bayesian Information Criterion (BIC) were used for downstream maximum likelihood (ML) and Bayesian inference (BI) phylogenetic analyses. We inferred the ML topology using RAxML v8.2.9 (Stamatakis, 2014) with 300 nonparametric rapid bootstrap replicates and a simultaneous search for the best likelihood tree on the Cipres Portal (Miller *et al.*, 2010). The GTR+G model was used as RAxML only permits the specification of a single model for an alignment and its partitions. To determine the effects of model choice and partitioning on topology and branch lengths, we also used the ML algorithm of IQ-TREE v1.5.2 (Minh *et al.*, 2013; Nguyen *et al.*, 2015) with the partitioning scheme and model choice suggested by PartitionFinder. Like RAxML, IQ-TREE implements a genetic algorithm that permits rapid likelihood calculation. With this in mind, we ran IQ-TREE for 1,000 ultrafast bootstrap replicates.

Given the number of loci used in this study and the general lack of informative sites in individual UCE loci, we assumed that there would be high levels of gene tree incongruence and incomplete lineage sorting (ILS) (Edwards, 2009). Multispecies coalescent methods, such as *BEAST (Heled & Drummond, 2010), that simultaneously estimate gene trees and species trees from sequence data while estimating complex parameters (i.e. effective population size) using MCMC are computationally impractical for datasets of this size (Edwards *et al.*, 2016). We therefore used the less computationally intensive ASTRAL II to estimate the species tree of the diplodactyloids (Mirarab & Warnow, 2015). This summary method is statistically consistent with the multispecies coalescent, taking a set of unrooted gene trees with known branch lengths as input as opposed to sequence data. The ASTRAL algorithm estimates the species tree by maximizing the number of quartet trees shared with a set of unrooted gene trees, penalizing low frequency quartet trees (Mirarab *et al.*, 2014; Sayyari & Mirarab, 2016). Rather than bootstrapping our individual gene trees, we relied on the local posterior probability (lpp) estimated by ASTRAL for node support (Sayyari & Mirarab, 2016). Understanding how many loci are required to obtain topological stability is critical for phylogenomic studies. We consequently used a random binning method ASTRALnaut (https://github.com/dportik) to determine how many loci were needed to converge on the optimal species tree topology recovered by ASTRAL for our full 4,200 locus data set. To do this we designated 10 bins with varying numbers of UCE loci (10, 20, 50, 100, 250, 500, 1000, 2000, 3000, 4000). Each bin was sampled 10 times randomly from the full set of 4,200

loci, resulting in 10 species trees per binning group. AstralNaut uses the Robinson-Foulds (RF) metric to compute the distance between each estimated species tree within a bin and the optimal topology (Robinson & Foulds, 1981; Ruane *et al.*, 2015). This method effectively bootstraps the UCE dataset for a given bin, as loci are sampled or potentially resampled at random. Lastly, we computed between RF distances for trees within each bin. We used custom python scripts developed in the Museum of Vertebrate Zoology to compute RF distances.

*Topological Consistency with Published Phylogenetic Estimates*

As a proxy for determining how much accounting for genealogy effects phylogenetic inference, we used the R package PHANGORN to estimate normalized Robinson-Foulds (nRF) between our concatenated and coalescent trees (Schliep, 2011). To determine the extent to which our phylogenomic estimates differed from those of published studies, we also computed nRF metrics for all comparisons of our two trees to that of Brennan and Oliver (2017) and the supertrees of Pyron *et al.* (2013b), Wright *et al.* (2015), and Tonini *et al.* (2016). While the Brennan and Oliver (2017) phylogeny was comprised of a mostly complete matrix of 6 loci, the three supertree alignments ranged 12 to 15 loci with up to 90% missing data (Pyron *et al.*, 2013b). However, the diplodactyloids were at most represented by 4 loci (ND2, RAG1, Cmos, and PDC). We took the published topologies and pruned them using APE to match our two trees for all topological comparisons.

*Divergence Dating*

Traditional Bayesian divergence dating methods, such as BEAST, that simultaneously infer divergence dates and topology from sequence data are computationally infeasible for datasets of this scale (Drummond & Rambaut, 2007). Thus, to infer divergence dates for diplodactyloids, we used the program MCMCTREE in PAML (YANG, 2007). The MCMCTREE algorithm circumvents the computational pitfalls of BEAST-like divergence dating methods by bypassing the tree building process, taking a known phylogeny without branch lengths as input. It then assigns substitution rates to different branches of the tree before estimating branch rates and divergence dates from sequence data. We used the species tree topology inferred from ASTRAL as the guide tree. However, our entire concatenated alignment of 4,268 UCE loci and 190 species proved too large for MCMCTREE, requiring the dataset to be pared down to the top 250 most complete loci. We first estimated the Hessian matrix from our sequence data with the default priors which was then used for the approximate likelihood calculation of divergence times. The burnin was set at 5,000 and the analysis was run until 60,000 samples from the mcmc had been attained. We ran MCMCTREE twice with the same prior settings and plotted the resulting divergence times of the two runs against one another to ensure they had converged. The HKY + G model was used for all dating analyses as this is the most complex model available in MCMCTREE and rate heterogeneity is prevalent in UCE datasets (Moyle *et al.*, 2016).

Geckos have a relatively sparse fossil record when compared to other squamates, with the majority of probable gekkotans being stem taxa from the Mesozoic (Bauer *et al.*, 2005; Arnold & Poinar, 2008; Daza *et al.*, 2013). To constrain the divergence between *Anolis* and Gekkota, we placed a normal distribution on the root (1.9 – 2.2) in MCMCTREE, a range largely congruent with the accepted divergence between Gekkota and Toxicofera (Evans, 2003; Vidal & Hedges, 2005; Hedges & Vidal, 2009; Vidal & Hedges, 2009; Hutchinson *et al.*, 2012; Zheng & Wiens, 2016). Relatively few taxa can be confidently assigned to crown gekkotan lineages and most of these are amber preserved sphaerodactylids from the Neogene (Daza *et al.*, 2014). The amber preserved

gecko *Cretaceogekko* was used to constrain the divergence between gekkonoids and diplodactyloids with a truncated Cauchy distribution (L = 1.0, $c$ = 0.5, $p$ = 0.2) (Arnold & Poinar, 2008). Our outgroup sampling allowed us to include the amber embedded Miocene sphaerodactyline *Sphaerodactylus dommeli* for the split between the Dominican *S. difficilis* and the Puerto Rican *S. nicholsi* and *S. townsendi* (truncated Cauchy: L = 0.23, $c$ = 0.1, $p$ = 0.2) (Daza *et al.*, 2014). We further used a normal distribution as a secondary calibration for the crown age of diplodactyloids based off of the findings of previous studies ($t_L$ = 0.5, $t_U$ = 0.7, $p_L$ = 0.25, $p_U$ = 0.25) (Oliver & Sanders, 2009; Skipwith *et al.*, 2016). The crown age of the New Zealand diplodactylids was constrained by unidentified Miocene cranial material from New Zealand (truncated Cauchy: L = 0.16, $c$ = 0.09, $p$ = 0.1) (Lee *et al.*, 2009b; Daza *et al.*, 2014).

**Results**

*Sequence Capture Performance*

Overall, all samples performed well with raw base pair yield averaging at 1,247.3 Mb per sample (range: 293 – 4,017.7 Mb). After cleaning and the removal of low complexity reads, duplicates, and bacterial contamination the average amount of recovered data was 463.5 Mb (range: 123.9 – 1786.7 Mb) with an average of 38.9% of reads passing all filtering stages.

*Sensitivity, Specificity, Sequencing Depth, and Informativeness*

Sensitivity, the proportion of bases that map to at least one read in in-target assemblies, was highly conserved across all samples with an average of 99.9% (range: 99.8 – 100%). No clear pattern was present in terms of phylogenetic bias in sensitivity in either the outgroup or ingroup taxa. We further tested specificity, the proportion of filtered bases that mapped to the target sequence, and found that our samples had an average specificity of 49.5% but a very wide range (range: 1.14 – 79.9%) (figure 2). Coverage for both the target and flanking regions varied widely between samples but was otherwise very high with the average of 220x and all but one sample having above 43x coverage (range: 12.9 – 732.9x) (figure 3). One sample, *Orraya occultus* QMJ62596, had extremely low coverage at 12.9x.

Our sequence capture recovered a total of 4,268 loci with a concatenated length of 2,180,083 bp where at least 70% of loci were recovered for all samples. However, no single locus contained all samples with average taxa-completeness per locus being 268.1 individuals (range: 196 – 281 individuals). Approximately 98% of loci had 75% or more taxa represented. *Orraya occultus* yielded the least amount of data, with data available for only 556 loci. Locus length averaged at 510.8 bp (range: 30 – 1,410 bp) and individual loci were largely complete in terms of gaps with an average of 8% of the alignment being composed of gaps (range: 0 – 94.2%). In terms of phylogenetic information content, loci ranged from invariable to highly variable with an average of 21.7% informative sites (range: 0 - 65.3%) for the ingroup. We found a correlation between locus length and the number of informative sites (equation = -30.9 + 0.29*sequence length: F (1, 4971) = 4266: $R^2$ = 0.54, p = < 0.001) (figure 4).

*Phylogenetic Analyses*: *Concatenation*

Among the outgroup taxa, our concatenated maximum likelihood analyses found identical relationships to previous studies, with eublepharids recovered as sister to the other gekkonoids, and sphaerodactylids placed outside of gekkonids + phyllodactylids (Feng *et al.*, 2007; Gamble *et al.*, 2008a; Gamble *et al.*, 2008b; Gamble *et al.*, 2011; Gamble *et al.*, 2012; Pyron *et al.*, 2013b; Gamble *et al.*, 2015) (figure 5). Relationships within the diplodactyloids were largely resolved,

with the utilization of thousands of loci resolving numerous problematic relationships. We found strong support (≥ 70 bootstrap) for the sister relationship between the carphodactylids and pygopodids. Three major lineages were recovered within Carphodactylidae, *Orraya* was placed as sister to a clade containing the *Carphodactylus* and knob-tail geckos (*Nephrurus*, *Underwoodisaurus*, and *Uvidicolus*), and a second clade composing the remaining leaf-tail geckos (*Saltuarius* and *Phyllurus*). The pygopodids can similarly be broken into three major clades, with *Delma* sister to a clade containing *Aprasia* and a second clade including the large-bodied genera (*Pletholax*, *Paradelma*, *Lialis*, and *Pygopus*).

Within the diplodactylids, *Pseudothecadactylus* was recovered as sister to the New Caledonian clade. Intergeneric relationships within the New Caledonian clade are nearly fully resolved. The giant species in the genera *Rhacodactylus* and *Mniarogekko* receive strong support as being sister to the remaining genera, though *R. leachianus* received low support for placement in this clade. *Correlophus* and *Eurydactylodes* are collectively sister to a clade containing the remaining small-bodied genera *Bavayia*, *Paniegekko*, *Oedodera*, and *Dierogekko*. Sister to the *Pseudothecadactylus* + New Caledonian clade is an assemblage composed of the Australian *Crenadactylus* which is in turn sister to the New Zealand clade and the remaining Australian genera. The New Zealand clade is divided into a broad-toed clade (*Woodworthia* and *Hoplodactylus*) and a narrow-toed clade (*Dactylocnemis*, *Mokopirirakau*, *Tukutuku*, *Toropuku*, and *Naultinus*). The base of the core Australian clade includes a number of short internodes. The concatenated tree has moderate support suggesting that *Amalosia* and *Nebulifera* are sister to the remaining genera and that *Nebulifera* renders *Amalosia* paraphyletic. There was low support for *Hesperoedura* being sister to *Oedura* and the *Diplodactylus* group. *Strophurus* was found to be sister to *Lucasium* + *Rhynchoedura* and *Diplodactylus*.

*Phylogenetic Analyses*: *Multispecies Coalescent*

ASTRAL recovered a topology largely congruent with the RAxML phylogeny, with most discordances occurring intragenerically and at short internodes (figure 6). The major points of intrageneric incongruence are within the New Caledonian and core Australian diplodactylids. Rather than being found in a sister relationship with *Eurydactylodes*, *Correlophus* receives low support as sister to the *Rhacodactylus – Mniarogekko* clade. *Eurydactylodes* is in turn found to be sister to all the remaining New Caledonian genera with strong support. In contrast to the clade of small-bodied taxa recovered by our concatenated analyses, the species tree finds strong support for a *Oedodera* + *Dierogekko* clade and a *Paniegekko* + *Bavayia* clade. The base of the core Australian clade received far lower support than the concatenated tree, finding weak support for *Hesperoedura* being part of the *Amalosia* + *Nebulifera* clade and that this group is sister to the remaining Australian genera. Examination of topological convergence revealed that there were drastic gains in improvement between 10 and 500 loci, where 90% of nodes from the full ASTRAL tree were recovered (figure 7). At 1,000 or more loci, minor topological improvements were noted.

*Topological Congruence*

Tests of topological congruence revealed that our concatenated tree and species tree shared a large proportion of nodes with one another (nRF = 0.17). However, both trees demonstrated very high RF distances from the four published studies, with none sharing more than 61% of its nodes with either of our trees (nRF RAxML: 0.42 – 0.43, ASTRAL: 0.39 – 0.45) (figure 8). Greater variation among tree distances was seen in comparisons to the species tree, where the concatenated Brennan

and Oliver (2017) topology exhibited closer topological congruence with our species tree than our concatenated tree (nRF of 0.39 vs. 0.44).

*Divergence Dating*

The split between gekkonoids and diplodactyloids yielded by MCMCTREE suggests a late Jurassic divergence (μ = 149 mya, CI = 118 – 181 mya) (figure 6). The crown age for diplodactyloids was dated to the late Cretaceous (μ = 76 mya, CI = 65 – 86 mya), with the ages of the carphodactylid – pygopodid split (μ = 67 mya, CI = 58 – 72 mya) and crown Diplodactylidae (μ = 60 mya, CI = 52 – 69 mya) being inferred as late Cretaceous and mid-Paleocene respectively. *Orraya*, being sister to the remaining carphodactylids, split off during the early Eocene (μ = 50 mya, CI = 40 – 59 mya), while the split between the knob-tail geckos and leaf-tail geckos is estimated to have occurred 42 mya (CI = 33 – 50 mya). *Delma* split from other pygopodids during the early Eocene (μ = 40 mya, CI = 32 – 50 mya), with many of the divergences within the *Aprasia – Lialis/Pygopus* group occurring during the mid-late Paleogene. The splits between *Pseudothecadactylus* – New Caledonia and *Crenadactylus* – New Zealand/core Australia occurred during the late Paleocene (μ = 58 mya, CI = 50 – 67 mya for both). With the exceptions of the New Caledonian and New Zealand taxa, most of the recognized diplodactylid genera appear to have been present by the mid-late Miocene (16 – 23 mya).

**Discussion**

*Sequence Capture Performance*

In this study, we implemented a generalized sequence capture probe set to sample genomic-scale data from geckos with high success. We were able to capture a total of 4,268 UCEs for 290 gecko samples representing 190 species from all 7 gekkotan families, a total divergence spanning over 100 My. The UCE probe set was initially designed for capturing sequences from a range of tetrapod taxa, with most of the genomic data being sourced from birds (Faircloth *et al.*, 2012; McCormack *et al.*, 2013; Smith *et al.*, 2014). Nevertheless, our 70% complete matrix suggests that this locus set is highly efficacious for use within squamates, both in terms of cost effectiveness and capture fidelity. Unlike studies relying on transcriptome-based exon capture or ddRADseq, there is little chance that capture efficiency will decrease as phylogenetic distance increases from the probe set (Portik *et al.*, 2016). Rather, investigation of the sensitivity of target capture reveals that in all samples nearly 100% of bases mapped to reads in in-target assemblies. However, the specificity of bases that mapped to the target sequence after filtering stages varied more widely than did sensitivity. No clear pattern is evident, though many of the samples with low specificity may be traced back to the initial low quality of the tissue in question. The same appears to hold true for overall coverage of the target and flanking regions. One sample, *Orraya occultus* QMJ62596, is a clear example of this trend. This sample was heavily degraded when acquired, being composed of very small liquefied tissue fragments that had been rehydrated in ethanol. Initial extraction attempts yielded extremely low amounts of DNA and, after 3 rounds of extraction, only ~125 ng of double stranded DNA was available for library preparation. The raw read estimates for this sample were initially very high, comparable to other individuals from the same pool, but less than 2% of these mapped to target sequences after cleaning. Given that decontamination filtering detected negligible amounts of bacterial DNA, we feel confident that the low proportion of sequence recovery is a reflection of high amounts of highly fragmented short sequences rather than contamination.

Ultraconserved elements proved to be informative at multiple phylogenetic levels and were remarkably variable within the ingroup. Our finding that phylogenetic information content increases with locus length is consistent with UCEs being conserved in the target region, with the flanking regions containing most of the information content. However, our UCE dataset demonstrated a somewhat weaker signal for increased information content with locus length when compared to datasets such as exons. Portik *et al.* (2016) found a stronger correlation between locus length and the number of informative sites in their exon capture experiment, despite their dataset being one-third the size of ours in terms of loci. Their investigation of phylogenetic informativeness suggested that for every base pair in a locus there was an increase of 0.38 informative sites, whereas our UCEs present an increase of 0.29 informative sites. This comparison is particularly appropriate as afrobatrachian frogs span a roughly comparable divergence time scale as diplodactyloid geckos (mid-late Cretaceous) (Portik & Blackburn, 2016). This pattern is attributable to the highly-conserved nature of UCEs and the trade-off between acquiring the variable flanking region and sequencing depth. The farther from the core target region, be it UCE or exon, sequencing depth can be expected to decrease. UCEs are expected to be less variable than exon capture probe sets as these were initially designed for birds with only a single squamate genome for reference. It follows that a *de-novo* UCE probe set designed for squamates or gekkotans would be highly informative in comparison to the general tetrapod probe set used in this study.

*Topological Comparisons*

We found that our concatenated and coalescent trees agreed on 83% of the nodes, suggesting that incomplete lineage sort was relatively common, but not pervasive across our 4,268 loci. In fact, all discordances occurred at node that received low statistical support in both trees (RAxML: bootstrap, ASTRAL: lpp) or at nodes where branch lengths were near zero in the concatenated tree. This is entirely consistent with what would be expected with gene tree-species tree discordance, particularly in case of rapid divergence (Edwards *et al.*, 2016). Our comparisons to the four published studies reveals that not only does our phylogenetic estimate resolve nearly all problematic nodes, but that many of the species-level relationships recovered are novel. This lends credence to the importance of implementing numerous loci. Even though, these studies are multilocus, the relationships within are largely unstable between studies. This may be an artifact of copious amounts of missing data, in the case of the supertrees, and the use of comparatively few loci that are individually uninformative or overridden by potentially misleading mitochondrial signal.

*Interfamilial Relationships of Gekkonoids and Diplodactyloids*:

Interfamilial relationships within the gekkonoids are consistent with previous molecular studies where the lidded and padless eublepharids are sister to the lidless predominately pad-bearing sphaerodactylids, phyllodactylids, and gekkonids with high support (Han *et al.*, 2004; Gamble *et al.*, 2008a; Gamble *et al.*, 2008b; Pyron *et al.*, 2013a). The placement of eublepharids as sister to a clade consisting of diplodactyloids and the remaining three gekkonoid families in morphology-only analyses is indicative of eublepharids possessing a suite of plesiomorphic traits seen nowhere else in Gekkota (i.e.- presence of lacrimal bones, moveable eyelids, etc.) (Reeder *et al.*, 2015). Both our concatenated maximum likelihood and multispecies coalescent analyses of the 70% complete matrix yield identical interfamilial relationships for the diplodactyloids, with diplodactylids found to be sister to the carphodactylid-pygopodid assemblage. This relationship is

entirely consistent with the findings of most molecular studies relying on Sanger data, though the carphodactylid-pygopodid relationship has typically received low support in those analyses based solely on mitochondrial DNA or a single nuclear locus (Han *et al.*, 2004; Oliver & Sanders, 2009). This familial arrangement is incongruent with studies relying solely on morphology or combined morphology and molecular data, in which the limbless pygopodids are typically reconstructed as sister to the limbed carphodactylids and diplodactylids or sister to the diplodactylids alone (Kluge, 1967; Kluge, 1976, 1983, 1987; Bauer, 1990; Reeder *et al.*, 2015). The interfamilial incongruence found between molecular studies, including this one, and most morphological studies may be attributable to a large number of plesiomorphic traits uniting carphodactylids and diplodactylids (i.e.- traits related to the presence of limbs) and the general lack of synapomorphies uniting the former with pygopodids.

Our assessment of topological convergence with ASTRAL suggests that 500 or more UCEs are required to achieve a RF distance of 0.1 or below, with small improvements beyond 1,000 loci. This pattern contrasts sharply with studies relying on exon or anchored tag data, where topological convergence can typically be achieved with comparatively few loci (Ruane *et al.*, 2015; Portik *et al.*, 2016). This harkens back to the comparatively low variability of UCEs and potentially high levels of ILS in this study system.

*Carphodactylidae*

Our dataset contained 24 of 29 carphodactylid species (83%) and all recognized genera. Both our maximum likelihood and ASTRAL trees recovered three well-supported major clades, presenting the leaf-tail *Orraya* as sister to the *Carphodactylus* – knob-tail and leaf-tail clades. The placement of *Orraya* has been historically problematic as the genus is superficially similar to the leaf-tails of the genera *Saltuarius* and *Phyllurus* and was initially placed within the former based on morphology (Couper *et al.*, 1993; Couper *et al.*, 2000). Due to the low quality of the starting tissue, we were only able to recover 556 loci for this enigmatic genus. However, we are confident in its placement at the base of the carphodactylid tree as investigation of the most variable loci for which we have data for this species also place it there, suggesting that this position is not an artifact of missing data. This arrangement contrasts sharply with most molecular datasets, which typically find *Orraya* as sister to the *Carphodactylus* – knob-tail clade (Pyron *et al.*, 2013b; Brennan & Oliver, 2017).

The placement of *Carphodactylus* at the base of the knob-tail clade is consistent with nearly all molecular studies investigating the phylogenetics of this clade with the exception of Oliver and Bauer (2011). We recover the same biome related clades within *Nephrurus* as Oliver and Bauer (2011), with strong support for the basal-most lineages being predominately tropical and temperate while the remainder are restricted to the arid zone. Both our concatenated and coalescent trees conflict with the findings of Oliver and Bauer (2011) and Brennan and Oliver (2017) for the interrelationships of the arid clade (*N. levis*, *N. stellatus*, *N. vertabralis*, and *N. laevissmus*). The ASTRAL topology is somewhat biogeographically concordant with biome transitions, with *N. stellatus* representing the southeast-most lineage with a grade leading to the northwest-most arid lineages (*N. laevissmus* + *N. levis*). We find the same relationships within *Saltuarius* as has a previous multilocus study (Brennan & Oliver, 2017). Our reconstruction for *Orraya* as sister to the remaining carphodactylids posits two scenarios for the evolution of the leaf-tail phenotype. One suggests that the leaf-tail morph was the ancestral form for carphodactylids and that the *Carphodactylus* knob-tail clade subsequently lost this trait. Alternatively, the leaf-tail morphology evolved twice independently within the Carphodactylidae. We prefer the former as there is a

potential morphological grade in the *Carphodactylus* – knob-tail clade, where *Carphodactylus* retains a long, albeit turnip-shaped tail. *Uvidicolus* and *Underwoodisaurus* have flattened tails that are highly ornamented while the greatest morphological derivation occurs in *Nephrurus*, particularly in the *N. sheai – N. asper* group, in which the tail has been reduced to a button.

*Pygopodidae*

Phylogenetic relationships within the Pygopodidae have historically been problematic when relying on morphology and molecules, but there is general consensus that *Delma* is either sister to the remaining genera or very close to the root (Kluge, 1976; Jennings *et al.*, 2003). We were only able to sample 28 of the 44 recognized pygopodid species (63.6%) and were unable to sample *Ophidiocephalus*, an unusual genus with extreme adaptations for a fossorial lifestyle. Our findings agree with those of Jennings *et al.* (2003), Brennan *et al.* (2016), and Brennan and Oliver (2017) in terms of *Delma* being recovered as sister to the remaining genera. Our concatenated and coalescent trees converge on identical topologies for *Delma* with the exception of the placement of *D. nasuta* and *D. grayii*. The likelihood tree finds high support for *D. grayii* being sister to *D. nasuta* + *D. haroldi – D. butleri*, whereas the ASTRAL topology finds low support for *D. nasuta* being sister *D. grayii* and a well-supported *D. haroldi – D. butleri* clade. The ASTRAL topology is somewhat congruent combined mitochondrial-nuclear topology of Brennan *et al.* (2016) and the low support from the multispecies coalescent is indicative of high levels of gene tree discordance. Though ASTRAL and the majority of multispecies coalescent methods assume that ILS is the primary source of species tree – gene tree discordance, we attribute the discordance noted here to ancient interspecific hybridization within *Delma*. This pattern fits well with the findings of Brennan *et al.* (2016) which suggest ancient mitochondrial introgression in the *D. fraseri – D. haroldi* clade. It stands to reason that some proportion of the loci in this phylogenomic dataset bear signatures of these historical introgression events, leading to conflicting gene tree – species tree topologies and the low statistical support present in the latter.

The intergeneric relationships within the *Aprasia – Pygopus* clade are entirely novel, with *Aprasia* receiving unambiguous support as sister to the remaining genera as opposed to being closer to *Pletholax* or *Paradelma* + *Pygopus* (Jennings *et al.*, 2003; Brennan *et al.*, 2016; Brennan & Oliver, 2017). Evans (2008) notes that *Delma* possesses the least derived cranial morphology of all the pygopodid genera, an observation that fits well with our new intergeneric reconstruction. Members of the *Aprasia – Pygopus* clade demonstrate some of the most extreme cranial specializations seen in gekkotans, with *Lialis* being highly mesokinetic and *Pletholax* and *Aprasia* being head-first burrowers. Both the concatenated and coalescent trees find unambiguous support for *Aprasia* being sister to the other genera and the former received high support for *Pletholax* being sister to *Lialis* and *Paradelma* + *Pygopus*. ASTRAL receives comparatively low support for the same placement of *Pletholax* at the base of this clade (lpp = 0.65), suggesting high levels of gene tree incongruence for this node. Kluge (1976) proposed a close relationship between *Aprasia, Pletholax*, and *Lialis* based on morphology alone. In terms of the former two genera, this arrangement is likely due to homoplasy associated with fossoriality and the general reduction of kinetic properties of the skull. Our topology suggests that fossoriality evolved multiple times within this clade, once within *Aprasia* and again in *Pletholax*. Though it is possible that it evolved once and the ancestor of *Lialis* and *Paradelma* + *Pygopus* reversed back to grass-swimming. Distinguishing these two scenarios is complicated by our inability to include *Ophidiocephalus* in our dataset, though it is highly probably that this enigmatic genus falls out somewhere within this clade (Gamble *et al.*, 2015; Brennan *et al.*, 2016; Brennan & Oliver, 2017).

*Higher-Level Relationships within the Diplodactylidae*

Our results are largely congruent with previous studies regarding relationships among the major diplodactyloid clades, including the finding that the two Tasmantis clades arose independently from unrelated Australian lineages (Nielsen *et al.*, 2011; Skipwith *et al.*, 2016). The Australian genus *Crenadactylus* represents an ancient sister taxon of the New Zealand – core Australian clade (Oliver *et al.*, 2009; Oliver & Sanders, 2009). While we sampled less than half of the species within *Crenadactylus*, we find strong support for the two monsoonal tropic species (*C. rostralis* and *C. naso*) forming a clade relative to the arid savannah inhabiting *C. occellatus* (Doughty et al., 2016).

*Pseudothecadactylus and New Caledonia*

We find *Pseudothecadactylus* to be sister to the ecologically diverse New Caledonian clade, though our ASTRAL tree received low support for this relationship (lpp = 0.91) hinting at some level of gene tree heterogeneity. The union of these two clades is consistent with most molecular phylogenies and agrees with a number of shared morphological traits suggesting a close relationship (Bauer, 1990; Nielsen *et al.*, 2011; Oliver *et al.*, 2014b; Skipwith *et al.*, 2016). Relationships within *Pseudothecadactylus* have been historically problematic, with most molecular datasets finding the phenotypically similar *P. cavaticus* and *P. lindneri* to be sister taxa with varying levels of statistical support (Oliver *et al.*, 2014b; Brennan & Oliver, 2017). In contrast, we find *P. australis* and *P. cavaticus* to be sister taxa despite the former possessing a rather aberrant phenotype in comparison to the other two species. Using morphology, Bauer (1990) placed *Pseudothecadactylus* in *Rhacodactylus* sensu lato, deep within the New Caledonian assemblage, with *P. australis* having the most shared derived characters with members of that genus. No molecular phylogeny has found *Pseudothecadactylus* to be imbedded within the New Caledonian clade, but we posit that *P. australis* independently transitioned to an arboreal lifestyle. This transition in turn led to significant convergence with the New Caledonian forms, as evidenced by the osteology of the two groups, while the two remaining species retained characteristics suited for more rupicolous ecologies.

Estimation of interspecific relationships within the New Caledonian clade has also been historically challenging. Short internodes are present throughout the tree and are even prevalent in the mitochondrial phylogeny, obscuring most intergeneric relationships (Bauer *et al.*, 2004; Bauer *et al.*, 2006, 2009; Bauer *et al.*, 2012; Skipwith *et al.*, 2014). Our phylogenomic dataset largely resolves all major conflicts and poorly supported nodes detected in previous multilocus studies (Skipwith *et al.*, 2016). The concatenated UCE topology is similar to the concatenated nuclear topology of Skipwith *et al.* (2016), in which *Correlophus* was recovered as sister to *Eurydactylodes* with high support, and with weak support for the former being allied to *Rhacodactylus*. Furthermore, this study highlights the close affinity between *Dierogekko* and *Oedodera*. However, neither our concatenated or coalescent trees find any association between *Mniarogekko* and *Eurydactylodes*. The sister relationship between these two morphologically divergent genera in prior studies appears to be driven entirely by the mitochondrial genome and may be evidence of an ancient introgressive hybridization event between the ancestor of *Eurydactylodes* and *Rhacodactylus*. We find strong support for *Mniarogekko* as the sister to the morphologically similar *Rhacodactylus trachyrhynchus* and *R. trachycephalus*, with *R. auriculatus* and *R. leachianus* forming a successive grade at the base. Morphologically, *Eurydactylodes* is most similar to *Rhacodactylus* sensu lato (including *Mniarogekko* and *Correlophus*), suggesting an interesting pattern of body-size evolution. Our species tree topology

and that of Skipwith *et al.* (2016) suggest that the evolution of true gigantism evolved once, whereas the concatenated trees of both studies imply that high levels of morphological homoplasy are present in the New Caledonian clade. Alternatively, it is possible *Eurydactylodes* and *Correlophus* represent another introgression event, albeit one with no signature in the mitogenome. Given the young age of this clade and overall lack on genealogical congruence, ILS is likely a major cause of topological incongruence.

Skipwith *et al.* (2016) and Bauer *et al.* (2012) found *Oedodera* and *Dierogekko* to form a clade at the base of New Caledonian radiation. Both our concatenated and coalescent trees find a similarly close union of these two genera, though this clade is in turn deeply nested within the New Caledonian clade. Concatenation finds overwhelming support for uniting both genera with *Bavayia* and *Paniegekko*, forming a clade of small-bodied geckos. This fits well with the osteology and certain scalation characters uniting some of these taxa (Bauer, 1990; Bauer & Sadlier, 2000). However, our coalescent topology differs markedly from these prior studies in the placements of *Paniegekko* and *Bavayia*. As opposed to the former genus being allied to *Dierogekko* as in the concatenated analyses, we find it to be sister *Bavayia*, the genus to which it was originally assigned (Bauer *et al.*, 2000). If our coalescent tree is accurate, we propose that large body size (> 70 mm SVL) evolved multiple times within the New Caledonian radiation. The giants formerly assigned to *Rhacodactylus* may represent a single transition to true gigantism (> 130 mm SVL), *Paniegekko* may represent a shift to relatively large body-size (> 75 mm SVL), while members of the *Bavayia cyclura* group (> 70 mm SVL) may represent another.

*New Zealand*

The New Zealand diplodactylid clade shares a number of similarities to the New Caledonian assemblage that led several previous authors to propose that they were sister taxa (Kluge, 1983, 1987; Chambers *et al.*, 2001) or even that the New Caledonian clade was derived from within the New Zealand group (Bauer, 1990). Both clades and *Pseudothecadactylus* share a number of osteological features as well possessing prehensile tails bearing distal adhesive lamellae. However, recent molecular data unambiguously place this clade closer to the core Australian diplodactylid clade (all Australian genera excluding *Pseudothecadactylus* and *Crenadactylus*) (Nielsen *et al.*, 2011; Skipwith *et al.*, 2016). We find a pattern of intergeneric relationships broadly similar to those of Nielsen *et al.* (2011), with a broad-toed clade containing the genera *Woodworthia* and *Hoplodactylus* and a narrow-toed clade comprise of *Mokopirirakau*, *Dactylocnemis*, *Tukutuku*, *Toropuku*, and *Naultinus*. However, we find that the giant *Hoplodactylus duvaucelii* is sister to *Woodworthia maculata*, rendering *Woodworthia* paraphyletic. *Hoplodactylus duvaucelii* represents the largest extant member of the New Zealand lineage with a maximum SVL of 160 mm, substantially larger than other members of the clade of which the next largest species only attains an SVL of 95 mm. *Hoplodactylus* being embedded within *Woodworthia* implies that gigantism was attained very rabidly in a clade that is otherwise rather homogenous in body-size (60-95 mm SVL).

We also find that within the narrow-toed clade, *Toropuku* is sister to the diurnal and ornately colored members of *Naultinus*, a novel finding. The interrelationships between *Toropuku*, *Tukutuku*, and *Naultinus* were historically unresolved (Nielsen *et al.*, 2011; Gamble *et al.*, 2015). Our new phylogeny suggests that ornate patterning, which is present in all of the narrow-toed genera, evolved prior to diurnality. If this is true, this trend would be unique among insular diplodactylids, as the only other diurnal genus, *Eurydactylodes*, relies heavily on crypsis and is comparatively somber in color (Bauer *et al.*, 2009).

*Core Australian Diplodactylids*

As with previous studies, we found it difficult to resolve the base of the core Australian diplodactylid clade (Oliver *et al.*, 2012; Nielsen *et al.*, 2016). All of our analyses place *Strophurus* as sister to the *Lucasium* + *Rhynchoedura* – *Diplodactylus* clade, an arrangement largely in agreement with Oliver *et al.* (2012). Both concatenated and coalescent analyses find low support for *Oedura* being sister to this clade (bootstrap = 68, lpp = 0.67). We find no support for a monophyletic *Oedura* sensu lato, as the concatenated topology places *Nebulifera* and *Amalosia* sister to all the core Australian genera while *Hesperoedura* is sister to the *Strophurus* – *Lucasium/Diplodactylus* clade. The ASTRAL tree alternatively places *Hesperoedura* as sister to the *Amalosia* – *Nebulifera* group with low support (lpp = 0.46). This finding is consistent with the hypothesis proposed by Oliver *et al.* (2012) that representatives of *Oedura* sensu lato represent a plesiomorphic grade. Nearly all species assigned to these genera are arboreal generalists, the primary exceptions being the *O. gracilis* – *O. fillicipoda* and monsoonal tropical *Oedura marmorata* species complex. Our finding that *Amalosia* is paraphyletic relative to *Nebulifera* is novel as most other studies have failed to sample *A. jacovae*. All species currently assigned to *Amalosia* possess tails that are rounded in cross-section, while the tail of *Nebulifera* is dorsoventrally flattened. The presence of a dorsoventrally flattened tail in *Nebulifera* suggests that this trait has evolved at least four times independently within *Oedura* sensu lato. Once in the *Amalosia*/*Nebulifera* group, then three times in the ecologically diverse *Oedura* (*O. castelnaui*, and the undescribed 'Kimberley *Oedura*', and 'Top End *Oedura*'), and potentially a fifth time in *Hesperoedura* if referring to the concatenated tree.

While relationships within *Lucasium* are identical between the concatenated and coalescent trees, there is strong topological discordance within *Strophurus* and *Diplodactylus*. *Strophurus* can be split into a longitudinally-striped small-bodied clade of graminicolous species and a clade of marble-patterned large-bodied scansorial species. We find discordance in the placement of *S. wilsoni*, a small species sharing a number of features with both of these clades, rendering its placement historically problematic (Nielsen *et al.*, 2016; Brennan & Oliver, 2017). ASTRAL places *S. wilsoni* as sister to *S. elderi* and *S. michaelseni* with low support (lpp = 0.56) and we attribute its placement in the concatenated tree at the base of the large-bodied scansorial clade to long-branch attraction. If the coalescent topology is accurate, it implies that a general scansorial lifestyle evolved twice independently in *Strophurus*, whereas the highly-specialized twig anole-like ecology of the graminicolous taxa is ancestral for the genus. While our topology differs at nearly all nodes with that of Nielsen *et al.* (2016), this hypothesis agrees with their ancestral state reconstructions of the ecology of *Strophurus*. All of our analyses yield relationships within *Diplodactylus* that conflict strongly with previous phylogenetic estimates of the genus (Oliver *et al.*, 2007b; Oliver *et al.*, 2007a; Doughty *et al.*, 2008; Hutchinson *et al.*, 2009; Oliver *et al.*, 2009; Brennan & Oliver, 2017). All members of this genus are small, largely terrestrial species occurring mainly in the Australian arid zone specializing on small invertebrate prey. Several species appear to have transitioned to eating small, swarming insects (*D. pulcher*, *D. conspicillatus*, *D. galaxias*, *D. klugei*, and *D. savagei*) and possess particularly small heads with pointed snouts reminiscent of *Rhynchoedura* and some *Lucasium* species. As this broad ecomorphological group crops up several times in the *Diplodactylus* – *Lucasium* + *Rhynchoedura* group, we propose that it represents independent exaptations of the established small-headed phenotype to exploit termites and other insects.

*Divergence Times and Biogeographic Implications*

Our divergence time estimates for diplodactyloids are broadly concordant with previous studies, although deeper nodes are on the whole older than previously proposed ages (Lee *et al.*, 2009a; Oliver & Sanders, 2009; Oliver *et al.*, 2010a; Nielsen *et al.*, 2011; Brennan *et al.*, 2016; Nielsen *et al.*, 2016; Skipwith *et al.*, 2016; Brennan & Oliver, 2017). This may be an artifact of these previous analyses relying on BEAST rather than MCMCTREE. While both methods are Bayesian and posterior date estimates are heavily influenced by prior choice for node calibrations, the two differ in how fossil constraints are treated as time priors. In order to simultaneously estimate topology and divergence times, BEAST multiplies the calibration densities by the tree prior which can result in the calibration priors violating the fossil constraints on which they are based (Heled & Drummond, 2012). MCMCTREE does not infer topology and so is not subject to the same potential pitfall. Our finding of comparatively old crown ages for diplodactyloids agrees with the findings of Warnock *et al.* (2015), whereas our BEAST analyses typically found young dates in comparison to MCMCTREE.

MCMCTREE places the gekkonoid – diplodactyloid divergence somewhere between the late-early Jurassic and late-early Cretaceous (181-118 My). This wide range predates the breakup of west-east Gondwana and most estimates for crown age Gekkota (Oliver & Sanders, 2009). However, our divergence time estimates place the crown age of diplodactyloids in either the late Campanian or the very end of the Cretaceous (86-65 My), which broadly overlaps the breakup of Australia and Antarctica (~80 My). This timing suggests that while stem gekkonoids and diplodactyloids must have been present prior to the Gondwanan breakup, both clades experienced extensive extinction prior to the KT boundary. We propose that diplodactyloids experienced ecological release after Australia split from Antarctica, as this clade likely represents a combination of adaptive and non-adaptive lineages.

The time scale for divergence we found for carphodactylids suggests a strong pattern of ancestrally tropical and temperate habitats for all clades with subsequent invasion of the arid zone by the knob-tail clade. Our topology and timing estimates suggest that this happened at least twice, once with *Underwoodisaurus* and the 'smooth knob-tails' identified by Oliver and Bauer (2011). However, it is possible that the smooth knob-tails were isolated in the arid zone due to vicariance, as the formation of this biome (~15 My) overlaps with the estimated crown age of this clade (Byrne *et al.*, 2008). We propose a similar tropical/temperate origin followed by numerous invasions of the arid zone for pygopodids. Invasions of the arid zone by these two families during post-Miocene cooling agrees largely with the findings of Brennan and Oliver (2017). Our placement of the *Lialis burtonis – L. jicarii* split in the early – mid Miocene necessitates the need to invoke extinction on the *L. jicarii* lineage on mainland Australia. Given the old divergence of these two taxa, we propose that *Lialis* dispersed to New Guinea when the two landmasses were contiguous prior to the end of the last glacial maxima. Patterns within the core Australian diplodactylids suggests that each of the major genera have independently colonized the arid zone, some of which have back-colonized the relictual tropical and mesic regions bordering this large biome. Brennan and Oliver (2017) used a taxonomically more complete but comparatively poorly resolved phylogeny to suggest that the arid zone has played a major role as a source of diversity for diplodactylids and our tree appears to corroborate this hypothesis.

Both New Zealand and New Caledonia are remnants of the mostly sunken landmass Tasmantis, a subcontinent that was formerly part of eastern Gondwana. Tasmantis split from Australia during the late Cretaceous, leading many authors to propose that lineages endemic to this region were relicts from this ancient vicariance event (Bauer, 1990; Chambers *et al.*, 2001).

Within the diplodactylids, we find dates that suggest late Paleogene and early Neogene dispersals to New Zealand and New Caledonia respectively. The recovery of splits from their respective sister taxa and crown ages that are vastly younger than the Australia – Tasmantis split agrees with all molecular divergence dating studies involving these two clades (Nielsen *et al.*, 2011; Skipwith *et al.*, 2016). Our estimates for the crown age of the New Caledonian clade are concordant with coalescent dates recovered by Skipwith *et al.* (2016). These estimates make the New Caledonian clade far younger than most animal taxa on the archipelago, though all endemic taxa investigated to date appear to be the result of Miocene-age over-water dispersals (Smith *et al.*, 2007; Grandcolas *et al.*, 2008; Murienne *et al.*, 2008; Chapple *et al.*, 2009; Murienne, 2009; Espeland & Johanson, 2010; Espeland & Murienne, 2011). In contrast to Nielsen *et al.* (2011) who found the crown age of the New Zealand clade to be late Oligocene to mid-Miocene (33.8 – 15.5 My), we find a mid-Eocene to late Oligocene time of divergence (41 – 24 My). Both timing schemes are congruent with there being no geological evidence for exposed land area during the Oligocene drowning period that rendered most if not all of Tasmantis submerged (Landis *et al.*, 2008). Despite being somewhat older than the New Caledonian clade, the New Zealand diplodactylids are remarkably conservative in form and habit. All of the New Zealand genera are viviparous, a trait that has only evolved once elsewhere within Gekkota, and this is likely an adaptation to the colder climate of the region. Given the relative climatic stability of New Zealand and the low temperatures of the region, it is likely that the New Zealand clade has been unable to explore the range of niches occupied by the New Caledonian and core Australian diplodactylids (Nielsen *et al.*, 2011). It is also probable that this clade has not been forced to expand its ecological breadth at a rapid rate as it arrived on New Zealand relatively early, filling the nocturnal lizard niche. The New Caledonian clade, however, stands in stark contrast with a wide array of ecologies having been explored in a substantially shorter time frame. Their late arrival and the subtropical climate of New Caledonia may have facilitated the rapid accumulation of diverse ecologies. The core Australian diplodactylids are far older than either Tasmantis lineage, and occupy a much greater breadth of ecomorphological space. The older age of this clade in combination with climatic instability of Australia during the Neogene likely presented opportunities for ecological expansion.

## Literature Cited


Arnold, E.N. & Poinar, G. (2008) A 100 million year old gecko with sophisticated adhesive toe pads, preserved in amber from Myanmar. *Zootaxa*, **1847**, 62-68.

Bankevich, A., Nurk, S., Antipov, D., Gurevich, A.A., Dvorkin, M., Kulikov, A.S., Lesin, V.M., Nikolenko, S.I., Pham, S., Prjibelski, A.D., Pyshkin, A.V., Sirotkin, A.V., Vyahhi, N., Tesler, G., Alekseyev, M.A. & Pevzner, P.A. (2012) SPAdes: A New Genome Assembly Algorithm and Its Applications to Single-Cell Sequencing. *Journal of Computational Biology*, **19**, 455-477.

Bauer, A.M. (1990) Phylogenetic systematics and biogeography of the Carphodactylini (Reptilia: Gekkonidae). *Bonner Zoologische Monographien*, **30**, 1-218.

Bauer, A.M. & Sadlier, R.A. (2000) *The Herpetofauna of New Caledonia*. The Society for the Study of Amphibians and Reptiles, in cooperation with the Institut de recherche pour le développement, Ithaca, NY.

Bauer, A.M., Jones, J.P.G. & Sadlier, R.A. (2000) A new high-elevation *Bavayia* (Reptilia: Squamata: Diplodactylidae) from northeastern New Caledonia. *Pacific Science*, **54**, 63-69.

Bauer, A.M., Jackman, T.R. & Kiebish, M. (2004) Molecular systematics of the New Caledonian geckos *Rhacodactylus* and *Eurydactylodes* (Squamata: Diplodactylidae). *New Zealand Journal of Zoology*, **31**, 100.

Bauer, A.M., Bohme, W. & Weitschat, W. (2005) An Early Eocene gecko from Baltic amber and its implications for the evolution of gecko adhesion. *Journal of Zoology*, **265**, 327-332.

Bauer, A.M., Jackman, T., Sadlier, R.A. & Whitaker, A.H. (2006) A new genus and species of diplodactylid gecko (Reptilia: Squamata: Diplodactylidae) from northwestern New Caledonia. *Pacific Science*, **60**, 125-135.

Bauer, A.M., Jackman, T., Sadlier, R.A. & Whitaker, A.H. (2009) Review and phylogeny of the New Caledonian diplodactylid genus *Eurydactylodes* Wermuth, 1965, with the description of a new species. *Zoologia Neocaledonica 7:Mémoires du Muséum National d'Histoire Naturelle* **198**, 13-36.

Bauer, A.M., Jackman, T., Sadlier, R. & Whitaker, A. (2012) Revision of the giant geckos of New Caledonia (Reptilia: Diplodactylidae: *Rhacodactylus*) *Zootaxa*, **3404**, 1-52.

Bi, K., Vanderpool, D., Singhal, S., Linderoth, T., Moritz, C. & Good, J.M. (2012) Transcriptome-based exon capture enables highly cost-effective comparative genomic data collection at moderate evolutionary scales. *Bmc Genomics*, **13**

Bi, K., Linderoth, T., Vanderpool, D., Good, J.M., Nielsen, R. & Moritz, C. (2013) Unlocking the vault: next-generation museum population genomics. *Molecular Ecology*, **22**, 6018-6032.

Bolger, A.M., Lohse, M. & Usadel, B. (2014) Trimmomatic: a flexible trimmer for Illumina sequence data. *Bioinformatics*, **30**, 2114-2120.

Brennan, I.G. & Oliver, P.M. (2017) Mass turnover and recovery dynamics of a diverse Australian continental radiation. *Evolution*, n/a-n/a.

Brennan, I.G., Bauer, A.M. & Jackman, T.R. (2016) Mitochondrial introgression via ancient hybridization, and systematics of the Australian endemic pygopodid gecko genus *Delma*. *Molecular Phylogenetics and Evolution*, **94**, 577-590.

Byrne, M., Yeates, D.K., Joseph, L., Kearney, M., Bowler, J., Williams, M.A.J., Cooper, S., Donnellan, S.C., Keogh, J.S., Leys, R., Melville, J., Murphy, D.J., Porch, N. & Wyrwoll, K.H. (2008) Birth of a biome: insights into the assembly and maintenance of the Australian arid zone biota. *Molecular Ecology*, **17**, 4398-4417.

Capella-Gutierrez, S., Silla-Martinez, J.M. & Gabaldon, T. (2009) trimAl: a tool for automated alignment trimming in large-scale phylogenetic analyses. *Bioinformatics*, **25**, 1972-1973.

Chambers, G.K., Boon, W.M., Buckley, T.R. & Hitchmough, R.A. (2001) Using molecular methods to understand the Gondwanan affinities of the New Zealand biota: three case studies. *Australian Journal of Botany*, **49**, 377-387.

Chapple, D.G., Ritchie, P.A. & Daugherty, C.H. (2009) Origin, diversification, and systematics of the New Zealand skink fauna (Reptilia: Scincidae). *Molecular Phylogenetics and Evolution*, **52**, 470-487.

Couper, P.J., Covacevich, J.A. & Moritz, C. (1993) A review of the leaf-tailed geckos endemic to eastern Australia: a new genus, four new species, and other new data. *Memoirs of the Queensland Museum*, **34**, 95-124.

Couper, P.J., Schneider, C.J., Hoskin, C.J. & Covacevich, J.A. (2000) Australian leaf-tailed geckos: phylogeny, a new genus, two new species and other new data. *Memoirs of the Queensland Museum*, **45**, 253-265.

Crawford, N.G., Faircloth, B.C., McCormack, J.E., Brumfield, R.T., Winker, K. & Glenn, T.C. (2012) More than 1000 ultraconserved elements provide evidence that turtles are the sister group of archosaurs. *Biology Letters*, **8**, 783-786.

Daza, J.D., Bauer, A.M. & Snively, E. (2013) *Gobekko cretacicus* (Reptilia: Squamata) and its bearing on the interpretation of gekkotan affinities. *Zoological Journal of the Linnean Society*, **167**, 430-448.

Daza, J.D., Bauer, A.M. & Snively, E.D. (2014) On the Fossil Record of the Gekkota. *Anatomical Record-Advances in Integrative Anatomy and Evolutionary Biology*, **297**, 433-462.

Donnellan, S.C., Hutchinson, M.N. & Saint, K.M. (1999) Molecular evidence for the phylogeny of Australian gekkonoid lizards. *Biological Journal of the Linnean Society*, **67**, 97-118.

Doughty, P., Oliver, P. & Adams, M. (2008) Systematics of stone geckos in the genus *Diplodactylus* (Reptilia: Diplodactylidae) from northwestern Australia, with a description of a new species from the northwest Cape, Western Australia. *Records of the Western Australian Museum*, **24**, 247-265.

Doughty, P., Ellis, R.J. & Oliver, P.M. (2016) Many things come in small packages: Revision of the clawless geckos (*Crenadactylus*: Diplodactylidae) of Australia. *Zootaxa*, **4168**, 239-278.

Doughty, P., Palmer, R., Sistrom, M., Bauer, A. & Donnellan, S. (2012) Two new species of *Gehyra* (Squamata: Gekkonidae) geckos from the north-west Kimberley region of Western Australia. *Records of the Western Australian Museum*, **27**, 117-134.

Drummond, A.J. & Rambaut, A. (2007) BEAST: Bayesian evolutionary analysis by sampling trees. *BMC Evolutionary Biology*, **7**, 214.

Edwards, S.V. (2009) Is a new and general theory of molecular systematics emerging? *Evolution*, **63**, 1-19.

Edwards, S.V., Xi, Z., Janke, A., Faircloth, B.C., McCormack, J.E., Glenn, T.C., Zhong, B., Wu, S., Lemmon, E.M., Lemmon, A.R., Leache, A.D., Liu, L. & Davis, C.C. (2016) Implementing and testing the multispecies coalescent model: A valuable paradigm for phylogenomics. *Molecular Phylogenetics and Evolution*, **94**, 447-62.

Espeland, M. & Johanson, K.A. (2010) The effect of environmental diversification on species diversification in New Caledonian caddisflies (Insecta: Trichoptera: Hydropsychidae). *Journal of Biogeography*, **37**, 879-890.

Espeland, M. & Murienne, J. (2011) Diversity dynamics in New Caledonia: towards the end of the museum model? *BMC Evolutionary Biology*, **11**, 254.

Evans, S.E. (2003) At the feet of the dinosaurs: the early history and radiation of lizards. *Biological Reviews*, **78**, 513-551.

Evans, S.E. (2008) The skull of lizards and tuatara. *Biology of the Reptilia: the Skull of Lepidosauria* (ed. by C. Gans, A.S. Gaunt and K. Adler), pp. 1-349. Society for the Study of Amphibians and Reptiles, Ithaca, New York, USA.

Faircloth, B.C., McCormack, J.E., Crawford, N.G., Harvey, M.G., Brumfield, R.T. & Glenn, T.C. (2012) Ultraconserved Elements Anchor Thousands of Genetic Markers Spanning Multiple Evolutionary Timescales. *Systematic Biology*, **61**, 717-726.

Feng, J., Han, D., Bauer, A.M. & Zhou, K. (2007) Interrelationships among gekkonid geckos inferred from mitochondrial and nuclear gene sequences. *Zoological Science*, **24**, 656-665.

Flecks, M., Schmitz, A., Bohme, W., Henkel, F.W. & Ineich, I. (2012) A new species of *Gehyra* Gray, 1834 (Squamata, Gekkonidae) from the Loyalty Islands and Vanuatu, and phylogenetic relationships in the genus Gehyra in Melanesia. *Zoosystema*, **34**, 203-221.

Fujita, M.K., McGuire, J.A., Donnellan, S.C. & Moritz, C. (2010) Diversification and persistence at the arid-monsoonal interface: Australia-wide biogeography of the Bynoe's gecko (*Heteronotia binoei*; Gekkoninae). *Evolution*, **64**, 2293-2314.

Gamble, T., Bauer, A.M., Greenbaum, E. & Jackman, T.R. (2008a) Evidence for Gondwanan vicariance in an ancient clade of gecko lizards. *Journal of Biogeography*, **35**, 88-104.

Gamble, T., Bauer, A.M., Greenbaum, E. & Jackman, T.R. (2008b) Out of the blue: a novel, trans-Atlantic clade of geckos (Gekkota, Squamata). *Zoologica Scripta*, **37**, 355-366.

Gamble, T., Greenbaum, E., Jackman, T.R. & Bauer, A.M. (2015) Into the light: diurnality has evolved multiple times in geckos. *Biological Journal of the Linnean Society*, **115**, 896-910.

Gamble, T., Greenbaum, E., Jackman, T., Russell, A.P. & Bauer, A.M. (2012) Repeated Origin and Loss of Adhesive Toepads in geckos. *PLoS ONE*, **7**, e39429.

Gamble, T., Bauer, A.M., Colli, G.R., Greenbaum, E., Jackman, T.R., Vitt, L.J. & Simons, A.M. (2011) Coming to America: multiple origins of New World geckos. *Journal of Evolutionary Biology*, **24**, 231-244.

Garcia-Porta, J. & Ord, T.J. (2013) Key innovations and island colonization as engines of evolutionary diversification: a comparative test with the Australasian diplodactyloid geckos. *Journal of Evolutionary Biology*, **26**, 2662-2680.

Grandcolas, P., Murienne, J., Robillard, T., Desutter-Grandcolas, L., Jourdan, H., Guilbert, E. & Deharveng, L. (2008) New Caledonia: A very old Darwinian island? *Philosophical Transactions of the Royal Society of London B Biological Sciences*, **363**, 3309-3317.

Han, D., Zhou, K. & Bauer, A.M. (2004) Phylogenetic relationships among gekkotan lizards inferred from C-mos nuclear DNA sequences and a new classification of the Gekkota. *Biological Journal of the Linnean Society*, **83**, 353-368.

Hedges, B.S. & Vidal, N. (2009) Lizards, snakes, and amphisbaenians. *The Timetree of Life* (ed. by B.S. Hedges and J.D. Kumar), pp. 383-389. Oxford University Press, New York.

Heinicke, M.P., Greenbaum, E., Jackman, T.R. & Bauer, A.M. (2011) Phylogeny of a trans-Wallacean radiation (Squamata, Gekkonidae, *Gehyra*) supports a single early colonization of Australia. *Zoologica Scripta*, **40**, 584-602.

Heled, J. & Drummond, A.J. (2010) Bayesian inference of species trees from multilocus data. *Molecular Biology and Evolution*, **27**, 570-580.

Heled, J. & Drummond, A.J. (2012) Calibrated Tree Priors for Relaxed Phylogenetics and Divergence Time Estimation. *Systematic Biology*, **61**, 138-149.

Horner, P. (2005) *Gehyra koira* sp. nov. (Reptilia: Gekkonidae), a new species of lizard with two allopatric subspecies from the Ord-Victoria region of north-western Australia and a key to the Gehyra australis species complex. *Beagle*, **21**, 165-174.

Hugall, A.F., Foster, R. & Lee, M.S.Y. (2007) Calibration choice, rate smoothing, and the pattern of tetrapod diversification according to the long nuclear gene RAG-1. *Systematic Biology*, **56**, 543-563.

Hutchinson, M.N., Doughty, P. & Oliver, P.M. (2009) Taxonomic revision of the stone geckos (Squamata: Diplodactylidae: *Diplodactylus*) of southern Australia. *Zootaxa*, 25-46.

Hutchinson, M.N., Skinner, A. & Lee, M.S.Y. (2012) *Tikiguania* and the antiquity of squamate reptiles (lizards and snakes). *Biology Letters*,

Jennings, W.B., Pianka, E.R. & Donnellan, S. (2003) Systematics of the lizard family pygopodidae with implications for the diversification of Australian temperate biotas. *Systematic Biology*, **52**, 757-780.

Katoh, K. & Standley, D.M. (2013) MAFFT Multiple Sequence Alignment Software Version 7: Improvements in Performance and Usability. *Molecular Biology and Evolution*, **30**, 772-780.

Kluge, A.G. (1967) Higher taxonomic categories of gekkonid lizards and their evolution. *Bulletin of the American Museum of Natural History*, **135**, 1-59.

Kluge, A.G. (1976) Phylogenetic relationships in the lizard family Pygopodidae: An evaluation of theory, methods and data. *Miscellaneous Publications Museum of Zoology University of Michigan*, **147**, 1-54.

Kluge, A.G. (1983) Cladistic relationships among gekkonid lizards. *Copeia*, **1983**, 465-475.

Kluge, A.G. (1987) Cladistic relationships in the Gekkonoidea (Squamata, Sauria). *Miscellaneous Publications Museum of Zoology University of Michigan*, i-iv, 1-54.

Landis, C.A., Campbell, H.J., Begg, J.G., Mildenhall, D.C., Paterson, A.M. & Trewick, S.A. (2008) The Waipounamu Erosion Surface: questioning the antiquity of the New Zealand land surface and terrestrial fauna and flora. *Geological Magazine*, **145**, 173-197.

Lanfear, R., Calcott, B., Ho, S.Y.W. & Guindon, S. (2012) PartitionFinder: Combined Selection of Partitioning Schemes and Substitution Models for Phylogenetic Analyses. *Molecular Biology and Evolution*, **29**, 1695-1701.

Langmead, B. & Salzberg, S.L. (2012) Fast gapped-read alignment with Bowtie 2. *Nature Methods*, **9**, 357-U54.

Lee, M.S.Y., Oliver, P.M. & Hutchinson, M.N. (2009a) Phylogenetic uncertainty and molecular clock calibrations: A case study of legless lizards (Pygopodidae, Gekkota). *Molecular Phylogenetics and Evolution*, **50**, 661-666.

Lee, M.S.Y., Sanders, K.L., King, B. & Palci, A. (2016) Diversification rates and phenotypic evolution in venomous snakes (Elapidae). *Royal Society Open Science*, **3**

Lee, M.S.Y., Hutchinson, M.N., Worthy, T.H., Archer, M., Tennyson, A.J.D., Worthy, J.P. & Scofield, R.P. (2009b) Miocene skinks and geckos reveal long-term conservatism of New Zealand's lizard fauna. *Biology Letters*, **5**, 833-837.

Li, H. & Durbin, R. (2009) Fast and accurate short read alignment with Burrows–Wheeler transform. *Bioinformatics*, **25**, 1754-1760.

Martin, M. (2011) Cutadapt removes adapter sequences from high-throughput sequencing reads. *2011*, **17**

McCormack, J.E., Faircloth, B.C., Crawford, N.G., Adair Gowaty, P., Brumfield, R.T. & Glenn, T.C. (2012) Ultraconserved elements are novel phylogenomic markers that resolve placental mammal phylogeny when combined with species-tree analysis. *Genome Research*, **22**, 746-754.

McCormack, J.E., Harvey, M.G., Faircloth, B.C., Crawford, N.G., Glenn, T.C. & Brumfield, R.T. (2013) A phylogeny of birds based on over 1,500 Loci collected by target enrichment and high-throughput sequencing. *Plos One*, **8**

McKenna, A., Hanna, M., Banks, E., Sivachenko, A., Cibulskis, K., Kernytsky, A., Garimella, K., Altshuler, D., Gabriel, S., Daly, M. & DePristo, M.A. (2010) The Genome Analysis Toolkit: A MapReduce framework for analyzing next-generation DNA sequencing data. *Genome Research*, **20**, 1297-1303.

Meyer, M. & Kircher, M. (2010) Illumina sequencing library preparation for highly multiplexed target capture and sequencing. *Cold Spring Harbor Protocols*, **2010**

Miller, M.A., Pfeiffer, W. & Schwartz, T. (2010) Creating the CIPRES Science Gateway for large phylogenetic trees. *Proceedings of the Gateway Computing Environments Workshop (GCE)* (ed by, pp. 1-8. New Orleans, LA.

Minh, B.Q., Nguyen, M.A.T. & von Haeseler, A. (2013) Ultrafast Approximation for Phylogenetic Bootstrap. *Molecular Biology and Evolution*, **30**, 1188-1195.

Mirarab, S. & Warnow, T. (2015) ASTRAL-II: coalescent-based species tree estimation with many hundreds of taxa and thousands of genes. *Bioinformatics*, **31**, 44-52.

Mirarab, S., Reaz, R., Bayzid, M.S., Zimmermann, T., Swenson, M.S. & Warnow, T. (2014) ASTRAL: genome-scale coalescent-based species tree estimation. *Bioinformatics*, **30**, I541-I548.

Mitchell, K.J., Pratt, R.C., Watson, L.N., Gibb, G.C., Llamas, B., Kasper, M., Edson, J., Hopwood, B., Male, D. & Armstrong, K. (2014) Molecular phylogeny, biogeography, and habitat preference evolution of marsupials. *Molecular Biology and Evolution*, **In press**

Moyle, R.G., Oliveros, C.H., Andersen, M.J., Hosner, P.A., Benz, B.W., Manthey, J.D., Travers, S.L., Brown, R.M. & Faircloth, B.C. (2016) Tectonic collision and uplift of Wallacea triggered the global songbird radiation. *Nature Communications*, **7**, 1-7.

Murienne, J. (2009) Testing biodiversity hypotheses in New Caledonia using phylogenetics. *Journal of Biogeography*, **36**, 1433-1434.

Murienne, J., Pellens, R., Budinoff, R.B., Wheeler, W.C. & Grandcolas, P. (2008) Phylogenetic analysis of the endemic New Caledonian cockroach *Lauraesilpha*. Testing competing hypotheses of diversification. *Cladistics*, **24**, 802-812.

Nguyen, L.T., Schmidt, H.A., von Haeseler, A. & Minh, B.Q. (2015) IQ-TREE: A Fast and Effective Stochastic Algorithm for Estimating Maximum-Likelihood Phylogenies. *Molecular Biology and Evolution*, **32**, 268-274.

Nielsen, S.V., Bauer, A.M., Jackman, T.R., Hitchmough, R.A. & Daugherty, C.H. (2011) New Zealand geckos (Diplodactylidae): Cryptic diversity in a post-Gondwanan lineage with trans-Tasman affinities. *Molecular Phylogenetics and Evolution*, **59**, 1-22.

Nielsen, S.V., Oliver, P.M., Laver, R.J., Bauer, A.M. & Noonan, B.P. (2016) Stripes, jewels and spines: further investigations into the evolution of defensive strategies in a chemically defended gecko radiation (*Strophurus*, Diplodactylidae). *Zoologica Scripta*, **45**, 481-493.

Oliver, P.M. & Sanders, K.L. (2009) Molecular evidence for Gondwanan origins of multiple lineages within a diverse Australasian gecko radiation. *Journal of Biogeography*, **36**, 2044-2055.

Oliver, P.M. & Bauer, A.M. (2011) Systematics and evolution of the Australian knob-tail geckos (*Nephrurus*, Carphodactylidae, Gekkota): Plesiomorphic grades and biome shifts through the Miocene. *Molecular Phylogenetics and Evolution*, **59**, 664-674.

Oliver, P.M. & Doughty, P. (2016) Systematic revision of the marbled velvet geckos (*Oedura marmorata* species complex, Diplodactylidae) from the Australian arid and semi-arid zones. *Zootaxa*, **4088**, 151-176.

Oliver, P.M., Hutchinson, M.N. & Cooper, S.J.B. (2007a) Phylogenetic relationships in the lizard genus *Diplodactylus* Gray and resurrection of *Lucasium* Wermuth (Gekkota, Diplodactylidae). *Australian Journal of Zoology*, **55**, 197-210.

Oliver, P.M., Adams, M. & Doughty, P. (2010a) Molecular evidence for ten species and Oligo-Miocene vicariance within a nominal Australian gecko species (*Crenadactylus ocellatus*, Diplodactylidae). *BMC Evolutionary Biology*, **10**, 386.

Oliver, P.M., Skipwith, P. & Lee, M.S. (2014a) Crossing the line: increasing body size in a trans-Wallacean lizard radiation (*Cyrtodactylus*, Gekkota). *Biology Letters*, **10**, 1-4.

Oliver, P.M., Laver, R.J., Smith, K.L. & Bauer, A.M. (2014b) Long-term persistence and vicariance within the Australian Monsoonal Tropics: the case of the giant cave and tree geckos (*Pseudothecadactylus*). *Australian Journal of Zoology*, **61**, 462-468.

Oliver, P.M., Hugall, A., Adams, M., Cooper, S.J.B. & Hutchinson, M. (2007b) Genetic elucidation of cryptic and ancient diversity in a group of Australian diplodactyline geckos: The *Diplodactylus vittatus* complex. *Molecular Phylogenetics and Evolution*, **44**, 77-88.

Oliver, P.M., Adams, M., Lee, M.S.Y., Hutchinson, M.N. & Doughty, P. (2009) Cryptic diversity in vertebrates: molecular data double estimates of species diversity in a radiation of Australian lizards (*Diplodactylus*, Gekkota). *Proceedings of the Royal Society B-Biological Sciences*, **276**, 2001-2007.

Oliver, P.M., Sistrom, M., Tjaturadi, B., Krey, K. & Richards, S. (2010b) On the status and relationships of the gecko species *Gehyra barea* Kopstein 1926, with description of new specimens and a range extension. *Zootaxa*, 45-55.

Oliver, P.M., Bauer, A.M., Greenbaum, E., Jackman, T. & Hobbie, T. (2012) Molecular phylogenetics of the arboreal Australian gecko genus *Oedura* Gray 1842 (Gekkota: Diplodactylidae): Another plesiomorphic grade? *Molecular Phylogenetics and Evolution*, **63**, 255-264.

Oliver, P.M., Smith, K.L., Laver, R.J., Doughty, P. & Adams, M. (2014c) Contrasting patterns of persistence and diversification in vicars of a widespread Australian lizard lineage (the *Oedura marmorata* complex). *Journal of Biogeography*, n/a-n/a.

Portik, D.M. & Blackburn, D.C. (2016) The evolution of reproductive diversity in Afrobatrachia: A phylogenetic comparative analysis of an extensive radiation of African frogs. *Evolution*, **70**, 2017-2032.

Portik, D.M., Smith, L.L. & Bi, K. (2016) An evaluation of transcriptome-based exon capture for frog phylogenomics across multiple scales of divergence (Class: Amphibia, Order: Anura). *Molecular Ecology Resources*, **16**, 1069-1083.

Pyron, R.A., Burbrink, F.T. & Wiens, J.J. (2013a) A phylogeny and revised classification of Squamata, including 4161 species of lizards and snakes. *BMC Evol Biol*, **13**, 93.

Pyron, R.A., Burbrink, F.T. & Wiens, J.J. (2013b) A phylogeny and revised classification of Squamata, including 4161 species of lizards and snakes. *BMC Evolutionary Biology*, **13**, 53.

Reeder, T.W., Townsend, T.M., Mulcahy, D.G., Noonan, B.P., Wood, P.L., Sites, J.W. & Wiens, J.J. (2015) Integrated Analyses Resolve Conflicts over Squamate Reptile Phylogeny and Reveal Unexpected Placements for Fossil Taxa. *Plos One*, **10**

Robinson, D.F. & Foulds, L.R. (1981) Comparison of Phylogenetic Trees. *Mathematical Biosciences*, **53**, 131-147.

Ruane, S., Raxworthy, C.J., Lemmon, A.R., Lemmon, E.M. & Burbrink, F.T. (2015) Comparing species tree estimation with large anchored phylogenomic and small Sanger-sequenced molecular datasets: an empirical study on Malagasy pseudoxyrhophiine snakes. *BMC Evolutionary Biology*, **15**, 221.

Sayyari, E. & Mirarab, S. (2016) Fast Coalescent-Based Computation of Local Branch Support from Quartet Frequencies. *Molecular Biology and Evolution*, **33**, 1654-1668.

Schliep, K.P. (2011) phangorn: phylogenetic analysis in R. *Bioinformatics*, **27**, 592-3.

Shea, G., Couper, P., Wilmer, J.W. & Amey, A. (2011) Revision of the genus *Cyrtodactylus* Gray, 1827 (Squamata: Gekkonidae) in Australia. *Zootaxa*, 1-63.

Singhal, S. (2013) De novo transcriptomic analyses for non-model organisms: an evaluation of methods across a multi-species data set. *Molecular Ecology Resources*, **13**, 403-416.

Sistrom, M., Donnellan, S. & Hutchinson, M.N. (2012) Delimiting species in recent radiations with low levels of morphological divergence: A case study in Australian *Gehyra* geckos. *Molecular Phylogenetics and Evolution*, **68**, 135-143.

Skinner, A., Hugall, A. & Hutchinson, M. (2011) Lygosomine phylogeny and the origins of Australian scincid lizards. *Journal of Biogeography*, **38**, 1044-1058.

Skipwith, P.L. & Oliver, P. (2014) A new *Gehyra* (Gekkonidae: Reptilia) from New Guinea with caudal ornamentation. *Zootaxa*, **3827**, 057-066.

Skipwith, P.L., Bauer, A.M., Jackman, T.R. & Sadlier, R.A. (2016) Old but not ancient: coalescent species tree of New Caledonian geckos reveals recent post-inundation diversification. *Journal of Biogeography*, **43**, 1266-1276.

Skipwith, P.L., Jackman, T.R., Whitaker, A., Sadlier, R.A. & Bauer, A.M. (2014) New data on *Dierogekko* (Squamata: Gekkota: Diplodactylidae), with the description of a new species from Île Baaba, Province Nord, New Caledonia. *Mémoires du Muséum National d'Histoire Naturelle*, **204**, 13-30.

Smit, A.F.A., Hubley, R. & Green, P. (2015) *RepeatMasker Open-4.0*. Available at: http:// www.repeatmasker.org (accessed

Smith, B.T., Harvey, M.G., Faircloth, B.C., Glenn, T.C. & Brumfield, R.T. (2014) Target Capture and Massively Parallel Sequencing of Ultraconserved Elements for Comparative Studies at Shallow Evolutionary Time Scales. *Systematic Biology*, **63**, 83-95.

Smith, S.A., Sadlier, R.A., Bauer, A.M., Austin, C.C. & Jackman, T. (2007) Molecular phylogeny of the scincid lizards of New Caledonia and adjacent areas: Evidence for a single origin of the endemic skinks of Tasmantis. *Molecular Phylogenetics and Evolution*, **43**, 1151-1166.

Stamatakis, A. (2014) RAxML version 8: a tool for phylogenetic analysis and post-analysis of large phylogenies. *Bioinformatics*, **30**, 1312-1313.

Tonini, J.F.R., Beard, K.H., Ferreira, R.B., Jetz, W. & Pyron, R.A. (2016) Fully-sampled phylogenies of squamates reveal evolutionary patterns in threat status. *Biological Conservation*, **204, Part A**, 23-31.

Uetz, P., Freed, P. & Hošek, J. (2017) *The Reptile Database*. Available at: http://www.reptile-database.org (accessed 9 January 2017).

Underwood, G. (1954) On the classification and evolution of geckos. *Proceedings of the Zoological Society of London*, **124**, 469-492.

Underwood, G. (1955) Classification of geckos. *Nature*, **175**, 1089.

Vidal, N. & Hedges, S.B. (2005) The phylogeny of squamate reptiles (lizards, snakes, and amphisbaenians) inferred from nine nuclear protein-coding genes. *Comptes Rendus Biologies*, **328**, 1000-1008.

Vidal, N. & Hedges, S.B. (2009) The molecular evolutionary tree of lizards, snakes, and amphisbaenians. *Comptes Rendus Biologies*, **332**, 129-139.

Vidal, N., Marin, J., Sassi, J., Battistuzzi, F.U., Donnellan, S., Fitch, A.J., Fry, B.G., Vonk, F.J., de la Vega, R.C.R., Couloux, A. & Hedges, S.B. (2012) Molecular evidence for an Asian origin of monitor lizards followed by Tertiary dispersals to Africa and Australasia. *Biology Letters*, **8**, 853-855.

Warnock, R.C.M., Parham, J.F., Joyce, W.G., Lyson, T.R. & Donoghue, P.C.J. (2015) Calibration uncertainty in molecular dating analyses: there is no substitute for the prior evaluation of time priors. *Proceedings of the Royal Society B-Biological Sciences*, **282**

Wright, A.M., Lyons, K.M., Brandley, M.C. & Hillis, D.M. (2015) Which came first: The lizard or the egg? Robustness in phylogenetic reconstruction of ancestral states. *Journal of Experimental Zoology Part B: Molecular and Developmental Evolution*, **324**, 504-516.

Yang, Z.H. (2007) PAML 4: Phylogenetic analysis by maximum likelihood. *Molecular Biology and Evolution*, **24**, 1586-1591.

Zheng, Y.C. & Wiens, J.J. (2016) Combining phylogenomic and supermatrix approaches, and a time-calibrated phylogeny for squamate reptiles (lizards and snakes) based on 52 genes and 4162 species. *Molecular Phylogenetics and Evolution*, **94**, 537-547.

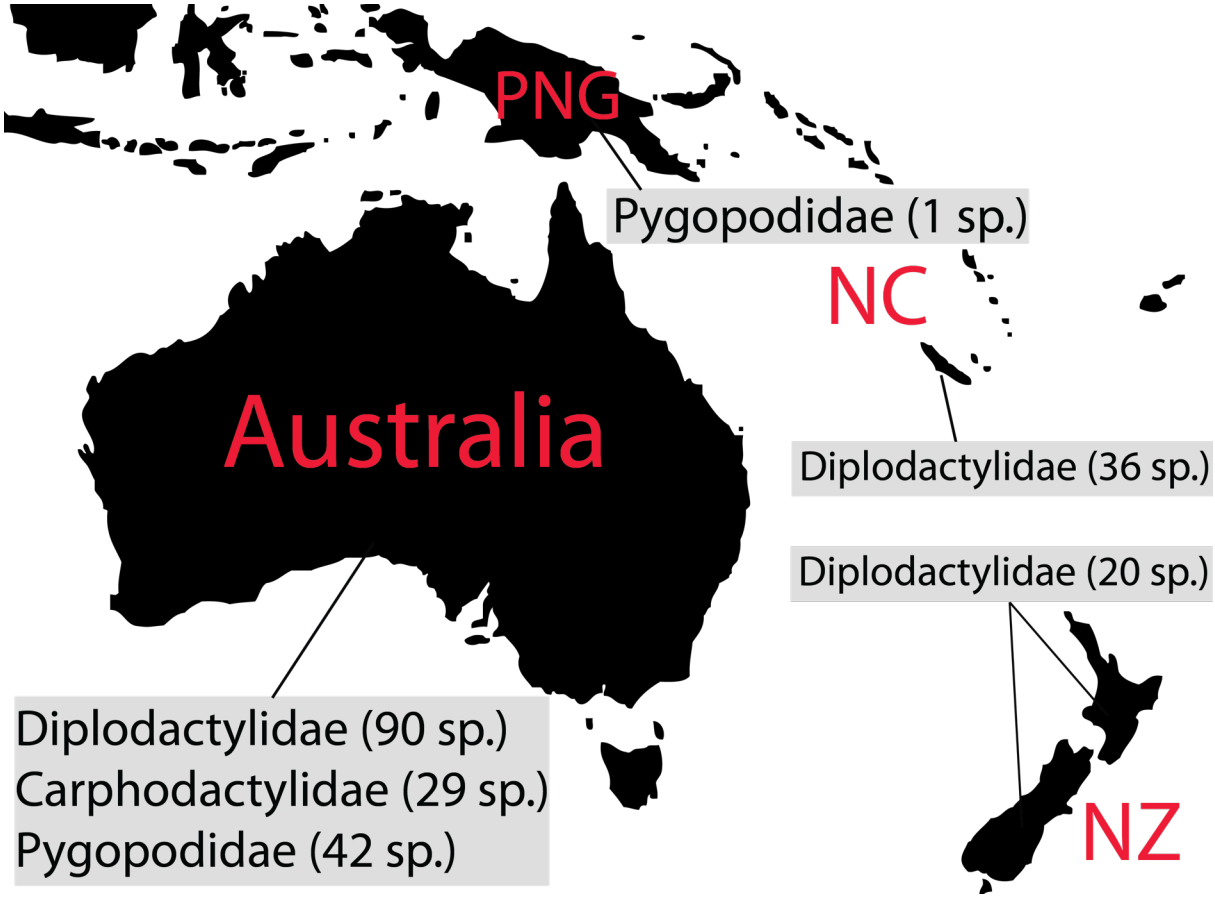


**Figure 1**: Map of Australasia displaying the number of species in each family present on mainland Australia, Papua New Guinea (PNG), New Caledonia (NC), and New Zealand (NZ).

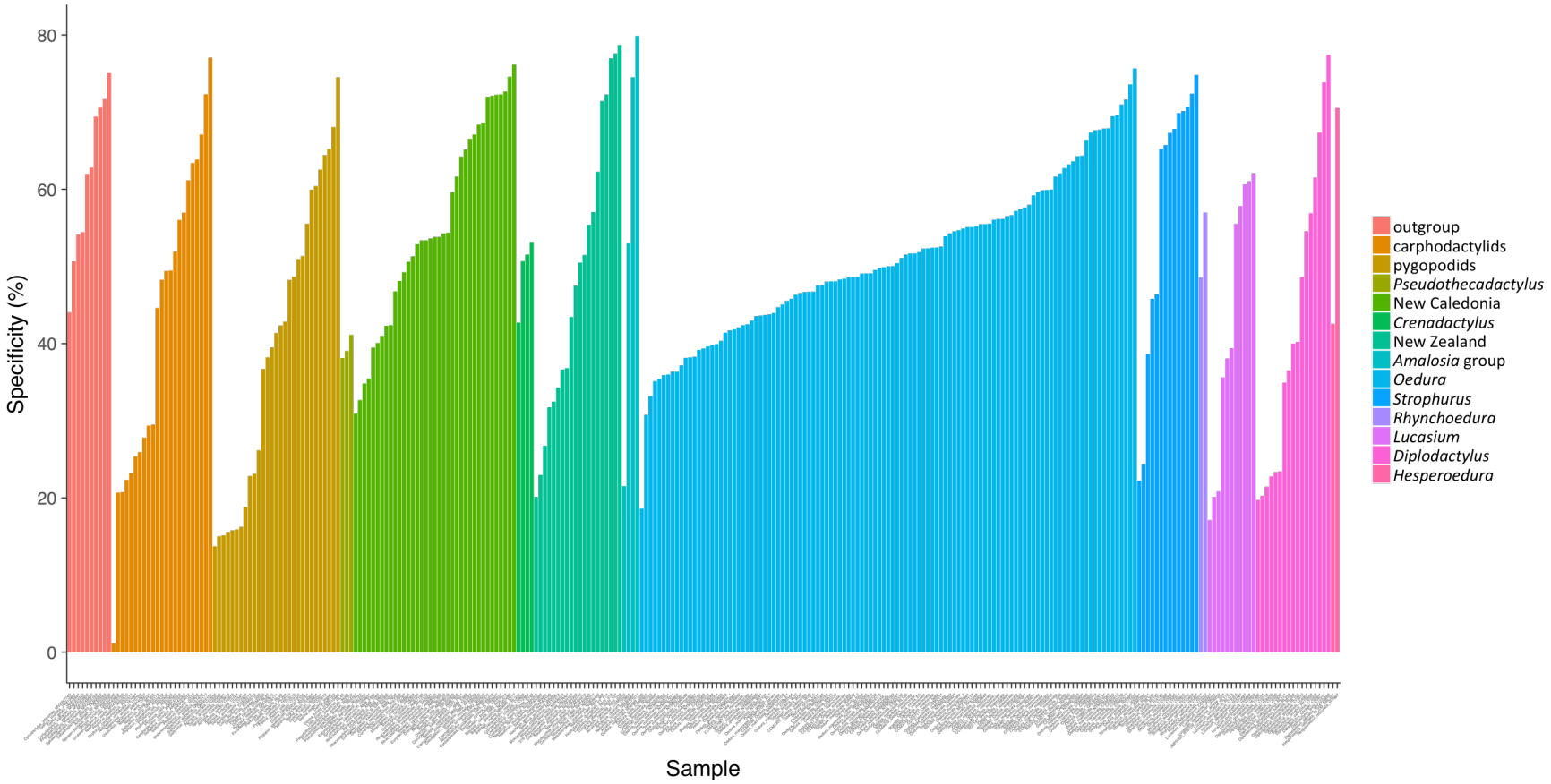


**Figure 2**: UCE capture specificity (%) for every individual library in this study.

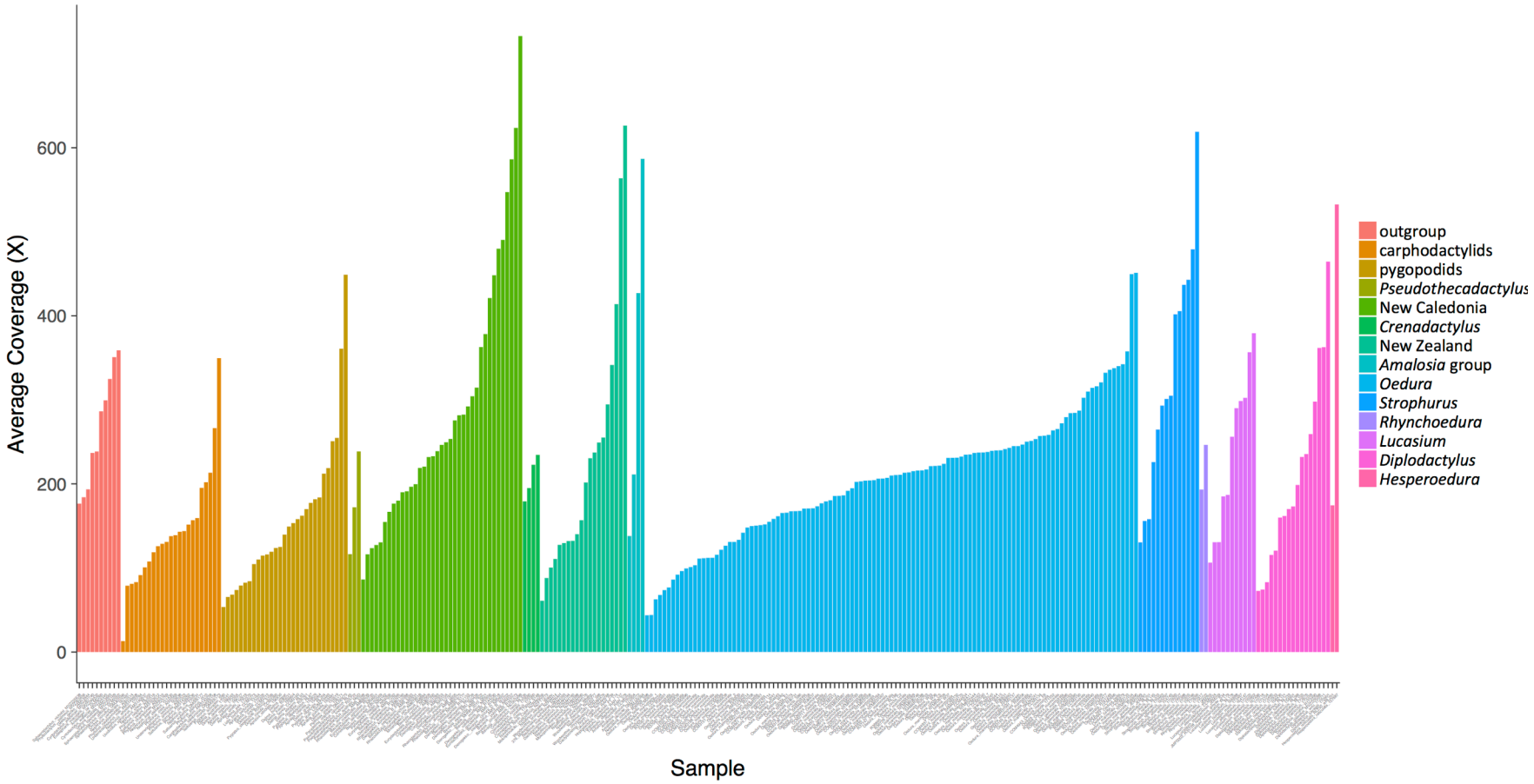


**Figure 3**: Average coverage (x) for all UCEs (target and flanging regions) for every individual library in this study.

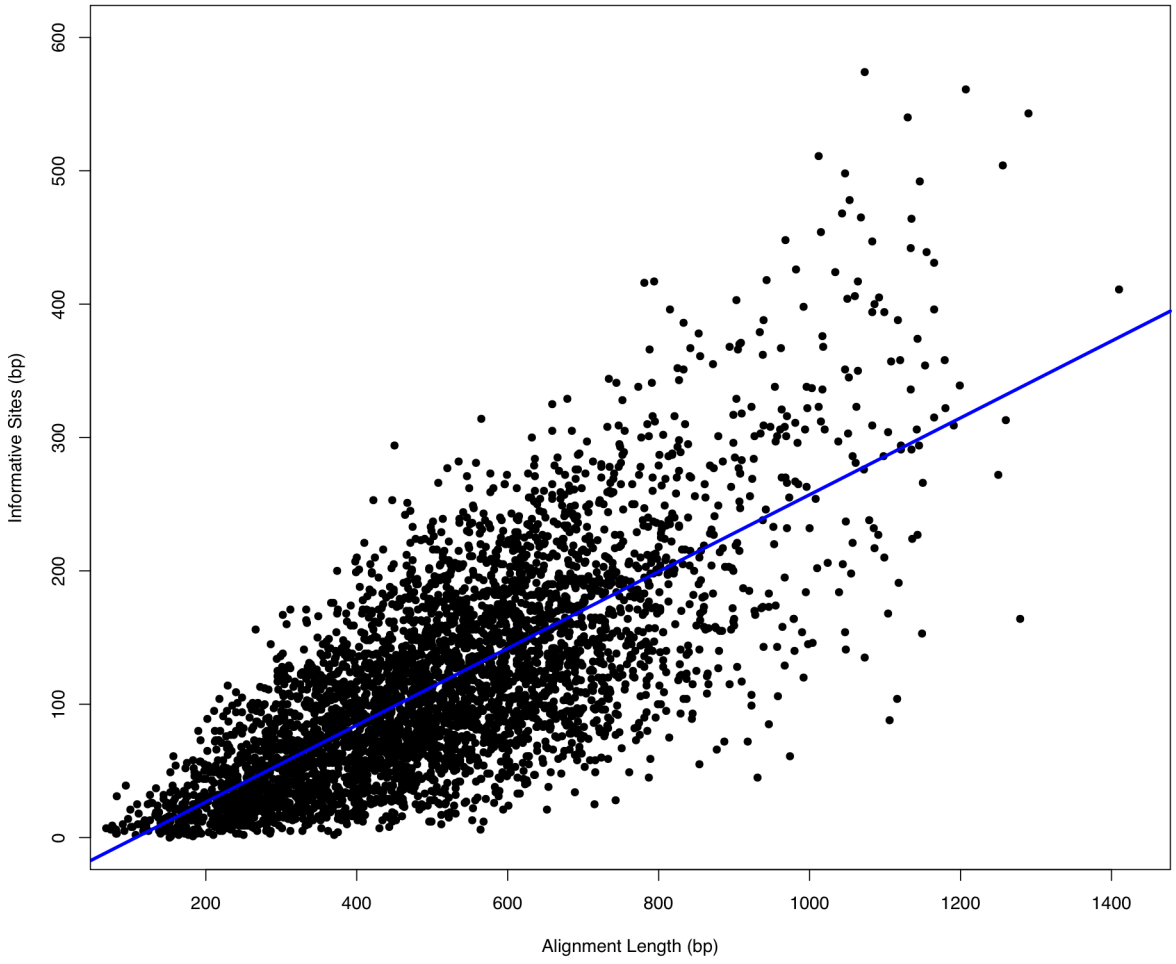


**Figure 4**: Linear regression of alignment length and the number of informative sites. Each represents a single UCE alignment for all taxa (n = 4,268). Equation = -30.9 + 0.29*sequence length: F (1, 4971) = 4266: $R^2 = 0.54$, p = < 0.001.

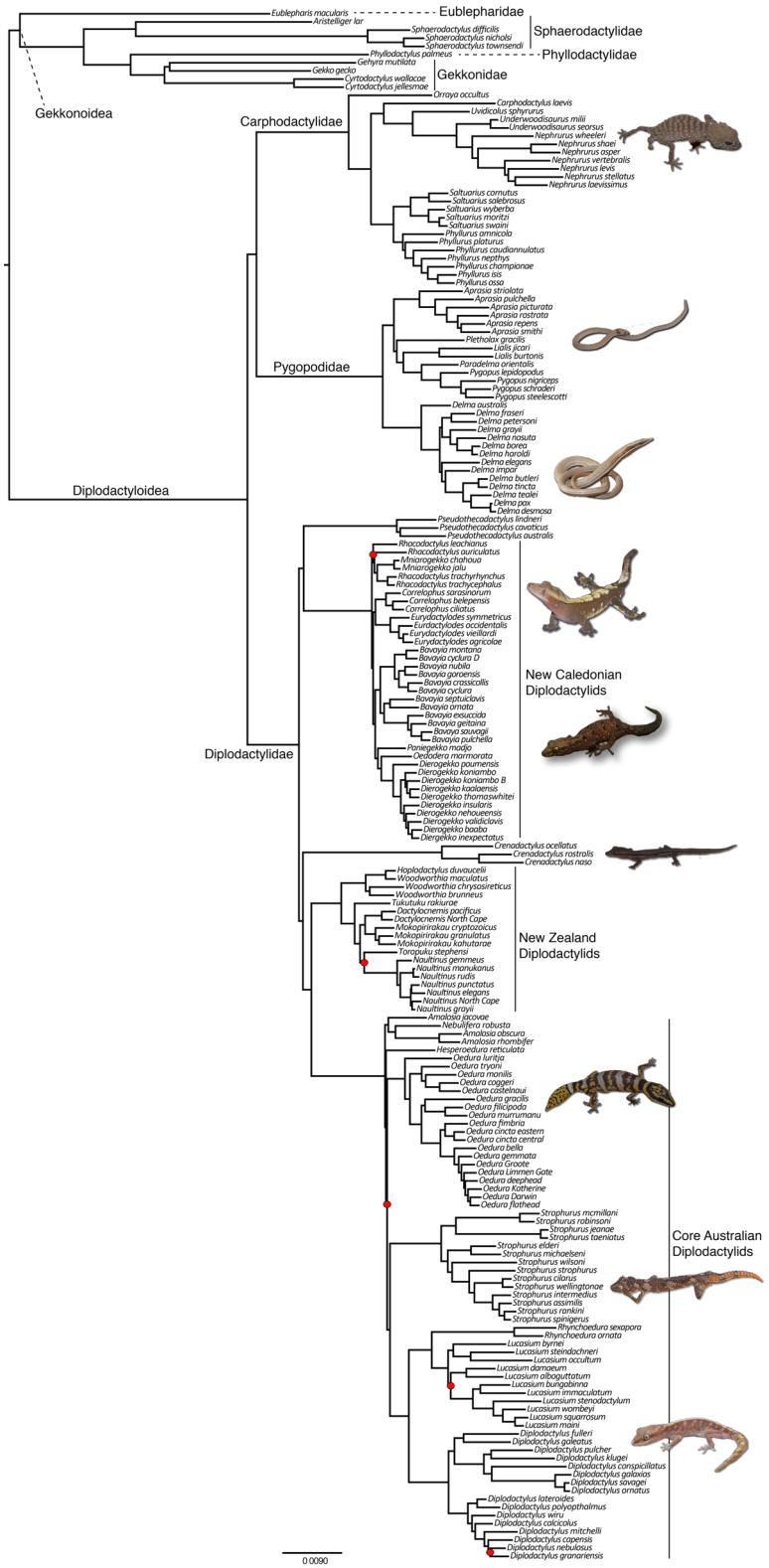


**Figure 5**: Maximum likelihood phylogram from RAxML of the concatenated 4,268 UCE alignment. This tree has been pruned down to a single representative per species for simplicity. Red dots denote nodes with rapid bootstrap proportions < 70. Unlabeled nodes all received bootstrap proportions between ≥ 90. See figure 36 for intraspecific relationships within the AMT *Oedura marmorata* complex. All photographs taken by Phillip L. Skipwith.

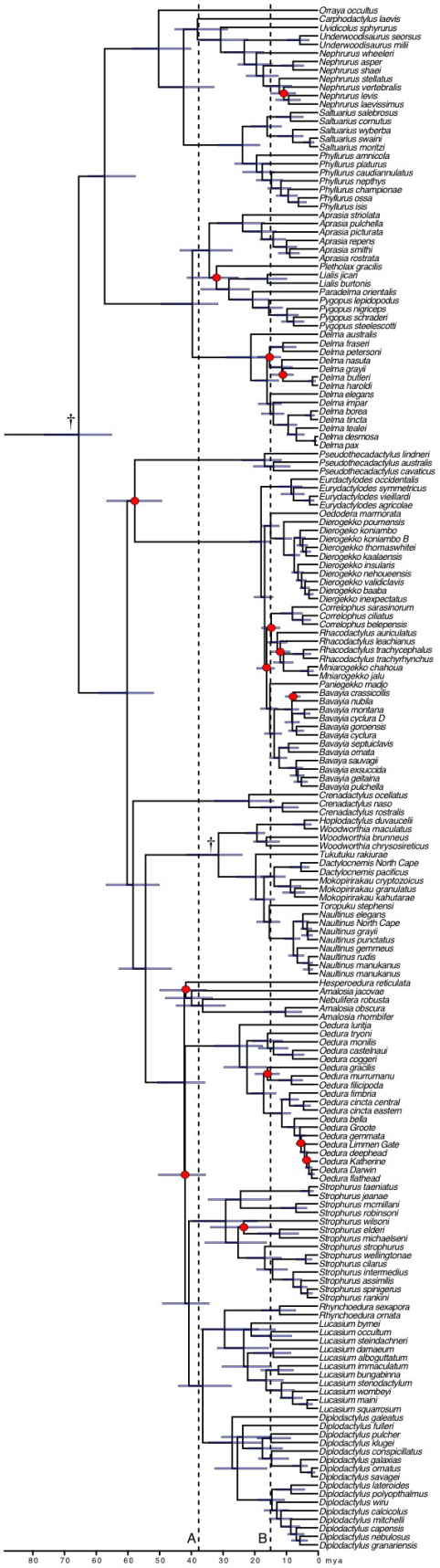


**Figure 6**: MCMCTREE timetree constrained to the ASTRAL topology, outgroup taxa removed. Red dots denote nodes with lpp < 0.95. All other nodes received lpp ≥ 0.95. '†' denotes nodes with a calibration. Line A represented to aerial emergence of the Tasmantis black. Line B represents the initial aridification of mainland Australia.

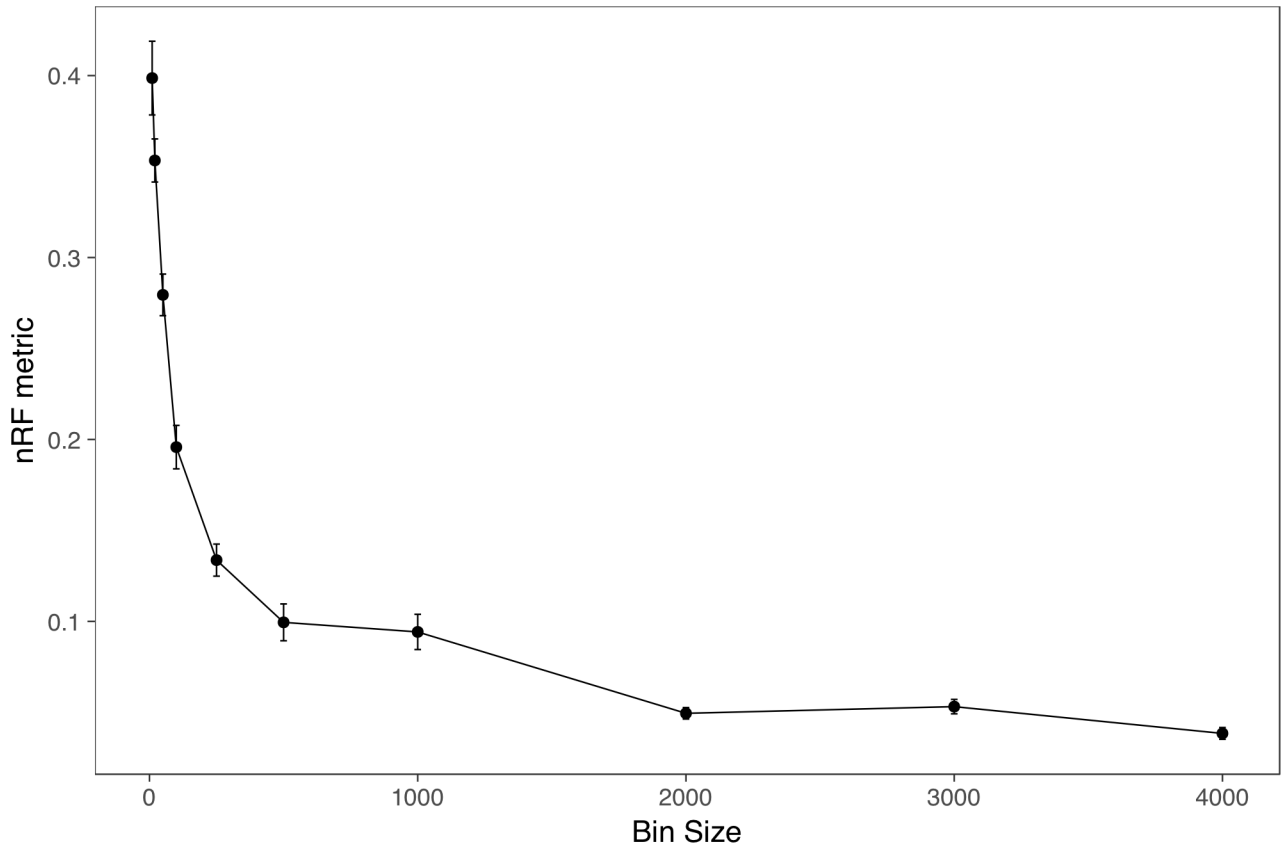


**Figure 7**: Normalized Robinson-Foulds (nRF) distances for each of the ASTRAL random bin replicates for the full 4,268 loci ASTRAL tree. Error bars are standard error of the mean of the 10 replicates/bin.

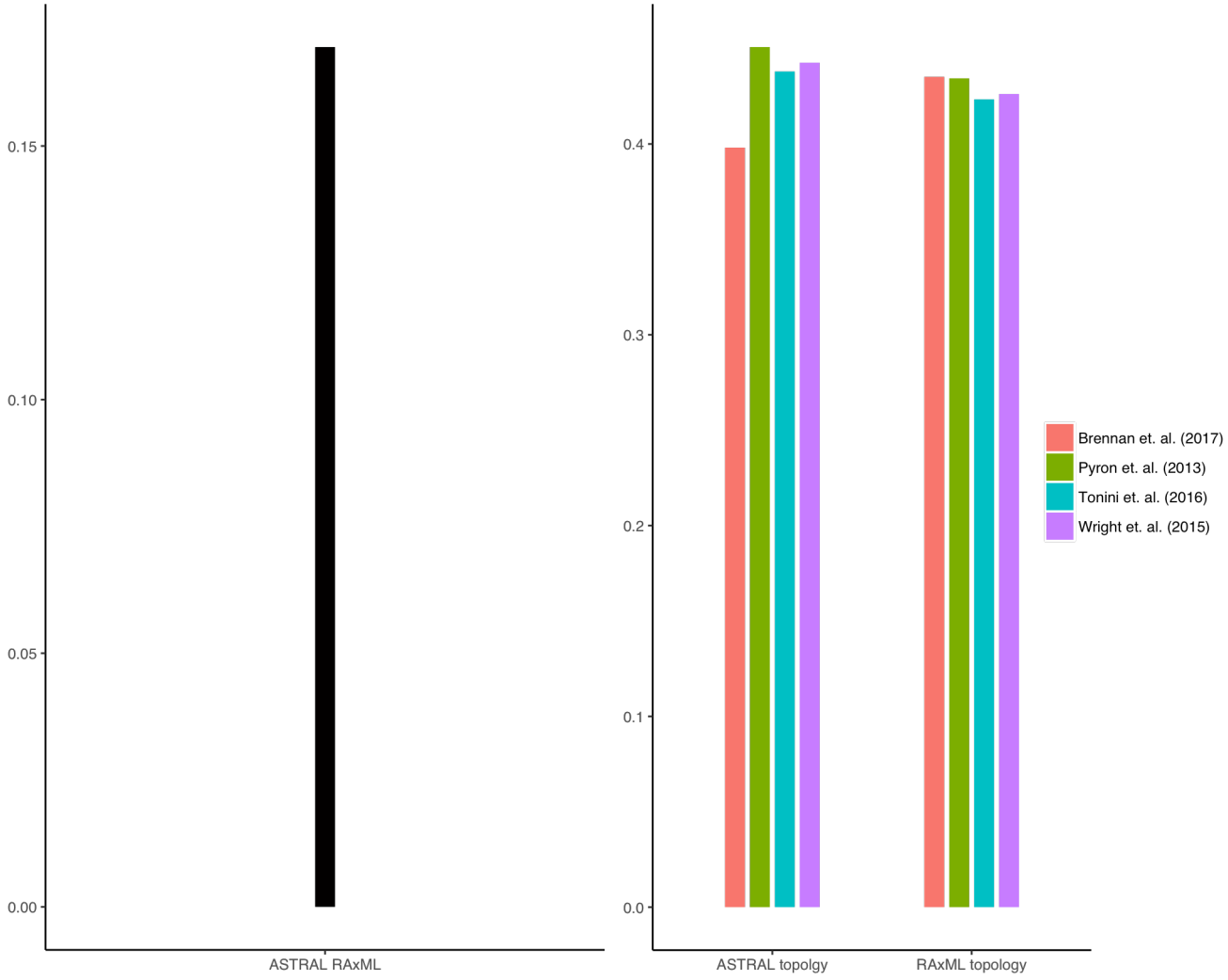


**Figure 8**: A) Normalized Robinson-Foulds (nRF) distances between the concatenated (RAxML) and coalescent (ASTRAL) topologies of this study. B) Robinson-Foulds distances between the coalescent and concatenated trees of this study and the phylogenetic estimates of the Diplodactyloidea of four previous studies.

**Table 1**: All specimens used in this study. Ordered by family.

| Family | Museum Number | Genus | Species |
|---|---|---|---|
| Eublepharidae | MVZ248432 | *Eublepharis* | *macularis* |
| Gekkonidae | MVZ267740 | *Cyrtodactylus* | *jellesmae* |
| | MVZ254345 | *Cyrtodactylus* | *wallacae* |
| | JAM13883 | *Gehyra* | *mutilata* |
| | JAM13944 | *Gekko* | *gecko* |
| Phyllodactylidae | MVZ263856 | *Phyllodactylus* | *palmeus* |
| Sphaerodactylidae | DLM2260 | *Aristelliger* | *lar* |
| | MVZ235638 | *Sphaerodactylus* | *nicholsi* |
| | DLM2002 | *Sphaerodactylus* | *difficilis* |
| | MVZ235169 | *Sphaerodactylus* | *townsendi* |
| Carphodactylidae | AMS143258 | *Carphodactylus* | *laevis* |
| | MVZ225769 | *Nephrurus* | *asper* |
| | 172233 | *Nephrurus* | *laevissimus* |
| | 172231 | *Nephrurus* | *levis* |
| | 18883 | *Nephrurus* | *sheai* |
| | 151430 | *Nephrurus* | *stellatus* |
| | 167487 | *Nephrurus* | *vertebralis* |
| | 170784 | *Nephrurus* | *wheeleri* |
| | QMJ 62596 | *Orraya* | *occultus* |
| | A002516 | *Phyllurus* | *nepthys* |
| | A002569 | *Phyllurus* | *ossa* |
| | A002523 | *Phyllurus* | *amnicola* |
| | A002514 | *Phyllurus* | *caudiannulatus* |
| | A002510 | *Phyllurus* | *championae* |
| | A002536 | *Phyllurus* | *isis* |
| | JS10 | *Phyllurus* | *platurus* |
| | AMS143262 | *Saltuarius* | *cornutus* |
| | QM005173 | *Saltuarius* | *moritzi* |
| | QM005158 | *Saltuarius* | *salebrosus* |
| | AMS163012 | *Saltuarius* | *swaini* |
| | QM005177 | *Saltuarius* | *wyberba* |
| | AMS149808 | *Underwoodisaurus* | *milii* |
| | NoID | *Underwoodisaurus* | *seorsus* |
| | AMS140837 | *Uvidicolus* | *sphyrurus* |
| Diplodactylidae | QMJ77272 | *Amalosia* | *jacovae* |
| | 172804 | *Amalosia* | *obscura* |
| | CCM3255 | *Amalosia* | *rhombifer* |
| | EBU50569 | *Bavayia* | *sauvagii* |

| | | |
|---|---|---|
| AMB8039 | *Bavayia* | *crassicollis* |
| NR2909 | *Bavayia* | *cyclura* |
| NR2607 | *Bavayia* | *cyclura D* |
| AMB 7822 | *Bavayia* | *exsuccida* |
| AMB 7282 | *Bavayia* | *geitaina* |
| NC00249B | *Bavayia* | *goroensis* |
| NR2856 | *Bavayia* | *montana* |
| NR3689 | *Bavayia* | *nubila* |
| AMS R167273 | *Bavayia* | *ornata* |
| NR4557 | *Bavayia* | *pulchella* |
| AMB 5383 | *Bavayia* | *septuiclavis* |
| R161283 | *Correlophus* | *belepensis* |
| NR3104 | *Correlophus* | *ciliatus* |
| NR4601 | *Correlophus* | *sarasinorum* |
| 170097 | *Crenadactylus* | *ocellatus* |
| 173360 | *Crenadactylus* | *ocellatus* |
| 172680 | *Crenadactylus* | *ocellatus* |
| TR653 | *Crenadactylus* | *ocellatus* |
| AMS R 161222 | *Dierogekko* | *inexpectatus* |
| EBU 560426 | *Dierogekko* | *koniambo* |
| MHNH 2010.0621 | *Dierogekko* | *baaba* |
| AMB 7853 | *Dierogekko* | *cf. validiclavis* |
| 52787 | *Dierogekko* | *insularis* |
| R161095 | *Dierogekko* | *kaalaensis* |
| EBU50388 | *Dierogekko* | *koniambo B* |
| R52739 | *Dierogekko* | *nehoueensis* |
| R161153 | *Dierogekko* | *thomaswhitei* |
| AMS R144230 | *Dierogekko* | *validiclavis* |
| 173359 | *Diplodactylus* | *calcicolus* |
| 154901 | *Diplodactylus* | *capensis* |
| WAMR168480 | *Diplodactylus* | *conspicillatus* |
| WAMR157965 | *Diplodactylus* | *fulleri* |
| 173076 | *Diplodactylus* | *galaxias* |
| MVZ229288 | *Diplodactylus* | *galeatus* |
| 167486 | *Diplodactylus* | *granariensis* |
| 90290 - listed as 90280 | *Diplodactylus* | *granariensis* |
| 158430 | *Diplodactylus* | *klugei* |
| 173104 | *Diplodactylus* | *lateroides* |
| 170718 | *Diplodactylus* | *mitchelli* |
| 172933 | *Diplodactylus* | *nebulosus* |

| | | |
|---|---|---|
| 173490 | *Diplodactylus* | *ornatus* |
| WAMR157753 | *Diplodactylus* | *polyophthalmus* |
| 172433 | *Diplodactylus* | *pulcher* |
| 170901 | *Diplodactylus* | *savagei* |
| 172211 | *Diplodactylus* | *wiru* |
| AMS R166218 | *Eurydactylodes* | *occidentalis* |
| R52720 | *Eurydactylodes* | *agricolae* |
| AMB7360 | *Eurydactylodes* | *symmetricus* |
| NR4206 | *Eurydactylodes* | *vieillardi* |
| 157887 | *Hesperoedura* | *reticulata* |
| WAMR114757 | *Hesperoedura* | *reticulata* |
| FT 174 | *Hoplodactylus* | *duvaucelii* |
| NZ RAH 14 | *Hoplodactylus* | *brunneus* |
| NZ RAH 476 | *Hoplodactylus* | *chrysosireticus* |
| NZ FT 7273 | *Hoplodactylus* | *cryptozoicus* |
| NZ RAH 90 | *Hoplodactylus* | *granulatus* |
| NZ RAH 376 | *Hoplodactylus* | *kahutarae* |
| NZ CD 277 | *Hoplodactylus* | *maculatus* |
| NZ RAH 194 | *Hoplodactylus* | *pacificus* |
| NZ RAH 248 | *Hoplodactylus* | *pacificus* |
| 164147 | *Lucasium* | *alboguttatum* |
| 166888 | *Lucasium* | *bungabinna* |
| JEM 255 | *Lucasium* | *byrnei* |
| 172220 | *Lucasium* | *damaeum* |
| NTMR35027 | *Lucasium* | *immaculatum* |
| 173487 | *Lucasium* | *maini* |
| NTMR35008 | *Lucasium* | *occultum* |
| 167475 | *Lucasium* | *squarrosum* |
| JEM 259 | *Lucasium* | *steindachneri* |
| CCM3324 | *Lucasium* | *stenodactylum* |
| 170902 | *Lucasium* | *wombeyi* |
| AMB 84 | *Mniarogekko* | *chahoua* |
| AMB 7801 B | *Mniarogekko* | *chahoua* |
| RAH 388 | *Naultinus* | *rudis* |
| NoID | *Naultinus* | *e. elegans* |
| NoID | *Naultinus* | *e. punctatus* |
| NZ RAH 190 | *Naultinus* | *gemmeus* |
| NZ RAH 176 | *Naultinus* | *grayii* |
| NZ RAH 393 | *Naultinus* | *manukanus* |
| NZ RAH 256 | *Naultinus* | *North Cape* |

| | | |
|---|---|---|
| NZ RAH 388 | *Naultinus* | *manukanus* |
| QMJ89364 | *Nebulifera* | *robusta* |
| R161249 | *Oedodera* | *marmorata* |
| R34843 | *Oedura* | *castelnaui* |
| QMJ94241 | *Oedura* | *coggeri* |
| 171552 | *Oedura* | *filicipoda* |
| R35753 | *Oedura* | *gemmata* |
| R34986 | *Oedura* | *gemmata* |
| NTMR34987 | *Oedura* | *gemmata* |
| NTMR35680 | *Oedura* | *gemmata* |
| SAMAR34170 | *Oedura* | *gemmata* |
| WAMR151005 | *Oedura* | *gracilis* |
| CCM5979 | *Oedura* | *luritja* |
| CCM2204 | *Oedura* | *marmorata* |
| CCM3163 | *Oedura* | *marmorata* |
| CCM3164 | *Oedura* | *marmorata* |
| CCM3132 | *Oedura* | *marmorata* |
| CCM2589 | *Oedura* | *marmorata* |
| CCM2590 | *Oedura* | *marmorata* |
| CCM3137 | *Oedura* | *marmorata* |
| NTMR37058 | *Oedura* | *marmorata* |
| R36893 | *Oedura* | *marmorata* |
| R36731 | *Oedura* | *marmorata* |
| NTMR37061 | *Oedura* | *marmorata* |
| R36830 | *Oedura* | *marmorata* |
| R36863 | *Oedura* | *marmorata* |
| NTMR37074 | *Oedura* | *marmorata* |
| NTMR37091 | *Oedura* | *marmorata* |
| NTMR36801 | *Oedura* | *marmorata* |
| NTMR37070 | *Oedura* | *marmorata* |
| R36858 | *Oedura* | *marmorata* |
| CCM3133 | *Oedura* | *marmorata* |
| R36892 | *Oedura* | *marmorata* |
| CCM4934 | *Oedura* | *marmorata* |
| NTMR37067 | *Oedura* | *marmorata* |
| CCM3162 | *Oedura* | *marmorata* |
| CCM4940 | *Oedura* | *marmorata* |
| CCM3134 | *Oedura* | *marmorata* |
| CCM3150 | *Oedura* | *marmorata* |
| NTMR37059 | *Oedura* | *marmorata* |

| | | |
|---|---|---|
| R36897 | *Oedura* | *marmorata* |
| NTMR37081 | *Oedura* | *marmorata* |
| R36889 | *Oedura* | *marmorata* |
| R36837 | *Oedura* | *marmorata* |
| R36839 | *Oedura* | *marmorata* |
| R36838 | *Oedura* | *marmorata* |
| R36890 | *Oedura* | *marmorata* |
| NTMR37091 | *Oedura* | *marmorata* |
| NTMR37069 | *Oedura* | *marmorata* |
| R37061 | *Oedura* | *marmorata* |
| R36831 | *Oedura* | *marmorata* |
| CCM3844 | *Oedura* | *marmorata* |
| CCM3151 | *Oedura* | *marmorata* |
| CCM4943 | *Oedura* | *marmorata* |
| CCM3188 | *Oedura* | *marmorata* |
| CCM4944 | *Oedura* | *marmorata* |
| R36894 | *Oedura* | *marmorata* |
| CCM4935 | *Oedura* | *marmorata* |
| CCM4936 | *Oedura* | *marmorata* |
| CCM4939 | *Oedura* | *marmorata* |
| CCM2214 | *Oedura* | *marmorata* |
| R36862 | *Oedura* | *marmorata* |
| CCM3135 | *Oedura* | *marmorata* |
| CCM3136 | *Oedura* | *marmorata* |
| CCM3149 | *Oedura* | *marmorata* |
| R36880 | *Oedura* | *marmorata* |
| CCM4941 | *Oedura* | *marmorata* |
| R37147 | *Oedura* | *marmorata* |
| R36891 | *Oedura* | *marmorata* |
| CCM2203 | *Oedura* | *marmorata* |
| CCM4937 | *Oedura* | *marmorata* |
| R36895 | *Oedura* | *marmorata* |
| R37067 | *Oedura* | *marmorata* |
| R36729 | *Oedura* | *marmorata* |
| CCM4195 | *Oedura* | *marmorata* |
| CCM4191 | *Oedura* | *marmorata* |
| CCM2667 | *Oedura* | *marmorata* |
| CCM2710 | *Oedura* | *marmorata* |
| R36910 | *Oedura* | *marmorata* |
| R36899 | *Oedura* | *marmorata* |

| | | |
|---|---|---|
| R37058 | *Oedura* | *marmorata* |
| CCM2711 | *Oedura* | *marmorata* |
| R35919 | *Oedura* | *marmorata* |
| R37059 | *Oedura* | *marmorata* |
| SAMAR38845 | *Oedura* | *marmorata* |
| NTMR18278 | *Oedura* | *marmorata* |
| SAMAR42883 | *Oedura* | *marmorata* |
| SAMAR54300 | *Oedura* | *marmorata* |
| SAMAR34188 | *Oedura* | *marmorata* |
| SAMAR34158 | *Oedura* | *marmorata* |
| NTMR22104 | *Oedura* | *marmorata* |
| NTMR22183 | *Oedura* | *marmorata* |
| NTMR22444 | *Oedura* | *marmorata* |
| NTMR35902 | *Oedura* | *marmorata* |
| NTMR36746 | *Oedura* | *marmorata* |
| NTMR36709 | *Oedura* | *marmorata* |
| WAMR102619 | *Oedura* | *marmorata* |
| WAMR154783 | *Oedura* | *marmorata* |
| WAMR105965 | *Oedura* | *marmorata* |
| WAMR110173 | *Oedura* | *marmorata* |
| WAMR119837 | *Oedura* | *marmorata* |
| WAMR160074 | *Oedura* | *marmorata* |
| WAMR132626 | *Oedura* | *marmorata* |
| CCM2655 | *Oedura* | *marmorata* |
| CCM2223 | *Oedura* | *marmorata* |
| CCM2202 | *Oedura* | *marmorata* |
| CCM2412 | *Oedura* | *marmorata* |
| CCM2477 | *Oedura* | *marmorata* |
| CCM2245 | *Oedura* | *marmorata* |
| CCM2666 | *Oedura* | *marmorata* |
| CCM2696 | *Oedura* | *marmorata* |
| CCM2614 | *Oedura* | *marmorata* |
| MCZA27114 | *Oedura* | *monilis* |
| CCM3365 | *Oedura* | *murrumanu* |
| CCM3366 | *Oedura* | *murrumanu* |
| AMS152045 (NR 5290) | *Oedura* | *tryoni* |
| NR4162 | *Paniegekko* | *madjo* |
| No ID | *Pseudothecadactylus* | *australis* |
| WAMR171453 | *Pseudothecadactylus* | *cavaticus* |
| R35722 | *Pseudothecadactylus* | *lindneri* |

| | | | |
|---|---|---|---|
| | AMB5375 | *Rhacodactylus* | *auriculatus* |
| | AMB 5398 | *Rhacodactylus* | *auriculatus* |
| | AMB 7190 | *Rhacodactylus* | *leachianus* |
| | AMB 6605 | *Rhacodactylus* | *trachycephalus* |
| | NR2931 | *Rhacodactylus* | *trachyrhynchus* |
| | 172222 | *Rhynchoedura* | *ornata* |
| | 172917 | *Rhynchoedura* | *sexapora* |
| | 154745 | *Strophurus* | *assimilis* |
| | WAMR108798 | *Strophurus* | *ciliaris* |
| | 172227 | *Strophurus* | *elderi* |
| | JEM 261 | *Strophurus* | *intermedius* |
| | JEM 1099 | *Strophurus* | *jeanae* |
| | 173095 | *Strophurus* | *mcmillani* |
| | 150196 | *Strophurus* | *michaelseni* |
| | WAMR132471 | *Strophurus* | *rankini* |
| | 172855 | *Strophurus* | *robinsoni* |
| | 165297 | *Strophurus* | *spinigerus* |
| | 172388 | *Strophurus* | *strophurus* |
| | NTMR36750 | *Strophurus* | *taeniatus* |
| | 170463 | *Strophurus* | *wellingtonae* |
| | 170260 | *Strophurus* | *wilsoni* |
| | RAH 378 | *Toropuku* | *stephensi* |
| | RAH 137 | *Toropuku* | *stephensi* |
| | RAH 239 | *Tukutuku* | *rakiurae* |
| Pygopodidae | 131647 | *Aprasia* | *picturata* |
| | 163481 | *Aprasia* | *pulchella* |
| | 172504 | *Aprasia* | *repens* |
| | 153829 | *Aprasia* | *rostrata* |
| | 116919 | *Aprasia* | *smithi* |
| | 156936 | *Aprasia* | *striolata* |
| | 172541 | *Delma* | *australis* |
| | CCM3160 | *Delma* | *borea* |
| | R35031 | *Delma* | *butleri* |
| | 166043 | *Delma* | *desmosa* |
| | WAMR110900 | *Delma* | *elegans* |
| | 169904 | *Delma* | *fraseri* |
| | 154064 | *Delma* | *grayii* |
| | 172326 | *Delma* | *haroldi* |
| | NoID | *Delma* | *impar* |
| | CCM3360 | *Delma* | *nasuta* |

| | | |
|---|---|---|
| 172570 | *Delma* | *pax* |
| 166727 | *Delma* | *petersoni* |
| 153819 | *Delma* | *tealei* |
| CCM3213 | *Delma* | *tincta* |
| CCM3273 | *Lialis* | *burtonis* |
| LSUMZ10483 | *Lialis* | *jicari* |
| QMJ92675 | *Paradelma* | *orientalis* |
| 106171 | *Pletholax* | *gracilis* |
| R35761 | *Pygopus* | *nigriceps* |
| NoID | *Pygopus* | *schraderi* |
| R35022 | *Pygopus* | *steelescotti* |
| R05328 | *Pygopus* | *lepidopodus* |

**Table 2:** All diplodactyloid genera with known distributions and habitat preference. Region abbreviations: Aust. = Australia, NC = New Caledonia, NZ = New Zealand, and PNG = Papua New Guinea. Number of described species is taken from the Reptile Database with estimates as of 2017 (Uetz *et al.*, 2017).

| Family | Genus | Distribution | Substrate | No. Described Species | No. Species Sampled |
|---|---|---|---|---|---|
| Carphodactylidae | *Carphodactylus* | Aust. | terrestrial/scansorial | 1 | 1 |
| | *Nephrurus* | Aust. | terrestrial | 9 | 7 |
| | *Orraya* | Aust. | rupicolous | 1 | 1 |
| | *Phyllurus* | Aust. | rupicolous/arboreal | 9 | 7 |
| | *Saltuarius* | Aust. | rupicolous | 7 | 5 |
| | *Underwoodisaurus* | Aust. | terrestrial | 2 | 2 |
| | *Uvidicolus* | Aust. | terrestrial | 1 | 1 |
| Diplodactylidae | *Amalosia* | Aust. | rupicolous/scansorial | 4 | 3 |
| | *Bavayia* | NC | rupicolous/scansorial | 12 | 11 |
| | *Correlophus* | NC | arboreal | 3 | 3 |
| | *Crenadactylus* | Aust. | terrestrial/scansorial | 7 | 3 |
| | *Dactylocnemis* | NZ | arboreal | 1 | 1 |
| | *Dierogekko* | NC | arboreal | 9 | 9 |
| | *Diplodactylus* | Aust. | terrestrial | 27 | 16 |
| | *Eurydactylodes* | NC | arboreal | 4 | 4 |
| | *Hesperoedura* | Aust. | arboreal | 1 | 1 |
| | *Hoplodactylus* | NZ | arboreal | 1 | 1 |
| | *Lucasium* | Aust. | terrestrial | 11 | 11 |
| | *Mniarogekko* | NC | arboreal | 2 | 2 |
| | *Mokopirirakau* | NZ | rupicolous/scansorial | 4 | 3 |
| | *Naultinus* | NZ | arboreal | 8 | 6 |
| | *Nebulifera* | Aust. | rupicolous/scansorial | 1 | 1 |
| | *Oedodera* | NC | arboreal | 1 | 1 |
| | *Oedura* | Aust. | rupicolous/scansorial | 14 | 13 |
| | *Paniegekko* | NC | arboreal | 1 | 1 |
| | *Pseudothecadactylus* | Aust. | rupicolous/scansorial | 3 | 3 |
| | *Rhacodactylus* | NC | arboreal | 4 | 4 |
| | *Rhynchoedura* | Aust. | terrestrial | 6 | 2 |
| | *Strophurus* | Aust. | scansorial/graminicolous | 18 | 14 |
| | *Toropuku* | NZ | arboreal | 1 | 1 |
| | *Tuktuku* | NZ | arboreal | 1 | 1 |
| | *Woodworthia* | NZ | arboreal | 3 | 3 |
| Pygopodidae | *Aprasia* | Aust. | fossorial | 14 | 6 |
| | *Delma* | Aust. | grass swimming | 22 | 14 |

| | | | | |
|---|---|---|---|---|
| *Lialis* | Aust./PNG | grass swimming | 2 | 2 |
| *Ophidiocephalus* | Aust. | fossorial | 1 | 0 |
| *Paradelma* | Aust. | grass swimming | 1 | 1 |
| *Pletholax* | Aust. | grass swimming | 1 | 1 |
| *Pygopus* | Aust. | grass swimming | 5 | 4 |

# Chapter 2

## ECOLOGICAL DIVERSIFICATION AND PHENOTYPIC CONVERGENCE IN DIPLODACTYLOID GECKOS

### Introduction

Adaptive radiations are very difficult to define across broad taxonomic and temporal scales, but most definitions agree that the accumulation of ecological diversity accompanies this phenomenon (Schluter, 2000). With this increased ecological breadth, adaptive radiations are frequently described as exhibiting high levels of convergent evolution (Losos *et al.*, 1998). This replication provides strong evidence that the environment plays a major role in adaptive diversification, leading to superficially similar phenotypes in distantly related taxa (Simpson, 1953). The presence of this pattern of replicated evolution in relatively closely related species suggests that there is a deterministic aspect of phenotypic diversification (Losos *et al.*, 1998; Losos & Ricklefs, 2009; Mahler *et al.*, 2013; Davis *et al.*, 2014; Esquerre & Keogh, 2016). As selection is the primary force that results in the pattern of homoplasy, truly convergent taxa must occupy the same adaptive peak due to similar environmental pressures (Schluter, 2000; Ingram & Mahler, 2013). A few exceptional clades, such as the Greater Antillean *Anolis* lizards and Neotropical cichlid fishes, have taken both inter and intraclade phenotypic replication to the extreme across islands and lakes (Pinto *et al.*, 2008; Mahler *et al.*, 2010; Mahler *et al.*, 2013; Arbour & Lopez-Fernandez, 2014). Distinguishing true convergence from plesiomorphy is exacerbated by poorly supported phylogenetic relationships. Furthermore, issues arise in the circularity of designating *a priori* morphological groups into which researchers must place putatively convergent taxa. Hence, well supported phylogenetic estimates and rigorous, model-based statistical methods that do not require *a priori* groups are becoming increasingly common in macroevolutionary studies of adaptive landscapes (Ingram & Mahler, 2013).

In this study, we explore the diplodactyloid geckos of Australasia to determine if this morphologically and ecologically diverse clade exhibits detectable signatures of convergent evolution. Broadly speaking, diplodactyloids vastly exceed another major clade of geckos, the gekkonoids, in morphological diversity. However, several clades occupy superficially similar ecological niches and some appear to have independently acquired similar phenotypes. We ascribe several *a priori* ecomorphological groups corresponding to substrate preference and diet that appear in distantly related but ecological equivalents across the diplodactyloid tree (figure 9). For limbed the carphodactylids and diplodactylids these are: a generalist arboreal ecomorph where species possess moderately broad toepads and intermediate length limbs, a rupicolous ecomorph characterized by dorsoventrally flattened heads and long limbs and digits, a general scansorial ecomorph intermediate between the arboreal and rupicolous morphs, a terrestrial ecomorph specializing on large prey characterized by long limbs and large heads, and a terrestrial ecomorph specializing in small prey defined by short limbs and short heads. We also define two broad ecomorph groups encompassing a generalized grass-swimming form where the head is relatively long and pointed, and a specialized fossorial form where the head is blunt and shortened. These putative ecomorphs are particularly interesting given that some occur multiple times across the diplodactyloid tree. For instance, several Australian carphodactylid and diplodactylid taxa have independently colonized rocky habitats. Of particular note are the leaf-tailed geckos of the genus *Saltuarius* and the three Kimberley *Oedura* species (*O. gracilis*, *O. fillicipoda*, and *O. murrumanu*). All of these taxa have comparatively long limbs and some degree of dorsoventral

flattening of the head, traits widely documented across phylogenetically disparate lizard clades as adaptations for a rupicolous lifestyle (Revell *et al.*, 2007). The *Diplodactylus – Lucasium* + *Rhynchoedura* clade is largely defined by its members being small-bodied and small headed, possessing reduced digital scansors. Several lineages within *Diplodactylus* (i.e., *D. conspicillatus*, etc.) and *Rhynchoedura* have exceptionally small heads with beak-like snouts, presumably traits for consuming small arthropod prey. When relying on morphology alone, the New Caledonian and New Zealand diplodactylids were inferred to be closely related, with some proposing that the latter gave rise to the former (Kluge, 1967; Kluge, 1987; Bauer, 1990). This is evidenced by the two clades being arboreal and, along with the Australian *Pseudothecadactylus*, sharing a number of osteological traits as well as broad toepads and prehensile tails tipped with adhesive lamellae. Given that these lineages are very distantly related and independently derived from Australian ancestors, it is likely that these similarities are the result of convergence. Lastly, members of the Australian *Amalosia*/*Nebulifera* and *Hesperoedura* groups are largely arboreal, bearing some similarities to the New Caledonian and New Zealand clades such as relatively large heads and broad toepads.

To address whether phenotypic convergence occurs both within and between clades, we used high throughput sequencing to generate a new and improved phylogenetic estimate for the diplodactyloids (see Chapter 1). We then measured a suit of external ecomorphological characters to map onto this new tree for comparative phylogenetic analyses. In addition to continuous variables, we used discrete character ancestral trait reconstruction to infer the ancestral ecology for this clade. Likelihood and Bayesian methods were implemented to statistically infer which clades have experienced shifts in morphospace and if multiple clades have converged on the same adaptive peaks. These analyses serve as a first pass at quantitatively determining whether diplodactyloids represent an amalgam of adaptive and non-adaptive radiations.

**Methods**

*Ecomorphological Data*

We measured 23 ecologically relevant external traits for 148 diplodactyloid species, totaling 993 specimens from museum collections in the United States, Australia, and New Zealand. To account for intraspecific variation, we attempted to measure at least 5 adult individuals for each species, specifically targeting males. All genera were sampled with the exception of the pygopodid *Pletholax*. However, a number of species are rare in museum collections and were often represented by a single specimen (mean = 6.3 individuals/species, range: 1 – 28 individuals/species. Adult males were targeted to standardize for sex, though 15% of species were only represented by females in the available collections. Species only represented by females were kept in all downstream analyses as geckos, while females are typically larger, do not exhibit sexual dimorphism in trait proportions to the same extent as iguanian lizards such as *Anolis* (Mahler *et al.*, 2010). Traits related to prey acquisition and locomotion (i.e.- head, limb, and toe traits) were measured with digital calipers and all measurements we collected by P. L. Skipwith. All measurements were taken on the left side unless that side was heavily deformed or otherwise damaged, in which case the right side was measured. We opted to measure well preserved specimens in the standardized preparation position of lizards. For species represented by poorly preserved specimens (i.e.- twisted or otherwise deformed), each measurement was taken 3 times and the average of those individual measures was used.

*Phylogenetic Inference*

We used a new phylogenomic dataset of 4,268 ultraconserved loci to infer the phylogenetic relationships of 180 species of diplodactyloid gecko. For all phylogenetic comparative analyses, the topology of the multispecies coalescent tree from ASTRAL II was used (Mirarab *et al.*, 2014; Mirarab & Warnow, 2015). Divergence dating was done with MCMCTREE in PAML using a combination of fossil and secondary calibrations (Yang, 2007). See Chapter 1 and figure 6 for details. As MCMCTREE takes a single topology onto which it estimates divergence times from sequence data, we were unable to account for phylogenetic uncertainty in our model testing and comparative phylogenetic analyses. See Chapter 1 for additional phylogenetic and divergence dating methods.

*Comparative Phylogenetic Analyses of Continuous Trait Data*

Of the 23 original measurements, we discarded all traits related to tail dimensions as well as for the humerus and femur, as these traits were subject to high levels of measurement error. Only 56% of the specimens in this study had original tails and most diplodactyloid species regenerate oddly shaped tails which are markedly different from the originals. This left us with 16 external measurements and these were: head length, head width, head depth, trunk length, forearm length (crus), tibia length, internarial width (EN), nares-eye distances (NEYE), orbit diameter (EYE), eye-ear distance (EyeEar), interorbital distance (IE), 4$^{th}$ finger width, 4$^{th}$ finger length, 4$^{th}$ toe width, and 4$^{th}$ toe length. All measurements were carried out by P. Skipwith using a pair of digital calipers. As some of these were likely not evolving under a single-rate Brownian motion process, we estimated the appropriate model for each trait using Akaike Information Criterion (AIC) and then AIC weights (AICw). We tested for single-rate Brownian motion (BM), single-peak Ornstein-Uhlenbeck (OU1) where a selection parameter ($\alpha$) influences the magnitude of the random walk process, early-burst (EB) where the rate of trait evolution increases or decreases exponentially through time, and lambda ($\lambda$) where the phylogeny explains the extent to which a trait varies between species. Model testing for continuous traits was done with the fitContinous function in GEIGER (Harmon *et al.*, 2008; Harmon *et al.*, 2010). All comparative phylogenetic analyses used the mean value of each log-transformed trait, though we incorporated the mean standard error for all traits into model testing. To correct for allometric scaling, all traits were regressed against body size (svl) using phylogenetic least squares (PGLS) regression in PHYTOOLS while optimizing for $\lambda$ (Revell, 2009). To reduce the dimensionality of our traits, we used a phylogenetic principal component analysis (pPCA) for our size-corrected traits and maximum body size for each species while optimizing for $\lambda$. We opted to use maximum body size from the literature as an independent trait to account for sampling bias in our dataset (Mahler *et al.*, 2013; Ingram & Kai, 2014). Examination of pPCA axes was done to determine if clades and *a priori* ecomorphs clustered together along the same morphological axes. A broken stick test of the variance explained was used to determine how many principle components to use in downstream comparative analyses. While the ideal scenario would involve reducing dimensionality under the appropriate model of trait evolution, no algorithm exists that allows for pPCAs to be fitted with OU and other complex models. We recognize that this computational pitfall can lead to the identification of misleading major axes of variation within a multivariate dataset (Uyeda *et al.*, 2015).

*Ecology and Discrete State Ancestral State Reconstruction*

To investigate the evolution of ecological diversity in the diplodactyloids, we coded our full 180 taxon time-calibrated species tree with discrete categories. These were: a) *terrestrial* – entirely restricted to the ground, b) *rupicolous* – occurring exclusively on rocks, c) *scansorial* – occurring

on rocks and low vegetation, d) *arboreal* – occurring on trees, e) *shrub-inhabiting* – occurring on low vegetation, f) *graminicolous* – occurring on bunch grass (i.e.- *Triodia*), g) *fossorial* – limbless and burrowing, and h) *grass-swimming* – limbless and terrestrial. Ecological states for each species were garnered from Wilson and Swan (2013) and Bauer and Sadlier (2000). As numerous states, in this case eight, can overparamaterize ancestral trait reconstruction, we reran our reconstruction analyses with pygopodids classified as terrestrial and again with pygopodids removed. The fitDiscrete function in GEIGER was used to determine the appropriate macroevolutionary model for these discrete data. All discrete ancestral trait reconstruction analyses were tested for the equal-rates (ER), symmetric (SYM), and all-rates-differ (ARD) models. We then used a likelihood-ratio test for each pairwise model comparison before using a Chi-square test to determine the appropriate model. We implemented a likelihood approach for estimating ancestral states via the ACE function in GEIGER on the ASTRAL topology (Felsenstein, 1973, 1985). Stochastic character mapping with the Bayesian algorithm SIMMAP was then used to estimate ancestral ecological states on the same tree with the MAKE.SIMMAP function in PHYTOOLS (Bollback, 2006). Each of the SIMMAP analyses was run with 1,000 simulations to estimate the posterior probabilities of node states. To determine if our likelihood and Bayesian ancestral reconstruction analyses converged on similar results, we compared the marginal ancestral states of ACE to the stochastic mapping posterior probabilities of SIMMAP by plotting one against the other.

*Testing Relationships Between Ecology and Continuous Traits*

In order to ascertain the relationship between our ecological groups and continuous traits, we implemented state-dependent trait diversification methods. We used OUWIE to fit various Hansen models under random-walk (BM) and stabilizing selection (OU) to body-size (SVL), limb-length (crus and tibia), and toepad width for each of the discrete ecological categories (O'Meara *et al.*, 2006; Beaulieu *et al.*, 2012). Continuous traits were fitted with a single-rate Brownian motion model (BM1), a Brownian motion model with different rate parameters for each discrete trait (BMS), an OU model with a single optimum across the whole tree (OU1), a multipeak OU model with different state means but global stochastic ($\sigma^2$) and selection ($\alpha$) parameters acting across the tree (OUM), and two multi-peak OU models that allow for different state means with multiple $\sigma^2$ (OUMV) and multiple $\alpha$ (OUMA). Model choice was determined by calculating $\Delta$AIC from the corrected AICs (AICc). The rates of $\sigma^2$ and $\alpha$ were then inspected for the appropriate trait to determine which ecological group had the highest rate of continuous trait evolution.

*Quantifying Phenotypic Convergence*

To test phenotypic convergence in our continuous trait data, we used two complementary methods that do not rely on *a priori* ecomorph designations. The likelihood program SURFACE was used to first identify shifts in morphospace and then determine if any clades had converged on the same adaptive peak (Ingram & Mahler, 2013). SURFACE uses the Hansen stabilizing selection model to fit OU processes to trait data and a phylogeny, estimating adaptive regimes and clade-specific shifts in ecomorphology (Hansen, 1997, 2012; Ingram & Mahler, 2013). SURFACE has two phases, the first of which estimates where shifts in morphospace have occurred on the phylogeny. It then uses stepwise AICc to determine if collapsing clades into the same adaptive regime improves the likelihood, suggesting convergence between two or more clades. To determine if diplodactyloids exhibited exceptional convergence beyond what would be expect by chance given a null expectation, we generated 100 simulated datasets each under BM, OU1, and a non-convergent Hansen model ($H_{NC}$) from the forward phase of SURFACE on our ASTRAL tree. Null distributions

of peak shifts were then created by running SURFACE on each of the simulated trait datasets with significance being determined with *simulations data* $\geq$ *empirical estimates/total simulations*. SURFACE is computationally expensive, making more replicates impractical. Ho and Ané (2014) demonstrated that using AIC to determine regime shifts can lead to overfitting of the model, resulting in overestimation of shifts and convergence events. Thus, we implemented l1OU, a complementary method for detecting regime shifts that uses Bayesian information criterion (BIC) and a derivation of the phylogenetic lasso (Khabbazian *et al.*, 2016). In short, the phylogenetic lasso methods implemented here minimize the magnitude of $\alpha$ and penalize shifts along a branch, increasing the chance of detecting significant shifts. l1OU was run with phylogenetic BIC (pBIC) which can account for phylogenetic correlation between species and is robust to overestimating the number of regime shifts. Both SURFACE and l1OU assume that each trait is evolving under its own OU process, but l1OU assumes that $\theta$ (the inferred adaptive optimum? of a trait) is constant along a given branch due to difficulties in accurately detecting multiple shifts in $\theta$ (Ho & Ané, 2014). To determine statistical support for regime shifts proposed by l1OU, 100 non-parametric bootstrap replicates were run on the phylogenetically-uncorrelated residuals calculated from the optimal shift configuration. SURFACE and l1OU were run with the pPCA scores of the most heavily loaded pPC axes that were correlated with our original, biologically meaningful traits (Ingram & Mahler, 2013; Mahler *et al.*, 2013; Ingram & Kai, 2014). Both methods were implemented on a pruned phylogeny of 129 diplodactylid and carphodactylid species.

**Results**

*Reconstruction of Morphospace*

We chose to keep the first 7 pPCs as determined by the broken stick test and the variance explained (88.7%) (figure 10). Furthermore, these pPCs had interpretable correlations with the original trait. These were: pPC1 – maximum svl (33.9%), pPC2 – head length (21%), pPC3 – 4$^{th}$ toe width (12.9%), pPC4 – 4$^{th}$ toe length (9.5%), pPC5 – forearm length (4.4%), pPC6 – nares to eye distance (3.8%), and pPC7 – eye to ear distance (3.2%). All principle components from the pPCA were negatively loaded.

*Continuous Trait Model Selection*

Most traits on the pruned carphodactylid and diplodactylid tree were fitted with a Brownian motion model (table 3). However, head length, eye diameter, and eye-ear distance strongly favored a OU1 model. Since multivariate size corrections for phylogenetic principle component analyses require correlation tests and estimation of the covariance matrix to be estimated under a common model, we chose to optimize $\lambda$ for phylogenetic regression and pPCA. For the 7 axes use here, axes 2-7 all found distinct clusters differentiating carphodactylids and diplodactylids (figure 11).

*Ancestral State Reconstruction and Association of Ecology with Trait Evolution*

Model testing of discrete ecological states revealed that the complex SYM and ARD models were not better fits for these data than the simple ER model. We found that the marginal ancestral states of ACE and stochastic mapping posterior probabilities of SIMMAP were highly correlated (figure 12). Both methods found strong support for the root of diplodactyloids being rupicolous (SIMMAP pos. prob. = 0.53, ACE marginal probability = 0.57), a rupicolous origin for the carphodactylids (SIMMAP pos. prob. = 0.77, ACE marginal probability = 0.79), and a grass-swimming origin for the pygopodids (SIMMAP pos. prob. = 0.8, ACE marginal probability = 0.8) (figure 13). Each of the major diplodactylid clades was recovered with a different ecology with the New Caledonian and

New Zealand clades being reconstructed as scansorial (NC: SIMMAP pos. prob. = 1, ACE marginal probability = 0.99/ NZ: SIMMAP pos. prob. = 0.4, ACE marginal probability = 0.37), and the core Australian clade as arboreal (SIMMAP pos. prob. = 0.41, ACE marginal probability = 0.42). SIMMAP estimated 43.8 changes in ecology across the diplodactyloid tree with the highest number of changes being transitions to arboreal/rupicolous and arboreal from other ecologies (table 4). Model comparisons with OUWIE selected the OUMV model with multiple $\sigma^2$ and examination of $\sigma^2$ revealed that arboreal lineages exhibit the highest rates of body-size evolution ($\sigma^2 = 0.26$) followed by the grass-swimming pygopodids ($\sigma^2 = 0.1$) (table 5).

*Detecting Convergence with Macroevolutionary Models*

The Hansen model in SURFACE detected 28 shifts in morphospace across carphodactylids and diplodactylids with a total *k'* = 22 distinct regimes. Of these 22 identifiable regimes, 6 were found to be convergent with more than one lineage approaching the same θ, resulting in a total of 12 shifts to the same adaptive peak. Overall, the Hansen model performed well with a 369.4 unit improvement in the AICc score during the forward phase and an additional 46.6 unit increase during the backward phase. The contribution of individual PCs to AICc improvement was negligible, with PC1 seemingly contributing the most to the combined ΔAICc (figure 14). Examination of the selection parameter α reveals that traits ranged from 67.3 to 469.9 in terms of strength of directed evolution with PC5 (forearm length) having the highest estimate of α followed by PC2 (head length: 335.4). The backward phase of SURFACE suggests that intraclade convergence is relatively more common than interclade convergence for these two families (figure 15). We found no evidence that the core Australian diplodactylids occupied the same optima as representatives from other clades nor is there any signature that any carphodactylids have converged on similar phenotypes as diplodactylids. Within the core Australian diplodactylids there is a single convergent regime where *Diplodactylus pulcher* and *Rhynchoedura* were found to have shifted to the same regime. We also found that the basal members of the knob-tail clade (*Carphodactylus* and *Uvidicolus*) converged on the same optima as *Phyllurus* (all species excluding *P. amnicola*). However, the New Caledonian clade shows exceedingly high levels of convergence, with exemplars sharing optima with other members of the same clade as well as with representatives from the New Zealand clade and the genus *Pseudothecadactylus* (figure 15). Simulations in SURFACE revealed that the empirical estimates of the number regime shifts and proportion of convergent regimes were not significantly different from the BM and OU1models, but significantly greater than non-convergent Hansen simulations (table 6).

Implementation of the phylogenetic lasso in l1OU yielded 17 shifts in morphospace across the diplodactyloid phylogeny, a substantially lower estimate than that indicated by SURFACE. Most of the shifts inferred by l1OU are congruent (47%) with those recovered by SURFACE though a number of intraclade shifts differ between the two algorithms (figure 16). l1OU found shifts along the branches leading to *Mniarogekko jalu*, *Strophurus wellingtonae*, *S. taeniatus*, *Lucasium maini*, and *L. stenodactylum*, all shifts that were undetected by SURFACE. However, l1OU failed to find several shifts detected by SURFACE including one at the base of the broad-toed New Zealand clade, many within the core Australian diplodactylids, within *Phyllurus*, shifts within *Bavayia*, and one at the base of *Dierogekko*. Bootstrap analysis provided strong statistical support for each of the shift configurations, with all shifts receiving a bootstrap value of 70 or higher (figure 16). Estimates of α were markedly different from those estimated by SURFACE and ranged from 0.3 (pPC5) to 7.13 (pPC6).

## Discussion

*Evolution of Ecomorphological Diversity*

Diplodactyloid geckos demonstrate an extraordinary array of phenotypes and associated ecologies, characteristics that are reflected in the complex macroevolutionary history of this clade. We find strong evidence that different phenotypic traits are evolving under different macroevolutionary processes and that the variation of some trait proportions (i.e. relative head size, relative toe width, etc.) are tied to ecology. Our finding that body-size (svl) explained the largest proportion of variance in our ecomorphological analyses agrees with the findings of most multivariate ecomorphological studies, though this trait explains substantially less of the variance in our dataset due to the extremely high morphological diversity of diplodactyloids (Mahler *et al.*, 2013; Ingram & Kai, 2014). Phylomorphspace of diplodactyloids is heavily influenced by phylogeny, with carphodactylids and diplodactylids being clearly distinguished by all pPC axes except pPC1 (svl). All other pPCs yield stronger ties to ecology with the terrestrial diplodactylids (*Diplodactylus*, *Lucasium*, and *Rhynchoedura*) all clustering on small-headed, narrow-toed end of morphospace while *Strophurus* and the largely arboreal and scansorial New Caledonian and New Zealand taxa cluster in the broad-toed, large-headed region. *Oedura* are typically rupicolous and bear relatively long toes, resulting in nearly all species being placed between the terrestrial and arboreal/scansorial taxa. While largely arboreal and scansorial, members of the *Amalosia – Hesperoedura* group do not cluster with the other arboreal taxa. The lack of overlap in morphospace among the arboreal taxa strongly suggests a that generalized broad-toed arboreal ecomorph does not exist but rather the generalized morphology of padded geckos allows them to explore other regions of morphospace without being forced to abandon arboreality. The Top End *Oedura marmorata* complex (including *O. bella* and *O. gemmata*) are somewhat distinct from their congeners along most pPC axes, with somewhat longer limbs and narrower toes. This trend may be the result of increased rock dwelling and the placement of other *Oedura* near the *Amalosia* group is likely due to a suite of plesiomorphic traits that led to the four genera being lumped together (Revell *et al.*, 2007; Oliver *et al.*, 2012). Nearly all of the leaf-tailed carphodactylids (*Phyllurus* and *Saltuarius*) are rupicolous and cluster separately from the terrestrial *Nephrurus* group, largely a result of the latter having comparatively massive heads for dealing with hard-bodied prey.

We find moderate support for diplodactyloids being ancestrally rupicolous in all reconstruction analyses. This pattern fits well with Australian climatic history as the region was dominated by tropical savannah and mesic vegetation until the mid-Neogene, being somewhat reminiscent of the modern monsoonal tropics of northern Australia in terms of vegetation (Byrne *et al.*, 2008; Bowman *et al.*, 2010; Byrne *et al.*, 2011). If this is the case, standing stony outcrops would have been ideal hiding places for nocturnal geckos, regardless of the presence of toepads. The New Caledonian and New Zealand diplodactylids were reconstructed as scansorial vegetation specialists with unambiguous and moderate support, respectively. All species in both clades as well as *Pseudothecadactylus* are characterized by possessing relatively large, broad toepads with no separate apical scansors and prehensile tails tipped with adhesive lamellae. Despite these morphological similarities, these three clades took very different trajectories in regards to ecological diversification despite being descended from a rupicolous ancestor. *Pseudothecadactylus* diverged very little from the ancestral ecology, with a single species, *P. australis*, transitioning to arboreality. This transition was likely accompanied by drastic morphological divergence as this species is easily distinguished from its two congeners (Oliver *et al.*, 2014). In contrast to the conservative ecology of their sister taxon, the New Caledonian clade transitioned to scansoriality with at least three transitions to arboreality and a single transition to

scansoriality/rupicoly. The New Zealand radiation, however, exhibits a somewhat more complex history in terms of substrate specialization, with a single transition to arboreality and at least three shifts to scansoriality/rupicoly. The discordance in substrate specialization between the two Tasmantis lineages is most likely a reflection of the geologic and climatic histories of these two related, but vastly different archipelagos. Both islands systems, particularly New Caledonia, were affected by the Oligocene drowning, resulting in much of if not all of their modern biotas being composed of recent overwater dispersals (Smith *et al.*, 2007; Grandcolas *et al.*, 2008; Chapple *et al.*, 2009; Murienne, 2009; Espeland & Murienne, 2011; Nielsen *et al.*, 2011; Pepper *et al.*, 2016; Skipwith *et al.*, 2016). New Caledonia experienced extensive orogenesis during the Eocene, though the elevational gradient is somewhat modest with the highest peak being a meagre ~1600m (Bauer & Sadlier, 2000; Cluzel *et al.*, 2001; Cluzel *et al.*, 2012). The region has been relatively stable since its proposed emergence ~37 My and the tropical Mediterranean climate has been largely maintained despite post-Oligocene climatic oscillations (Nattier *et al.*, 2013). New Zealand has had a far more complex geologic history with extensive mountain-building during the Neogene, and with peaks exceeding 3700m (Landis *et al.*, 2008). Furthermore, recent orogenesis altered New Zealand's post Oligocene cooling warm/temperate climate to a much cooler one after Pliocene-Pleistocene glacial formation (Pepper *et al.*, 2016). The proliferation of serpentine soils during the Cenozoic permitted the expansion of maquis vegetation that now dominated two-thirds of New Caledonia's flora, an axis that may have allowed for the rapid diversification of the numerous scansorial taxa in the New Caledonian lineages. The relictual distribution sclerophyll and humid forests in New Caledonia may have granted the giants of *Rhacodactylus*/*Mniarogekko* and the larger-bodied *Bavayia cyclura* group to adapt to near exclusive arboreal ecologies. The cooler climate and comparatively high topographical complexity of New Zealand likely forced the New Zealand radiation to explore other substrates. This is evidenced by members of the *Mokopirirakau*/*Dactylocnemis* assemblage being tied to rocky areas, sometimes coastal, and the broad-toed clade making multiple transitions to the higher canopy, which is reminiscent of the unrelated New Caledonian giants.

The core Australian diplodactylids and *Crenadactylus* represent a far more ecologically diverse fauna than either of the Tasmantis radiations, though our estimates suggest that the generation of this diversity has occurred over a much longer timescale. There is extremely high phylogenetic signal for substrate in this group, with nearly all members of *Oedura* being rupicolous and the *Diplodactylus*-*Lucasium* group being exclusively terrestrial. Both *Strophurus* and *Crenadactylus* contain graminicolous species found almost exclusively on spinifex bunch grass (*Triodia*), with phenotypes somewhat reminiscent of the Greater Antillean twig-specialist *Anolis* ecomorphs. These geckos are primarily restricted to the relictual mesic regions of Australia where bunch grass dominates open savannah. The transition from graminicoly to terrestriality in *Crenadactylus occellatus* may be tied to isolation in the recent Australian Arid Zone. Most *Oedura* have in all likelihood retained the ancestral condition of rupicoly and species diversity is highest in the northern monsoonal and wet tropics, suggesting that these climatically stable biomes have done little to force this clade to expand its morphological and ecological envelope. One might suspect that the recent emergence and expansion of the AAZ has influenced the origin and proliferation of terrestrial carphodactylids and diplodactylids. Our divergence dating and ancestral state reconstructions suggest that this may not be the case as both the *Nephrurus* and *Diplodactylus* – *Lucasium* groups were recovered as substantially older than the development of this biome (31 and 36 My, respectively). Rather, we propose that terrestriality evolved very early in these lineages

and that the expansion of the AAZ opened up niche space within which terrestrial, reduced-pad/padless diplodactyloids could explore and diversify.

Investigation of the relationship between body-size evolution and ecology with OU-based Hansen models revealed heterogeneity in trait diversification and our *a-priori* ecological groupings. Here, we found that arboreal taxa had higher rates of body size evolution than any of the other ecological groups. This pattern is due to the wide range of body-sizes present in this grouping (49 – 280 mm svl), with both of the extremes being represented by New Caledonian species. In fact, while arboreal species are present in other clades, nearly half of those in our dataset are from the New Caledonian radiation. This clade is exemplified by short internal branches, which in turn resulted in bolstered estimates of the rate of trait evolution. We found that the grass-swimming pygopodids had the next highest rate of undirected body-size evolution, with a five-fold difference between species (75 – 311 mm svl). Rapid increase in body-size in limbless squamates is well documented. In the case of pygopodids, the increase in trunk vertebrae associated with limb loss may have opened a corridor for this clade to greatly increase the rate of body-size evolution (Lee, 1998). Conversely, fossorial taxa demonstrated the lowest rate of body-size evolution. *Aprasia*, the only fossorial genus represented in our dataset, is remarkably conserved along this axis. It should be noted that we were able to include less than half of the *Aprasia* described species and this non-random sampling may have resulted in long branches, whereas more complete sampling would have been interspersed with shorter internal nodes. Furthermore, we were unable to sample the fossorial pygopodid *Ophidiocephalus*. While the placement of this genus in our analyses, be it with *Aprasia* or the *Pletholax – Pygopus* clade, may have influenced our ancestral state reconstructions, we are confident that our estimates of body-size evolution for our *a priori* ecological groups were unaffected. Being a rather small pygopodid, *Ophidiocephalus* is comparable in size with most *Aprasia*, thus our finding that fossorial species are rather conserved in body-size is likely robust to taxonomic sampling. We propose that while arboreal and grass-swimming diplodactyloids have experienced little constraint in the way of body-size evolution, subterranean taxa may be under higher selective pressures to maintain comparatively small body size for fossoriality. These findings suggest that graminicolous taxa (*Strophurus taeniatus* group and *Crenadactylus rostralis* group) are also likely under this selective pressure to retain small body size to facilitate locomotion through dense, thin vegetation.

*Adaptive Regimes in Diplodactyloids*

Our investigation of phenotypic convergence using Hansen models revealed that not only have there been numerous shifts in morphospace across the carphodactylid-diplodactylid tree, but that convergence was widespread. Under these models, we were able to determine that several lineages have adapted to multiple adaptive peaks. We find an exceedingly high number of shifts in morphospace for these two families, 28 under stepwise AICc and 17 using the phylogenetic lasso, with most shifts being seen in the Diplodactylidae (SURFACE 78.6%, l1OU 82.4%). Our simulations evidence that the diplodactyloids exhibit a higher amount of convergence than would be expected under no stabilizing selection, but under random walk (BM) or single optimum OU processes. In the BM, OU1, and non-convergent Hansen models, taxa occupying the same trait space is attributed to phenotypic constraint and not independent colonization of the same adaptive peak due to similar selective pressures. Thus, these findings make a strong case that phenotypic diversification in carphodactylids and diplodactylids is subject to some degree of determinism. Unlike the Greater Antillean *Anolis* or *Sebastes* rockfishes, we find that interclade convergence is

relatively rare in diplodactyloids, being greatly exceeded by intraclade convergence (Ingram & Mahler, 2013; Mahler *et al.*, 2013; Ingram & Kai, 2014).

Carphodactylids are morphologically and ecologically diverse and do not overlap with the mostly padded diplodactylids in morphospace. This is likely the result of the former possessing relatively short, padless toes and proportionally robust heads, traits that are comparatively uncommon among diplodactylids. It follows that SURFACE found no signature that any carphodactylid and diplodactylid lineages had converged on the same adaptive peak. However, the genera *Carphodactylus* and *Uvidicolus* were found to be convergent to all *Phyllurus* except *P. amnicola*. This may be attributable to *P. amnicola* being somewhat longer-snouted than its congeners, sharing the same morphospace as the larger-bodied *Saltuarius*. However, we recognize that this may be a spurious finding with little biological significance as these three genera are ecologically distinct. Most *Phyllurus* are strictly rupicolous, while *Carphodactylus* and *Uvidicolus* are scansorial and terrestrial, respectively. Furthermore, our inability to include tail measurements may have heavily biased pPCA loadings onto cranial measurements, as these three genera possess extremely divergent tail morphologies that are ecologically informative.

Within diplodactylids, we found a great deal of heterogeneity in the proportion of nodes that had experienced shifts in morphospace between major clades. Within the core Australian diplodactylids, the largest clade, only 18.4% of nodes contained shifts in contrast to 29.4% of nodes in the New Caledonian clade. While the core Australian diplodactylids are morphologically diverse and occupy a much larger region of morphospace than any of the other diplodactylid clades, only a single convergent regime was recovered. SURFACE found that adaptive regimes had only been converged upon twice (4% of nodes) by *Diplodactylus pulcher* and *Rhynchoedura ornata*. Both species are exemplified by small heads with pointed snouts and toes bearing reduced pads or are completely padless, presumably specializing in small arthropods and larvae. In contrast to the carphodactylids and core Australian diplodactylids, several New Caledonian diplodactylid clades were found to occupy the same adaptive peaks with the distantly related *Pseudothecadactylus* and New Zealand clade. The morphological phylogenetics of these three lineages have been historically problematic and it is not surprising that *Oedodera*, *Paniegekko*, and the *Bavayia cyclura* group were recovered as convergent with the smaller members of broad-toed *Woodworthia* clade. In fact, the placement of *Pseudothecadactylus australis* with *Rhacodactylus/Mniarogekko* and the *Bavayia sauvagii* group with *Dierogekko* further falls in line with previous phylogenetic hypotheses relying solely on morphology (Sadlier, 1989; Bauer, 1990; Bauer *et al.*, 2006). All of the interclade convergence events detected by SURFACE between the New Zealand, New Caledonia, and *Pseudothecadactylus* tie heavily to substrate, where all taxa are scansorial or arboreal. Traits with the highest signatures of adaptive evolution ($\alpha$) were tied to diet and locomotion which, by proxy, reflects substrate choice. All of the scansorial and arboreal members of these lineages have very broad, spatulate toepads and proportionally large heads when compared to most members of the core Australian clade. The possession of the former may be highly advantageous for efficient climbing in complex vegetation and examination of trait space reveals that only some members of the largely arboreal *Amalosia* group possess broader toepads within the Diplodactylidae. Large heads are widespread across these clades, particularly among the New Caledonian giants, which are presumably adaptations for consuming comparatively large prey. However, members of the Australian genus *Oedura* also consume large prey but possess comparatively modest size heads relative to body-size. Given that most *Oedura* species are rupicolous, it is conceivable that these species are constrained to have shorter heads in order to take advantage of the rocky crevices in which they take refuge.

The high levels convergence between and within the two Tasmantis clades and *Pseudothecadactylus* is likely the result of two phenomena. Both New Caledonia and New Zealand have experienced climatic oscillations during the Cenozoic, with Neogene cooling drastically changing the flora for both regions (Stevenson & Dodson, 1995; Hope & Pask, 1998; Lee *et al.*, 2001; Pintaud *et al.*, 2001; Stevenson & Hope, 2005; Nattier *et al.*, 2013; Pepper *et al.*, 2016). In the case of the broad-toed New Zealand taxa and the New Caledonian forms, the relative conservatism of phenotypes may have facilitated the rapid colonization of the same adaptive peaks. While similar adaptive pressures likely drove phenotypic convergence between these clades, constraint may have played a role in reducing the area of morphospace explored by both clades. In contrast, *Pseudothecadactylus* represents an ancient lineage where climatic stability has maintained a relatively conservative ecological breadth (Oliver *et al.*, 2014). The transition to arboreality in the *P. australis* lineage may be a direct result of an ancient vicariance event that led to the relictual distribution of the genus.

SURFACE is a powerful tool for detecting shifts in morphospace and convergent regimes occupied by disparate lineages, its power increasing both with taxa and independent traits (Ingram & Mahler, 2013). However, its reliance on stepwise AICc may result in the detection of biologically unrealistic shifts with high confidence. Our use of a single topology, while unavoidable, renders our inference of ecomorphological diversification in diplodactyloids subject to SURFACE's sensitivity to the order of peak shifts (Ingram & Kai, 2014; Khabbazian *et al.*, 2016). The implementation of the phylogenetic lasso in l1OU suggested significantly fewer shifts among carphodactylids and diplodactylids, with some degree of congruence between the two algorithms. Notable incongruences, particularly within *Lucasium* and the New Caledonian genera, are reminiscent of shifts detected by SURFACE when using pPCA scores under Brownian motion rather than Pagel's lambda. In fact, only 47% of the shifts proposed by l1OU agree with those detected by SURFACE. This incongruence can be attributed to the use of the more conservative pBIC in l1OU versus AICc in SURFACE, the latter of which has been attributed to the detection of unreasonably high shift configurations with high statistical support (Khabbazian *et al.*, 2016). Despite the conservative nature of the phylogenetic lasso, we defer to the shift configuration proposed by SURFACE. Based on our knowledge of the natural history and morphological diversity of diplodactyloids, many of the shifts detected by the Hansen model appear to be entirely reasonable. Rather, the incongruent shifts recovered by l1OU seem spurious and may be the result of the low variances of pPCs 6 and 7, which warrants further investigation. Most notable are the shifts along the *Mniarogekko jalu* and *Dierogekko baaba* branches. While these shifts receive strong bootstrap support, these species differ from their congeners primarily in body size and occupy the same morphospace as their respective sister taxa. Even more worrisome is the failure of l1OU to detect a shift along the *Diplodactylus pulcher* branch, a species that lies well outside of morphospace occupied by most other *Diplodactylus* and *Lucasium*. This may be the result of the difficulties in detecting the exact position of a shift along a branch when using the phylogenetically-uncorrelated residuals, where slightly different shift configurations along adjacent branches can be equally likely (Khabbazian *et al.*, 2016).

*Diplodactyloid Geckos as an Adaptive Radiation*

We find strong evidence that diplodactyloids represent an adaptive radiation with a much wider ecological and morphological breadth than the oft-cited *Anolis* radiation (Losos & Miles, 1994; Losos *et al.*, 1998; Schluter, 2000; Pinto *et al.*, 2008; Losos, 2009; Mahler *et al.*, 2010; Mahler *et al.*, 2013). While restricted to the Australasian region, diplodactyloids have radiated into a wide

array of niches unexplored by other geckos. Specialization to specific substrates seems to correspond broadly with shifts in ecomorphology within diplodactylids and carphodactylids. These shifts in ecology and morphology are likely the combination of vicariance and dispersal events to new climatic and vegetation regimes across the mainland and Pacific islands. We propose that the diplodactyloid radiation is a composite of both non-adaptive and adaptive radiations. Some clades, such as the Tasmantis diplodactylid and pygopodid radiations, are extremely diverse in terms of ecology and morphology, having explored a number of ecological niches and novel regions of morphospace during relatively short time-spans. Conversely, other clades, such as the *Amalosia*/*Nebulifera – Hesperoedura* clade and *Oedura*, are remarkably conserved despite their respective crown ages being comparable to more morphologically diverse diplodactyloid clades. Convergence to similar adaptive peaks are somewhat more common among closely related taxa but poorly documented across deeper timescales, though the exact mechanisms of this pattern are poorly understood (Schluter, 2000; Kassen, 2009). The high proportion of phenotypic shifts and shared adaptive peaks between the two Tasmantis radiations indicate that shared environmental pressures in combination with similar initial ecologies shaped the pattern of diverse phenotypes and widespread convergence seen today. While recent dispersal to Tasmantis resulted in some degree of ecological release for these two radiations, constraint may have restricted ecomorphological space, allowing diversification along different axes than for other diplodactyloids. The core Australian diplodactylids, while exhibiting substantially less convergence, are by far the most ecologically and phenotypically diverse of the limbed forms. This may reflect the relative environmental instability of mainland Australia, which increased ecological opportunity along different ecomorphological axes at the expense of shared adaptive peaks with other taxa.

## Literature Cited


Arbour, J.H. & Lopez-Fernandez, H. (2014) Adaptive landscape and functional diversity of Neotropical cichlids: implications for the ecology and evolution of Cichlinae (Cichlidae; Cichliformes). *Journal of Evolutionary Biology*, **27**, 2431-2442.

Bauer, A.M. (1990) Phylogenetic systematics and biogeography of the Carphodactylini (Reptilia: Gekkonidae). *Bonner Zoologische Monographien*, **30**, 1-218.

Bauer, A.M. & Sadlier, R.A. (2000) *The Herpetofauna of New Caledonia*. The Society for the Study of Amphibians and Reptiles, in cooperation with the Institut de recherche pour le développement, Ithaca, NY.

Bauer, A.M., Jackman, T., Sadlier, R.A. & Whitaker, A.H. (2006) A revision of the *Bavayia validiclavis* group (Squamata: Gekkota: Diplodactylidae), a clade of New Caledonian geckos exhibiting microendemism. *Proceedings of the California Academy of Sciences*, **57**, 503-547.

Beaulieu, J.M., Jhwueng, D.-C., Boettiger, C. & O'Meara, B.C. (2012) Modeling stablizing selection: Expanding the Ornstein-Uhlenbeck model of adaptive evolution. *Evolution*, **66**, 2369-2383.

Bollback, J.P. (2006) SIMMAP: Stochastic character mapping of discrete traits on phylogenies. *Bmc Bioinformatics*, **7**

Bowman, D.M.J.S., Brown, G.K., Braby, M.F., Brown, J.R., Cook, L.G., Crisp, M.D., Ford, F., Haberle, S., Hughes, J., Isagi, Y., Joseph, L., McBride, J., Nelson, G. & Ladiges, P.Y.

(2010) Biogeography of the Australian monsoon tropics. *Journal of Biogeography*, **37**, 201-216.

Byrne, M., Yeates, D.K., Joseph, L., Kearney, M., Bowler, J., Williams, M.A.J., Cooper, S., Donnellan, S.C., Keogh, J.S., Leys, R., Melville, J., Murphy, D.J., Porch, N. & Wyrwoll, K.H. (2008) Birth of a biome: insights into the assembly and maintenance of the Australian arid zone biota. *Molecular Ecology*, **17**, 4398-4417.

Byrne, M., Steane, D.A., Joseph, L., Yeates, D.K., Jordan, G.J., Crayn, D., Aplin, K., Cantrill, D.J., Cook, L.G., Crisp, M.D., Keogh, J.S., Melville, J., Moritz, C., Porch, N., Sniderman, J.M.K., Sunnucks, P. & Weston, P.H. (2011) Decline of a biome: evolution, contraction, fragmentation, extinction and invasion of the Australian mesic zone biota. *Journal of Biogeography*, **38**, 1635-1656.

Chapple, D.G., Ritchie, P.A. & Daugherty, C.H. (2009) Origin, diversification, and systematics of the New Zealand skink fauna (Reptilia: Scincidae). *Molecular Phylogenetics and Evolution*, **52**, 470-487.

Cluzel, D., Aitchison, J.C. & Picard, C. (2001) Tectonic accretion and underplating of mafic terranes in the Late Eocene intraoceanic fore-arc of New Caledonia (Southwest Pacific): geodynamic implications. *Tectonophysics*, **340**, 23-59.

Cluzel, D., Maurizot, P., Collot, J. & Sevin, B. (2012) An outline of the Geology of New Caledonia; from Permian-Mesozoic Southeast Gondwanaland active margin to Cenozoic obduction and supergene evolution. *Episodes*, **35**, 72-86.

Davis, A.M., Unmack, P.J., Pusey, B.J., Pearson, R.G. & Morgan, D.L. (2014) Evidence for a multi-peak adaptive landscape in the evolution of trophic morphology in terapontid fishes. *Biological Journal of the Linnean Society*, **113**, 623-634.

Espeland, M. & Murienne, J. (2011) Diversity dynamics in New Caledonia: towards the end of the museum model? *BMC Evolutionary Biology*, **11**, 254.

Esquerre, D. & Keogh, J.S. (2016) Parallel selective pressures drive convergent diversification of phenotypes in pythons and boas. *Ecology Letters*, **19**, 800-809.

Felsenstein, J. (1973) Maximum-Likelihood Estimation of Evolutionary Trees from Continuous Characters. *American Journal of Human Genetics*, **25**, 471-492.

Felsenstein, J. (1985) Phylogenies and the Comparative Method. *American Naturalist*, **125**, 1-15.

Grandcolas, P., Murienne, J., Robillard, T., Desutter-Grandcolas, L., Jourdan, H., Guilbert, E. & Deharveng, L. (2008) New Caledonia: A very old Darwinian island? *Philosophical Transactions of the Royal Society of London B Biological Sciences*, **363**, 3309-3317.

Hansen, T.F. (1997) Stabilizing selection and the comparative analysis of adaptation. *Evolution*, **51**, 1341-1351.

Hansen, T.F. (2012) Adaptive landscapes and macroevolutionary dynamics. *Adaptive Lanscape in Evolutionary Biology* (ed. by E. Svensson and R. Calsbeek), pp. 205-226. Oxford University Press, Oxford, UK.

Harmon, L.J., Weir, J.T., Brock, C.D., Glor, R.E. & Challenger, W. (2008) GEIGER: investigating evolutionary radiations. *Bioinformatics*, **24**, 129-31.

Harmon, L.J., Losos, J.B., Jonathan Davies, T., Gillespie, R.G., Gittleman, J.L., Bryan Jennings, W., Kozak, K.H., McPeek, M.A., Moreno-Roark, F., Near, T.J., Purvis, A., Ricklefs, R.E., Schluter, D., Schulte Ii, J.A., Seehausen, O., Sidlauskas, B.L., Torres-Carvajal, O., Weir, J.T. & Mooers, A.O. (2010) Early bursts of body size and shape evolution are rare in comparative data. *Evolution*, **64**, 2385-96.

Ho, L.S.T. & Ané, C. (2014) Intrinsic inference difficulties for trait evolution with Ornstein-Uhlenbeck models. *Methods in Ecology and Evolution*, **5**, 1133-1146.
Hope, G. & Pask, J. (1998) Tropical vegetational change in the late Pleistocene of New Caledonia. *Palaeogeography Palaeoclimatology Palaeoecology*, **142**, 1-21.
Ingram, T. & Mahler, D.L. (2013) SURFACE: detecting convergent evolution from comparative data by fitting Ornstein-Uhlenbeck models with stepwise Akaike Information Criterion. *Methods in Ecology and Evolution*, **4**, 416-425.
Ingram, T. & Kai, Y. (2014) The Geography of Morphological Convergence in the Radiations of Pacific *Sebastes* Rockfishes. *American Naturalist*, **184**, E115-E131.
Kassen, R. (2009) Toward a General Theory of Adaptive Radiation: Insights from Microbial Experimental Evolution. *Year in Evolutionary Biology 2009*, **1168**, 3-22.
Khabbazian, M., Kriebel, R., Rohe, K. & Ane, C. (2016) Fast and accurate detection of evolutionary shifts in Ornstein-Uhlenbeck models. *Methods in Ecology and Evolution*, **7**, 811-824.
Kluge, A.G. (1967) Higher taxonomic categories of gekkonid lizards and their evolution. *Bulletin of the American Museum of Natural History*, **135**, 1-59.
Kluge, A.G. (1987) Cladistic relationships in the Gekkonoidea (Squamata, Sauria). *Miscellaneous Publications Museum of Zoology University of Michigan*, i-iv, 1-54.
Landis, C.A., Campbell, H.J., Begg, J.G., Mildenhall, D.C., Paterson, A.M. & Trewick, S.A. (2008) The Waipounamu Erosion Surface: questioning the antiquity of the New Zealand land surface and terrestrial fauna and flora. *Geological Magazine*, **145**, 173-197.
Lee, D.E., Lee, W.G. & Mortimer, N. (2001) Where and why have all the flowers gone? Depletion and turnover in the New Zealand Cenozoic angiosperm flora in relation to palaeogeography and climate. *Australian Journal of Botany*, **49**, 341-356.
Lee, M.S.Y. (1998) Convergent evolution and character correlation in burrowing reptiles: towards a resolution of squamate relationships. *Biological Journal of the Linnean Society*, **65**, 369-453.
Losos, J.B. (2009) *Lizards in an Evolutionary Tree: Ecology and Adaptive Radiation of Anoles*. University of California Press.
Losos, J.B. & Miles, D.B. (1994) Adaptation, constraint, and the comparative method: phylogenetic issues and methods. *Ecological morphology: integrative organismal biology* (ed. by P.C. Wainwright and S.M. Reilly), pp. 60-98. University Chicago Press, Chicago.
Losos, J.B. & Ricklefs, R.E. (2009) Adaptation and diversification on islands. *Nature*, **457**, 830-836.
Losos, J.B., Jackman, T.R., Larson, A., de Queiroz, K. & Rodriguez-Schettino, L. (1998) Contingency and determinism in replicated adaptive radiations of island lizards. *Science*, **279**, 2115-2118.
Mahler, D.L., Revell, L.J., Glor, R.E. & Losos, J.B. (2010) Ecological Opportunity and the Rate of Morphological Evolution in the Diversification of Greater Antillean Anoles. *Evolution*, **64**, 2731-2745.
Mahler, D.L., Ingram, T., Revell, L.J. & Losos, J.B. (2013) Exceptional Convergence on the Macroevolutionary Landscape in Island Lizard Radiations. *Science*, **341**, 292-295.
Mirarab, S. & Warnow, T. (2015) ASTRAL-II: coalescent-based species tree estimation with many hundreds of taxa and thousands of genes. *Bioinformatics*, **31**, 44-52.

Mirarab, S., Reaz, R., Bayzid, M.S., Zimmermann, T., Swenson, M.S. & Warnow, T. (2014) ASTRAL: genome-scale coalescent-based species tree estimation. *Bioinformatics*, **30**, I541-I548.

Murienne, J. (2009) Testing biodiversity hypotheses in New Caledonia using phylogenetics. *Journal of Biogeography*, **36**, 1433-1434.

Nattier, R., Grandcolas, P., Pellens, R., Jourdan, H., Couloux, A., Poulain, S. & Robillard, T. (2013) Climate and Soil Type Together Explain the Distribution of Microendemic Species in a Biodiversity Hotspot. *Plos One*, **8**

Nielsen, S.V., Bauer, A.M., Jackman, T.R., Hitchmough, R.A. & Daugherty, C.H. (2011) New Zealand geckos (Diplodactylidae): Cryptic diversity in a post-Gondwanan lineage with trans-Tasman affinities. *Molecular Phylogenetics and Evolution*, **59**, 1-22.

O'Meara, B.C., Ane, C., Sanderson, M.J. & Wainwright, P.C. (2006) Testing for different rates of continuous trait evolution using likelihood. *Evolution*, **60**, 922-933.

Oliver, P.M., Laver, R.J., Smith, K.L. & Bauer, A.M. (2014) Long-term persistence and vicariance within the Australian Monsoonal Tropics: the case of the giant cave and tree geckos (*Pseudothecadactylus*). *Australian Journal of Zoology*, **61**, 462-468.

Oliver, P.M., Bauer, A.M., Greenbaum, E., Jackman, T. & Hobbie, T. (2012) Molecular phylogenetics of the arboreal Australian gecko genus *Oedura* Gray 1842 (Gekkota: Diplodactylidae): Another plesiomorphic grade? *Molecular Phylogenetics and Evolution*, **63**, 255-264.

Pepper, M.R., Keogh, J.S. & Chapple, D.G. (2016) Molecular biogeography of Australian and New Zealand reptiles and amphibians. (ed. by M.C. Ebach), pp. 295-328. CRC Press.

Pintaud, J.C., Jaffré, T. & Puig, H. (2001) Chorology of New Caledonian palms and possible evidence of Pleistocene rain forest refugia. *Comptes Rendus De l'Académie Des Sciences Serie Iii-Sciences de la Vie-Life Sciences*, **324**, 453-463.

Pinto, G., Mahler, D.L., Harmon, L.J. & Losos, J.B. (2008) Testing the island effect in adaptive radiation: rates and patterns of morphological diversification in Caribbean and mainland Anolis lizards. *Proceedings of the Royal Society B-Biological Sciences*, **275**, 2749-2757.

Revell, L.J. (2009) Size-Correction and Principal Components for Interspecific Comparative Studies. *Evolution*, **63**, 3258-3268.

Revell, L.J., Johnson, M.A., Schulte, J.A., II, Kolbe, J.J. & Losos, J.B. (2007) A phylogenetic test for adaptive convergence in rock-dwelling lizards. *Evolution*, **61**, 2898-2912.

Sadlier, R.A. (1989) *Bavayia validiclavis* and *Bavayia septuiclavis*, two new species of gekkonid lizard from New Caledonia. *Records of the Australian Museum*, **40**, 365-370.

Schluter, D. (2000) *The Ecology of Adaptive Radiation*. Oxford University Press, New York.

Simpson, G.G. (1953) *The Major Features of Evolution*. Columbia University Press, New Yor, NY.

Skipwith, P.L., Bauer, A.M., Jackman, T.R. & Sadlier, R.A. (2016) Old but not ancient: coalescent species tree of New Caledonian geckos reveals recent post-inundation diversification. *Journal of Biogeography*, **43**, 1266-1276.

Smith, S.A., Sadlier, R.A., Bauer, A.M., Austin, C.C. & Jackman, T. (2007) Molecular phylogeny of the scincid lizards of New Caledonia and adjacent areas: Evidence for a single origin of the endemic skinks of Tasmantis. *Molecular Phylogenetics and Evolution*, **43**, 1151-1166.

Stevenson, J. & Dodson, J.R. (1995) Palaeoenvironmental evidence for human settlement of New Caledonia. *Archaeology in Oceania*, **30**, 36-41.

Stevenson, J. & Hope, G. (2005) A comparison of late Quaternary forest changes in New Caledonia and northeastern Australia. *Quaternary Research*, **64**, 372-383.
Uyeda, J.C., Caetano, D.S. & Pennell, M.W. (2015) Comparative Analysis of Principal Components Can be Misleading. *Systematic Biology*, **64**, 677-689.
Wilson, S. & Swan, G. (2013) *A Complete Guide to Reptiles of Australia*, 4th edn. New Holland Publishers, Chatswood, Australia.
Yang, Z.H. (2007) PAML 4: Phylogenetic analysis by maximum likelihood. *Molecular Biology and Evolution*, **24**, 1586-1591.

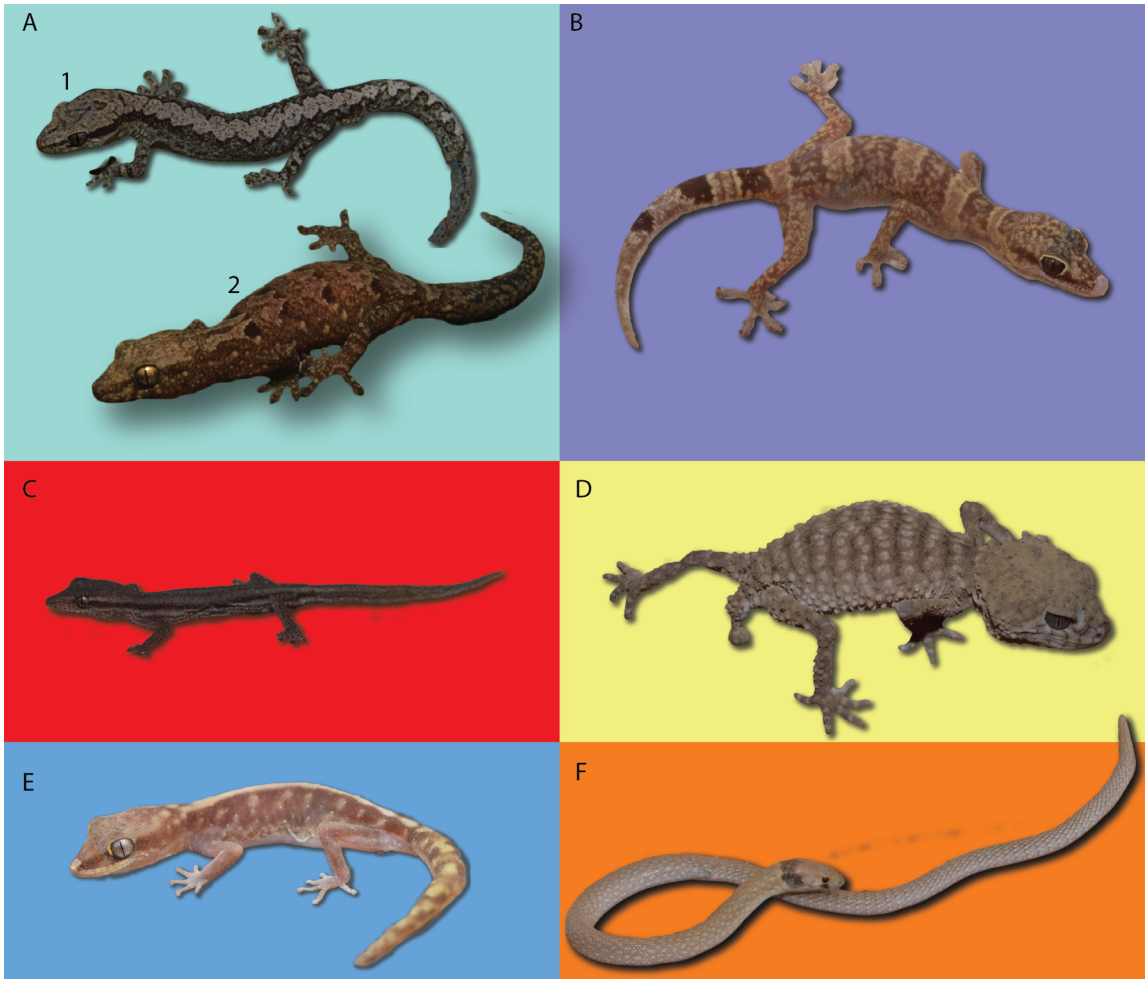


**Figure 9**: Representatives of some of the *a priori* ecomorphs described in this study. A) Generalized arboreal: 1. *Amalosia rhombifer*. 2. *Bavayia sauvagii*. B) Rupicolous: *Oedura murrumanu*. C) Generalized scansorial: *Crenadactylus rostralis*. D) Large-headed terrestrial: *Nephrurus sheai*. E) Small-headed terrestrial: *Lucasium stenodactylum*. F) Grass-swimming: *Pygopus schraderi*. **Note:** We were unable to obtain images of fossorial pygopodids. All photographs taken by Phillip L. Skipwith.

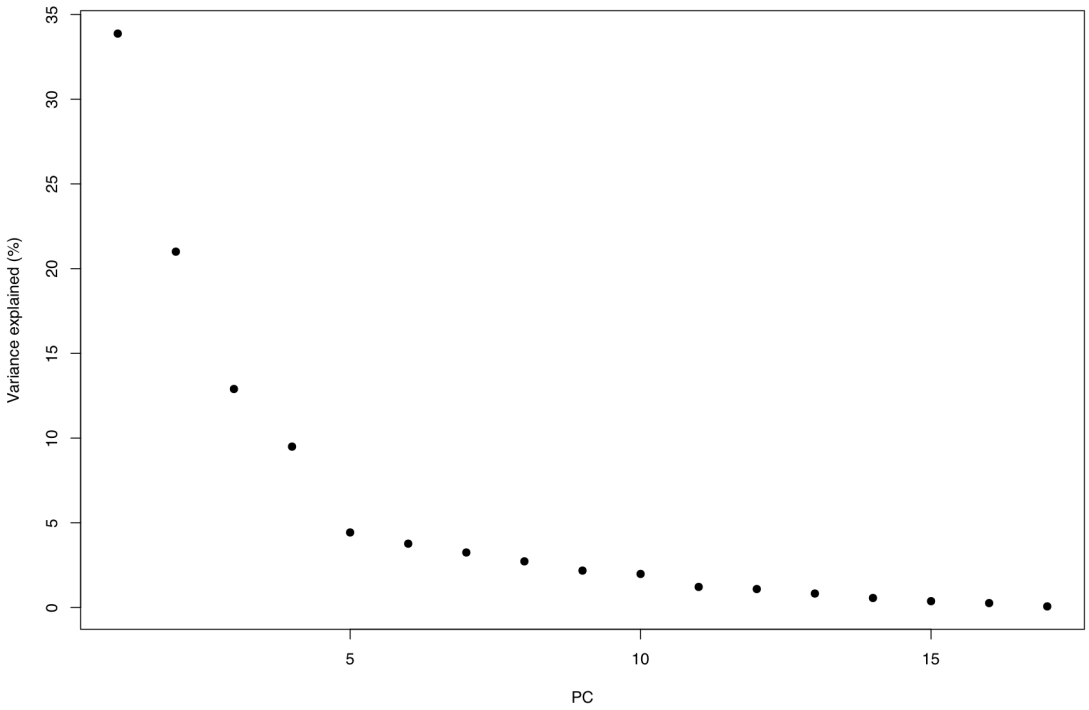


**Figure 10**: Broken stick plot of eigenvalues of pPCA. We opted to include the top 7 pPCs in all downstream continuous trait analyses.

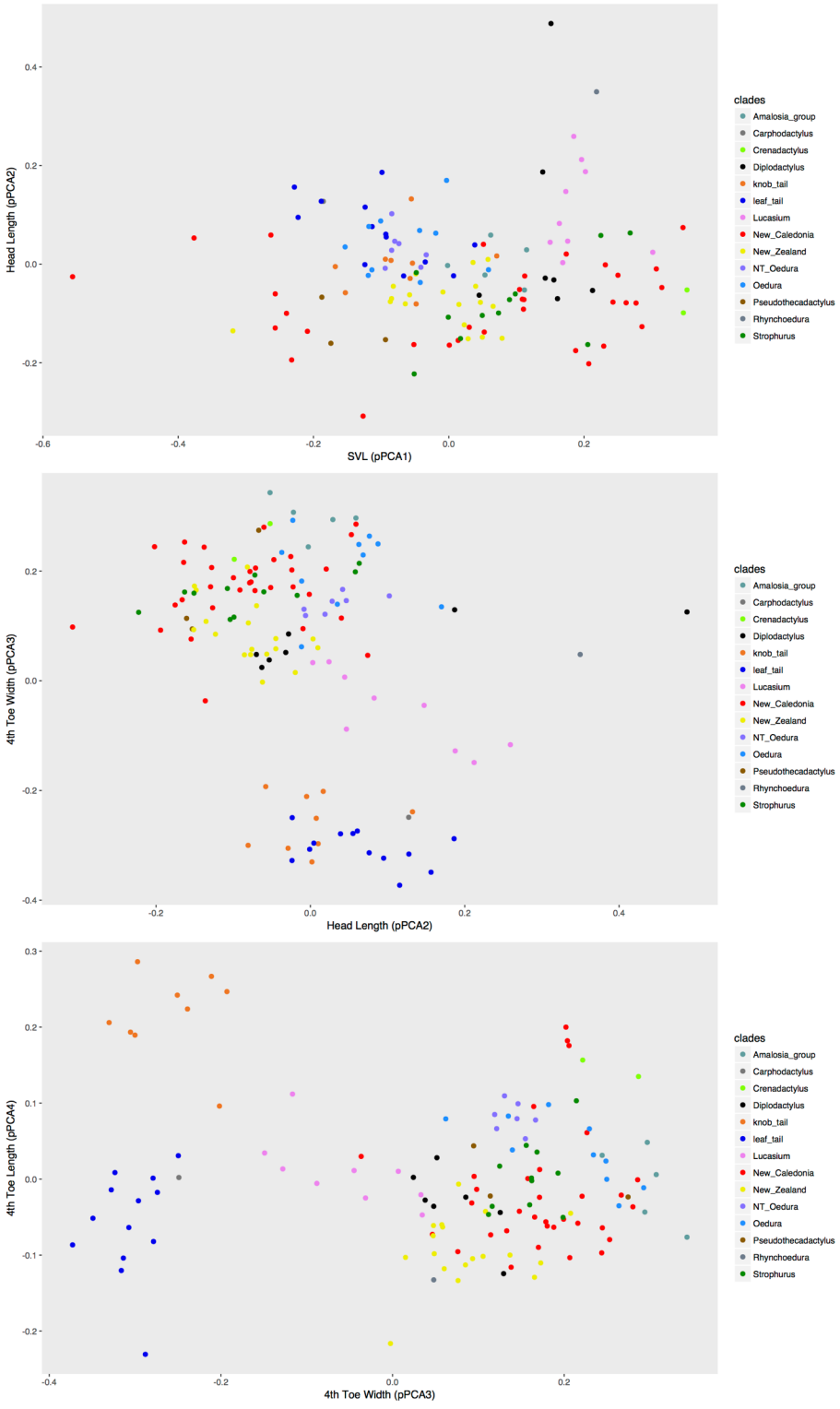


**Figure 11**: pPCA plots of pPCs 1-3. Colored by clade.

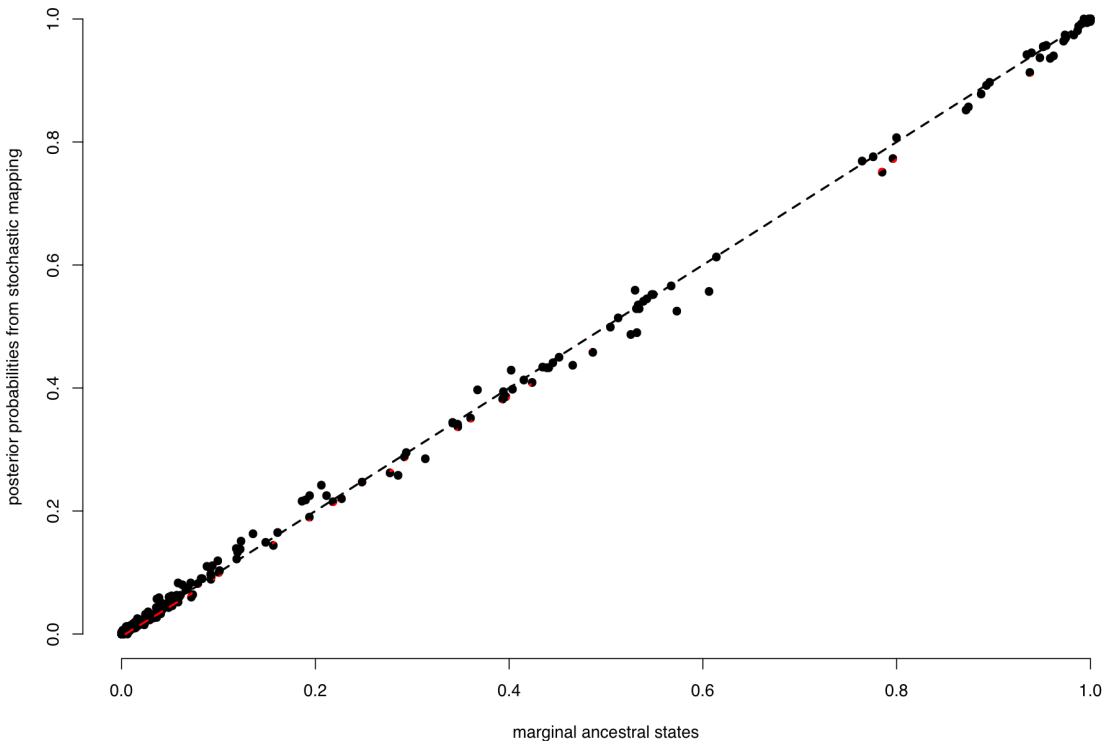


**Figure 12**: Comparison of ancestral marginal states from ACE and the stochastic mapping posterior probabilities from SIMMAP.

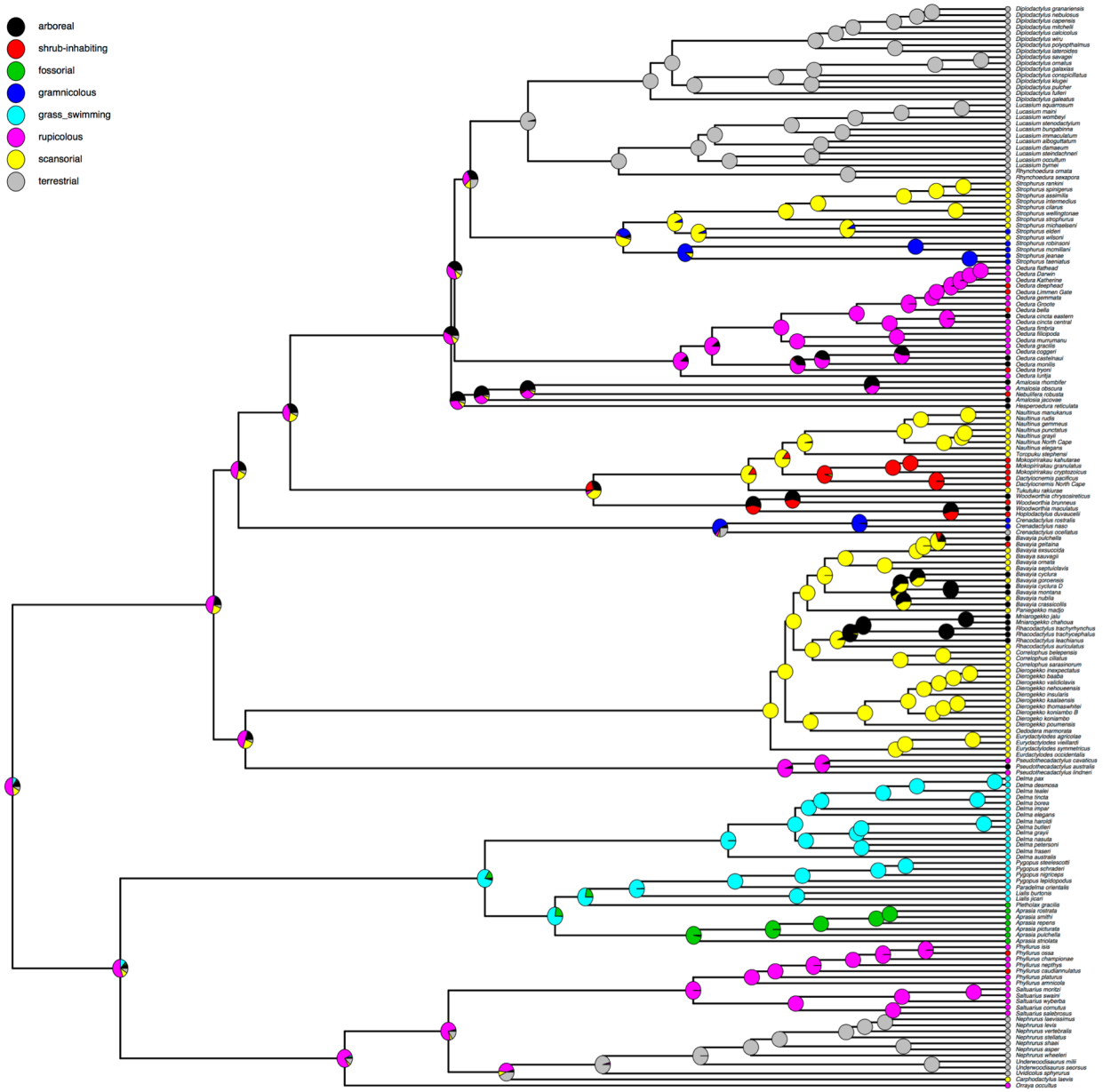


**Figure 13**: Stochastic mapping ancestral state reconstruction from SIMMAP. We opted to not display the results from ACE as they are identical.

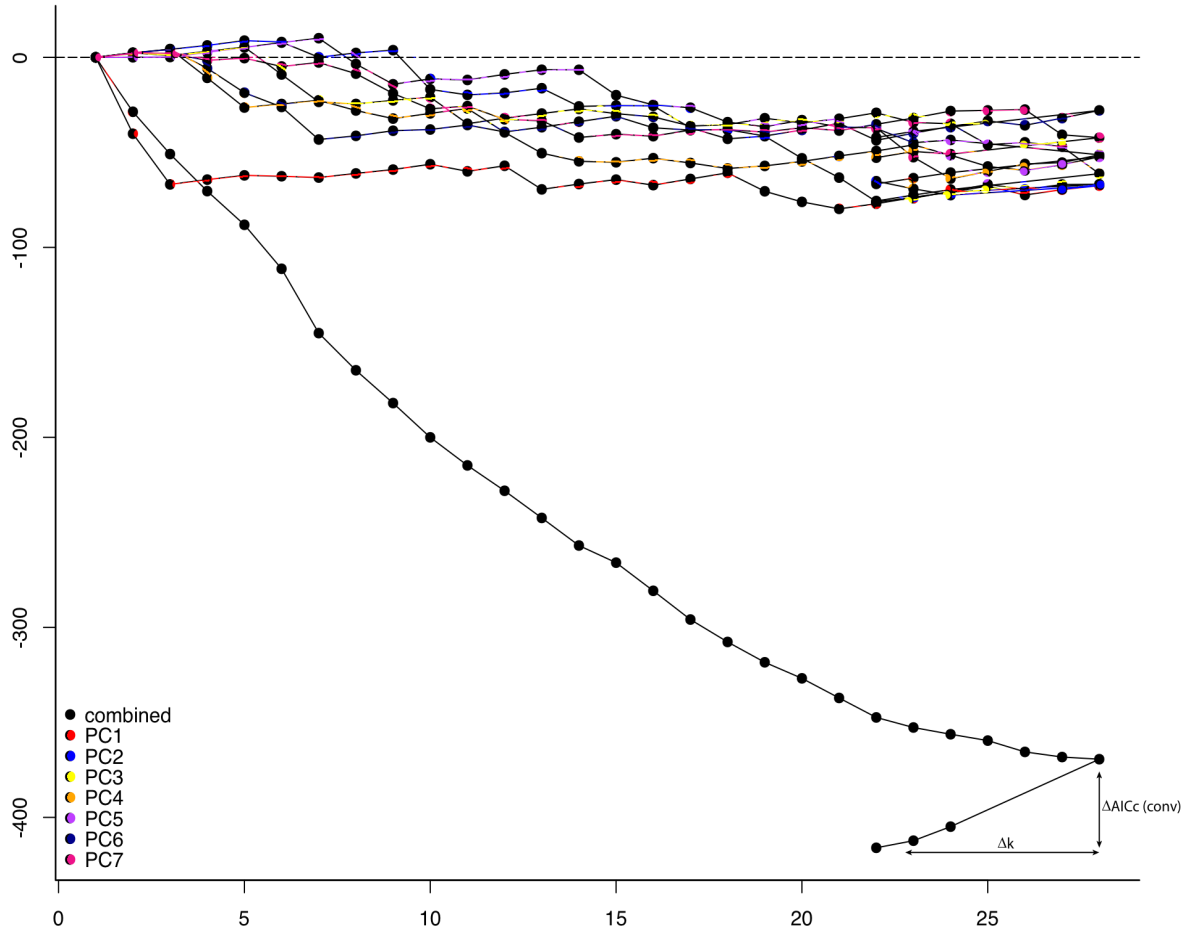


**Figure 14**: Line graph depicting how the AICc changed during the backward phase of SURFACE for each of the variables run and the change in AICc for the combined variables.

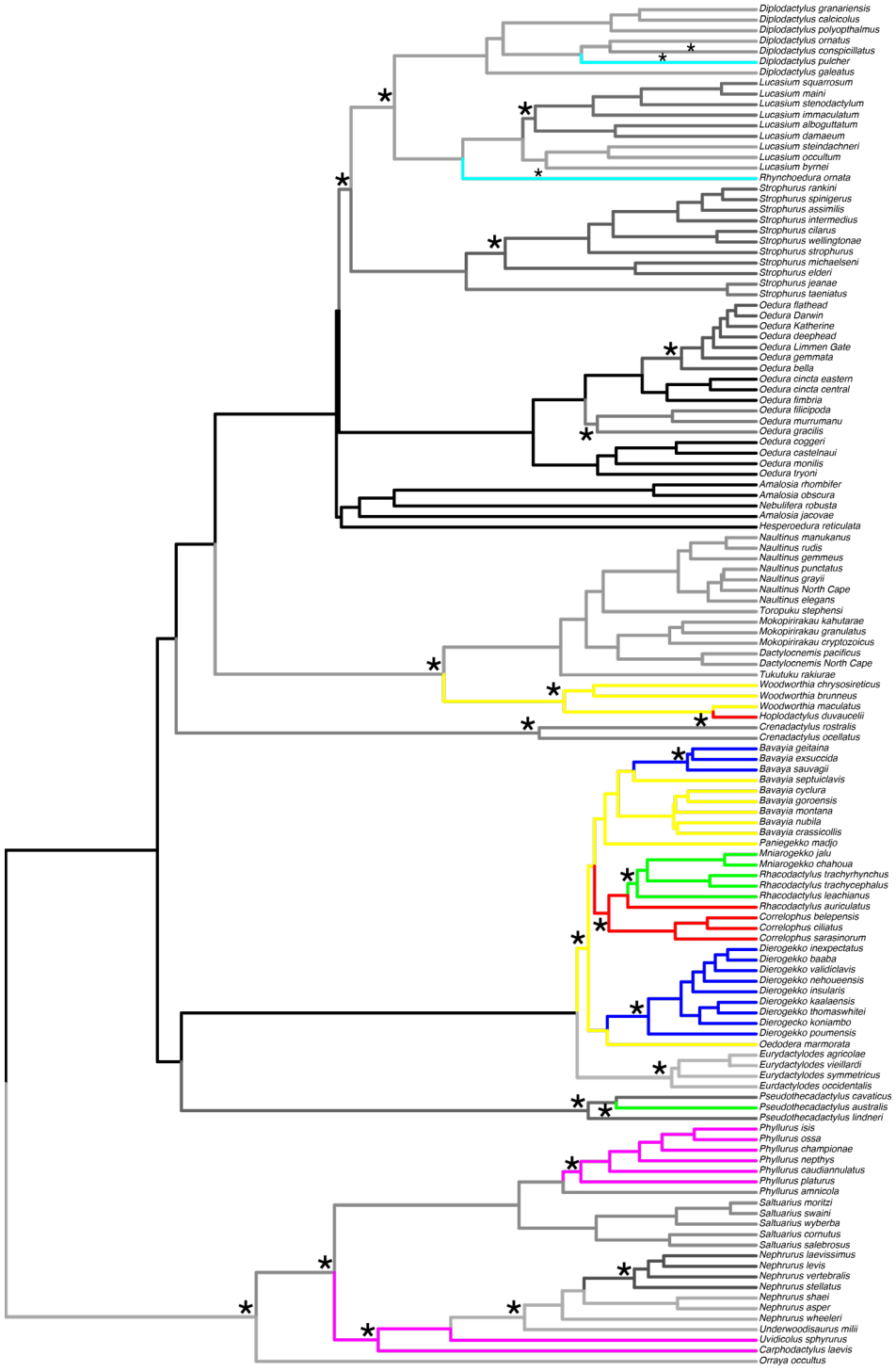


**Figure 15**: Results from the backward phase of SURFACE, revealing 28 regime shifts in morphospace and 6 regimes that have been converged on at least twice by distantly related species. All grayscale branches are non-convergent regimes while colored branches are convergent. Regime shifts are denoted with '*' at the nearest node.

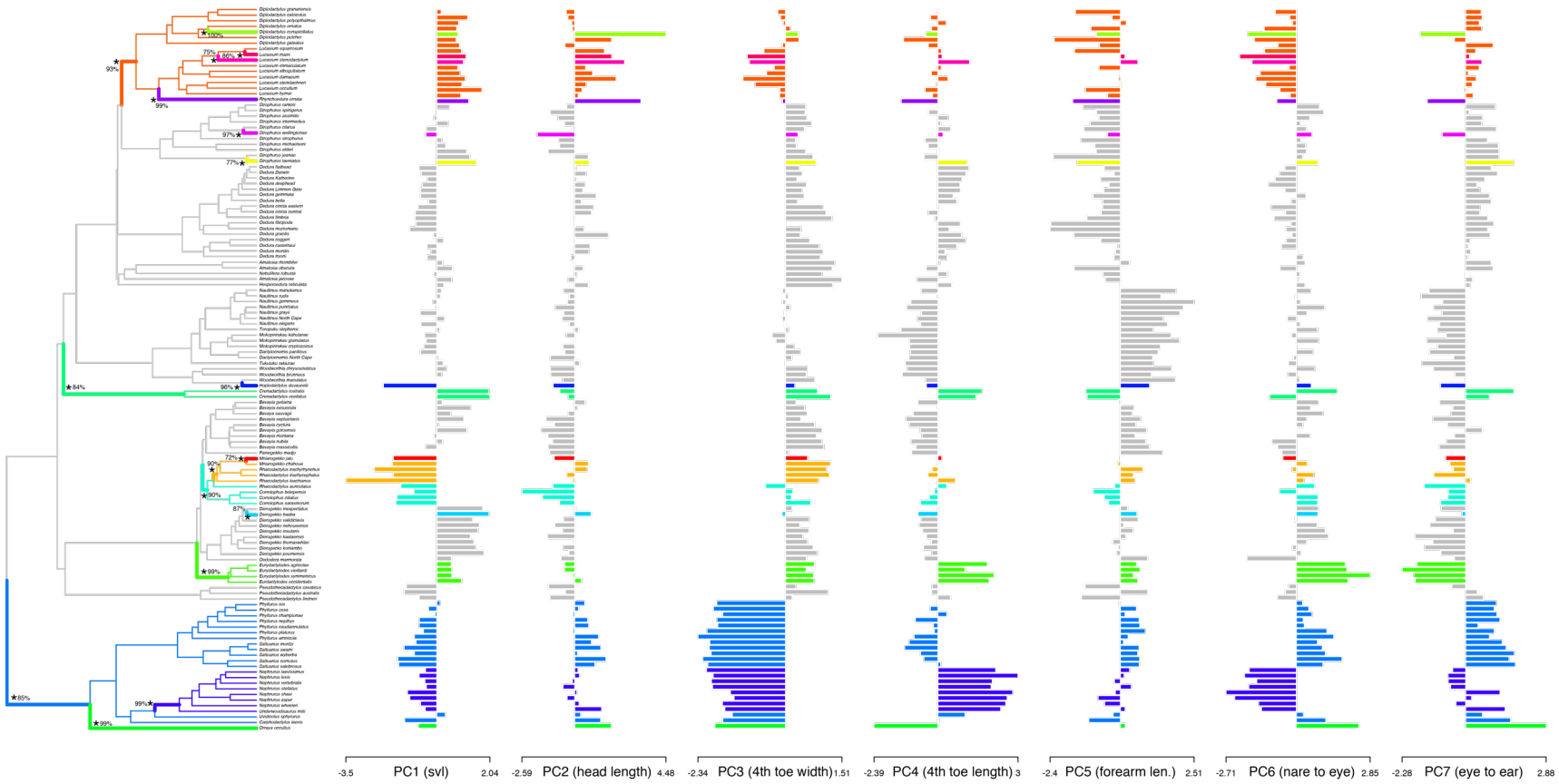


**Figure 16**: Results from the backward phase of l1OU under pBIC, revealing only 17 regime shifts in morphospace but no quantifiable signature of convergence. Numbers on node correspond to bootstrap proportions for each shift. Barplots to right are the loadings of each trait for species from the original pPCA.

**Table 3**: AIC weights (AICw) for models of trait evolution for diplodactyloids. Bold numbers indicate the best model.

| | Head width | Head depth | Head length | Retroarticular length | Trunk length | Forearm length | Tibia length | Inernarial distance | Nares -eye | Eye diameter | Eye-ear | Interorbital | 4th finger width | 4th finger length | 4th toe width | 4th toe length | SVL |
|---|---|---|---|---|---|---|---|---|---|---|---|---|---|---|---|---|---|
| BM | **0.42** | 0.00 | 0.00 | **0.43** | 0.00 | 0.**41** | **0.39** | **0.40** | **0.45** | 0.09 | 0.16 | 0.00 | **0.47** | **0.38** | **0.44** | **0.32** | **0.47** |
| OU | 0.15 | **1.00** | **1.00** | 0.16 | **1.00** | 0.16 | 0.22 | 0.15 | 0.16 | **0.83** | **0.70** | **1.00** | 0.17 | 0.14 | 0.18 | 0.27 | 0.17 |
| EB | 0.28 | 0.00 | 0.00 | 0.25 | 0.00 | 0.28 | 0.25 | 0.31 | 0.22 | 0.05 | 0.08 | 0.00 | 0.18 | 0.34 | 0.22 | 0.29 | 0.18 |
| Lambda | 0.15 | 0.00 | 0.00 | 0.16 | 0.00 | 0.15 | 0.14 | 0.15 | 0.16 | 0.03 | 0.06 | 0.00 | 0.17 | 0.14 | 0.16 | 0.12 | 0.17 |

**Table 4**: Stochastic mapping transition rates from SIMMAP for substrate preference and general ecology for diplodactyloids.

| | Substrate/Ecology | | | | |
|---|---|---|---|---|---|
| Transition Rate | arboreal, shrub-inhabiting | arboreal, fossorial | arboreal, graminicolous | arboreal, grass swimming | arboreal, rupicolous |
| x -> y | 2.121 | 0.187 | 0.399 | 0.233 | 1.876 |
| | arboreal, scansorial | arboreal, terrestrial | shrub-inhabiting, arboreal | shrub-inhabiting, fossorial | |
| x -> y | 1.975 | 0.663 | 1.202 | 0.081 | |
| | shrub-inhabiting, graminicolous | shrub-inhabiting, grass swimming | shrub-inhabiting, rupicolous | | |
| x -> y | 0.158 | 0.086 | 0.238 | | |
| | shrub-inhabiting, scansorial | shrub-inhabiting, terrestrial | fossorial, arboreal | fossorial, shrub-inhabiting | |
| x -> y | 0.552 | 0.133 | 0.193 | 0.158 | |
| | fossorial, graminicolous | fossorial, grass swimming | fossorial, rupicolous | fossorial, scansorial | fossorial, terrestrial |
| x -> y | 0.076 | 0.42 | 0.152 | 0.167 | 0.117 |
| | graminicolous, arboreal | graminicolous, shrub-inhabiting | graminicolous, fossorial | graminicolous, grass swimming | |
| x -> y | 0.215 | | 0.178 | 0.081 | 0.095 |
| | graminicolous, rupicolous | graminicolous, scansorial | graminicolous, terrestrial | grass swimming, arboreal | |
| x -> y | 0.165 | 0.63 | 0.591 | 0.235 | |
| | grass swimming, shrub-inhabiting | grass swimming, fossorial | grass swimming, graminicolous | grass swimming, rupicolous | |
| x -> y | | 0.228 | 1.48 | 0.148 | 0.281 |

| | grass swimming, scansorial | grass swimming, terrestrial | rupicolous, arboreal | rupicolous, shrub-inhabiting | rupicolous, fossorial |
|---|---|---|---|---|---|
| x -> y | 0.275 | 0.199 | 4.566 | 6.033 | 0.385 |
| | rupicolous, graminicolous | rupicolous, grass swimming | rupicolous, scansorial | rupicolous, terrestrial | scansorial, arboreal |
| x -> y | 0.714 | 0.699 | 1.401 | 1.544 | 4.304 |
| | scansorial, shrub-inhabiting | scansorial, fossorial | scansorial, graminicolous | scansorial, grass swimming | scansorial, rupicolous |
| x -> y | 2.141 | 0.188 | 1.708 | 0.275 | 0.625 |
| | scansorial, terrestrial | terrestrial, arboreal | terrestrial, shrub-inhabiting | terrestrial, fossorial | terrestrial, graminicolous |
| x -> y | 0.489 | 0.395 | 0.249 | 0.151 | 0.511 |
| | terrestrial, grass swimming | terrestrial, rupicolous | terrestrial, scansorial | | |
| x->y | 0.193 | 0.568 | 0.719 | | |

**Table 5**: Rates of directional ($\alpha$) and stochastic ($\sigma^2$) trait evolution (svl) under the OUMV model in OUWIE for each of the substrate preference and general ecology categories for diplodactyloids.

| | Arboreal | Shrub-inhabiting | Fossorial | Graminicolous | Grass-swimming | Rupicolous | Scansorial | Terrestrial |
|---|---|---|---|---|---|---|---|---|
| Stabilizing ($\alpha$) | 1.7 | 1.7 | 1.7 | 1.7 | 1.7 | 1.7 | 1.7 | 1.7 |
| Stochastic ($\sigma^2$) | 0.26 | 0.03 | 0.01 | 0.02 | 0.11 | 0.03 | 0.09 | 0.03 |

**Table 6**: Empirical estimates from SURFACE of shifts and regimes in comparison to simulations (n = 100) under single rate Brownian motion (BM), single optimum Ornstein-Uhlenbeck (OU1), and true non-convergence $H_{NC}$.

| **Parameter** | **Empirical Estimate** | **BM** | **p(BM)** | **OU1** | **p(OU1)** | **$H_{NC}$** | **p($H_{NC}$)** |
|---|---|---|---|---|---|---|---|
| No. Shifts (*k*) | 28 | 4 - 26 | *0* | 3-25 | *0* | 27-33 | 0.13 |
| No. Regimes (*k'*) | 22 | 3 - 23 | *0.01* | 2-19 | *0* | 23-31 | 1 |
| Convergence ($\Delta k$) | 6 | 0 - 12 | 0.23 | 0-8 | 0.13 | 0-6 | 0.9 |
| Convergent Regimes (*k'c*) | 6 | 0 - 9 | 0.13 | 0-8 | 0.06 | 0-5 | *0* |
| Pairwise Convergence (*c*) | 12 | 0 - 19 | 0.19 | 0-16 | 0.08 | 0-11 | *0* |
| Proportion conv. (*c*/*k*) | 0.43 | 0 - 0.9 | 0.59 | 0-0.79 | 0.67 | 0-0.38 | *0* |

# Chapter 3

## DIVERSIFICATION AND MACROEVOLUTIONARY DYNAMICS OF DIPLODACTYLOID GECKOS

### Introduction

Our planet harbors an astounding diversity of life, yet we know very little of the patterns of diversity for many groups or the underlying processes under which they were generated. Species richness is not evenly distributed among clades and this asymmetry in diversity has been known for some time. This pattern is often true for phenotypic diversity as well. Even clades of relatively closely related species can demonstrate extremely high levels of phenotypic diversity relative to their nearest relatives (Vidal-Garcia *et al.*, 2014). Globally, clades have experienced bouts of speciation and subsequently lost species through extinction leading to the diversity we observe today (Morlon, 2014; Höhna *et al.*, 2016). A number of factors are known to influence both speciation and extinction including intrinsic properties of members of a clade such as generation time, evolutionary constraint, and niche availability (Losos & Miles, 1994; Losos *et al.*, 1998; Mahler *et al.*, 2010; Vidal-Garcia *et al.*, 2014). Extrinsic abiotic factors that influence resource availability and habitat suitability such as mountain building and climate change have also been invoked to explain diversity patterns (Santini *et al.*, 2013; McGuire *et al.*, 2014; Rabosky, 2014; Shi & Rabosky, 2015). Clades that occur in a range of habitats and have undergone dispersal events or major geologic alterations to the ancestral range that have fragmented their ranges offer special opportunities to investigate the processes driving diversity (Linder *et al.*, 2014; Lee *et al.*, 2016; Moyle *et al.*, 2016).

The diplodactyloid geckos are an ideal group for the investigation of the processes that have generated species and phenotypic diversity. While restricted to Australia and three nearby archipelagos, this clade occupies a wide variety of ecological niches which is reflected in morphological diversity that far exceeds that seen elsewhere within Gekkota (Oliver & Sanders, 2009; Garcia-Porta & Ord, 2013) (figures 5, 9, and 17). For example, this clade includes the only gecko lineage with limb reduction, and viviparity has evolved twice within the Diplodactylidae, whereas it is absent in the remainder of Gekkota. Diplodactyloids occur in a wide array of climate regimes ranging from deserts to humid rainforests to high-altitude temperate forests. The limb-reduced pygopodids have diversified into a number of niches with some, such as *Lialis, Delma, Pygopus*, *Pletholax,* and *Paradelma* being grass swimmers, and others such as *Aprasia* and *Ophidiocephalus* being semi-fossorial (Jennings *et al.*, 2003; Brennan *et al.*, 2016). Most carphodactylids and diplodactylids are scansorial to some degree with many being specialized to high canopy habitats and others adapted to rupicolous lifestyles. Several lineages within both of these families have adapted to terrestrial niches, often resulting in the corresponding reduction or complete loss of adhesive toepads. Cranial morphology varies extensively within carphodactylids and diplodactylids as well, primarily relating to diet. Carphodactylids in the *Nephrurus* clade have large, highly ossified skulls likely adapted to hard-sheleld arthropods while several diplodactylids in the *Diplodactylus*/*Lucasium* clade have evolved small heads adapted to consuming small invertebrates. The pygopodid genus *Lialis* stands as the gecko lineage with the most extreme adaptations for subduing vertebrate prey, possessing a highly kinetic skull and hinged teeth (Evans, 2008). Substrate choice may have also been a major axis of diversification for this clade. Multiple carphodactylids and diplodactylid lineages are rupicolous and some show adaptations closely associated with this substrate such as flattened heads and correspondingly long limbs (Revell *et al.*, 2007).

Macroevolutionary patterns within this clade remain largely unexplored, though Garcia-Porta and Ord (2013), Skipwith *et al.* (2016), and Brennan and Oliver (2017) examined speciation dynamics and phenotypic diversification. Habitat change, either due to major geologic events or climate change, and the colonization of novel regions have been associated with shifts in diversification rate and rates of phenotypic diversification (Pinto *et al.*, 2008; Mahler *et al.*, 2010; Espeland & Murienne, 2011). The colonization of the islands New Caledonia and New Zealand by diplodactylids has been hypothesized to have influenced speciation dynamics for these clades (Garcia-Porta & Ord, 2013). Both clades exhibit high ecological diversity as exemplified by independent instances of gigantism (*Hoplodactylus, Rhacodactylus, Mniarogekko,* and *Correlophus*), viviparity (*Rhacodactylus trachyrhynchus* group and all the New Zealand species), and diurnality (*Naultinus* and *Eurydactylodes*) having evolved on both islands. Garcia-Porta and Ord (2013) and Skipwith *et al.* (2016) suggested that diversification trajectories for these groups were non-linear and fit well with what would be expected for clades after the colonization of open regions. The former study also proposed that the rate of body size evolution for these island radiations was higher than the background rate for the Diplodactyloidea.

Climatic oscillations during the Neogene led to the development of the deserts that now cover two-thirds of mainland Australia (Byrne *et al.*, 2008; Bowman *et al.*, 2010). Few studies have attempted to address the tempo of diversification of Australian radiations after their colonization from surrounding areas or *in-situ* diversification following these invasion events (but see Fujita et al. 2010). Recent studies investigating diversification dynamics across Australian squamates have found that there exist high levels of heterogeneity in diversification rates in certain groups (Lee *et al.*, 2016; Title & Rabosky, 2016). There have been multiple invasions of the Australian Arid Zone (AAZ) by distantly related diplodactyloid lineages. Many taxa in the AAZ, such as *Oedura*, are phenotypically similar to their mesic and temperate sister taxa while others have diverged substantially (Oliver *et al.*, 2007; Oliver *et al.*, 2012). This biome presents an opportunity to investigate how open niche space influences speciation dynamics and trait evolution. The Eocene-Oligocene boundary (EOb) cooling period (~34 Mya) has been linked to global biotic turnover (Stadler, 2011). Brennan and Oliver (2017) suggest that the EOb played a large role in the diversification dynamics of Australian diplodactyloids, where mass extinction resulted in turnover and recovery within the clade.

In this study, we investigate the dynamics of speciation and trait evolution of diplodactyloids using a phylogenomic data set consisting of ~4,200 UCE loci screened for 180 species (~75% of the described diversity). Using maximum likelihood and Bayesian methods, we test speciation rates across the time-calibrated diplodactyloid tree. To elucidate how this clade has diversified phenotypically, we used body size and several ecomorphologically relevant traits to test if rates of trait evolution differ between clades for different traits. We further tested if speciation rate and the rate of trait evolution are correlated or decoupled. Testing the tempo of diversification for this clade is particularly pertinent given that previous studies have shown that diversification dynamics are neither constant nor homogenous for this clade (Garcia-Porta & Ord, 2013; Skipwith *et al.*, 2016; Brennan & Oliver, 2017). Lastly, several clades have dispersed to nearby islands and geologically recent bioregions in Australia. We use these methods to determine if these clades have experienced ecological release in terms of diversification rates and trait evolution. Previous studies relied on smaller, poorly supported molecular datasets and only examined body size to investigate morphological diversification. Brennan and Oliver (2017) excluded the two Tasmantis radiations in their analysis as to whether the EOb influenced the diversification dynamics of diplodactyloid geckos. Our use of a robust phylogenomic estimate, a

taxonomically comprehensive phylogeny, and multiple ecomorphological traits is ideal for the implementation of more complex models of diversification that allow us to test for signatures of modularity in trait evolution. Given the ecological diversity exemplified by diplodactyloids, these data allow us to address if this clade is indeed a diverse lineage composed of both adaptive and non-adaptive radiations.

**Methods**

*Taxon Sampling*

We sampled 170 of the 213 currently recognized diplodactyloid species and all genera with the exception of the pygopodid *Ophidiocephalus*. An additional 10 diplodactylid species were included in this dataset as these were treated as potential cryptic species based of the findings of previous studies and novel results from our own phylogenetic estimates (Nielsen *et al.*, 2011; Oliver *et al.*, 2014; Oliver & Doughty, 2016; Skipwith *et al.*, 2016). Our ecomorphological dataset only included 148 species for all traits in question and the phylogeny was pruned to include just these 148 species for trait analyses beyond body size. Because body size data were available for all species, analyses of body size were based on the complete phylogenetic estimate.

*Phylogeny and Time Tree*

We used the time tree estimate from Skipwith (Chapter 1) as the phylogenetic framework for all downstream comparative analyses. Briefly, the time tree of Skipwith (Chapter 1) was generated in a two-stage process. First, a summary multispecies coalescent tree was estimated from 4268 ultraconserved loci using ASTRAL-II(Mirarab *et al.*, 2014; Mirarab & Warnow, 2015). Then, the ASTRAL-II topology served as constraint tree for a divergence dating analysis using MCMCTREE in PAML (Yang, 2007; Mirarab *et al.*, 2014; Mirarab & Warnow, 2015)

*Ecomorphological Data, Continuous Trait Modeling, and Phylogenetic Correction*

We measured body size and 16 linear, external, ecomorphologically relevant traits for 148 diplodactyloid species, sampling all genera except *Pletholax*. These were: head length, head width, head depth, trunk length, forearm length (crus), tibia length, internarial width (EN), nares-eye distances (NEYE), orbit diameter (EYE), eye-ear distance (EyeEar), interorbital distance (IE), $4^{th}$ finger width, $4^{th}$ finger length, $4^{th}$ toe width, and $4^{th}$ toe length. All measurements were carried out by P. Skipwith using a pair of digital calipers. Details on trait models and phylogenetic size correction can be found in chapter 2.

*Diversification Dynamics and Rate Heterogeneity*

We first used the gamma statistic ($\gamma$) to determine if diplodactyloids exhibit a linear pattern of diversification under a constant birth process with the gamstat function in PHYTOOLS (Pybus & Harvey, 2000; Revell, 2012). Previous studies have suggested that diversity dependence has played a role in the diversification of at least some diplodactyloid lineages (Skipwith *et al.*, 2016). The fitAICrc function in LASER was used to test constant rate pure-birth, constant rate birth-death, rate variable pure-birth (Yule-2-rate), and two density dependent models (DDX and DDL) of diversification (Rabosky, 2006). We attempted to account for extinction processes in a likelihood framework using DDD, testing constant rate pure-birth, constant rate birth-death, diversity dependence without extinction (DDL – E), and diversity dependence with extinction (DDL + E) (Etienne *et al.*, 2012). LASER models were evaluated with the $\Delta AIC_{rv}$ statistic ($\Delta AIC_{rv} = AIC_{rv} - AIC_{rc}$), whereas model choice for DDD was done with AIC weights (AICw). Both LASER and

DDD were run on the whole diplodactyloid clade, Carphodactylidae, Pygopodidae, Diplodactylidae, New Caledonian diplodactylids, New Zealand diplodactylids, core Australian diplodactylids, and non-insular diplodactyloids. Clade specific incomplete taxon sampling was accounted for in all DDD analyses.

In recent years, a number of analytical methods have become available to estimate speciation ($\lambda$), extinction ($\mu$), and net diversification ($\delta = \lambda - \mu$) from molecular trees (Rabosky, 2006; Morlon *et al.*, 2011; Etienne *et al.*, 2012; Morlon, 2014). While intrinsic issues arise when trying to estimate extinction from a molecular phylogeny with known branch lengths, recent advances using simulations have made it possible to detect rate heterogeneity (Quental & Marshall, 2009, 2010; Rabosky, 2010; Quental & Marshall, 2011). However, we have opted not to employ methods such as MEDUSA (Alfaro *et al.*, 2009) in which the algorithm assigns diversification parameters to branches in a phylogeny before integrating over them with AIC, as such methods have been shown to be highly susceptible to the recovery of false shifts in diversification rate (May & Moore, 2016).

To test for net diversification and rate heterogeneity, we used Bayesian analysis of macroevolutionary mixtures (BAMM;(Rabosky, 2014). BAMM simulates changes in $\lambda$ and $\mu$ along branches via reversible-jump Markov Chain Monte Carlo (rjMCMC) under a compound Poisson process that accounts for rate heterogeneity. This method decouples $\lambda$ and $\mu$, permitting the detection of rate heterogeneity within the tree in the form of clade-specific shifts in diversification (Rabosky *et al.*, 2013; Rabosky, 2014). We used BAMMTOOLS in R to specify priors, and four BAMM 'speciation extinction' analyses each run for 1,000,000 generations sampling every 10,000 generations, discarding the first 10% as burnin (Rabosky *et al.*, 2014). As taxon sampling can have serious impacts on diversification rate estimation, we accounted for genus-specific incomplete taxon sampling in BAMM. Due to parameter estimation in BAMM being driven by MCMC, issues arise when inferring the correct or probable pattern of parameter shifts within a phylogeny. Identifying the exact placement of a shift along a branch is unlikely, requiring the use of the 95% credible set of the shift configurations to reflect the most likely shift pattern.

Recent concern has been raised regarding the likelihood function implemented in BAMM and the algorithm's sensitivity to prior specification. Moore *et al.* (2016) demonstrated that the failure of the likelihood function to account for rate shifts on extinct lineages resulted in BAMM only being able to accurately estimate the number and magnitude of shifts in phylogenies under a constant-rate birth-death process, but not under a variable-rate birth-death process. Furthermore, the compound Poisson process prior model was shown to be extremely sensitive to prior specification, specifically the specification of the prior on the expected number of shifts. Mitchell and Rabosky (2016) note that the pathological behavior of the likelihood function has been addressed as of BAMM v2.5 and the estimation of the correct number of shifts via model selection with Bayes factor (BF) support alleviates problems associated with prior specification. We followed the thresholds outlined by Kass and Raftery (1995) when determining significant differences between models where BF < 2 is interpreted as negative (supports $M_1$), BF = 2 - 6 as moderate support for $M_2$, BF = 6 – 10 as substantial support for $M_2$, and BF = > 10 as very strong support for $M_2$.

To further assess the tempo of diversification of diplodactyloid geckos we used TESS (Höhna *et al.*, 2016) to estimate the appropriate model and parameters of diversification as well as signatures of mass extinction. Like BAMM, TESS simulates diversification parameters on a phylogeny using rjMCMC, estimating the joint posterior density of these parameters to detect

shifts under a birth-death process. TESS allows for the estimation of rate heterogeneity across the whole tree though rates among subclades remain constant at a given time. Mass turnover dynamics are estimated via the magnitude of a predefined survival probability parameter, in this case we used the sampling fraction of species included in our analysis. In order to determine if mass turnover had played a role in the diversification dynamics of diplodactyloids, we tested five birth-death models including: (1) constant-rate birth-death null model (CrBD), (2) a birth-death model with continuously varying diversification rates (BDVar), (3) a birth-death model with continuously varying diversification rates that incorporates explicit mass extinctions (BDVarEx), (4) a birth-death model with episodically varying diversification rates (BDep), and (5) a constant-rate birth-death model that incorporates explicit mass extinctions (CrBDex). Models were evaluated using stepping-stone simulation, a method analogous to standard MCMC where the probability of the data is estimated from a defined number of points between the prior and the posterior. Using the likelihoods and priors of the abovementioned models, we used stepping-stone sampling to estimate Bayes factors. Stepping-stone sampling was run for 10,000 iterations and sampled every 100 steps with the first 1,000 iterations discarded as burnin. The criteria defined by Kass and Raftery (1995) were used to determine which model best fit these data.

To determine the timing of putative shifts in diversification parameters and mass extinction events, we used the TESS extension COMET (May *et al.*, 2016). Theoretically, there are an infinite number of birth-death processes with or without extinction, varying rates, and episodically varying rates that can be tested for a dataset, and stepping-stone sampling may be computationally unfeasible for this level of model testing. The COMET model uses rjMCMC to simulate over all possible episodically varying birth-death processes by treating shifts in rate parameters as random variables from which it estimates their joint posterior probabilities for model comparison. In addition to analyzing the full diplodactyloid tree, we ran a second COMET analysis on the 'Australian-only' diplodactyloids. We estimated the timing of shifts in speciation and extinction rate as well as mass extinction events with COMET from empirically estimated hyperpriors. Four independent COMET analyses were run for 200,000 iterations with the first 10% discarded as burnin while requiring a minimum ESS value of 500. We also ran COMET analyses on the diplodactyloid tree with all insular species removed for comparison to the findings of Brennan and Oliver (2017) who used the COMET model in their analysis of diplodactyloid diversification.

Lastly, we tested birth-death models of diversification using RPANDA in R, a method that complements BAMM and TESS (Morlon *et al.*, 2011; Morlon, 2014; Morlon *et al.*, 2016). RPANDA allows the user to fit different rate-constant and rate-varying birth-death models to a phylogeny using maximum likelihood to subclades defined *a-priori*. We split the Diplodactyloidea into seven smaller clades representing the Carphodactylidae, Pygopodidae, Diplodactylidae, New Caledonian diplodactylids, New Zealand diplodactylids, core Australian diplodactylids (excluding *Pseudothecadactylus* and *Crenadactylus*), and all diplodactyloids excluding the insular radiations. Four birth-death models were then fitted to each of the seven subclades including (1) constant rate birth-death (BcstDcst), (2) varying birth with constant death (BvarDcst), (3) constant birth with varying death (BcstDvar), and (4) varying birth-death (BvarDvar) processes. For these analyses, corrected AIC (AICc) was used for model comparisons and to determine model choice. We also used the spectR function in RPANDA to characterize potential diversification rate shifts within the diplodactyloid tree by summarizing tree shape using the spectral density (Lewitus & Morlon, 2016; Morlon *et al.*, 2016).

*Phenotypic Diversification and the Role of Biogeography in Diversification Dynamics*

Diplodactyloids are incredibly diverse in terms of morphology and we tested if rate heterogeneity was present for continuous trait evolution. We investigated body size evolution and used size-corrected residuals for all other traits. To infer ancestral states for our continuous traits, the likelihood-based FASTANC function through CONTMAP in PHYTOOLS was implemented (Felsenstein, 1973, 1985; Revell, 2013). We used BAMM to determine if certain traits had experienced clade-specific shifts in diversification, specifically body size, head length (corrected for body size), head depth (corrected for head length), fourth toe width (corrected to toe length), and lower limb measurements (corrected for svl). These traits were selected as they were found to have relatively high signatures of adaptive evolution (see chapter 2) or are closely tied to the diverse habitats occupied by this lineage. BAMM estimates the rate of trait evolution under a Brownian motion process where the occurrence of a shift decouples the parent rate and those of its daughter processes (Rabosky *et al.*, 2013). We ran four separate BAMM 'trait' runs with the same MCMC settings as the abovementioned 'speciation extinction' analyses. These included the full 180 species tree for body size (svl), a reduced 148 species tree for head measurements (length and depth relative to head length), and a tree with 129 carphodactylids and diplodactylids for toepad and limb dimensions. We additionally tested for trait dependent diversification using the STRAPP function in BAMMTOOLS (Rabosky & Huang, 2016). Here, diversification rates along the tree are estimated independently of the traits in question. The STRAPP method then determines the association between species-level traits and the diversification rate at the tips of the tree, comparing the empirical rates to a null distribution. To determine which species occupied the same macroevolutionary rate regime for trait evolution, we estimated the pairwise correlation of rate regimes using the macroevolutionary cohort analysis in BAMMTOOLS. Occupation of the same rate regime is estimated as the proportion of samples from the posterior where two taxa share the same regimes.

We used OUWIE to fit several Hansen models under random-walk (BM) and stabilizing selection (OU) for discrete biogeographic states and body-size (svl) (O'Meara *et al.*, 2006; Beaulieu *et al.*, 2012). Species were coded as 1) mainland or island and 2) Australia, New Caledonia, New Zealand, or New Guinea. Continuous traits were fitted with a single-rate Brownian motion model (BM1), a Brownian motion model with different rate parameters for each discrete trait (BMS), an OU model with a single optimum across the whole tree (OU1), a multipeak OU model with different state means but global stochastic ($\sigma^2$) and selection ($\alpha$) parameters acting across the tree (OUM), and two multipeak OU models that allow for different state means with multiple $\sigma^2$ (OUMV) and multiple $\alpha$ (OUMA). Model choice was determined by calculating $\Delta$AIC from AICc. The rates of $\sigma^2$ and $\alpha$ were then inspected to determine which geographic groupings had the highest rate of continuous trait evolution.

**Results**

*Net Diversification Dynamics*

The $\gamma$-statistic revealed that the diplodactyloid tree deviated significantly from a pure-birth process, having experienced a downshift in net diversification towards the present ($\gamma$ = -3.3, p = < 0.001). Diversification model evaluation with LASER yielded positive $\Delta AIC_{rv}$ values for diplodactyloids and all subclades with the exception of the New Zealand diplodactylids, where the Yule-2-rate model was preferred (table 7). All Yule-2-rate models revealed a decrease in speciation rate towards the present. The diversity dependent process without extinction (DDL – E) was found to fit all clades except the New Zealand diplodactylids, though speciation rates varied greatly between lineages. Like LASER, DDD found that the New Zealand diplodactylids fit a pure-

birth process (table 7). The BAMM 'speciation-extinction' analyses detected no significant clade-specific shifts in diversification as indicated by Bayes factors. This is further supported by the 95% credible shift set finding overwhelming support for there being no clade specific shifts (pos. prob. = 1) (figure 18). Mean speciation rate for diplodactyloids was estimated to be 7.3 species/My with an inferred extinction rate of 0.38 species/My. Clade-specific rates of mean speciation for the carphodactylids, pygopodids, New Caledonian and New Zealand diplodactylids, and the core Australian diplodactylids were all within 0.05 units of the global mean for diplodactyloids (table 7). Diversification rate through time plots reveal stable rates for all diplodactyloids and all subclades examined (figure 19).

Investigation of the tempo of diversification with TESS additionally reveals that diversification has been non-linear. Model comparison of the marginal likelihoods yields overwhelming support for models incorporating mass extinction (BF > 3.2) (table 8). These estimates place the occurrence of the mass extinction very close to the base of the diplodactyloid tree, around the late Campanian of the Cretaceous (75 My). Our COMET analyses also found evidence for deviation from a pure-birth process. However, COMET failed to find any signature of mass extinction across the whole diplodactyloid tree or for the Australia only diplodactyloid tree (BF < 3). While extinction rate was found to be constant, COMET found strong support for a downshift in the rate of speciation and, by extension, net diversification across the whole tree (figure 20). Highest support from the posterior and BF evidence (> 9) for this decrease in speciation rate is placed around 4 My.

RPANDA found that the BcstDcst model best fit the Carphodactylidae, Pygopodidae, Diplodactylidae, New Zealand diplodactylids, and non-insular diplodactyloids (table 7, figure 21). The New Caledonian and core Australian diplodactylids were both found to fit a BvarDcst process, where the former experienced an increase in speciation rate ($\lambda_1 = 5.2$, $\lambda_2 = 12.1$) while the latter experienced a decrease ($\lambda_1 = 4.9$, $\lambda_2 = 2.3$) (figure 21). Analysis of rate heterogeneity using the spectral density revealed a single modality for the entire diplodactyloid tree, indicating no clade-specific rate shifts (figure 22).

*Trait Evolution and Biogeography*

All traits were found to have high phylogenetic signal (table 9). Ancestral state reconstructions using likelihood recover a small ancestral body size for diplodactyloids, but intermediate proportions for the other size corrected traits (figure 23 – 28). BAMM yielded strong evidence for rate heterogeneity in trait evolution for body size and relative head length. The rate of body size evolution was found to have shifted twice across the tree, one along the *Hoplodactylus duvaucelii – Woodworthia maculata* branch and another on the *Correlophus*, *Rhacodactylus*, and *Paniegekko – Bavayia* clade (figure 29). Both clades demonstrate a greater than three-fold increase in the rate of body size evolution (β means = 0.37 and 0.22 respectively) over the background rate for the diplodactyloids (β mean = 0.06) (table 10). Rate heterogeneity was also found in relative head length, where a single shift in the rate of trait evolution were detected (figure 30). The pygopodids (β mean = 0.05) experienced increased rates of head size evolution over the background for diplodactyloids (β mean = 0.02). BAMM also found very low support from the credible set of rate shifts for a second shift along the *Strophurus jeanae – S. taeniatus* branch (frequency = 0.18). The only other trait found to exhibit rate heterogeneity was fourth toe width where increased rates were found for the *Lucasium – Rhynchoedura* clade (β mean = 0.07) over the background rate (β mean = 0.02) (figure 31). Macroevolutionary cohort analyses of body size (figure 32), head length (figure 33), or toepad width (figure 34) revealed that no two clades on which a shift occurred occupied

the same rate regime. We found no signature of rate shifts in the diversification of relative head depth, forearm length, or hind limb length with BAMM. STRAPP analysis found no significant correlation between diversification rates and trait diversification. Hansen model testing with OUWIE revealed that the BMS model best fit the binary (island vs. mainland) and multistate geographic categories for body-size. Insular forms were found to have a higher rate of stochastic body-size evolution than mainland forms (table 11) and the New Caledonian and New Zealand clades had vastly higher rates than Papua New Guinea or Australia (table 12).

**Discussion**

*Rate Heterogeneity and Extinction*

Our finding of homogenous diversification rates within diplodactyloids refutes the hypothesis that the recent colonization of the two Tasmantis islands and AAZ led to increased rates of speciation. Both LASER and DDD recovered extremely high estimates of speciation rate for the New Caledonian diplodactylids in comparison to the other clades, a four-fold difference in some cases. Rather, our BAMM analyses strongly suggest that the background rate of net diversification for all diplodactyloids is high, with a slight trend towards increasing. This is further supported by the complementary spectR analysis in RPANDA, which found a single modality in speciation rate. These findings indicate that consistently high diversification rates have led to the rapid generation of diplodactyloid species, and the generation of the high diversity seen in the two Tasmantis lineages has been facilitated by this high background rate. High ancestral diversification rates allowed the New Caledonian clade to explosively diversify and explore morphospace. This rapid increase in species and ecological diversity likely limited the amount of competition with the five unrelated gekkonid genera that colonized the New Caledonian archipelago much later in the Neogene (Bauer & Sadlier, 2000; Grant-Mackie *et al.*, 2003). The same hypothesis of early endemism and competitive exclusion can be invoked to explain the high species diversity but lack of rate heterogeneity on mainland Australia. Australian gekkonids are substantially more diverse than those of New Caledonia, with several genera having undergone *in situ* diversification. Nevertheless, these lineages were late arrivals from Asia and elsewhere in Oceania and morphological diversity is comparatively low when compared to diplodactyloid clades of comparable age (Fujita *et al.*, 2007; Fujita *et al.*, 2010; Heinicke *et al.*, 2011). The rate homogeneity seen in the Australian diplodactyloids is particularly striking given the growing evidence of heterogeneity in other Australian squamates (Lee *et al.*, 2016; Title & Rabosky, 2016). However, the absence of rate heterogeneity found across all diplodactyloids is consistent with the findings of Brennan and Oliver (2017). New Zealand remained gekkonid free until the arrival of humans, making the absence of explosive diversification in this clade all the more surprising.

Using TESS, Brennan and Oliver (2017) found overwhelming BF evidence for a mass extinction event and faunal turnover within the Australian diplodactyloids corresponding to the EOb (37- 22 My). This pattern is consistent with mass extinctions elsewhere on the planet during this time (Stadler, 2011; Sun *et al.*, 2014). Our failure to recover the same findings across all model testing methods in TESS conflicts with these studies (figure 20). The diplodactyloid phylogeny used in the present study differs from that of Brennan and Oliver (2017) at many nodes, particularly at the generic level. Our tree has much higher resolution in terms of statistical support, a benefit of implementing thousands of independent loci over a handful dominated by mitochondrial signal. In addition to topological incongruences between our phylogenies, we recover overall older crown ages. This combination of topological and divergence time discordance likely had a large influence on differing mass extinction estimates. Our phylogeny includes the two Tasmantis clades, lineages with high species diversity and younger crown ages than the mainland taxa. The use of a more

taxonomically complete phylogeny may have resulted in fewer artificially long branches with our phylogeny, preventing the COMET algorithm from finding signatures of mass extinction. While this may be true in part, the failure of our 'Australia only' tree to show signatures of mass extinction suggests that divergence times rather than taxonomic sampling played a larger role in incongruent model characterization. In this case, older crown age estimates also removed the presence of long branches devoid of cladogenic events, a pattern consistent with the node density effect observed by Hugall and Lee (2007). This observation falls in line with the findings of Title and Rabosky (2016) who found that divergence time estimates have a heavy influence on the estimation of parameters underlying diversification.

While Brennan and Oliver (2017) estimated divergence dates with the widely used BEAST algorithm, we implemented the Bayesian program MCMCTREE. The two methods are largely complementary, but handle tree priors and time priors very differently. BEAST simultaneously estimates the topology and divergence times, a feature that results in the posterior estimates of divergences broadly violating the overlying priors, a phenomenon noted by Warnock *et al.* (2015). In fact, our timetree places all of the familial crown ages in the Paleocene or early Eocene, well prior to the EOb. In light of this, we are more confident in our temporal estimates using MCMCTREE and a well-supported phylogenomic dataset than in the timetree estimated by Brennan and Oliver (2017). We note, however, that Brennan and Oliver (2017) were able to integrate over the trees from the posterior of BEAST, a feature unavailable in MCMCTREE. Running TESS on set of divergence time estimates would allow us to account for temporal uncertainty in our dataset. That being said, our credibility intervals are rather narrow for all clades, suggesting that analyzing the posterior trees would make little difference. We also note that model testing with the tess.mcmc function offers more rigorous model selection through stepping stone simulation than is possible with COMET, which relies on rjMCMC (Höhna *et al.*, 2016; May *et al.*, 2016). Our analysis with this function yields results more congruent with those of Brennan and Oliver (2017), finding strong support for a mass extinction event. However, where the previous study recovered mass extinction broadly overlapping the EOb, ours found one very near the base of the Diplodactyloidea. This implies that, if there was indeed a mass extinction event, it had nothing to do with the EOb but rather events occurring during the Mesozoic. This putative event predates the KT boundary by ten million years, but there are documented marine mass extinctions corresponding to the Campanian (Yazykova, 1996). Examples of terrestrial mass extinction from this time period, however, are largely lacking, although decreases in squamate diversity have been documented near the Campanian-Maastrichtian boundary (Longrich *et al.*, 2012; DeMar *et al.*, 2017). While an extinction event may have occurred at some point in diplodactyloid diversification, any inference of the magnitude and timing of such an event must treated with a great deal of caution. These methods, whether relying on AIC statistics, stepping stone simulation, or rjMCMC, are notoriously unreliable in estimating realistic extinction rates (Quental & Marshall, 2010; Rabosky, 2010). With their very limited fossil record, any trends estimated for diplodactyloids cannot be independently verified.

*Equilibrium Dynamics within Diplodactyloids*

Our multifaceted analysis of the macroevolutionary dynamics of diplodactyloids reveals that this clade has experienced a complex pattern of diversification. The whole diplodactyloid complex and most of the subclades demonstrate an initially rapid speciation rate followed by a decline, a pattern consistent with a number of processes. Disentangling diversity dependent rate variation and extinction processes is problematic, as the latter is difficult if not impossible to extract from

molecular-only phylogenies (Quental & Marshall, 2010, 2011). In short, molecular phylogenies have considerable power to tell us if and when there have been shifts in net diversification, but not the underlying processes governing these shifts (Quental & Marshall, 2010). Furthermore, molecular phylogenies, by virtue of only containing extant species, are by definition increasing towards the present, often resulting in the signature of increasing diversification (Nee *et al.*, 1994; Pagel, 1999).

Given these limitations in the power of diversification methods to realistically estimate the processes underlying diversification, we are hesitant to place high confidence in their parameter estimates. Likelihood analysis using LASER and DDD reveal that diplodactyloids on the whole and most of the subclades have experienced downshifts in speciation rate towards the present. This finding is broadly consistent with equilibrium dynamics, particularly diversity dependence, where speciation is initially rapid before slowing down as ecological niche space is filled. This process has likely played an important role in shaping the diversity dynamics of this clade at different time intervals, and this may be particularly true for the insular clades occupying smaller land areas and likely with less open niche space (Pinto *et al.*, 2008; Losos & Ricklefs, 2009; Skipwith *et al.*, 2016). The colonizations of New Caledonia and New Zealand may have granted diplodactylids the opportunity to rapidly explore niche space and increase in diversity, following a classic diversity dependent pattern. The relatively young crown age and extremely high diversity in body size and ecomorphology in both clades supports this idea, especially in comparison to the mainland diplodactyloids. However, all of the abovementioned methods, whether relying on likelihood or rjMCMC, fail to recover realistic estimates of extinction for diplodactyloids. This is exacerbated by the general paucity of the diplodactyloid fossils, a record that would present an opportunity to critically evaluate these extinction rate estimates (Quental & Marshall, 2010). The climatic instability of mainland Australia likely drove ecological differentiation within carphodactylids, pygopodids, and core Australian diplodactylids, making equilibrium dynamics plausible (Rabosky & Glor, 2010). It should be noted that while ecological controls almost certainly shaped diplodactyloid diversity, the complex interplay between environmental history and immigration rates between changing biomes needs to be considered. Most of the Australian genera have colonized the geologically young AAZ and some have back-colonized the relictual mesic and tropical regions of the continent. This pattern necessitates the implementation of fine-scale, clade-specific tests of diversification that account for biogeographic history.

Signatures of decline are common in studies investigating diversification dynamics using molecular phylogenies. Furthermore, for complex scenarios involving widely distributed (indeed continental scale) clades that include sympatric species that are only distantly related to one another, the importance of diversity dependence can be difficult to discern (Quental & Marshall, 2011; Morlon, 2014). If diversity dependence has indeed played a role with Diplodactyloidea, it is likely that the magnitude of and speed at which subclades reached equilibrium varied extensively. This is exemplified by the findings recovered by RPANDA, the only likelihood-based model used in this study that does not allow for the fitting of diversity dependent models. We fitted birth-death models to the diplodactyloid subtrees in RPANDA and only the New Caledonian and core Australian diplodactylids deviated from a constant rate birth-death process, both falling under a model with varying speciation and constant extinction (Morlon *et al.*, 2011; Morlon, 2014; Morlon *et al.*, 2016). This finding suggests that the magnitude of change between initial speciation ($\lambda_1$) and current speciation ($\lambda_2$) was estimated to be far greater than those of the subclades that best fit constant rate processes. Both the New Caledonian and core Australian diplodactylids are exemplified by short internodes near the crown with high topological variation among gene trees,

a pattern consistent with rapid initial speciation. Furthermore, both clades are among the most ecologically diverse of the diplodactyloids, where the colonization of novel regions likely drove the diversification of new ecomorphs during the Cenozoic.

The New Zealand diplodactylids did not show signatures of declining speciation rate with LASER, DDD, or RPANDA (table 7). This is surprising because previous studies have concluded that the New Zealand diplodactylid fauna was very similar to the New Caledonian clade in regards to biogeography and the generation of phenotypic diversity (Nielsen *et al.*, 2011; Skipwith *et al.*, 2016). The pattern of linear diversification under a pure-birth process for this clade is likely the combination of our older divergence estimates and its relatively low species diversity. Stable speciation rates for this clade may be attributable to the New Zealand group's recent transition to a temperate climate, a regime shift that may have negatively impacted generation time.

*Tempo of phenotypic diversification in Diplodactyloids*

For many clades, it has been implicitly assumed that rates of speciation and phenotypic diversification are positively correlated and there is a long history in evolutionary biology supporting this view. For instance Schluter (2000) argues that early in the history of an adaptive radiation, the rise of new phenotypes due to ecological differentiation will lead to increased speciation rates. Additionally, Ricklefs (2006) suggests that, in the presence of heterogeneity in speciation rate, phenotypic diversification will occur at cladogenic events. Indeed, many radiations may demonstrate a combination of these processes leading to a strong signature of coupling between the rates of phenotypic diversification and speciation (Rabosky *et al.*, 2013). However, the two processes may be decoupled where the entire clade is phenotypically conservative or if there is high phylogenetic signal in the traits in question as documented by Adams *et al.* (2009).

Despite being species-rich and the most phenotypically diverse clade of geckos, we find that speciation rates are decoupled from phenotypic diversification as the former was found to be homogenous across the clade. Rather we find that different traits are evolving at different rates for different clades (table 10). Our finding that most of the traits examined showed no signs of rate heterogeneity is surprising given that the limbs of these geckos are their direct interface with their environment. This observation is particularly pertinent given the ecological diversity exhibited by diplodactyloids where high variation is seen in limb proportions. This pattern is likely due to the relatively high phylogenetic conservatism seen within these traits. Individual clades may have rapidly converged on one peak for each of these traits, placing some level of constraint on the rate at which new areas morphospace could be explored.

In contrast to the conservatism in rates for limb traits, we found that body size, head length, and hind limb length demonstrate lower phylogenetic signal and rate heterogeneity across diplodactyloids. The increased rates observed for all three traits in the New Caledonian and New Zealand diplodactylids fits well with our hypothesis of heightened rates of phenotypic diversification for the Tasmantis radiations. Within these two clades, the rate of body size evolution vastly exceeds that seen within other diplodactyloid clades of comparable age. Our likelihood reconstructions of ancestral body size inferred small ancestral size (< 60 mm) for both lineages, indicating that large sizes attained by *Hoplodactylus duvaucelii* and the *Rhacodactylus* group were attained shortly after their respective colonization events. Open ecological space granted the opportunity to rapidly expand their respective size envelopes in the absence of competitors. In both clades, this is particularly evident in that the largest of the *Rhacodactylus* clade (*R. leachianus*, *R. trachyrhynchus*, *R. trachycephalus*, *Mniarogekko chahoua*, and *M. jalu*) and *Hoplodactylus duvaucelii* are all canopy specialists, much like the crown giants of *Anolis*

(Losos *et al.*, 1998; Bauer & Sadlier, 2000; Losos, 2009; Bauer *et al.*, 2012). This level of niche partitioning is a common feature of adaptive radiations (Schluter, 2000).

Where body size often plays a large role in determining which ecological guild an organism occupies, cranial morphology influences diet. Most diplodactyloids are insectivorous to some degree, though there is wide range of invertebrates taken and some species specialize on vertebrate prey or nectar (Bauer & Sadlier, 2000; Cogger, 2000; Wilson & Swan, 2013). We found that the rate of relative head size evolution increased for the pygopodids, but not for any of the limbed forms. This is attributable not necessarily to changes in head size, but rather a consequence of lengthening the axial skeleton. Pygopodids, like most limbless squamates, have proportionately small heads and the rate shift recovered by BAMM occurred early in the diversification of the family, presumably coinciding with initial limb reduction. This concurrent loss of limbs may have freed up the skull to diversify along a number of axes not seen in diplodactylids or carphodactylids. Of the more than 1,700 species of extant gecko, pygopodids are the only ones that display extreme cranial kinesis (*Lialis*) and head-first burrowing (*Aprasia* and *Ophidiocephalus*). Examination of diplodactyloid toepad width revealed rate heterogeneity along the *Lucasium – Rhynchoedura* clade. This lineage demonstrates the only example of pad reduction or loss among the Diplodactylidae, a clear adaptation towards an entirely terrestrial lifestyle.

The lack of rate variation in head depth relative to head length, forearm length, and hind limb length is surprising. In rupicolous lineages such as some *Oedura* and the leaf-tails (*Phyllurus*, *Saltuarius*, and *Orraya*), the head is notably dorsoventrally compressed. Within the Diplodactylidae and Carphodactylidae, limb length varies and appears to be closely related to the substrate as exemplified by arboreal taxa possessing short limbs and most terrestrial and rupicolous taxa possessing longer limbs. This pattern of homogeneity indicates that there are high levels of modularity where certain elements of skull differ in rates diversification as well as distinct rate regimes between the axial and appendicular skeletal elements. The elements modulating skull length (frontals, maxilla, nasals, dentary and mandibular elements, etc.) appear to be evolving under different controls than those modulating skull depth (quadrate, parietals, squamosal, etc.) (Sanger *et al.*, 2012). Appendicular elements are known to develop independently of the axial skeleton. Both the posterior cranial and appendicular elements may be under higher constraint for most clades. Ancestral state reconstructions reveal that these traits, while variable between clades, are relatively conserved within clades indicating that each clade initially colonized a 'peak' in morphospace and deviated very little as it diversified. For example, all carphodactylids possess long limbs when compared to nearly all diplodactylids, but this clade is reasonably old with long internal branches and long limbs were attained near the crown. In clades with short internodes, such as the New Caledonian and core Australian diplodactylids, these traits also show very little intraclade variation. If these groups demonstrated higher variation in the proportions of these traits or if clades like the carphodactylids contained short internodes, the signature of rate heterogeneity would likely be much higher.

Investigation of the prevalence of phenotypic convergence and adaptive peaks within diplodactyloids (Chapter 2) have shown that both relative head length and toepad width are under some degree of stabilizing selection. These traits are directly influenced by diet and substrate, ecological characteristics that are strongly conserved among clades (chapter 2). The relationship between rates of trait evolution and their independence from one another and speciation rate warrant further investigation. However, information regarding the developmental factors influencing the degree of modularity for each these traits are unknown for geckos.

*The Role of Biogeography in Ecomorphological Diversification*

Our finding that body size demonstrated higher rates of diversification on New Caledonia and New Zealand than on New Guinea and in Australia strengthens the argument that these two lineages represent adaptive radiations. The recent colonization of Tasmantis by their respective ancestors allowed them to rapidly fill the nocturnal lizard niche, diversifying along a number of ecomorphological axes, primarily size (Garcia-Porta & Ord, 2013; Skipwith *et al.*, 2016). Body size appears to be the least conserved of the traits examined in this study and in related studies investigating adaptive evolution (chapter 2). Following the colonization of these archipelagos, this labile trait was likely the primary skeletal trait for which rapid diversification was possible. Other traits, such as toepad dimensions and limb proportions were probably tightly constrained to fit the available habitat space available on the smaller landmasses. This is exemplified by the observation that all representatives of the two Tasmantis radiations are either scansorial (occurring primarily on some form of vegetation) or arboreal. Terrestriality has only evolved once within diplodactylids, being the basal condition for the *Diplodactylus – Lucasium* group. While Australian diplodactyloids are far more ecologically diverse than the insular lineages, the morphological diversification seen within these taxa has occurred over a much longer timescale. Furthermore, Australia is far more diverse in terms of biomes than either archipelago and its warmer climate may have facilitated the evolution of novel ecologies not seen in the more temperate New Zealand. The Tasmantis lineages had far shorter time intervals in which to generate species and accumulate morphological diversity (22 – 15 My in the case of New Caledonia), suggesting that they represent an adaptive radiation more in-line with the criteria proposed by Schluter (2000) than their mainland counterparts. The relationship between diversification rate, phenotypic diversification, and island also warrants further study.

## Literature Cited


Adams, D.C., Berns, C.M., Kozak, K.H. & Wiens, J.J. (2009) Are rates of species diversification correlated with rates of morphological evolution? *Proceedings of the Royal Society B: Biological Sciences*, **276**, 2729-38.

Alfaro, M.E., Santini, F., Brock, C.D., Alamilla, H., Dornburg, A., Rabosky, D.L., Carneval, G. & Harmon, L.J. (2009) Nine exceptional radiations plus high turnover explain species diversity in jawed vertebrates. *Proceedings of the Academy of Natural Sciences of Philadelphia*, **106**, 13410-13414.

Bauer, A.M. & Sadlier, R.A. (2000) *The Herpetofauna of New Caledonia*. The Society for the Study of Amphibians and Reptiles, in cooperation with the Institut de recherche pour le développement, Ithaca, NY.

Bauer, A.M., Jackman, T., Sadlier, R. & Whitaker, A. (2012) Revision of the giant geckos of New Caledonia (Reptilia: Diplodactylidae: *Rhacodactylus*) *Zootaxa*, **3404**, 1-52.

Beaulieu, J.M., Jhwueng, D.-C., Boettiger, C. & O'Meara, B.C. (2012) Modeling stablizing selection: Expanding the Ornstein-Uhlenbeck model of adaptive evolution. *Evolution*, **66**, 2369-2383.

Bowman, D.M.J.S., Brown, G.K., Braby, M.F., Brown, J.R., Cook, L.G., Crisp, M.D., Ford, F., Haberle, S., Hughes, J., Isagi, Y., Joseph, L., McBride, J., Nelson, G. & Ladiges, P.Y. (2010) Biogeography of the Australian monsoon tropics. *Journal of Biogeography*, **37**, 201-216.

Brennan, I.G. & Oliver, P.M. (2017) Mass turnover and recovery dynamics of a diverse Australian continental radiation. *Evolution*, n/a-n/a.

Brennan, I.G., Bauer, A.M. & Jackman, T.R. (2016) Mitochondrial introgression via ancient hybridization, and systematics of the Australian endemic pygopodid gecko genus *Delma*. *Molecular Phylogenetics and Evolution*, **94**, 577-590.

Byrne, M., Yeates, D.K., Joseph, L., Kearney, M., Bowler, J., Williams, M.A.J., Cooper, S., Donnellan, S.C., Keogh, J.S., Leys, R., Melville, J., Murphy, D.J., Porch, N. & Wyrwoll, K.H. (2008) Birth of a biome: insights into the assembly and maintenance of the Australian arid zone biota. *Molecular Ecology*, **17**, 4398-4417.

Cogger, H. (2000) *Reptiles and Amphibians of Australia*. New Holland Publishers, Ltd, Chatswood, NSW Australia.

DeMar, D.G., Jr., Conrad, J.L., Head, J.J., Varricchio, D.J. & Wilson, G.P. (2017) A new Late Cretaceous iguanomorph from North America and the origin of New World Pleurodonta (Squamata, Iguania). *Proc Biol Sci*, **284**

Espeland, M. & Murienne, J. (2011) Diversity dynamics in New Caledonia: towards the end of the museum model? *BMC Evolutionary Biology*, **11**, 254.

Etienne, R.S., Haegeman, B., Stadler, T., Aze, T., Pearson, P.N., Purvis, A. & Phillimore, A.B. (2012) Diversity-dependence brings molecular phylogenies closer to agreement with the fossil record. *Proceedings of the Royal Society Biological Sciences Series B*, **279**, 1300-1309.

Evans, S.E. (2008) The skull of lizards and tuatara. *Biology of the Reptilia: the Skull of Lepidosauria* (ed. by C. Gans, A.S. Gaunt and K. Adler), pp. 1-349. Society for the Study of Amphibians and Reptiles, Ithaca, New York, USA.

Felsenstein, J. (1973) Maximum-Likelihood Estimation of Evolutionary Trees from Continuous Characters. *American Journal of Human Genetics*, **25**, 471-492.

Felsenstein, J. (1985) Phylogenies and the Comparative Method. *American Naturalist*, **125**, 1-15.

Fujita, M.K., Boore, J.L. & Moritz, C. (2007) Multiple origins and rapid evolution of duplicated mitochondrial genes in parthenogenetic geckos (*Heteronotia binoei*; squamata, gekkonidae). *Molecular Biology and Evolution*, **24**, 2775-2786.

Fujita, M.K., McGuire, J.A., Donnellan, S.C. & Moritz, C. (2010) Diversification and persistence at the arid-monsoonal interface: Australia-wide biogeography of the Bynoe's gecko (*Heteronotia binoei*; Gekkoninae). *Evolution*, **64**, 2293-2314.

Garcia-Porta, J. & Ord, T.J. (2013) Key innovations and island colonization as engines of evolutionary diversification: a comparative test with the Australasian diplodactyloid geckos. *Journal of Evolutionary Biology*, **26**, 2662-2680.

Grant-Mackie, J.A., Bauer, A.M. & Tyler, M.J. (2003) Stratigraphy and herpetofauna of mé auré cave (site WMD007), Miondu, New Caledonia. *Les Cahiers de l'Archeologie en Nouvelle-Calédonie* **15**, 295-306.

Heinicke, M.P., Greenbaum, E., Jackman, T.R. & Bauer, A.M. (2011) Phylogeny of a trans-Wallacean radiation (Squamata, Gekkonidae, *Gehyra*) supports a single early colonization of Australia. *Zoologica Scripta*, **40**, 584-602.

Höhna, S., May, M.R. & Moore, B.R. (2016) TESS: an R package for efficiently simulating phylogenetic trees and performing Bayesian inference of lineage diversification rates. *Bioinformatics*, **32**, 789-791.

Hugall, A.F. & Lee, M.S.Y. (2007) The likelihood node density effect and consequences for evolutionary studies of molecular rates. *Evolution*, **61**, 2293-2307.

Jennings, W.B., Pianka, E.R. & Donnellan, S. (2003) Systematics of the lizard family pygopodidae with implications for the diversification of Australian temperate biotas. *Systematic Biology*, **52**, 757-780.

Kass, R. & Raftery, A. (1995) Bayes factors. *Journal of the American Statistical Association*, **90**

Lee, M.S.Y., Sanders, K.L., King, B. & Palci, A. (2016) Diversification rates and phenotypic evolution in venomous snakes (Elapidae). *Royal Society Open Science*, **3**

Lewitus, E. & Morlon, H. (2016) Characterizing and Comparing Phylogenies from their Laplacian Spectrum. *Systematic Biology*, **65**, 495-507.

Linder, H.P., Rabosky, D.L., Antonelli, A., Wüest, R.O. & Ohlemüller, R. (2014) Disentangling the influence of climatic and geological changes on species radiations. *Journal of Biogeography*, **41**, 1313-1325.

Longrich, N.R., Bhullar, B.-A.S. & Gauthier, J.A. (2012) Mass extinction of lizards and snakes at the Cretaceous–Paleogene boundary. *Proceedings of the National Academy of Sciences*, **109**, 21396-21401.

Losos, J.B. (2009) *Lizards in an Evolutionary Tree: Ecology and Adaptive Radiation of Anoles*. University of California Press.

Losos, J.B. & Miles, D.B. (1994) Adaptation, constraint, and the comparative method: phylogenetic issues and methods. *Ecological morphology: integrative organismal biology* (ed. by P.C. Wainwright and S.M. Reilly), pp. 60-98. University Chicago Press, Chicago.

Losos, J.B. & Ricklefs, R.E. (2009) Adaptation and diversification on islands. *Nature*, **457**, 830-836.

Losos, J.B., Jackman, T.R., Larson, A., de Queiroz, K. & Rodriguez-Schettino, L. (1998) Contingency and determinism in replicated adaptive radiations of island lizards. *Science*, **279**, 2115-2118.

Mahler, D.L., Revell, L.J., Glor, R.E. & Losos, J.B. (2010) Ecological Opportunity and the Rate of Morphological Evolution in the Diversification of Greater Antillean Anoles. *Evolution*, **64**, 2731-2745.

May, M.R. & Moore, B.R. (2016) How Well Can We Detect Lineage-Specific Diversification-Rate Shifts? A Simulation Study of Sequential AIC Methods. *Systematic Biology*, **65**, 1076-1084.

May, M.R., Höhna, S. & Moore, B.R. (2016) A Bayesian approach for detecting the impact of mass-extinction events on molecular phylogenies when rates of lineage diversification may vary. *Methods in Ecology and Evolution*, **7**, 947-959.

McGuire, J.A., Witt, C.C., Remsen, J.V., Jr., Corl, A., Rabosky, D.L., Altshuler, D.L. & Dudley, R. (2014) Molecular Phylogenetics and the Diversification of Hummingbirds. *Current Biology*, **24**, 910-916.

Mirarab, S. & Warnow, T. (2015) ASTRAL-II: coalescent-based species tree estimation with many hundreds of taxa and thousands of genes. *Bioinformatics*, **31**, 44-52.

Mirarab, S., Reaz, R., Bayzid, M.S., Zimmermann, T., Swenson, M.S. & Warnow, T. (2014) ASTRAL: genome-scale coalescent-based species tree estimation. *Bioinformatics*, **30**, I541-I548.

Mitchell, J.S. & Rabosky, D.L. (2016) Bayesian model selection with BAMM: effects of the model prior on the inferred number of diversification shifts. *Methods in Ecology and Evolution*, n/a-n/a.

Moore, B.R., Höhna, S., May, M.R., Rannala, B. & Huelsenbeck, J.P. (2016) Critically evaluating the theory and performance of Bayesian analysis of macroevolutionary mixtures. *PNAS*, **113**, 9569-9574.

Morlon, H. (2014) Phylogenetic approaches for studying diversification. *Ecology Letters*, **17**, 508-525.

Morlon, H., Parsons, T.L. & Plotkin, J.B. (2011) Reconciling molecular phylogenies with the fossil record. *Proceedings of the National Academy of Sciences of the United States of America*, **108**, 16327-16332.

Morlon, H., Lewitus, E., Condamine, F.L., Manceau, M., Clavel, J. & Drury, J. (2016) RPANDA: an R package for macroevolutionary analyses on phylogenetic trees. *Methods in Ecology and Evolution*, **7**, 589-597.

Moyle, R.G., Oliveros, C.H., Andersen, M.J., Hosner, P.A., Benz, B.W., Manthey, J.D., Travers, S.L., Brown, R.M. & Faircloth, B.C. (2016) Tectonic collision and uplift of Wallacea triggered the global songbird radiation. *Nature Communications*, **7**, 1-7.

Nee, S., May, R.M. & Harvey, P.H. (1994) The Reconstructed Evolutionary Process. *Philosophical Transactions of the Royal Society of London Series B-Biological Sciences*, **344**, 305-311.

Nielsen, S.V., Bauer, A.M., Jackman, T.R., Hitchmough, R.A. & Daugherty, C.H. (2011) New Zealand geckos (Diplodactylidae): Cryptic diversity in a post-Gondwanan lineage with trans-Tasman affinities. *Molecular Phylogenetics and Evolution*, **59**, 1-22.

O'Meara, B.C., Ane, C., Sanderson, M.J. & Wainwright, P.C. (2006) Testing for different rates of continuous trait evolution using likelihood. *Evolution*, **60**, 922-933.

Oliver, P.M. & Sanders, K.L. (2009) Molecular evidence for Gondwanan origins of multiple lineages within a diverse Australasian gecko radiation. *Journal of Biogeography*, **36**, 2044-2055.

Oliver, P.M. & Doughty, P. (2016) Systematic revision of the marbled velvet geckos (*Oedura marmorata* species complex, Diplodactylidae) from the Australian arid and semi-arid zones. *Zootaxa*, **4088**, 151-176.

Oliver, P.M., Hutchinson, M.N. & Cooper, S.J.B. (2007) Phylogenetic relationships in the lizard genus *Diplodactylus* Gray and resurrection of *Lucasium* Wermuth (Gekkota, Diplodactylidae). *Australian Journal of Zoology*, **55**, 197-210.

Oliver, P.M., Bauer, A.M., Greenbaum, E., Jackman, T. & Hobbie, T. (2012) Molecular phylogenetics of the arboreal Australian gecko genus *Oedura* Gray 1842 (Gekkota: Diplodactylidae): Another plesiomorphic grade? *Molecular Phylogenetics and Evolution*, **63**, 255-264.

Oliver, P.M., Smith, K.L., Laver, R.J., Doughty, P. & Adams, M. (2014) Contrasting patterns of persistence and diversification in vicars of a widespread Australian lizard lineage (the *Oedura marmorata* complex). *Journal of Biogeography*, n/a-n/a.

Pagel, M. (1999) Inferring the historical patterns of biological evolution. *Nature*, **401**, 877-84.

Pinto, G., Mahler, D.L., Harmon, L.J. & Losos, J.B. (2008) Testing the island effect in adaptive radiation: rates and patterns of morphological diversification in Caribbean and mainland Anolis lizards. *Proceedings of the Royal Society B-Biological Sciences*, **275**, 2749-2757.

Pybus, O.G. & Harvey, P.H. (2000) Testing macro-evolutionary models using incomplete molecular phylogenies. *Proceedings of the Royal Society Biological Sciences Series B*, **267**, 2267-2272.

Quental, T.B. & Marshall, C.R. (2009) Extinction during evolutionary radiations: reconciling the fossil record with molecular phylogenies. *Evolution*, **63**, 3158-3167.
Quental, T.B. & Marshall, C.R. (2010) Diversity dynamics: molecular phylogenies need the fossil record. *Trends in Ecology & Evolution*, **25**, 434-441.
Quental, T.B. & Marshall, C.R. (2011) The molecular phylogenetic signature of clades in decline. *PLoS ONE*, **6**, e25780.
Rabosky, D.L. (2006) LASER: A maximum likelihood toolkit for detecting temporal shifts in diversification rates from molecular phylogenies. *Bioinformatics*, **2**, 247-250.
Rabosky, D.L. (2010) Extinction rates should not be estimated from molecular phylogenies. *Evolution*, **64**, 1816-1824.
Rabosky, D.L. (2014) Automatic Detection of Key Innovations, Rate Shifts, and Diversity-Dependence on Phylogenetic Trees. *Plos One*, **9**, 1-15.
Rabosky, D.L. & Glor, R.E. (2010) Equilibrium speciation dynamics in a model adaptive radiation of island lizards. *Proceedings of the National Academy of Sciences of the United States of America*, **107**, 22178-22183.
Rabosky, D.L. & Huang, H.T. (2016) A Robust Semi-Parametric Test for Detecting Trait-Dependent Diversification. *Systematic Biology*, **65**, 181-193.
Rabosky, D.L., Santini, F., Eastman, J., Smith, S.A., Sidlauskas, B., Chang, J. & Alfaro, M.E. (2013) Rates of speciation and morphological evolution are correlated across the largest vertebrate radiation. *Nature Communications*, **4**
Rabosky, D.L., Grundler, M., Anderson, C., Title, P., Shi, J.J., Brown, J.W., Huang, H. & Larson, J.G. (2014) BAMMtools: an R package for the analysis of evolutionary dynamics on phylogenetic trees. *Methods in Ecology and Evolution*, **5**, 701-707.
Revell, L.J. (2012) phytools: an R package for phylogenetic comparative biology (and other things). *Methods in Ecology and Evolution*, **3**, 217-223.
Revell, L.J. (2013) Two new graphical methods for mapping trait evolution on phylogenies. *Methods in Ecology and Evolution*, **4**, 754-759.
Revell, L.J., Johnson, M.A., Schulte, J.A., II, Kolbe, J.J. & Losos, J.B. (2007) A phylogenetic test for adaptive convergence in rock-dwelling lizards. *Evolution*, **61**, 2898-2912.
Ricklefs, R.E. (2006) Time, species, and the generation of trait variance in clades. *Syst Biol*, **55**, 151-9.
Sanger, T.J., Mahler, D.L., Abzhanov, A. & Losos, J.B. (2012) Roles for Modularity and Constraint in the Evolution of Cranial Diversity among Anolis Lizards. *Evolution*, **66**, 1525-1542.
Santini, F., Nguyen, M.T.T., Sorenson, L., Waltzek, T.B., Lynch Alfaro, J.W., Eastman, J.M. & Alfaro, M.E. (2013) Do habitat shifts drive diversification in teleost fishes? An example from the pufferfishes (Tetraodontidae). *Journal of Evolutionary Biology*, **26**, 1003-1018.
Schluter, D. (2000) *The Ecology of Adaptive Radiation*. Oxford University Press, New York.
Shi, J.J. & Rabosky, D.L. (2015) Speciation dynamics during the global radiation of extant bats. *Evolution*, **69**, 1528-1545.
Skipwith, P.L., Bauer, A.M., Jackman, T.R. & Sadlier, R.A. (2016) Old but not ancient: coalescent species tree of New Caledonian geckos reveals recent post-inundation diversification. *Journal of Biogeography*, **43**, 1266-1276.
Stadler, T. (2011) Mammalian phylogeny reveals recent diversification rate shifts. *Proc Natl Acad Sci U S A*, **108**, 6187-92.

Sun, J., Ni, X., Bi, S., Wu, W., Ye, J., Meng, J. & Windley, B.F. (2014) Synchronous turnover of flora, fauna, and climate at the Eocene–Oligocene Boundary in Asia. **4**, 7463.

Title, P.O. & Rabosky, D.L. (2016) Do Macrophylogenies Yield Stable Macroevolutionary Inferences? An Example from Squamate Reptiles. *Systematic Biology*, **Advanced Access**, 1-14.

Vidal-Garcia, M., Byrne, P.G., Roberts, J.D. & Keogh, J.S. (2014) The role of phylogeny and ecology in shaping morphology in 21 genera and 127 species of Australo-Papuan myobatrachid frogs. *Journal of Evolutionary Biology*, **27**, 181-192.

Warnock, R.C.M., Parham, J.F., Joyce, W.G., Lyson, T.R. & Donoghue, P.C.J. (2015) Calibration uncertainty in molecular dating analyses: there is no substitute for the prior evaluation of time priors. *Proceedings of the Royal Society B-Biological Sciences*, **282**

Wilson, S. & Swan, G. (2013) *A Complete Guide to Reptiles of Australia*, 4th edn. New Holland Publishers, Chatswood, Australia.

Yang, Z.H. (2007) PAML 4: Phylogenetic analysis by maximum likelihood. *Molecular Biology and Evolution*, **24**, 1586-1591.

Yazykova, E.A. (1996) Post-crisis recovery of Campanian desmoceratacean ammonites from Sakhalin, far east Russia. *Geological Society of London Special Publications* (ed. by M.B. Hart), pp. 299-308. Geological Society of London, London, UK.

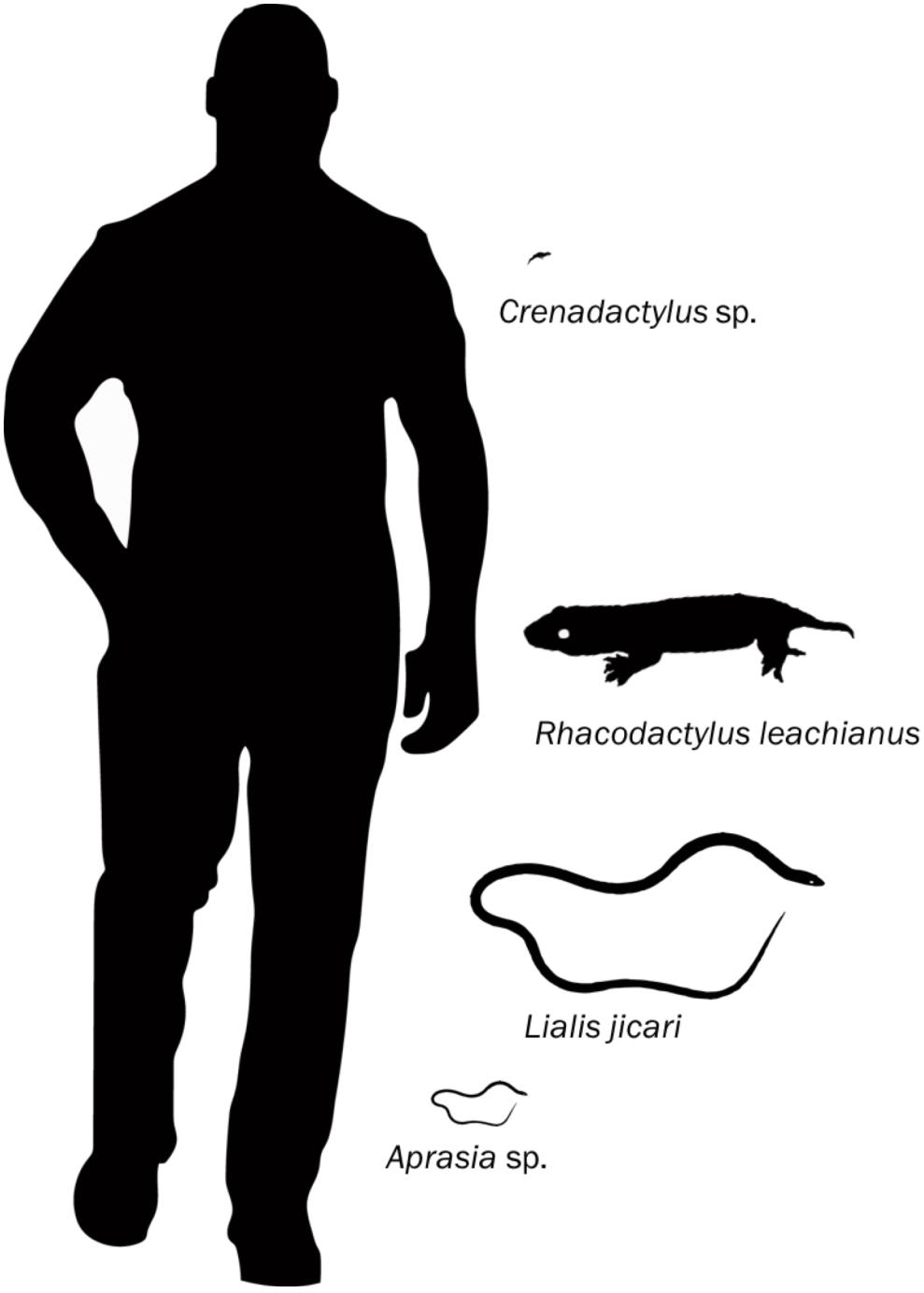


**Figure 17**: Silhouettes illustrating the comparative sizes of the largest and smallest limbed dipodactyloids as well as the largest and smallest pygopodids.

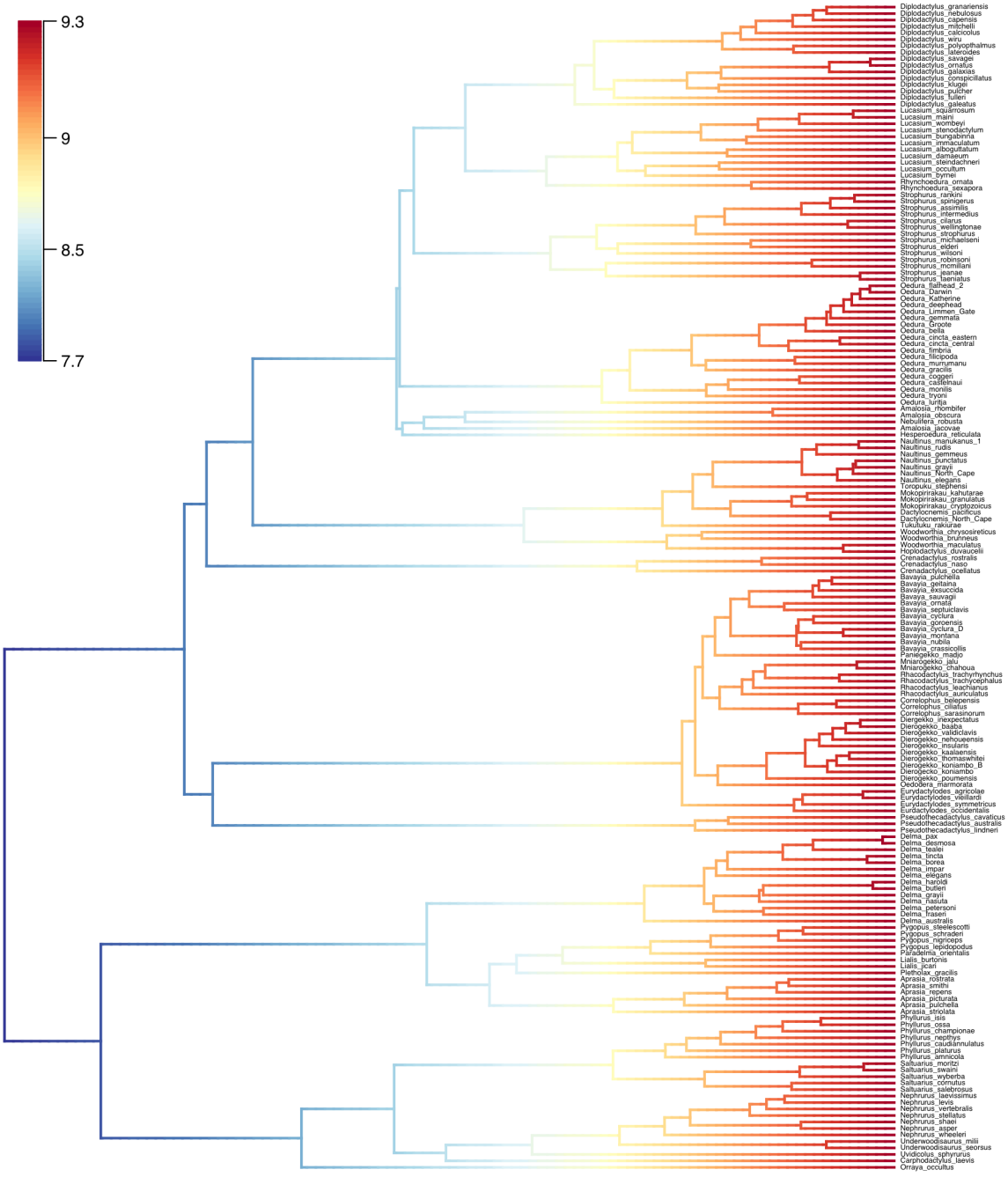


**Figure 18**: BAMM speciation-extinction analysis from best shift configuration. Red node dots indicate where a shift in diversification rate has occurred. Legend corresponds net diversification rate.

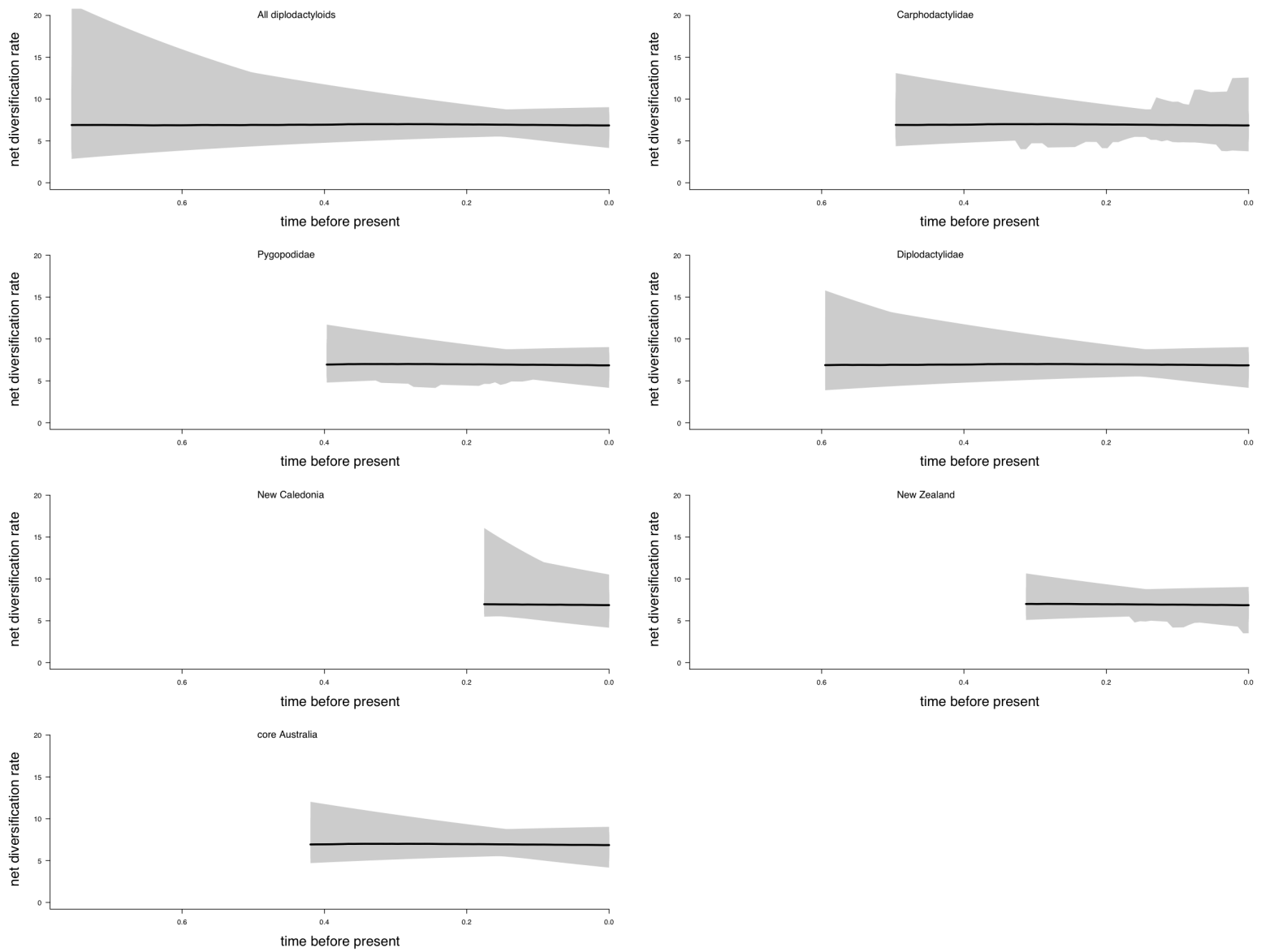


**Figure 19**: Net diversification through time plots from BAMM speciation-extinction analysis for all diplodactyloids and individual clades.

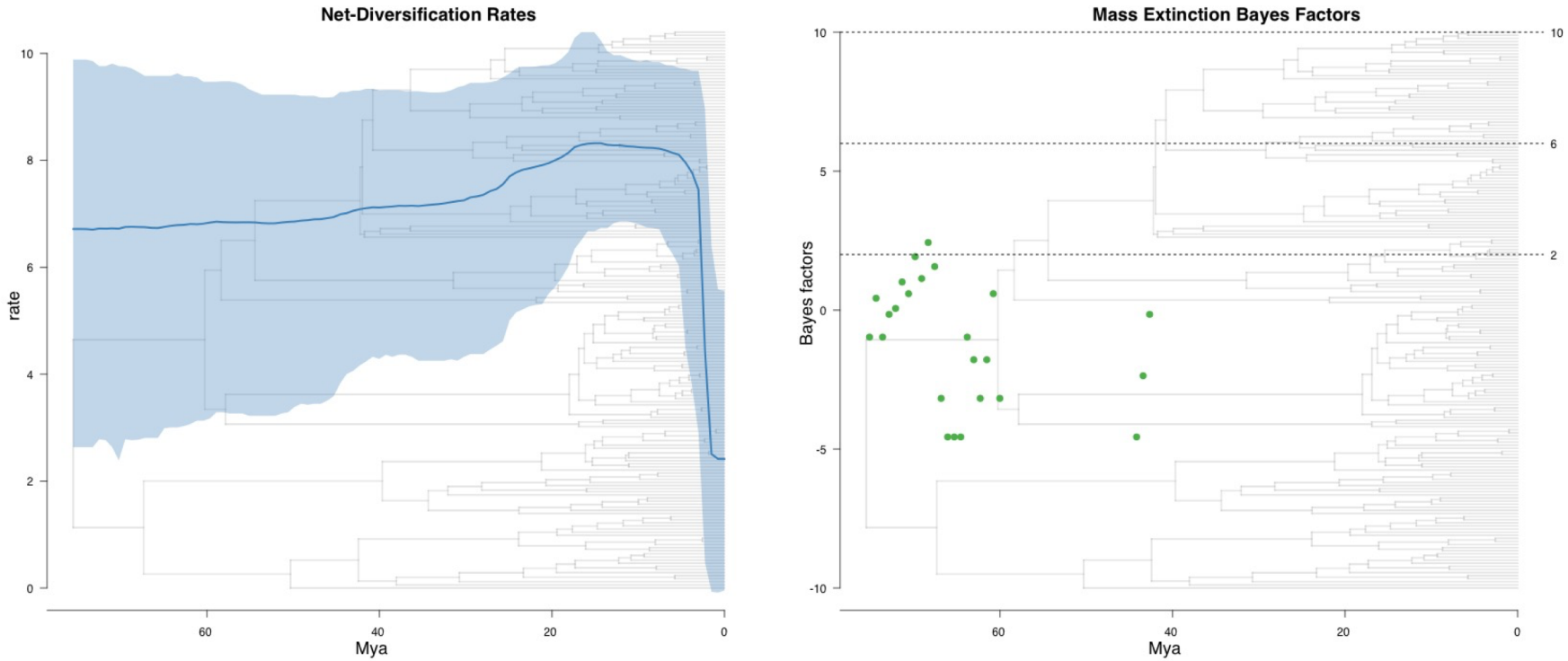


**Figure 20**: COMET analysis from TESS. A) Net diversification of the whole diplodactyloid tree. Note drop in diversification around 4 My. B) Bayes factor (BF) support for mass extinction events across the whole tree. No such event received strong BF evidence.

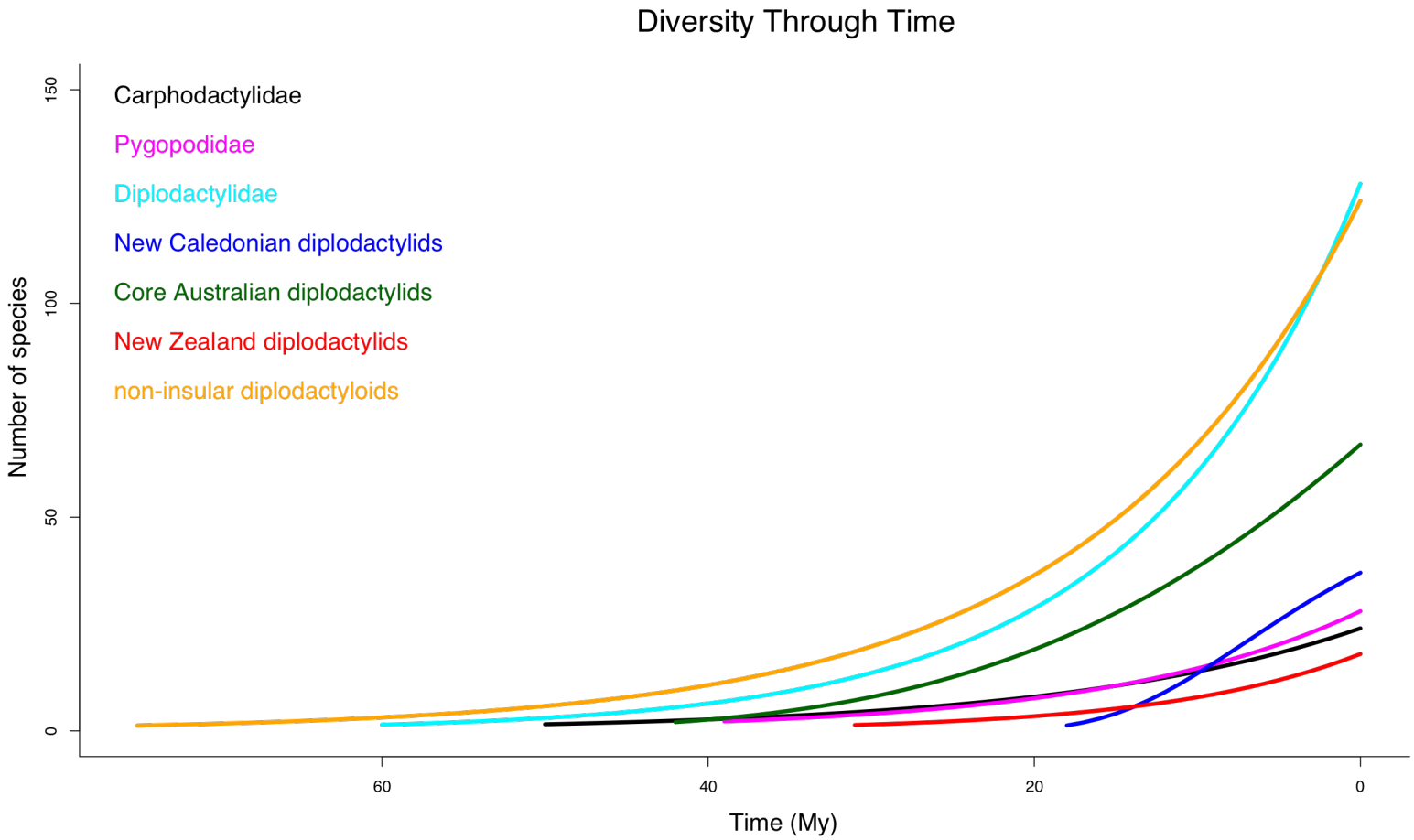


**Figure 21**: Diversity through time plots from RPANDA for clades examined.


**Figure 22**: Spectral density plot from RPANDA. Uniformity in color reveals a single modality across the whole diplodactyloid tree.


**Figure 23**: CONTMAP ancestral state reconstruction of svl for all 180 diplodactyloid species. Bars on right represent svl (mm).


**Figure 24**: CONTMAP ancestral state reconstruction of relative head length (corrected for body svl) for 148 diplodactyloid species. Bars on right represent relative head length.

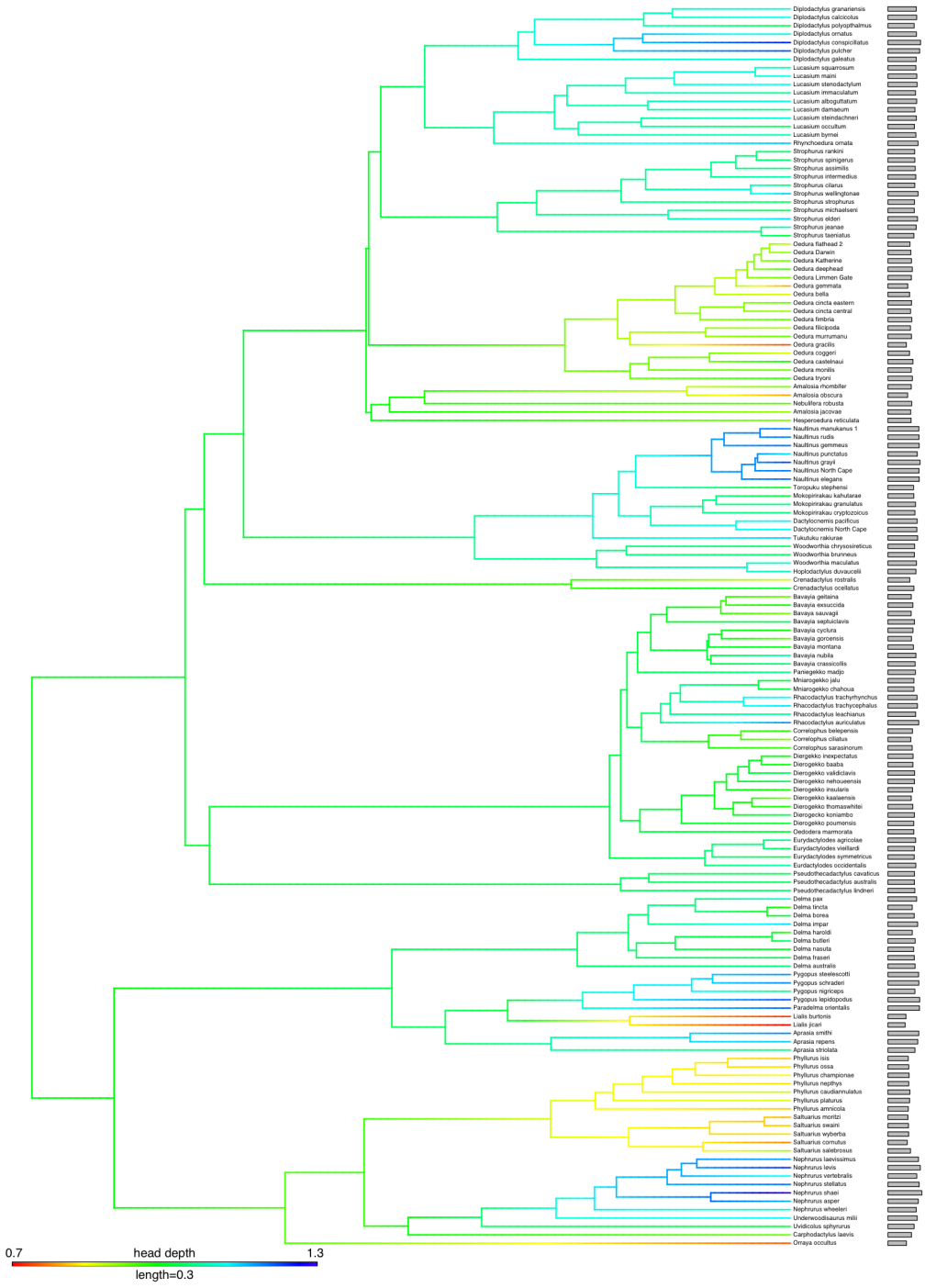


**Figure 25**: CONTMAP ancestral state reconstruction of relative head depth (corrected for head length) for 148 diplodactyloid species. Bars on right represent relative head depth.

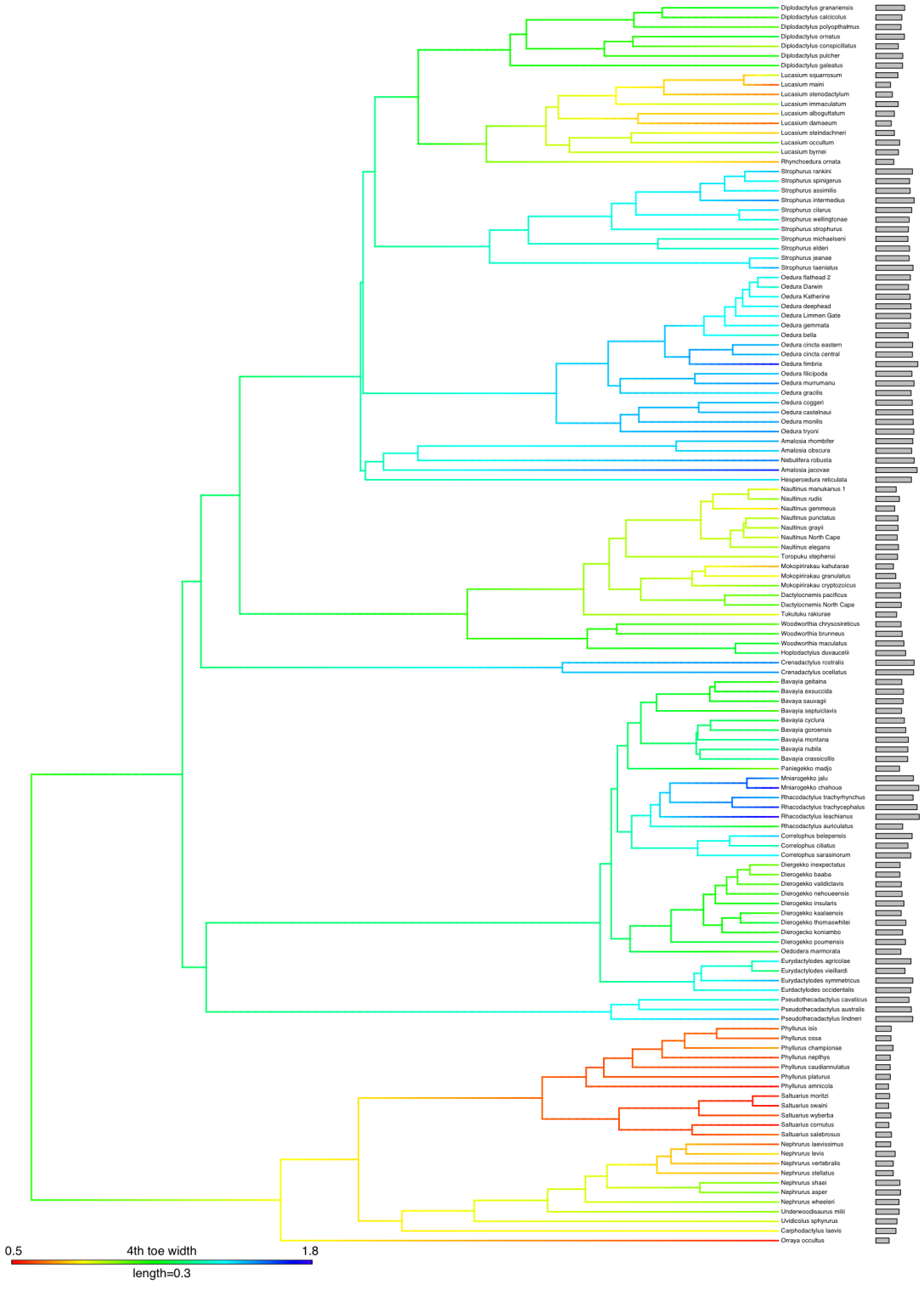


**Figure 26**: CONTMAP ancestral state reconstruction of relative toe width (corrected for toe length) for 129 diplodactyloid species. Bars on right represent relative toe width.

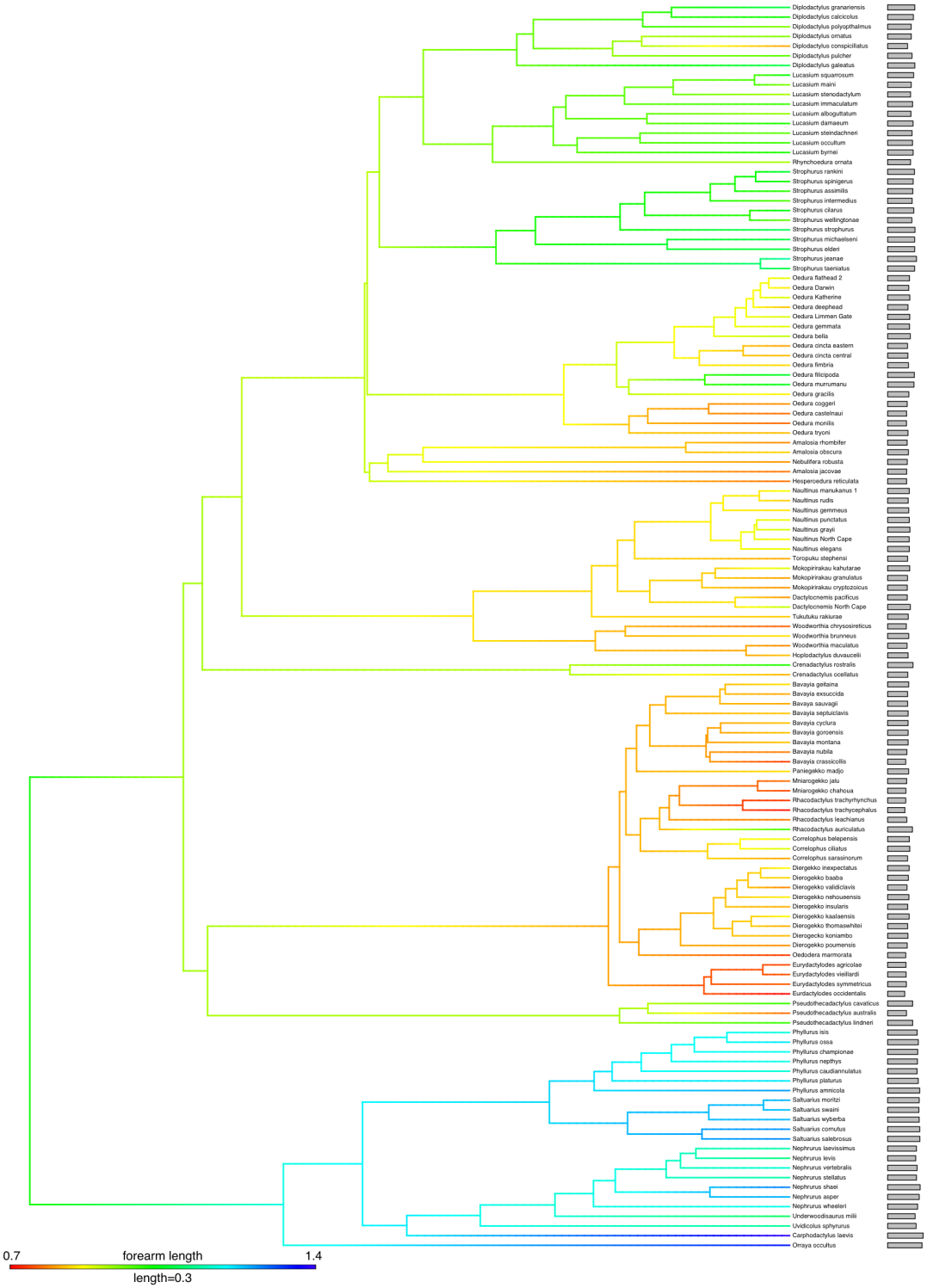


**Figure 27**: CONTMAP ancestral state reconstruction of relative forearm length (corrected for svl) for 129 diplodactyloid species. Bars on right represent relative forearm length.

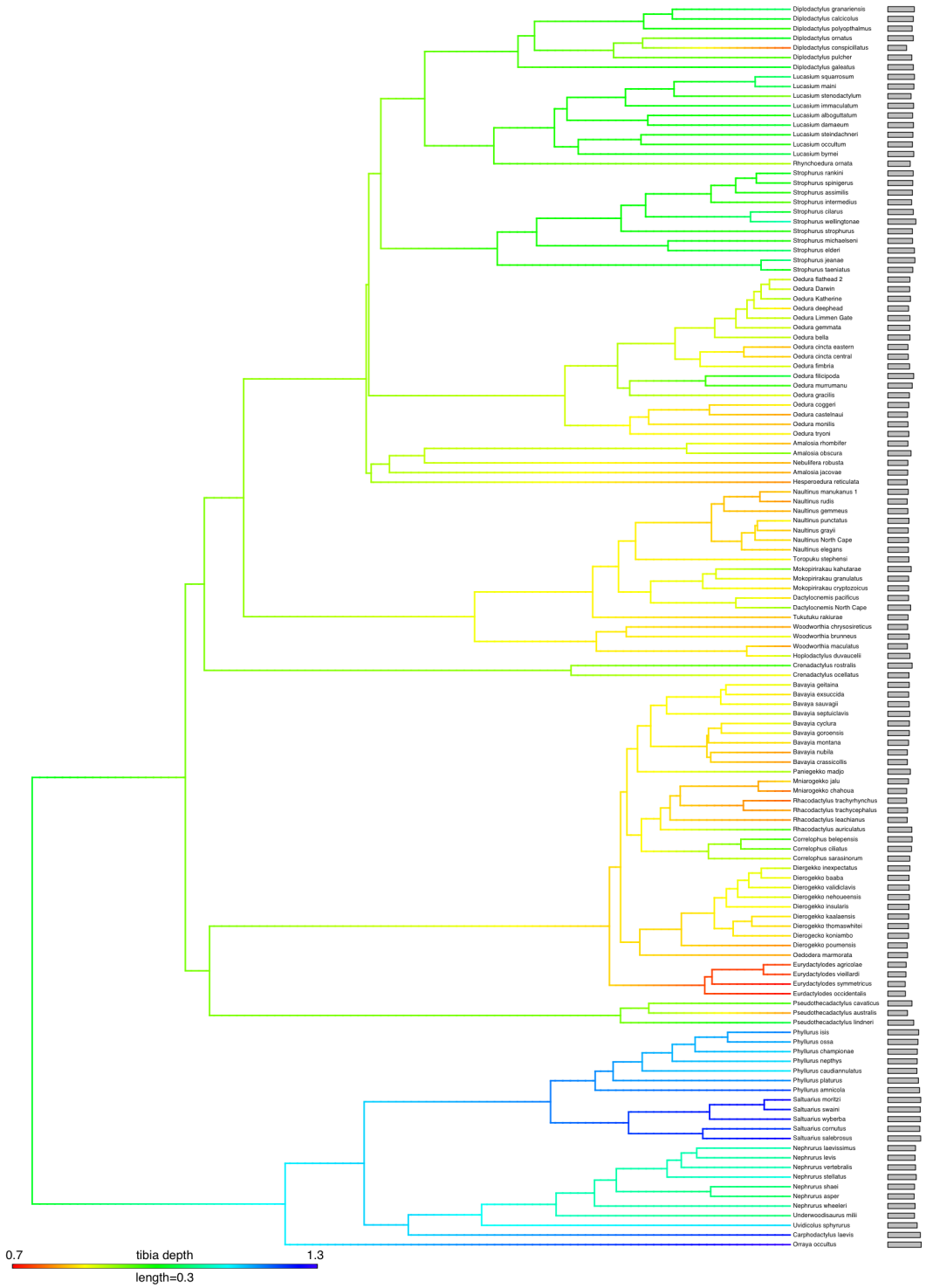


**Figure 28**: CONTMAP ancestral state reconstruction of relative tibia length (corrected for svl) for 129 diplodactyloid species. Bars on right represent relative tibia length.

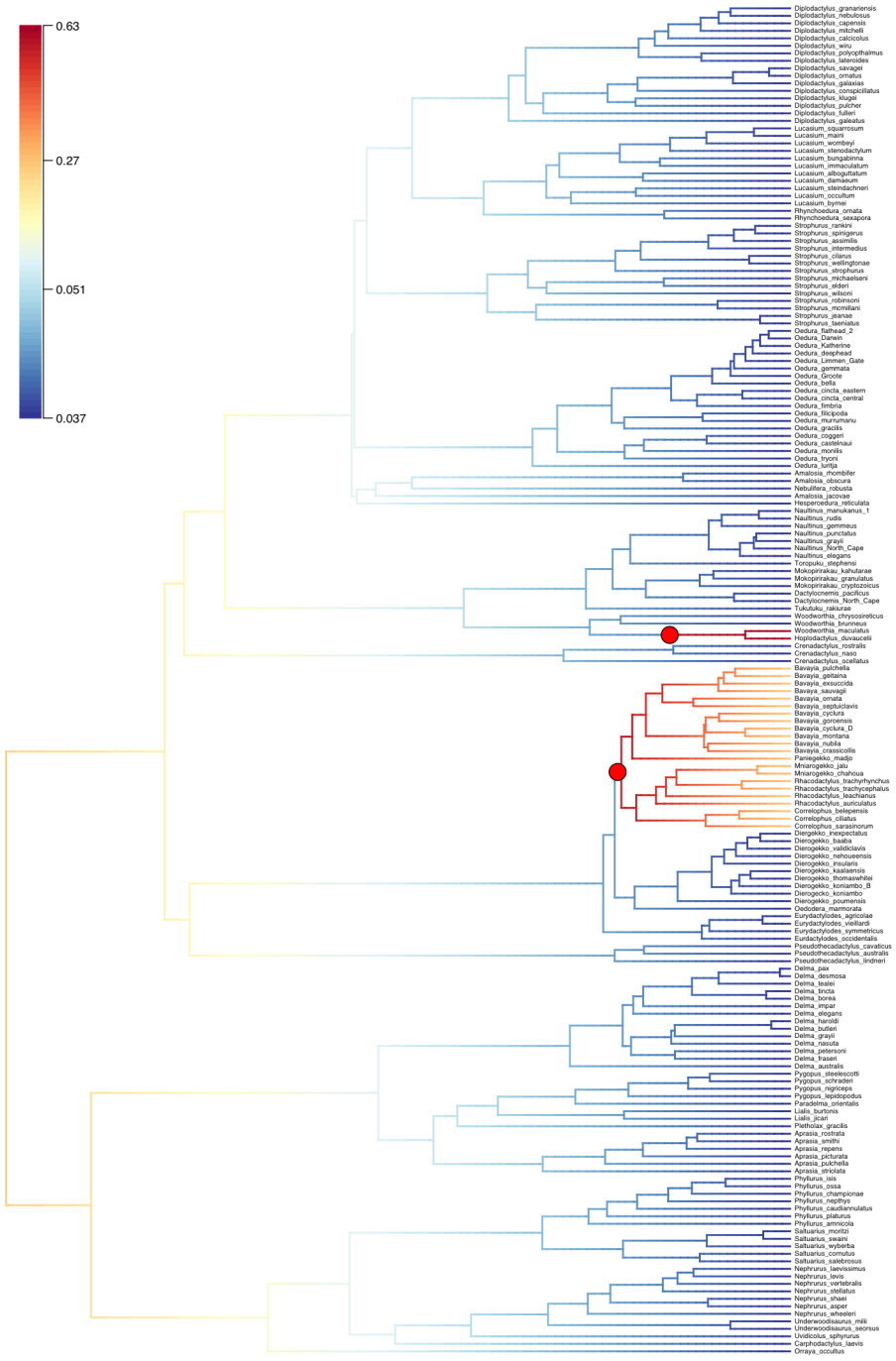


**Figure 29**: BAMM trait analysis of svl from best shift configuration. Red node dots indicate where a shift in diversification rate has occurred.

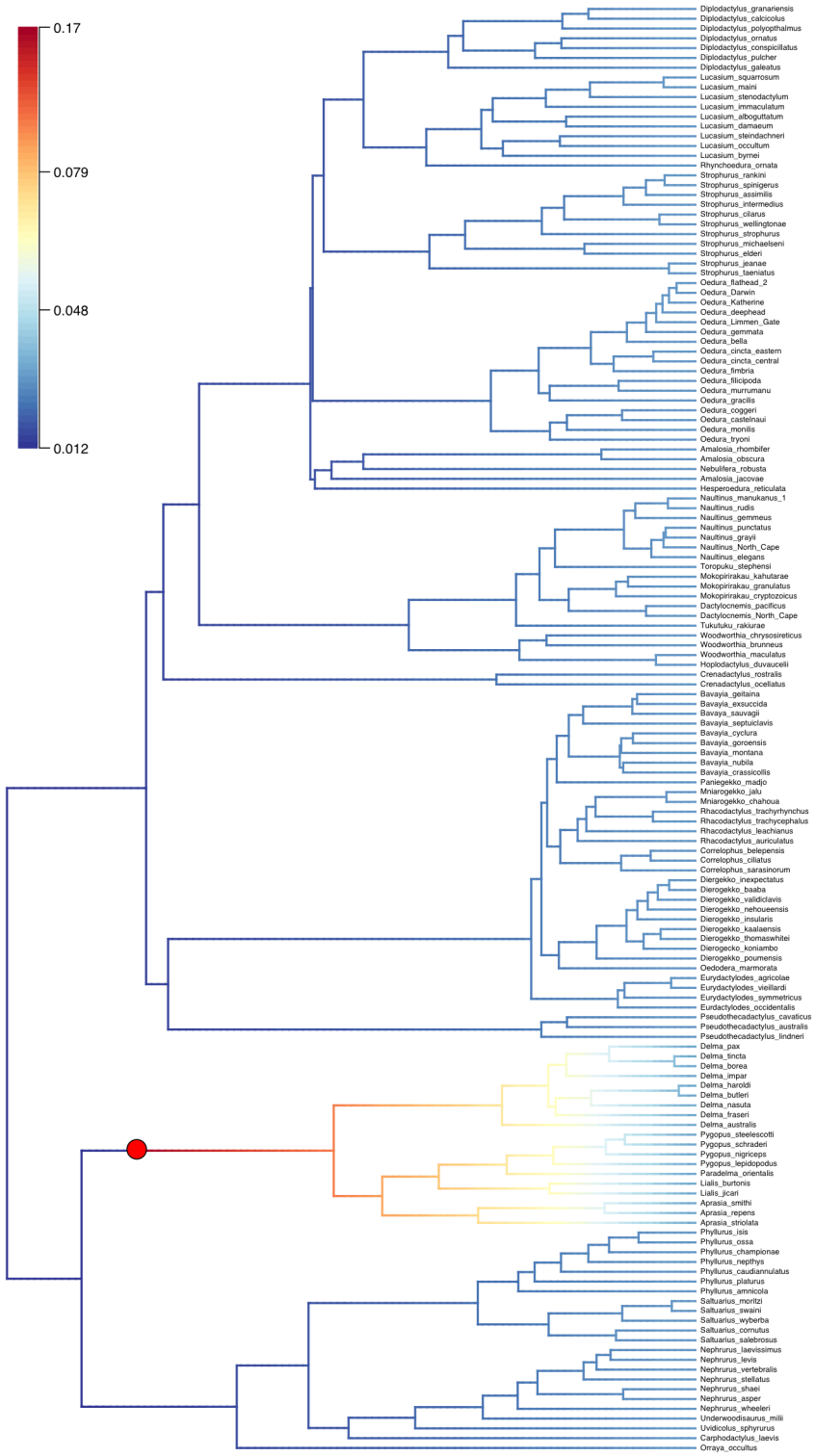


**Figure 30**: BAMM trait analysis of relative head length from best shift configuration. Red node dots indicate where a shift in diversification rate has occurred.

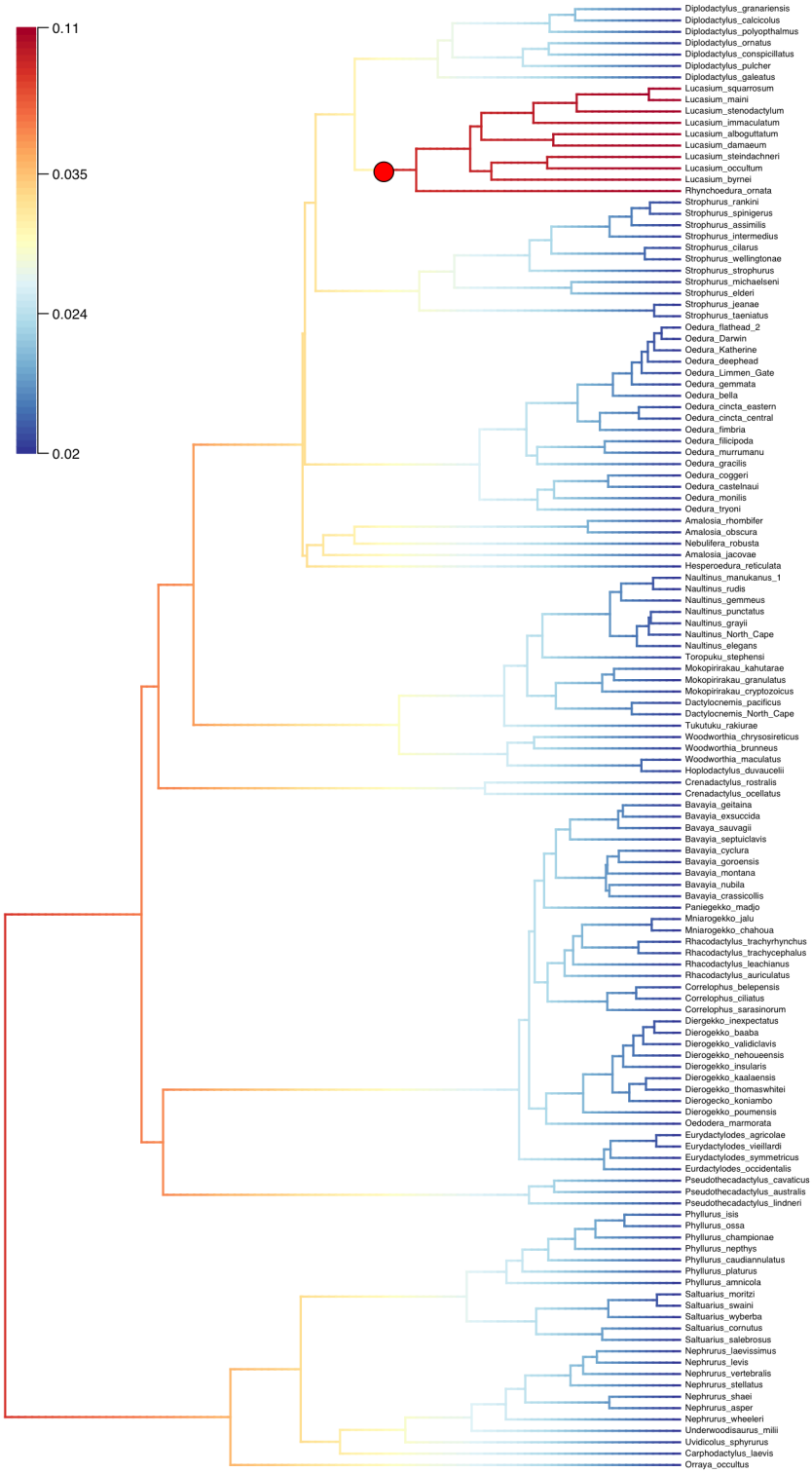


**Figure 31**: BAMM trait analysis of relative toe width from best shift configuration. Red node dots indicate where a shift in diversification rate has occurred.

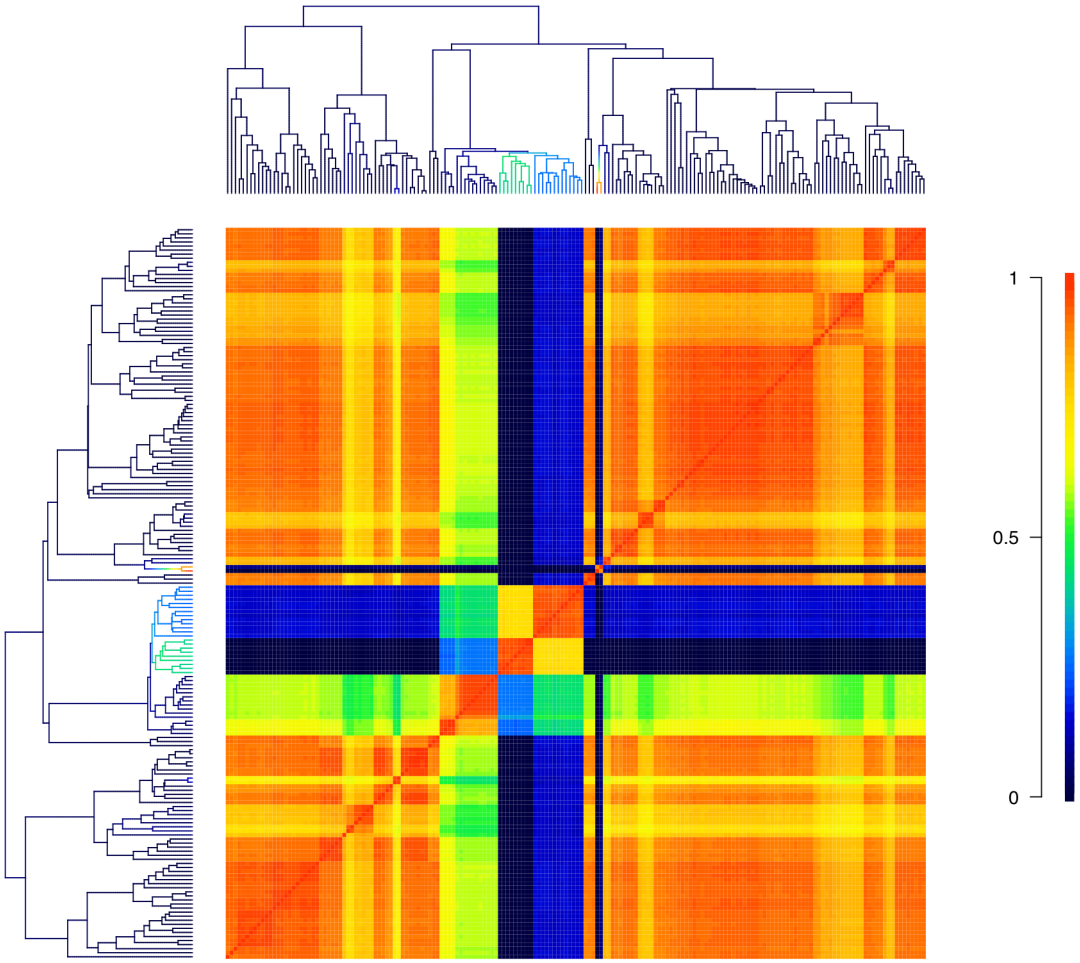


**Figure 32**: BAMM macroevolutionary cohort analysis of svl. Warm colors in a matrix column indicates that two species share the same rate regime for most samples from the BAMM trait analysis posterior. Cool colors for any pairwise comparison mean that those two species do not share a common rate regime, indication a distinct rate shift has occurred.

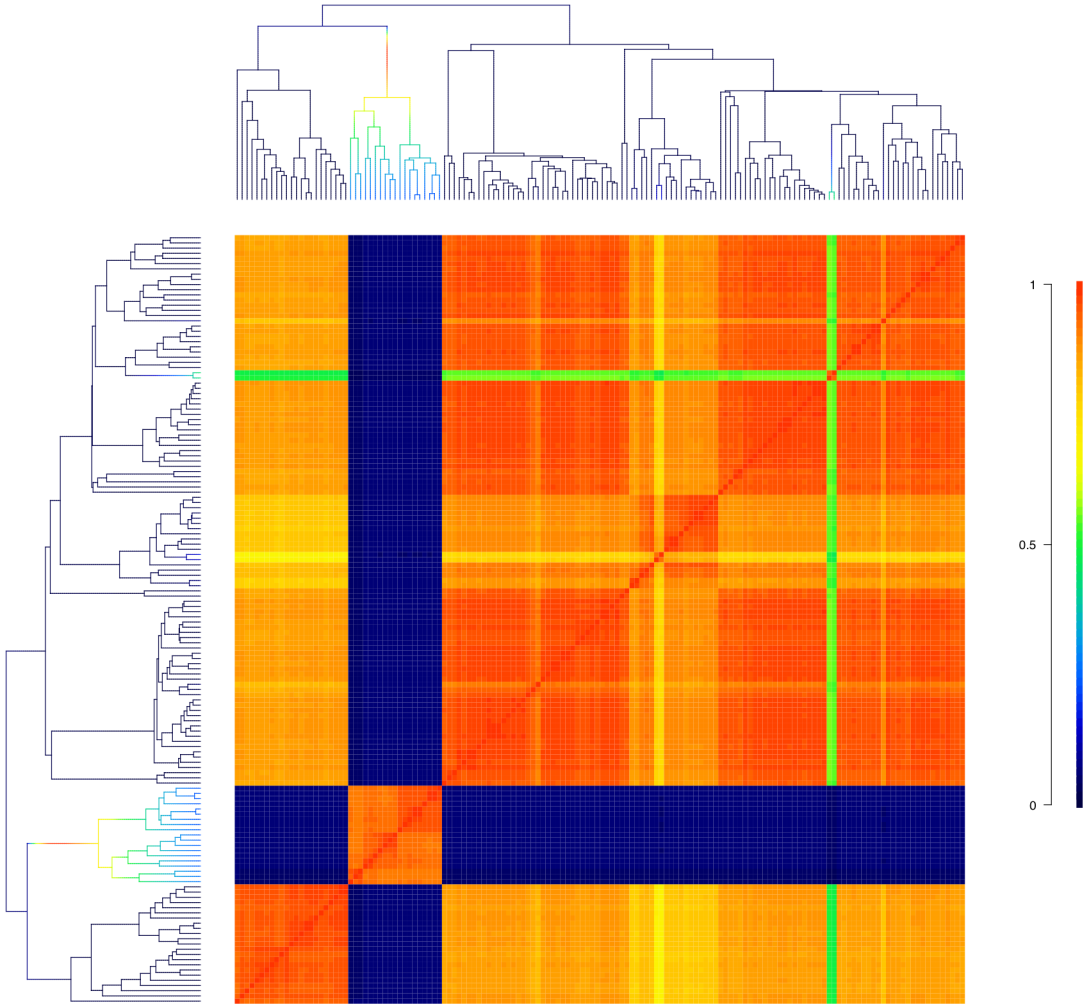


**Figure 33**: BAMM macroevolutionary cohort analysis of relative head length. Warm colors in a matrix column indicates that two species share the same rate regime for most samples from the BAMM trait analysis posterior. Cool colors for any pairwise comparison mean that those two species do not share a common rate regime, indication a distinct rate shift has occurred.

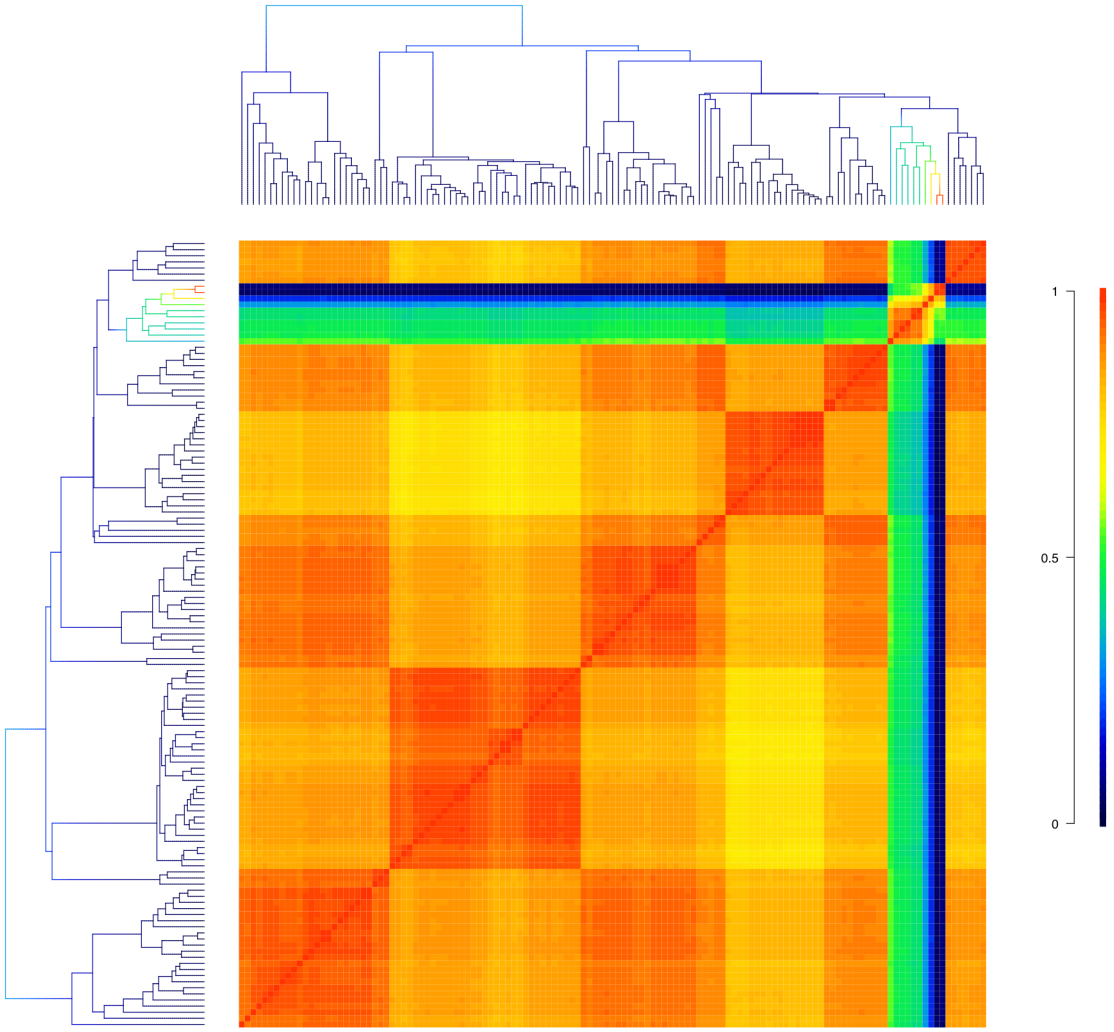


**Figure 34**: BAMM macroevolutionary cohort analysis of relative toe width. Warm colors in a matrix column indicates that two species share the same rate regime for most samples from the BAMM trait analysis posterior. Cool colors for any pairwise comparison mean that those two species do not share a common rate regime, indication a distinct rate shift has occurred.

**Table 7**: Model selection for LASER, DDD, and RPANDA for all diplodactyloids and minor clades. $\lambda$ = speciation rate, $\mu$ = extinction rate, and $k$ = species carrying capacity. BAMM speciation and extinction rate estimates for same clades.

| | | **Diplodactyloidea** | **Carphodactylidae** | **Pygopodidae** | **Diplodactylidae** | **New Caledonia** | **New Zealand** | **core Australia** | **Non-Insular** |
|---|---|---|---|---|---|---|---|---|---|
| LASER | Model | Y2R | Y2R | Y2R | Y2R | DDL | PB | Y2R | Y2R |
| | $\lambda_1$ | 7.01 | 6.42 | 6.12 | 7.97 | 33.86 | 7.29 | 7.08 | 6.01 |
| | $\lambda_2$ | 0.55 | 1.38 | 3.19 | 0.59 | — | — | 1.04 | 0.79 |
| | $k$ | — | — | — | — | 38.5 | — | — | — |
| DDD | Model | DDL - E | DDL - E | DDL - E | DDL - E | DDL - E | PB | DDL - E | DDL - E |
| | $\lambda$ | 9.18 | 9.46 | 13.46 | 10.03 | 33.91 | 8.24 | 11.1 | 8.95 |
| | $k$ | 466.2 | 41.9 | 63.3 | 333.1 | 39.6 | — | 121.8 | 196 |
| RPANDA | Model | — | BcstDcst | BcstDcst | BcstDcst | BvarDcst | BcstDcst | BvarDcst | BcstDcst |
| | $\lambda_1$ | — | 5.47 | 6.49 | 7.48 | 5.22 | 8.27 | 4.97 | 6.12 |
| | $\lambda_2$ | — | — | — | — | 1.21 | — | 2.26 | — |
| | $\mu$ | — | 2.16e-6 | 3.77e-6 | -2.03e-7 | -3.77e-6 | -4.11e-6 | 3.12e-6 | 1.21e-6 |
| BAMM | $\lambda$ | 7.33 | 7.33 | 7.31 | 7.32 | 7.33 | 7.3 | 7.3 | — |
| | $\mu$ | 0.38 | 0.38 | 0.37 | 038 | 0.39 | 0.37 | 0.38 | — |

**Table 8**: TESS BF support of the top 8 model comparisons.

| $M_0$ | $M_1$ | BF |
|---|---|---|
| CrBDex | BDep | 219.3 |
| BDVar | BDep | 190.8 |
| BDVarEx | BDep | 190.7 |
| CrBDex | CrBD | 144.1 |
| BDVar | CrBD | 115.6 |
| BDVarEx | CrBD | 115.5 |
| CrBD | BDep | 75.2 |
| CrBDex | BDVarEx | 28.6 |
| CrBDex | BDVar | 28.5 |
| BDVar | BDVarEx | 219.3 |

**Table 9**: Estimates for Pagel's $\lambda$ and Blomberg's K for all traits with BAMM estimates of shift number as inferred from BF evidence and the best credible set of shift configurations.

| | | SVL | head length | head depth | toepad width | forearm length | hind limb length |
|---|---|---|---|---|---|---|---|
| $\lambda$ | | 0.98 | 0.99 | 0.98 | 0.97 | 0.99 | 1.0 |
| | p | < 0.001 | < 0.001 | < 0.001 | < 0.001 | < 0.001 | < 0.001 |
| K | | 0.91 | 2.45 | 0.74 | 1.41 | 1.71 | 1.61 |
| | p | < 0.001 | < 0.001 | < 0.001 | < 0.001 | < 0.001 | < 0.001 |
| BAMM shifts | | 2 | 1 | 0 | 1 | 0 | 0 |

**Table 10**: BAMM rate estimates of beta (β) for each trait investigated. Italicized bold values correspond to clades for which a shift was detected using BF evidence and the best credible set of shift configurations.

| | SVL | head length | head depth | toepad width | forearm length | hind limb length |
|---|---|---|---|---|---|---|
| Diplodactyloidea | 0.06 | 0.02 | 0.01 | 0.02 | 0.01 | 0.01 |
| Carphodactylidae | 0.04 | 0.01 | 0.01 | 0.02 | 0.01 | < 0.01 |
| Pygopodidae | 0.05 | ***0.05*** | 0.01 | — | — | — |
| Diplodactylidae | 0.07 | 0.01 | 0.02 | 0.03 | 0.01 | 0.01 |
| New Caledonia | 0.15 | 0.01 | 0.01 | 0.02 | 0.01 | 0.01 |
| *Rhacodactylus – Bavayia* group | ***0.22*** | 0.01 | 0.01 | 0.02 | 0.01 | 0.01 |
| New Zealand | 0.08 | 0.01 | 0.01 | 0.02 | 0.01 | 0.01 |
| *Hoplodactylus duvaucelii – Woodworthia maculata* group | ***0.37*** | 0.02 | 0.01 | 0.02 | 0.01 | 0.01 |
| core Australia | 0.04 | 0.01 | 0.01 | 0.03 | 0.01 | 0.01 |
| *Lucasium* group | 0.04 | 0.01 | 0.01 | ***0.07*** | 0.01 | 0.01 |

**Table 11**: Rates stochastic ($\sigma^2$) trait evolution (svl) under the BMS model in OUWIE for each of island and mainland diplodactyloids.

| | Island | Mainland |
|---|---|---|
| Stochastic ($\sigma^2$) | 0.13 | 0.03 |

**Table 12**: Rates stochastic ($\sigma^2$) trait evolution (svl) under the BMS model in OUWIE for each of the bioregions for diplodactyloids.

| | New Caledonia | New Zealand | New Guinea | Australia |
|---|---|---|---|---|
| Stochastic ($\sigma^2$) | 0.13 | 0.12 | 0.04 | 0.02 |

# Chapter 4

## PHYLOGEOGRAPHY OF THE *OEDURA MARMORATA* COMPLEX IN THE MONSOONAL TROPICS OF AUSTRALIA

### Introduction

Together with New Guinea, New Caledonia, and New Zealand, Australia has been isolated from other landmasses since the breakup of Gondwana, thus, much of its biota had correspondingly ancient origins (Oliver & Sanders, 2009; Pepper *et al.*, 2016). Despite its great age, Australia has a remarkably stable geologic history in comparison to surrounding areas in Wallacea and Oceania. Its climatic history, on the other hand, has been much more varied, as exemplified by the cooling event that initiated the gradual appearance and expansion of the arid zone during the Miocene that now dominates two-thirds of Australia's land area. While this biome has become a hallmark for the continent, northern Australia is dominated by the monsoonal tropics, a climatic region stretching from the Kimberley of Western Australia to the Cape York Peninsula of Queensland. This region contrasts sharply with the Australian Arid Zone (AAZ), being characterized by extreme shifts in precipitation during the austral spring and summer (November-April). This cycle is driven by westerly monsoon winds, a component of the Asian-Australian monsoon system (Bowman *et al.*, 2010). Unlike the AAZ, the Australian Monsoonal Tropics (AMT) dates back to the mid-Paleogene, as evidenced by sediment deposits suggesting high seasonality in precipitation following the continent's separation from the remainder of Gondwana. However, there is evidence that annual oscillations in rainfall may not have been as extreme in the Paleogene as they are today (Herold *et al.*, 2011). Given the antiquity of the AMT, several biogeographic barriers have been proposed as mechanisms in generating population structure in taxa that inhabit this region. These include (1) the Bonaparte Gap (a putative barrier separating the Kimberley [west] and Top End [east]), (2) the Ord Arid Intrusion, (3) the Arnhem Plateau, (4) the Carpentarian Gap, and (5&6) the Victoria and Daly River drainages (Bowman *et al.*, 2010; Eldridge *et al.*, 2011; Criscione *et al.*, 2012). While the monsoonal tropics harbor substantial diversity, few studies have investigated the importance of these proposed barriers in a phylogeographic context. However, there is evidence that river drainages, such as the Victoria and Daly Rivers, and the intervening arid habitat have been attributed to geographic structure in macropod marsupials (Potter *et al.*, 2012; Eldridge *et al.*, 2014).

The monsoonal tropics have played a large role in the generation and maintenance of species diversity for a number of squamate lineages. The *Oedura marmorata* complex exemplifies this as it is a species group comprised of five described species found over much of Australia. Until recently, nearly all forms restricted to northern Australia, particularly the Arnhem Plateau, were restricted to a large-bodied form referred to as *O. gemmata*. Despite displaying an array of phenotypes and ecologies, all other populations found in the AMT and AMZ were relegated to *O. marmorata* until Oliver and McDonald (2016). *Oedura marmorata sensu lato* can be divided into a clade containing the arid forms *O. fimbria* (western AAZ) and *O. cincta* (eastern and central AAZ) which are in turn sister to a monsoonal tropics clade containing *O. gemmata* (Arnhem Plateau), *O. bella* (Gulf of Carpentaria), and *O. marmorata* (restricted to the Top End). The Top End clade is of particular interest as it possesses high mitochondrial diversity when compared to its sister lineage (Oliver *et al.*, 2012; Oliver *et al.*, 2014; Oliver & Doughty, 2016; Oliver & McDonald, 2016). In addition to *O. gemmata* and *O. bella*, these studies identified at least five other mitochondrial lineages. Furthermore, mtDNA suggests that *O. gemmata* renders *O.*

*marmorata* paraphyletic, being sister to a phenotypically similar lineage restricted to the central portion of the Top End. These mitochondrial lineages are largely allopatric and preliminary evidence suggests that there are distinct morphological differences between them (figure 35). A small-bodied form with distinct yellow barring on a black background is restricted to the northwestern portion of the Top End, just north of the Daly River drainage (hereby referred to as the Darwin clade). Another is confined to the east, north of the Daly River drainage and is larger than the Darwin form, possessing an overall lighter color with complex reticulating patterns of white and yellow (flathead clade). A clade phenotypically similar to the flathead mito-lineage is restricted to the karstic areas surrounding the Katherine region (Katherine clade). Two lineages are known from comparatively few localities, one isolated on the island of Groote Eylandt in the Gulf of Carpentaria and the other to the region associated with the Limmen National Park south of the Roper River drainage (Groote and Limmen respectively). Members of the Groote clade superficially resemble *O. bella* while the Limmen forms are large-bodied with yellow-white markings on a dark background. The last clade occurs over a much greater longitudinal breadth of the Top End than the other lineages, ranging south of the Daly River Drainage to Marchinbar Island to the northeast while skirting around the Arnhem Coast (deephead clade). These putative clades differ in morphology and, based off of personal and anecdotal evidence, are also ecologically distinct (Oliver, P. M. *pers. comm.*). The Groote lineage and *O. bella* are moderately sized (< 90 mm SVL) with conical, somewhat dorsoventrally flattened tails and appear to be scansorial generalists. In contrast to this, *O. gemmata* along with the Katherine, Darwin, and flathead lineages are strongly rupicolous with shortened tails that are compressed dorsoventrally. Intermediate between these two extremes are the large-bodied (> 95 mm SVL) Limmen and deephead lineages, with the former being rupicolous and the latter seemingly a scansorial generalist, occurring on both trees and rocks. Both of these lineages possess large turnip-shaped tails that are neither conical nor dorsoventrally flattened.

Previous studies relying on mtDNA have failed to resolve the interrelationships of these eight lineages. However, there is evidence for a strong relationship between *O. gemmata* and the flathead clade and for *O. bella* being sister the remaining seven mito-lineages (Oliver *et al.*, 2014; Oliver & Doughty, 2016). Furthermore, there is little concordance between the mitochondrial phylogeny and morphology and little correspondence to recognized biogeographic barriers and refugia in the Top End. Lastly, several of the lineages, namely the deephead, Darwin, flathead, and Katherine taxa, come into close contact with one another. This pattern warrants further investigation into whether or not introgression has occurred in neighboring allopatric lineages. In this study, we use a phylogenomic dataset of over 4,200 ultraconserved elements to resolve the phylogeny and divergence times of the Top End *O. marmorata* complex. In addition to traditional phylogenetic methods we implement population delimitation methods as well as the coalescent to infer the species tree and demographic history of the eight candidate lineages.

## Methods

### *Taxon Sampling and Molecular Data*

This study represents a subset of a broader investigation of the phylogenomics of diplodactyloid geckos. We included 83 individuals of the Top End *Oedura marmorata* complex for our phylogeographic analyses, with representatives from each of the eight mito-lineages (table 13). Our intra-lineage sampling ranged from 2 individuals, in the case of recently discovered Groote Eylandt form, to 27 representing the deephead form on the continental mainland. In conjunction with 1,259 bp of ND2 mitochondrial sequence, we implemented 4,268 ultraconserved element

(UCE) loci totaling 2.1 Mb. These nuclear loci were sequenced on an Illumina HiSeq 4000 platform with 150 bp paired-end reads. All assemblies and downstream bioinformatics were performed with custom Perl scripts (Bi *et al.*, 2012).

*Phylogenetic Inference*

We inferred the ML topology for all 4,268 UCEs using RAxML v8.2.9 (Stamatakis, 2014) with 300 nonparametric rapid bootstrap replicates and a simultaneous search for the best likelihood tree on the Cipres Portal (Miller *et al.*, 2010). The GTR+G model was used, as RAxML only permits the specification of a single model for an alignment and its partitions. Intraspecific topological incongruence between the mitochondrial and UCE tree for the Top End clade was assessed with the Robinson-Foulds metric (RF) (Robinson & Foulds, 1981). To account for gene tree heterogeneity, we used ASTRAL II to estimate the diplodactyloid species tree (Mirarab & Warnow, 2015). This summary multispecies coalescent method has been shown to be statistically consistent, taking a set of unrooted gene trees with known branch lengths as input as opposed to sequence data. The ASTRAL algorithm estimates the species tree by maximizing the number of quartet trees shared with a set of unrooted gene trees, penalizing low frequency quartet trees (Mirarab *et al.*, 2014; Sayyari & Mirarab, 2016). Rather than bootstrapping our individual gene trees, we relied on the local posterior probability (lpp) estimated by ASTRAL for node support (Sayyari & Mirarab, 2016). Given the near sympatry of several lineages, we attempted to visualize reticulate evolution with phylogenetic networks of the full UCE dataset for the Top End *Oedura* in SPLITSTREE4 using the distance-based NeighborNet method (Bryant & Moulton, 2002; Huson & Bryant, 2006).

To infer divergence dates for the eight lineages of Top End *O. marmorata*, we used the program MCMCTREE in PAML on the whole diplodactyloid tree (YANG, 2007). The MCMCTREE algorithm circumvents the computational pitfalls of BEAST-like divergence dating methods by bypassing the tree building process, taking a known phylogeny without branch lengths as input. It then assigns substitution rates to different branches of the tree before estimating branch rates and divergence dates from sequence data. We used the species tree topology inferred from ASTRAL as the guide tree. However, our entire concatenated alignment of 4,268 UCEs and 190 species proved too large for MCMCTREE, requiring the dataset to be pared down to the top 250 most complete loci (see Chapter 1 for details).

*Population Genetic Analyses*

Previous studies have shown the utility of UCEs in delimiting populations and elucidating demographic processes below the species level (Smith *et al.*, 2014). Genetic distances between our eight *a priori* populations (*O. bella*, *O. gemmata*, Limmen, Groote, deephead, Katherine, Darwin, and flathead) for 4,035 SNPs were determined with Nei's distance in the R package ADEGENET v2.0.1 (Nei, 1972; Jombart, 2008; Jombart & Ahmed, 2011). Population differentiation was initially tested with Nei's pairwise $F_{ST}$ in ADEGENET, where expected heretozygosities are weighted by group size (Nei, 1973, 1977; Holsinger & Weir, 2009). We visualized population-specific variation in alleles for the 4,035 SNP dataset using principle component analysis (PCA) again using ADEGENET.

While the findings of previous studies and our own preliminary mitochondrial data for the Top End *Oedura marmorata* strongly suggest the reciprocal monophyly of the eight putative lineages, we implemented population assignment methods to assess levels of admixture (Oliver *et al.*, 2014). This is particularly pertinent as multiple lineages come into near sympatry. Using Perl

scripts developed by Singhal (2013), the UCE dataset was first reduced to a single, informative single nucleotide polymorphism (SNP) per UCE locus, resulting in 4,035 SNPs across the whole Top End complex. First, we used the find.clusters function in ADEGENET, a method that first ordinates the data with PCA then partitions the it into *K* groups before minimizing the sum-squared distance of samples to the center of their assigned cluster. The Bayesian Information Criterion (BIC) was used to determine the best scoring estimate of *K*s 1-35. While this complex likely demonstrates high levels of geographically concordant structure, isolation by distance (IBD) may play a role in the patterns observed. ADEGENET was used test for signatures of IBD at the individual and population levels with a Mantel test using 999 simulations (Mantel, 1967; Ishida, 2009). Given its wide distribution across the eastern portion of the Top End, we also tested IBD for the deephead clade.

The Bayesian clustering program STRUCTURE v2.3.4 was implemented to determine population assignments for the SNP dataset (Pritchard *et al.*, 2000; Besnier & Glover, 2013). Using allele frequencies, STRUCTURE simultaneously estimates the number of populations in a sample and probabilistically assigns individuals to populations at random using MCMC. The ancestry coefficient (*Q* matrix) that a given sample belongs to one or more populations indicates the extent of admixture in a dataset. STRUCTURE was run on the SNP dataset for *K*s 2-10 seven times each with a burnin of 50,000 generations, a chain length of 150,000 generations, with the admixture model on the Cipres Portal (Miller *et al.*, 2010). Evanno *et al.* (2005) noted that examination of the standard mean log probability of the data output by STRUCTURE could lead to unreliable estimates of *K* and so proposed a second order derivative of the rate of change between log probabilities of successive estimates of *K* ($\Delta K$). We used the R package POPHELPER to estimate Evanno's *K* from all of the *Q* matrices output by STRUCTURE (Francis, 2017). POPHELPER was also used to implement the CLUMPP algorithm to deal with potential label switching on admixture plots between STRUCTURE runs (Jakobsson & Rosenberg, 2007).

In addition to STRUCTURE, we ran the R package TESS3r on our 4,035 SNP data set, a complementary clustering algorithm (Caye *et al.*, 2016). TESS3 incorporates spatial data in the form of coordinates for each sample, using them in combination with the genetic data to estimate ancestry coefficients distributed continuously over geographic space. Whereas STRUCTURE relies on MCMC, TESS3r uses least-squares optimization to estimate individual ancestry coefficients. The TESS3r algorithm is not likelihood-based and is thus model-free. Furthermore, this program makes no assumptions about linkage or Hardy-Weinberg equilibrium. Here, the sampling probabilities of each individual genotype for *K* ancestral genotypes correspond to their admixture coefficients (Caye *et al.*, 2016). The coordinate data is then used as a spatial constraint to ensure that individuals that are geographically close to one another are more likely to share ancestral genotypes than those that are far apart. We ran TESS3r ten times for *K*s 2-25 and the cross-entropy method described by (Frichot *et al.*, 2014) was then implemented to infer the number of ancestral clusters before the cross-validation scores were used to choose the best *K*, where a plateau or increase indicates the best estimate of *K* (Frichot & François, 2015). Plots of the cross-validation curve, admixture coefficient bar plots, and ancestry maps were all done with built-in TESS3r functions.

## Results

### *Phylogenetic Results*

Both mtDNA and phylogenomic data place *Oedura bella*, *O. gemmata*, and the remainder of the Top End *Oedura* as sister to the AAZ forms (*O. fimbria* and *O. cincta*) with strong support and

both clades in turn being sister to the Kimberley *Oedura* (*O. fillicipoda*, *O. murrumanu*, and *O. gracilis*) (figure 36). The *O. marmorata* complex (AAZ and AMT) and Kimberley forms represent a clade of large-bodied *Oedura* that are in turn sister to the Wet Tropics (AWT) species (*O. monilis*, *O. tryoni*, *O. coggeri*, and *O. castelnaui*). We found unambiguous support in the UCEs for *O. luritja* being at the base of *Oedura.* Within the AMT clade, both datasets recover the same eight lineages with *O. bella* being at the base, though the relationships between the remaining seven differ substantially. The mtDNA failed to recover most of the intraclade relationships between the western lineages, though *O. gemmata* was found to cluster with the deephead and flathead clades with strong support (bootstrap = 84). Conversely, the UCEs fully resolved intraclade relationships in the concatenated likelihood tree with *O. gemmata* being sister to an east-west clade where Groote was successively sister to Limmen, deephead, Katherine, flathead, and Darwin. Further structure was detected by RAxML with moderate support for a west-northeast split within the deephead lineage detected (figure 36a). The multispecies coalescent with ASTRAL revealed largely congruent results with the concatenated UCE tree though the Groote and *O. gemmata* lineages swapped positions and the deephead group received poor support for placement with the western rupicolous clades. Both concatenated and coalescent analyses of the UCEs place the phenotypically and ecologically similar northwestern lineages in a clade exclusive of the remaining taxa. Comparison of the mtDNA and UCE topologies revealed extensive incongruence (normalized RF = 0.78). SPLITSTREE recovered an identical topology to the RAxML tree (figure 37).

Divergence dating with MCMCTREE resulted in an estimated crown divergence for *Oedura* to have occurred sometime between the early Oligocene and early Miocene ($\mu$ = 24.8 mya, CI = 32.7 – 17.5) (figure 38). Divergence between *O. bella* and the other Top End lineages was found to be relatively young ($\mu$ = 7.5 mya, CI = 9.7 – 5.6), occurring during the late Miocene. The forms west of the Gulf of Carpentaria appear to have split sometime around the very end of the Miocene or earliest Pliocene ($\mu$ = 5.2 mya, CI = 7.4 – 4.2).

*Population Genetic Results*

Most SNP loci were found to be biallelic (93.5%) though 6.4% were triallelic and 0.18% possessed four alleles. Genetic distances for mtDNA and UCEs were highest between *Oedura bella* and the other seven lineages (mtDNA: 19 – 25%, UCEs: 13 – 15%), while the remaining taxa exhibited much lower values of Nei's estimator between one another (mtDNA: 7 – 20%, UCEs: 3 – 8%) (tables 14 – 15). Testing genetic differentiation with Nei's pairwise $F_{ST}$ exhibited a similar pattern where *O. bella* demonstrated the highest division between the other lineages (0.39 – 0.52) as opposed to the western clades to one another (0.13 – 0.49). We note that all $F_{ST}$ comparisons to the insular Groote lineage may be unreliable due the low number of individuals sampled (n = 2) (table 16). Principle component analysis of allele frequencies yielded concordant results with all combinations of the first three axes placing *O. bella* well outside of the other lineages. PC analysis of the SNP dataset with *O. bella* excluded revealed three major clusters: one with the Darwin and flathead forms, one with deephead, Limmen, Groote, and *O. gemmata*, and one containing Katherine only (figure 39). Mantel tests revealed stronger correlations between the genetic and coordinate distance matrices for the individual (p = 0.001) and population level (p = 0.004) IBD analyses than would be expected with no population structure (figures 40 a and b respectively). Examination of the deephead clade alone yielded concordant results of strong correlation between the two matrices (p = 0.001) (figure 40c).

All population structure analyses recovered strong signatures of population subdivision using the SNP dataset, though the results differ greatly between algorithms. The simplest method, ordination with ADEGENET, found unambiguous BIC support for 10 clusters. These corresponded to the eight clades recovered by conventional phylogenetic analysis, though additional subdivision was recovered. Both *O. bella* and the deephead lineage were split into two distinct eat-west clusters. Very little admixture was detected with the exception of the Darwin group where small a percentage of alleles was found to occupy the same cluster as the deephead and flathead groups (figure 41). Initial inspection of the mean log probability of *K* STRUCTURE suggested that 9 clusters were present in the Top End *Oedura*. Implementation of Evanno's Δ*K* resulted in overwhelming support for the presence of 5 clusters (figure 42). However, inspection of the ancestry coefficients and visualization of the assignment probabilities revealed very little admixture, but that individuals rarely clustered in the phylogenetic clades recovered above or in geographically concordant units (figure 43). TESS3r found strong signatures of population structure, though the exact estimate of *K* was highly ambiguous. Though there was no plateau, examination of the cross-validation curve revealed that there were as many as 16 clusters and potentially more (figure 44). Given the uncertainty of the appropriate *K*, we visualized several assignment schemes from *Q* matrix estimates 8-16. *K*s 8 and 9 found clusters concordant with conventional phylogenetic analyses with the eastern and western *O. bella* falling into different clusters with little admixture. Both *K*s 8 and 9 present strong signatures of admixture within the Groote lineage, the majority of cluster assignments placing them with *O. gemmata* with much lower ancestry proportions assigned to the remaining lineages (figures 45 – 48). All *K*s above 8 find additional structure with the deephead lineage corresponding to the northeast-southwest clades. However, *K*s 10 to 16 fail to find strong signatures of admixture within the Groote samples. *K* of 16 indicates extensive substructure within the deephead clade, recovering southwestern, southern, southeastern, northeastern, and northwestern clusters as well western and eastern clusters for both the flathead and *O. gemmata* groups (figure 49). The ancestry coefficients of *K*16 suggest extensive admixture between the flathead, Katherine, and deephead groups in the regions surrounding the Katherine River area southwest of Nitmiluk National Park (figure 50).

**Discussion**

*Phylogeographic Patterns*

We find that both mitochondrial and phylogenomic data support the presence of eight major phylogenetic clades within the Top End *Oedura marmorata* complex, with complete agreement in terms of individual assignment to specific clades. While our methods are largely exploratory and we were unable to implement population genetic methods incorporating the coalescent (Gronau *et al.*, 2011), we are confident that our findings here have broad ecological and biogeographical implications. The recovery of exceedingly high genetic diversity in a complex that is relatively conservative morphologically fits well with the Monsoonal Tropics being a significant source for biodiversity and short-range endemics. The AMT represents the world's largest tropical savannah and studies of Australian mammals and squamates have corroborated its importance in generating phylogeographic structure and phylogenetic diversity (Bowman *et al.*, 2010; Eldridge *et al.*, 2011; Melville *et al.*, 2011; Potter *et al.*, 2012; Eldridge *et al.*, 2014). The comparative range restriction of most of the Top End *O. marmorata* lineages suggests that ancient vicariance events played a major role in the formation of phylogeographic diversity, not dispersal. While the mitochondrial dataset provides little insight into the interrelationships between the clades, the UCEs recover relationships that are both morphologically and geographically concordant. The only well

supported clades in the mtDNA tree are the placement of *O. bella* outside of the remaining taxa and the union of *O. gemmata* with the flathead and deephead lineages. While this highlights a potential pattern where at least some of the lineages west of the Gulf of Carpentaria diverged relatively recently, the failure of all the northwestern populations to form a clade is problematic when attempting to infer biogeographic processes. Rather, the UCEs paint a clear east to west picture of divergence, where the four most nested lineages (flathead, Katherine, deephead, and Darwin) occur in near sympatry across the northwestern portion for the Top End. Furthermore, the flathead, Darwin, and Katherine taxa are all known to be exclusively rupicolous and possess relatively long dorsoventrally flattened tails. With the exception of *O. gemmata* and Limmen, the remaining Top End lineages occur on both vegetation and rocks. Phylogenetic analyses suggest that at least some of the previously proposed biogeographic barriers may have played a major role in the maintenance of genetic isolation. These include the Gulf of Carpentaria, Arnhem Plateau, and Daly River. Additionally, there is evidence that several river drainages not previously proposed to be biogeographic barriers may have played historical roles in allopatric divergence. Given its concordance with external morphology, ecology, and clade distributions, we defer to our UCE data for most the inferences henceforth.

Phylogenetic analyses strongly support the monophyly of each lineage with exceedingly high mitochondrial pairwise divergence estimates with correspondingly low nuclear estimates. Taken alone, these analyses present a strong argument that each of these represent candidate species. This pattern of high genetic diversity in the AMT is consistent with Oliver *et al.* (2014), though our UCE divergence time estimates for the northwestern AMT taxa are somewhat older. This discordance is likely due to inconsistences in how BEAST and MCMCTREE handle time priors for divergence estimation, with the former's implementation allowing for the violation of calibration priors (Warnock *et al.*, 2015). Oliver *et al.* (2014) further suggest that, in comparison to their AAZ sister taxa, the candidate lineages of AMT *Oedura* are comparatively ancient and the Top End taxa exhibit much higher levels of genetic diversity, indicating long-term isolation and persistence. While we did not attempt to include extensive intraspecific sampling for the AAZ *Oedura*, we agree with the above study's conclusion as we find the species-level divergences for the AMT (Top End and Kimberley) and AWT to predate those within the AAZ clade (figure 4.4). This reflects the comparatively young age of the AAZ (Byrne *et al.*, 2008). Indeed, our estimates place the split between the AAZ and Top End *Oedura* in the mid-Miocene ($\mu$ = 11.5 mya, CI = 14.5 – 8.7), corresponding nicely with the onset of Australia's rapid aridification after the initiation of the Antarctic circumpolar current (Dawson & Dawson, 2006; Byrne *et al.*, 2008).

We found strong signatures of isolation by distance in our tests at the individual and clade level. Given the high amount of phylogenetic structuring within the AMT *Oedura*, this is not surprising as all but one the clades are known from relatively small geographic regions. When considering the AMT, this pattern suggests that there several barriers that have historically restricted gene flow across parapatric and allopatric lineages. This is corroborated by strong signatures of IBD in the deephead lineage, the most well sampled clade in this study. The deephead group is by far the widest ranging of the eight lineages and it follows that genetic differentiation would occur somewhere across its distribution. Population assignment with STRUCTURE failed to recover even one of the eight phylogenetic groups. In the face of IBD or high genetic diversity, STRUCTURE has been shown to yield unreliable results, particularly in the form of spuriously high estimates of *K* (Meirmans, 2012). Interestingly, we find low amounts of structure with this algorithm, suggesting that, at least in our case, models that rely on assigning individuals to Hardy-Weinberg populations are inappropriate for this system. The pattern of nonsensical individual

assignments and a low estimate of *K* we recover is entirely consistent with simulation work done by Kalinowski (2011). The high degree of geographic isolation, genetic structure, and long divergence times in the AMT clade almost certainly confounded the estimation of *K* based on the log probability from (see high variance of log probability in figure 4.8) and, by extension, accurate estimation of Evanno's Δ*K* (Evanno et al., 2005).

Datasets, such as these, with patterns of high divergence necessitate the use of spatially informed clustering analyses (Meirmans, 2012). Thus, we defer to our spatially informed TESS analyses in determining population structure. All iterations of *K* with TESS resulted in geographically coherent clusters that largely corresponded to our initial concatenated and coalescent phylogenetic estimates. While our taxon sampling for the Groote clade is admittedly low, lower *K*s indicated that this insular form shared a large proportion of alleles with *O. gemmata* and Limmen, with smaller ancestry coefficients for the remaining clusters (< 10% assignment to a cluster). Low estimates of $F_{ST}$ between Groote, *O. gemmata*, and deephead lends further credence to ancient allele sharing between these lineages. However, higher estimates of *K* ($\geq$ 10) fail to reveal strong signatures of admixture. The Gulf of Carpentaria, a shallow sea, has a complex history through the Pleistocene, particularly during the last glacial maxima (LGM). Geologic evidence supports the presence of contiguous land across what is now the Gulf of Carpentaria during the late Pleistocene, periodically joining northern Australia with New Guinea until 9.7 kya (Chivas *et al.*, 2001; Byrne *et al.*, 2008). This land would have been dominated by tropical savannah, similar to much of the savannah that now covers the AMT. In place of a sea was a shallow lake, Lake Carpentaria, which has been implicated in generating phylogeographic patterns in freshwater taxa (Torgersen *et al.*, 1983; De Bruyn *et al.*, 2004). Our divergence time estimates on the species tree topology place the Groote lineage and the remaining western mainland taxa during the late Miocene or Early Pliocene ($\mu$ = 5.7 mya, CI = 4.2 – 7.4), well prior to drowning of areas surrounding Groote Eylandt. In light of this, we propose, if there is true admixture, divergence with secondary contact where the Groote taxon diverged early and subsequently introgressed with mainland taxa during Pleistocene sea level oscillations. Alternatively, the Groote lineage may represent an ancient hybridization event with recent insular isolation. In either case, the ambiguous placements of this taxon and *O. gemmata* in the species tree are conducive of a portion of gene trees reflecting ancient admixture. Conflicting topologies due to multiple parental lineages confound the multispecies coalescent which can only account for incomplete lineage sorting as a source of gene tree-species tree discordance (Mirarab & Warnow, 2015).

Within our mitochondrial data, the only well-supported interclade relationship recovered was the placement of *O. gemmata* with the deephead and flathead clades. This nested arrangement strongly conflicts with the more basal position of this species in the concatenated and coalescent UCE phylogenies. The poorly supported sister relationship between *O. gemmata* and the flathead clade would be concordant with morphology, as both lineages are large-bodied (> 100 mm svl), possess complex dorsal patterning, and are exclusively rupicolous with dorsoventrally flattened tails. Given this incongruence between the mitochondrial and nuclear genomes, it is possible that *O. gemmata* historically introgressed into the western AMT clade during the late Neogene, suggesting female biased dispersal. Though they do come into relatively close contact in regions surrounding Nitmiluk National Park, the two lineages are allopatric with the flathead form being known from limestone escarpments and *O. gemmata* occurring exclusively on sandstone outcrops in and adjacent to the Arnhem Land region. While ancient mitochondrial introgression is possible between two recently diverged lineages, interspecific mitonuclear discordance in the form of Bateson–Dobzhansky–Muller incompatibilities (BDM) may explain this pattern (Dobzhansky,

1934). Functional constraints from intergenomic interactions have been documented as prezygotic reproductive barriers in other squamate taxa (Singhal & Moritz, 2013; Haines *et al.*, 2016). However, further investigation is needed to determine if this is a simple case of sex-biased introgression or ancient hybridization with BDM incompatibility or both, a study that would benefit from broader geographic sampling and complementary molecular data such as karyotyping. At higher estimates of *K*, we found a high degree of subdivision within the deephead lineage, with all values consistently finding a southwestern cluster near the Katherine region, one directly to the east south of Nitmiluk National Park, and another southeast of the Arnhem Plateau. This supports our hypothesis that isolation by distance has played a large role in the generation of genetic diversity in this lineage and the remaining AMT taxa. Surprisingly, this pattern of longitudinal division is eroded by the presence of samples from the northeastern Top End south of the Koolatong River which cluster with the southwesternmost deephead group. Furthermore, clustering analyses relying on both minimizing the sum of squared distances and least-squares optimization found signatures that not only did the southwestern deephead group share alleles with eastern members of that clade, but with the adjacent flathead and Katherine taxa to the northwest. Patterns such as these, also seen in the flathead group, support our hypothesis that the eight candidate lineages diverged very early and have intermittently come into secondary contact. We argue that barriers to gene flow between adjacent clades, both geological and biotic, have been transient through the Plio- Pleistocene.

While the concatenated and multispecies coalescent trees disagree on the placement of *Oedura gemmata* and the Groote clade, both permit the inference of ecological state transitions in substrate choice. In chapter 2 we used stochastic mapping to reconstruct the ancestral ecology of all diplodactyloids using the time-calibrated ASTRAL topology (Bollback, 2006). Here, we found that *Oedura* was inferred to be ancestrally rupicolous and that there were three independent transitions to scansorial-rupicolous ecology by *O. bella*, deephead, and Groote. The ecological transitions likely facilitated the wide geographic ranges of the first two lineages, promoting further genetic differentiation at the limits of their respective distributions.

*Biogeographical Processes and Barriers*

A number of biogeographic barriers and refugia have been proposed to limited gene flow and shape phylogeographic patterns in monsoonal tropics taxa (De Bruyn *et al.*, 2004; Alpin, 2006; Bowman *et al.*, 2010; Eldridge *et al.*, 2011; Potter *et al.*, 2012; Eldridge *et al.*, 2014). Our UCE data reveals that some of these may have acted as effective or semipermeable barriers to gene flow in the Top End *Oedura*. The Top End clade is restricted to the AMT northeast of the Kimberley, so the Ord Arid Intrusion and Victoria River drainage were unlikely barriers. Rather, we propose that the Daly River and Adelaide Rivers to the northeast acted as barriers between the Darwin and flathead lineages, groups that are sister taxa in both the concatenated and coalescent trees. Ancestry coefficients reveal that the two share very few alleles, supporting our hypothesis that they diverged very recently (within the last 2 my) and the intervening river systems have effectively prevented dispersal and gene flow. In contrast to the clear pattern of division between these two clades, we found a far more complex story to be told in the Katherine region where the Katherine, flathead, and deephead lineages all come into close contact and appear to have shared alleles. Even more intriguing is the preliminary observation that, based on our exploratory clustering analyses, introgression has not been unilateral between the three groups. Instead, we find that eastern flatheads north of Katherine share a portion of their ancestry with the Katherine group, as do the adjacent deephead samples to the east. Furthermore, the Katherine samples show very little

admixture with the flathead or deephead groups, indicating biased introgression. However, we note that our clustering analyses have little power in distinguishing introgression and high levels of incomplete lineage sorting (ILS) and that accurate estimates of migration will require methods that operate under a fully coalescent framework (Gronau *et al.*, 2011; Petkova *et al.*, 2016). Nevertheless, we feel comfortable attributing biased introgression in the Katherine region as spatially explicit clustering analyses indicate geographically proximate samples exhibit admixture, not all samples from groups recovered by phylogenetic analyses. The later would lend more support for ILS. It is feasible that the Katherine River system has been a historically semipermeable barrier to gene flow for these three groups.

Our phylogenetic, IBD, and spatially explicit clustering analyses support the presence of underlying genetic structure in the deephead group. All methods at the very least recover southwestern and eastern groupings, the former of which occurs on the Arnhem Plateau. In the east, it is likely that the Roper River has acted as a semipermeable barrier between the western and eastern deephead groups. This is evidenced both the low statistical support received by the western clade in concatenated likelihood analyses and by both groups demonstrating some degree of admixture with one another. The Limmen clade is relatively close to the remaining western lineages, being very similar phenotypically to the deephead group albeit somewhat larger. Despite discordance between concatenation and the multispecies coalescent, we find very limited evidence of admixture with groups to the west. The Limmen River to the west may have been an effective barrier between the Limmen clade and eastern deephead group, at least in the Quaternary. In contrast to the potentially semipermeable nature of AMT river drainages, the Arnhem Plateau and Carpentarian Gap seem to have been hard barriers? that promoted isolation rather than mixing in *O. gemmata* and *O. bella*. The Arnhem Land region is ancient, dating back to the Proterozoic, and is characterized by the extensive sandstone outcroppings to which *O. gemmata* is endemic (Randal *et al.*, 1968; Bowman *et al.*, 2010). As mentioned above, the Carpentarian Gap and adjoining sea have not been stable geologic features, having experienced bouts of emergence and submersion during the Pleistocene (Chivas *et al.*, 2001). While the divergence between the western and eastern *O. bella* likely predates the dramatic sea level oscillations of the Plio-Pleistocene or the formation of the McArthur River, these formations likely acted as mechanisms maintaining genetic isolation.

While sandstone dominates the Arnhem Plateau, Arnhem Coast, and Central Arnhem, the central and more western reaches of the Top End are defined by limestone (Moulds & Bannink, 2012). This region supports the short range endemic lineages assigned to the Darwin, Katherine, and flathead groups. While undetected by tree-based methods, population genetic methods potentially detect a signature of gradual admixture in a west to east pattern. This is likely a reflection of the relative specialization of these taxa to rupicouly and the static nature of the karstic formations that define the Darwin-Katherine region (Randal *et al.*, 1968). With climatic changes during the Plio-Pleistocene, the vegetation intervening these escarpments would have alternated between grass-dominated savannah and tropical forest (Bowman *et al.*, 2010). During periods in which forest dominated and river drainages were at their lowest, it is possible that the western Top End *Oedura* were able to disperse to some degree and admix intermittently. These data, while largely exploratory, suggest that the climatic history of the AMT has played a profound role in the diversification of *Oedura* and a number of other vertebrates. Moreover, this assemblage may represent a non-adaptive radiation where vicariance events have driven genetic divergence while ecological and morphological divergence has been minimal (Schluter, 2000).

In addition to more extensive population genetic analyses integrating the coalescent, this clade warrants further investigation into the generation of high genetic diversity in the absence of

corresponding phenotypic diversity. This is particularly interesting given that *Oedura* on the whole is as old or older than the insular diplodactylid clades, but exhibits much reduced ecomorphological disparity (Oliver *et al.*, 2012; Oliver *et al.*, 2014; Oliver & Doughty, 2016; Oliver & McDonald, 2016; Skipwith *et al.*, 2016). Finally, these geckos illustrate the importance of the AMT, specifically the Top End, in generating biodiversity across multiple timescales (Rosauer *et al.*, 2016).

## Literature Cited


Alpin, K.P. (2006) Ten million years of rodent evolution in Australasia: phylogenetic evidence and a speculative histor- ical biogeography. *Evolution and Biogeography of Australasian Vertebrates* (ed. by J.R. Merrick, M. Archer, G.M. Hickey and M.S.Y. Lee), pp. 707-774. Australian Scientific Publishing, Oatlands, NSW Australia.

Besnier, F. & Glover, K.A. (2013) ParallelStructure: a R package to distribute parallel runs of the population genetics program STRUCTURE on multi-core computers. *PLoS One*, **8**, e70651.

Bi, K., Vanderpool, D., Singhal, S., Linderoth, T., Moritz, C. & Good, J.M. (2012) Transcriptome-based exon capture enables highly cost-effective comparative genomic data collection at moderate evolutionary scales. *Bmc Genomics*, **13**

Bollback, J.P. (2006) SIMMAP: Stochastic character mapping of discrete traits on phylogenies. *Bmc Bioinformatics*, **7**

Bowman, D.M.J.S., Brown, G.K., Braby, M.F., Brown, J.R., Cook, L.G., Crisp, M.D., Ford, F., Haberle, S., Hughes, J., Isagi, Y., Joseph, L., McBride, J., Nelson, G. & Ladiges, P.Y. (2010) Biogeography of the Australian monsoon tropics. *Journal of Biogeography*, **37**, 201-216.

Bryant, D. & Moulton, V. (2002) NeighborNet: An agglomerative method for the construction of planar phylogenetic networks. *Algorithms in Bioinformatics, Proceedings*, **2452**, 375-391.

Byrne, M., Yeates, D.K., Joseph, L., Kearney, M., Bowler, J., Williams, M.A.J., Cooper, S., Donnellan, S.C., Keogh, J.S., Leys, R., Melville, J., Murphy, D.J., Porch, N. & Wyrwoll, K.H. (2008) Birth of a biome: insights into the assembly and maintenance of the Australian arid zone biota. *Molecular Ecology*, **17**, 4398-4417.

Caye, K., Deist, T.M., Martins, H., Michel, O. & Francois, O. (2016) TESS3: fast inference of spatial population structure and genome scans for selection. *Molecular Ecology Resources*, **16**, 540-8.

Chivas, A.R., García, A., van der Kaars, S., Couapel, M.J.J., Holt, S., Reeves, J.M., Wheeler, D.J., Switzer, A.D., Murray-Wallace, C.V., Banerjee, D., Price, D.M., Wang, S.X., Pearson, G., Edgar, N.T., Beaufort, L., De Deckker, P., Lawson, E. & Cecil, C.B. (2001) Sea-level and environmental changes since the last interglacial in the Gulf of Carpentaria, Australia: an overview. *Quaternary International*, **83–85**, 19-46.

Criscione, F., Law, M.L. & KÖHler, F. (2012) Land snail diversity in the monsoon tropics of Northern Australia: revision of the genus *Exiligada* Iredale, 1939 (Mollusca: Pulmonata: Camaenidae), with description of 13 new species. *Zoological Journal of the Linnean Society*, **166**, 689-722.

Dawson, T.J. & Dawson, L. (2006) Evolution of Arid Australia and Consequences for Vertebrates. *Evolution and Biogeography of Australasian Vertebrates* (ed. by J.R. Merrick, M. Archer,

G.M. Hickey and M.S.Y. Lee), pp. 51-70. Australian Scientific Publishing, Oatlands, NSW Australia.
De Bruyn, M., Wilson, J.C. & Mather, P.B. (2004) Reconciling geography and genealogy: phylogeography of giant freshwater prawns from the Lake Carpentaria region. *Molecular Ecology*, **13**, 3515-3526.
Dobzhansky, T. (1934) Studies on hybrid sterility. I. Spermatogenesis in pure and hybrid *Drosophila pseudoobscura*. *Cell and Tissue Research*, **21**, 169-223.
Eldridge, M.D., Potter, S., Johnson, C.N. & Ritchie, E.G. (2014) Differing impact of a major biogeographic barrier on genetic structure in two large kangaroos from the monsoon tropics of Northern Australia. *Ecology and Evolution*, **4**, 554-67.
Eldridge, M.D.B., Potter, S. & Cooper, S.J.B. (2011) Biogeographic barriers in north-western Australia: an overview and standardisation of nomenclature. *Australian Journal of Zoology*, **59**, 270-272.
Evanno, G., Regnaut, S. & Goudet, J. (2005) Detecting the number of clusters of individuals using the software STRUCTURE: a simulation study. *Molecular Ecology*, **14**, 2611-2620.
Francis, R.M. (2017) pophelper: an R package and web app to analyse and visualize population structure. *Mol Ecol Resour*, **17**, 27-32.
Frichot, E. & François, O. (2015) LEA: An R package for landscape and ecological association studies. *Methods in Ecology and Evolution*, **6**, 925-929.
Frichot, E., Mathieu, F., Trouillon, T., Bouchard, G. & Francois, O. (2014) Fast and efficient estimation of individual ancestry coefficients. *Genetics*, **196**, 973-83.
Gronau, I., Hubisz, M.J., Gulko, B., Danko, C.G. & Siepel, A. (2011) Bayesian inference of ancient human demography from individual genome sequences. *Nat Genet*, **43**, 1031-1034.
Haines, M.L., Melville, J., Sumner, J., Clemann, N., Chapple, D.G. & Stuart-Fox, D. (2016) Geographic variation in hybridization and ecological differentiation between three syntopic, morphologically similar species of montane lizards. *Molecular Ecology*, **25**, 2887-2903.
Herold, N., Huber, M., Greenwood, D.R., Müller, R.D. & Seton, M. (2011) Early to Middle Miocene monsoon climate in Australia. *Geology*, **39**, 3-6.
Holsinger, K.E. & Weir, B.S. (2009) Genetics in geographically structured populations: defining, estimating and interpreting FST. *Nature Reviews Genetics*, **10**, 639-650.
Huson, D.H. & Bryant, D. (2006) Application of phylogenetic networks in evolutionary studies. *Molecular Biology and Evolution*, **23**, 254-267.
Ishida, Y. (2009) Sewall Wright and Gustave Malecot on Isolation by Distance. *Philosophy of Science*, **76**, 784-796.
Jakobsson, M. & Rosenberg, N.A. (2007) CLUMPP: a cluster matching and permutation program for dealing with label switching and multimodality in analysis of population structure. *Bioinformatics*, **23**, 1801-1806.
Jombart, T. (2008) adegenet: a R package for the multivariate analysis of genetic markers. *Bioinformatics*, **24**, 1403-1405.
Jombart, T. & Ahmed, I. (2011) adegenet 1.3-1: new tools for the analysis of genome-wide SNP data. *Bioinformatics*, **27**, 3070-3071.
Kalinowski, S.T. (2011) The computer program STRUCTURE does not reliably identify the main genetic clusters within species: simulations and implications for human population structure. *Heredity*, **106**, 625-632.

Mantel, N. (1967) The detection of disease clustering and a generalized regression approach. *Cancer Research*, **27**, 209-20.
Meirmans, P.G. (2012) The trouble with isolation by distance. *Mol Ecol*, **21**, 2839-46.
Melville, J., Ritchie, E.G., Chapple, S.N.J., Glor, R.E. & Schulte, J.A., II (2011) Evolutionary origins and diversification of dragon lizards in Australia's tropical savannas. *Molecular Phylogenetics and Evolution*, **58**, 257-270.
Miller, M.A., Pfeiffer, W. & Schwartz, T. (2010) Creating the CIPRES Science Gateway for large phylogenetic trees. *Proceedings of the Gateway Computing Environments Workshop (GCE)* (ed by, pp. 1-8. New Orleans, LA.
Mirarab, S. & Warnow, T. (2015) ASTRAL-II: coalescent-based species tree estimation with many hundreds of taxa and thousands of genes. *Bioinformatics*, **31**, 44-52.
Mirarab, S., Reaz, R., Bayzid, M.S., Zimmermann, T., Swenson, M.S. & Warnow, T. (2014) ASTRAL: genome-scale coalescent-based species tree estimation. *Bioinformatics*, **30**, I541-I548.
Moulds, T. & Bannink, P. (2012) Preliminary notes on the cavernicolous arthropod fauna of Judbarra/Gregory karst area, northern Australia. *Helictite*, **41**, 75-85.
Nei, M. (1972) Genetic Distance between Populations. *The American Naturalist*, **106**, 283-292.
Nei, M. (1973) Analysis of gene diversity in subdivided populations. *Proc Natl Acad Sci U S A*, **70**, 3321-3.
Nei, M. (1977) F-statistics and analysis of gene diversity in subdivided populations. *Ann Hum Genet*, **41**, 225-33.
Oliver, P.M. & Sanders, K.L. (2009) Molecular evidence for Gondwanan origins of multiple lineages within a diverse Australasian gecko radiation. *Journal of Biogeography*, **36**, 2044-2055.
Oliver, P.M. & McDonald, P.J. (2016) Young relicts and old relicts: a novel palaeoendemic vertebrate from the Australian Central Uplands. *Royal Society Open Science*, **3**
Oliver, P.M. & Doughty, P. (2016) Systematic revision of the marbled velvet geckos (*Oedura marmorata* species complex, Diplodactylidae) from the Australian arid and semi-arid zones. *Zootaxa*, **4088**, 151-176.
Oliver, P.M., Bauer, A.M., Greenbaum, E., Jackman, T. & Hobbie, T. (2012) Molecular phylogenetics of the arboreal Australian gecko genus *Oedura* Gray 1842 (Gekkota: Diplodactylidae): Another plesiomorphic grade? *Molecular Phylogenetics and Evolution*, **63**, 255-264.
Oliver, P.M., Smith, K.L., Laver, R.J., Doughty, P. & Adams, M. (2014) Contrasting patterns of persistence and diversification in vicars of a widespread Australian lizard lineage (the *Oedura marmorata* complex). *Journal of Biogeography*, n/a-n/a.
Pepper, M.R., Keogh, J.S. & Chapple, D.G. (2016) Molecular biogeography of Australian and New Zealand reptiles and amphibians. (ed. by M.C. Ebach), pp. 295-328. CRC Press.
Petkova, D., Novembre, J. & Stephens, M. (2016) Visualizing spatial population structure with estimated effective migration surfaces. *Nature Genetics*, **48**, 94-103.
Potter, S., Eldridge, M.D.B., Taggart, D.A. & Cooper, S.J.B. (2012) Multiple biogeographical barriers identified across the monsoon tropics of northern Australia: phylogeographic analysis of the *brachyotis* group of rock-wallabies. *Molecular Ecology*, **21**, 2254-2269.
Pritchard, J.K., Stephens, M. & Donnelly, P. (2000) Inference of population structure using multilocus genotype data. *Genetics*, **155**, 945-959.

Randal, M.A., Dunn, P.R. & Walpole, B.P. (1968) Geology of the Katherine-Darwin region, Northern Territory. In. Bureau of Mineral Resources, Geology and Geophysics

Robinson, D.F. & Foulds, L.R. (1981) Comparison of Phylogenetic Trees. *Mathematical Biosciences*, **53**, 131-147.

Rosauer, D.F., Blom, M.P.K., Bourke, G., Catalano, S., Donnellan, S., Gillespie, G., Mulder, E., Oliver, P.M., Potter, S., Pratt, R.C., Rabosky, D.L., Skipwith, P.L. & Moritz, C. (2016) Phylogeography, hotspots and conservation priorities: an example from the Top End of Australia. *Biological Conservation*, **204, Part A**, 83-93.

Sayyari, E. & Mirarab, S. (2016) Fast Coalescent-Based Computation of Local Branch Support from Quartet Frequencies. *Molecular Biology and Evolution*, **33**, 1654-1668.

Schluter, D. (2000) *The Ecology of Adaptive Radiation*. Oxford University Press, New York.

Singhal, S. (2013) De novo transcriptomic analyses for non-model organisms: an evaluation of methods across a multi-species data set. *Molecular Ecology Resources*, **13**, 403-416.

Singhal, S. & Moritz, C. (2013) Reproductive isolation between phylogeographic lineages scales with divergence. *Proceedings of the Royal Society B: Biological Sciences*, **280**

Skipwith, P.L., Bauer, A.M., Jackman, T.R. & Sadlier, R.A. (2016) Old but not ancient: coalescent species tree of New Caledonian geckos reveals recent post-inundation diversification. *Journal of Biogeography*, **43**, 1266-1276.

Smith, B.T., Harvey, M.G., Faircloth, B.C., Glenn, T.C. & Brumfield, R.T. (2014) Target Capture and Massively Parallel Sequencing of Ultraconserved Elements for Comparative Studies at Shallow Evolutionary Time Scales. *Systematic Biology*, **63**, 83-95.

Stamatakis, A. (2014) RAxML version 8: a tool for phylogenetic analysis and post-analysis of large phylogenies. *Bioinformatics*, **30**, 1312-1313.

Torgersen, T., Hutchinson, M.F., Searle, D.E. & Nix, H.A. (1983) General bathymetry of the Gulf of Carpentaria and the Quaternary physiography of Lake Carpentaria. *Palaeogeography, Palaeoclimatology, Palaeoecology*, **41**, 207-225.

Warnock, R.C.M., Parham, J.F., Joyce, W.G., Lyson, T.R. & Donoghue, P.C.J. (2015) Calibration uncertainty in molecular dating analyses: there is no substitute for the prior evaluation of time priors. *Proceedings of the Royal Society B-Biological Sciences*, **282**

Yang, Z.H. (2007) PAML 4: Phylogenetic analysis by maximum likelihood. *Molecular Biology and Evolution*, **24**, 1586-1591.

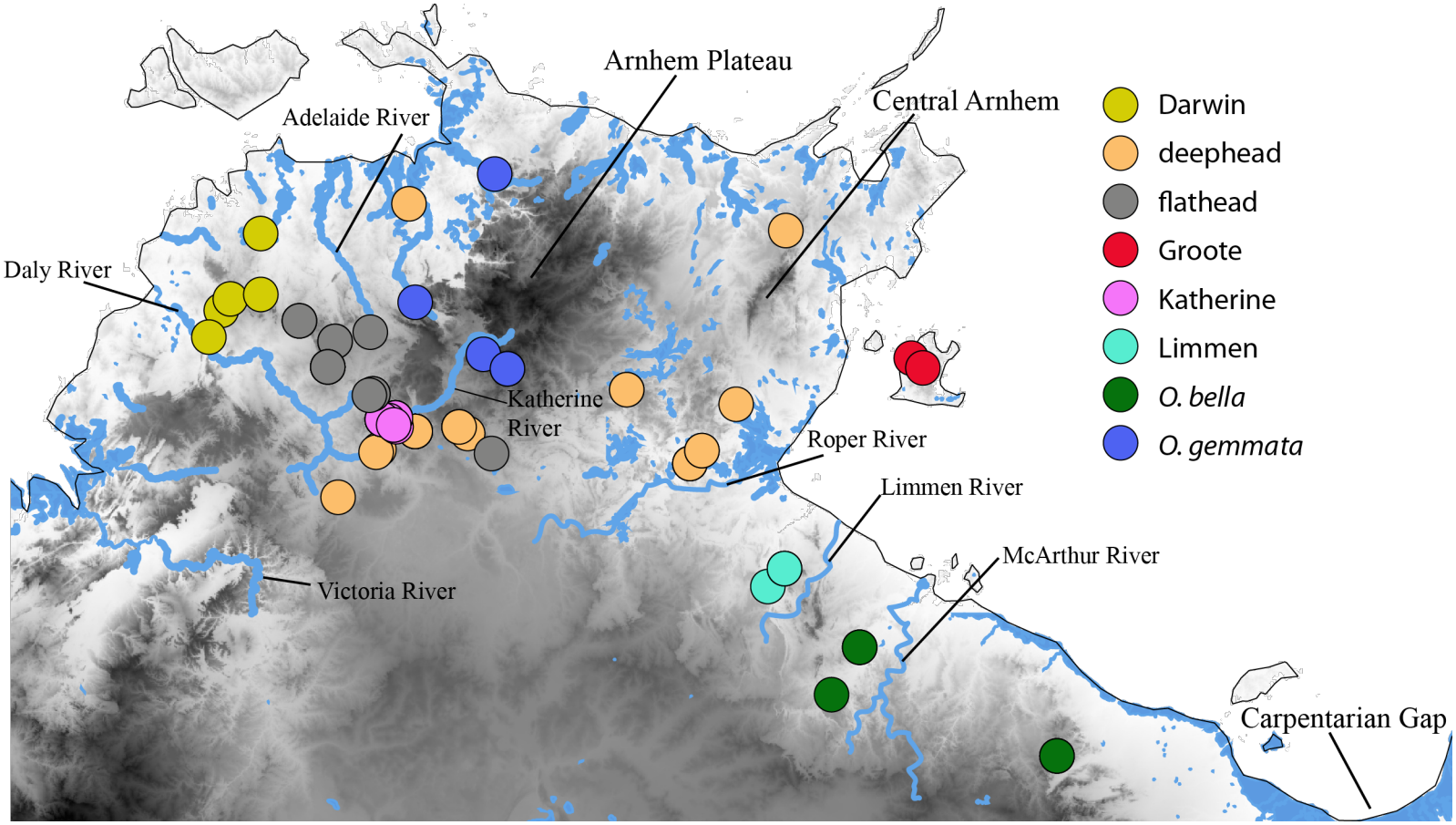


**Figure 35**: Map of the Top End with each clade color coded. Major rivers and biogeographic barriers labeled.

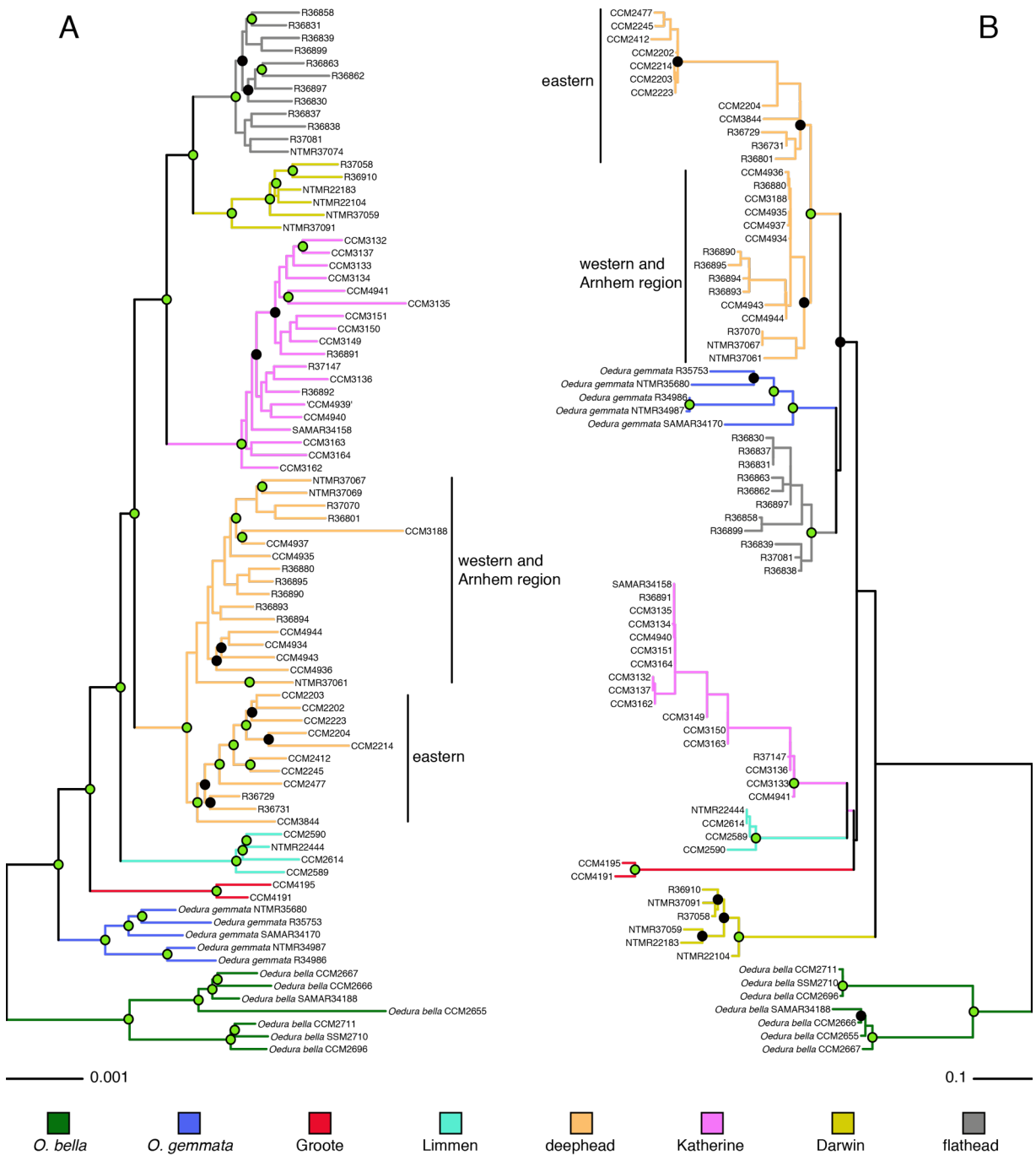


**Figure 36**: Maximum likelihood phylograms of 83 Top End *Oedura marmorata* samples from RAxML of A) 4,268 UCEs (2.1 Mb) and B) ND2 (1.2 Kb). Green node circles represent bootstrap proportions ≥ 90, while black circles denote bootstrap proportions 70 – 90. Nodes with below 70 bootstrap proportions are not annotated.

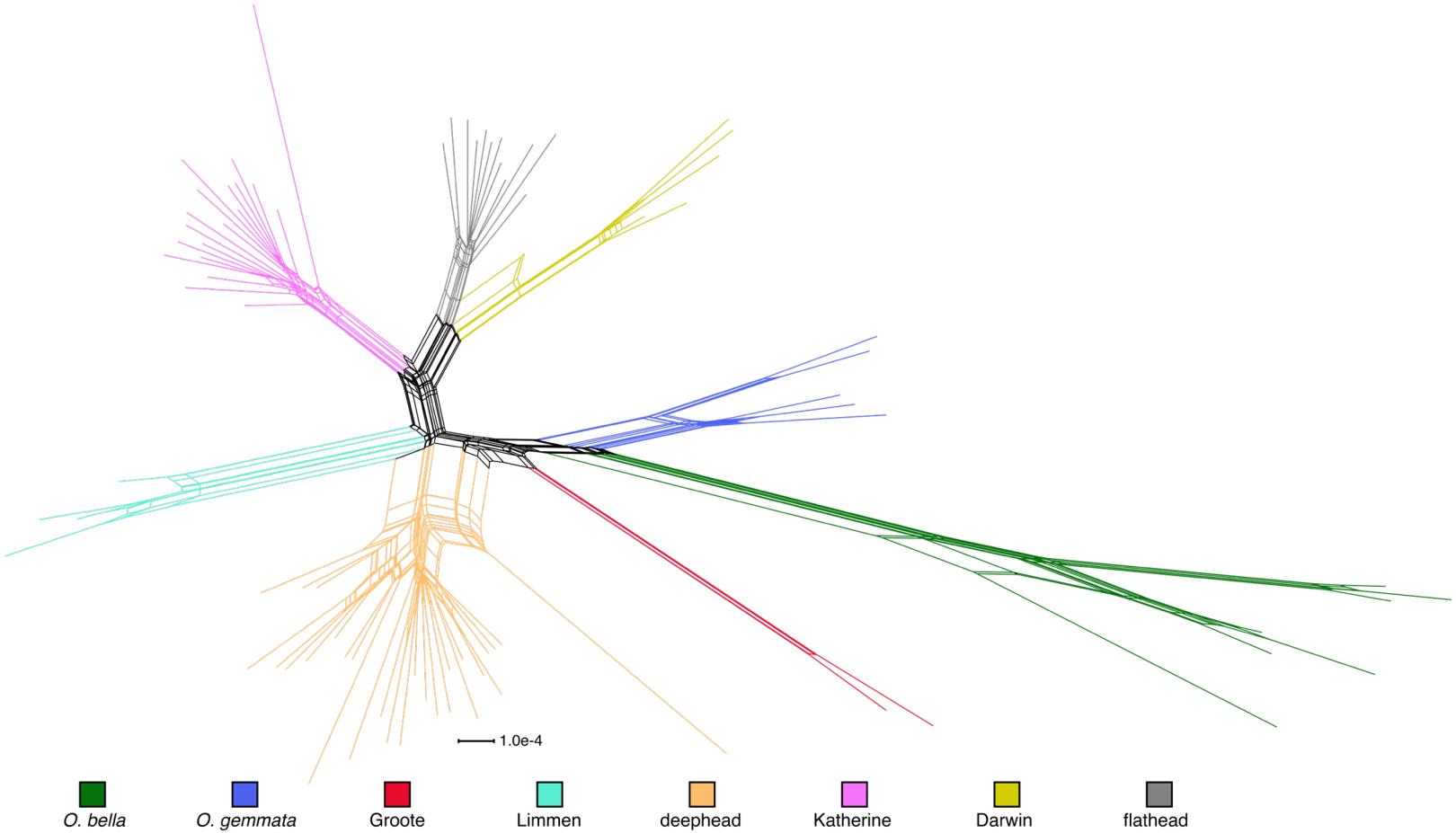


**Figure 37**: Neighbor net distance tree from SPLITSTREE.

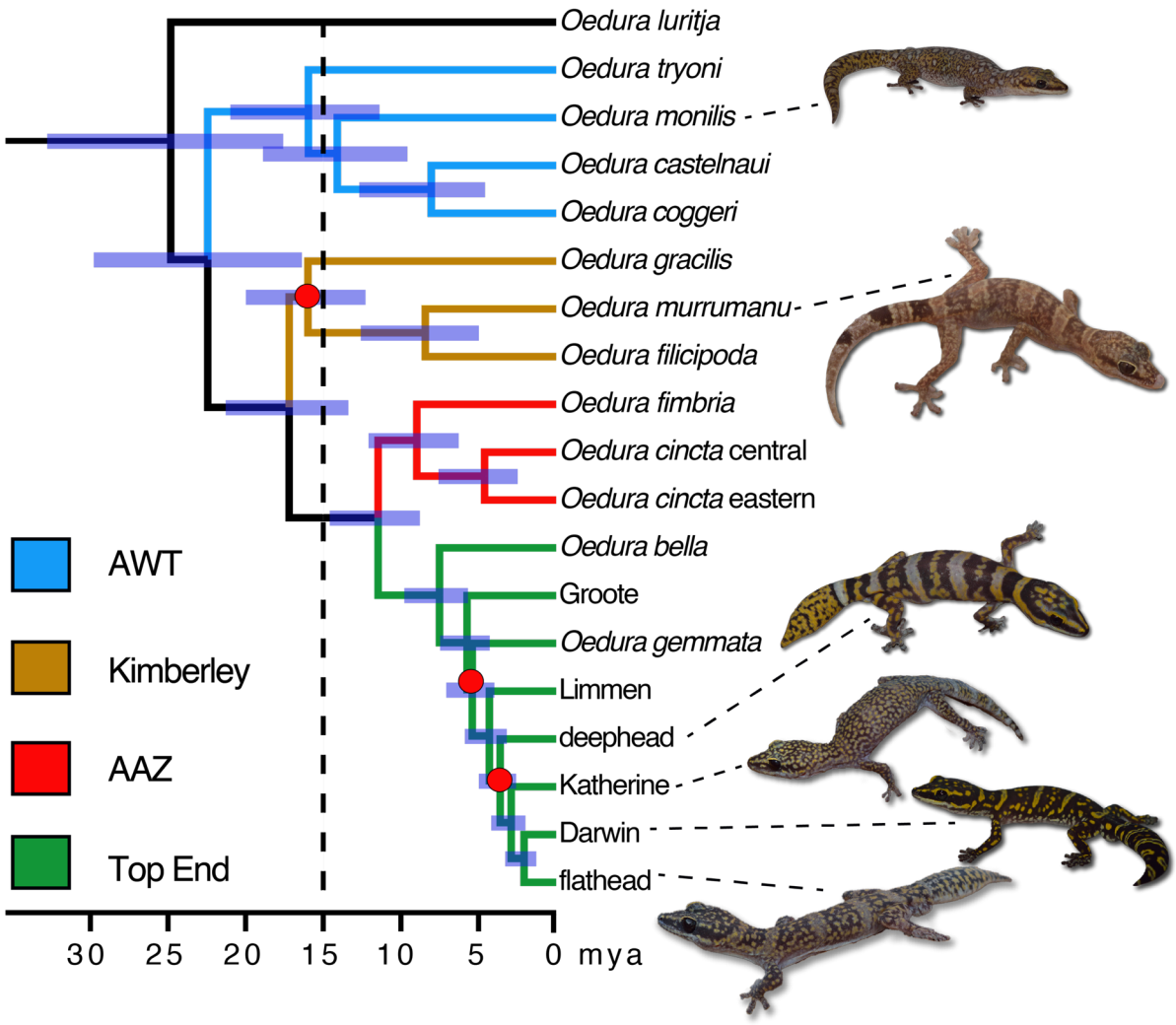


**Figure 38**: ASTRAL Timetree of *Oedura* from MCMCTREE. Red circles denote nodes with lpp < 0.95. AWT = Australia Wet Tropics, AAZ = Australian Arid Zone.

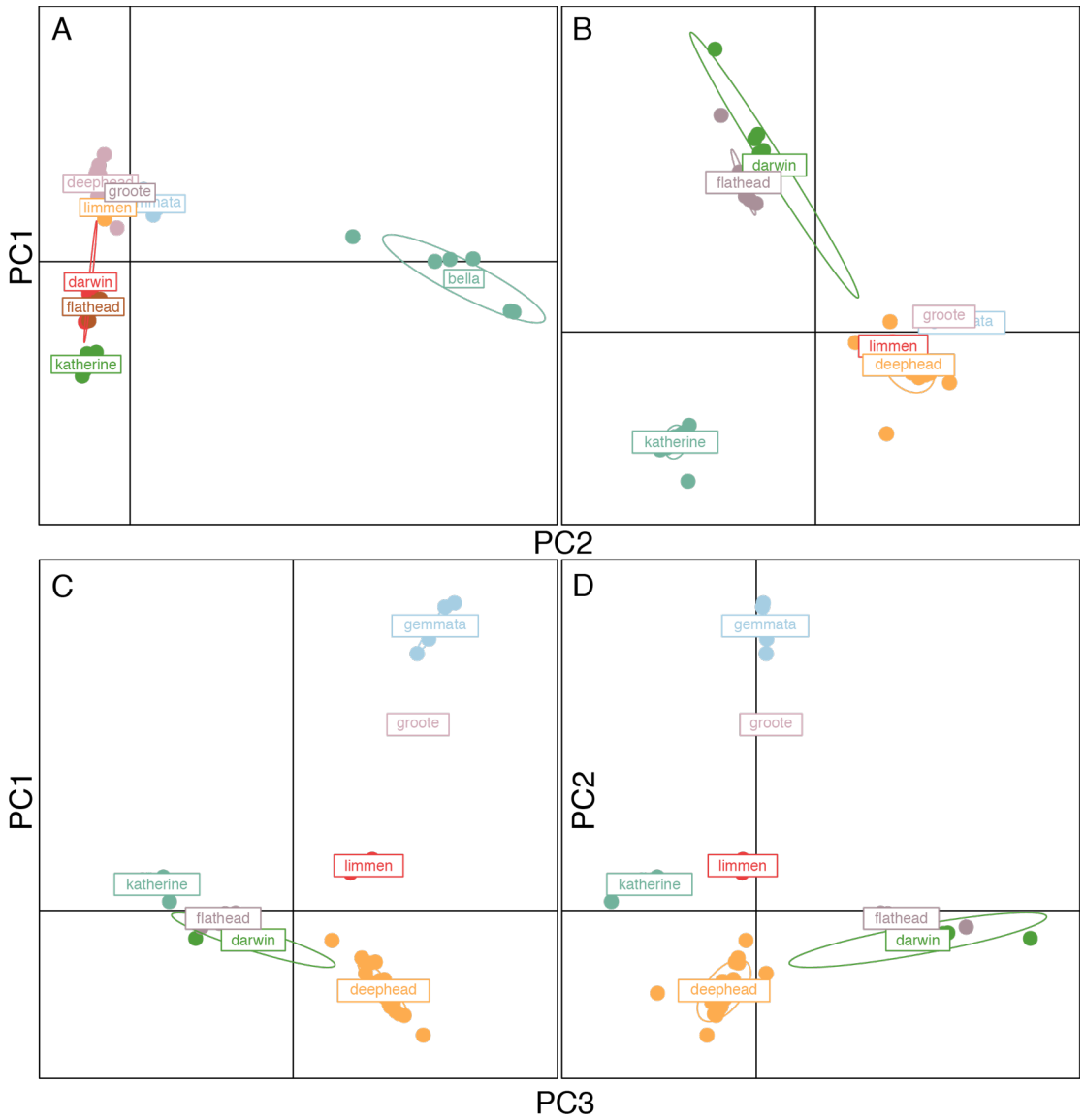


**Figure 39**: A) Allele frequency for all 8 phylogenetic lineages from 4,035 SNPs PCA plots of PCs 1 and 2. B) Allele frequency from 4,035 SNPs PCA plots of PCs 1 and 2. *O. bella* excluded. C) Allele frequency from 4,035 SNPs PCA plots of PCs 1 and 3. *O. bella* excluded. D) Allele frequency from 4,035 SNPs PCA plots of PCs 2 and 3. *O. bella* excluded.

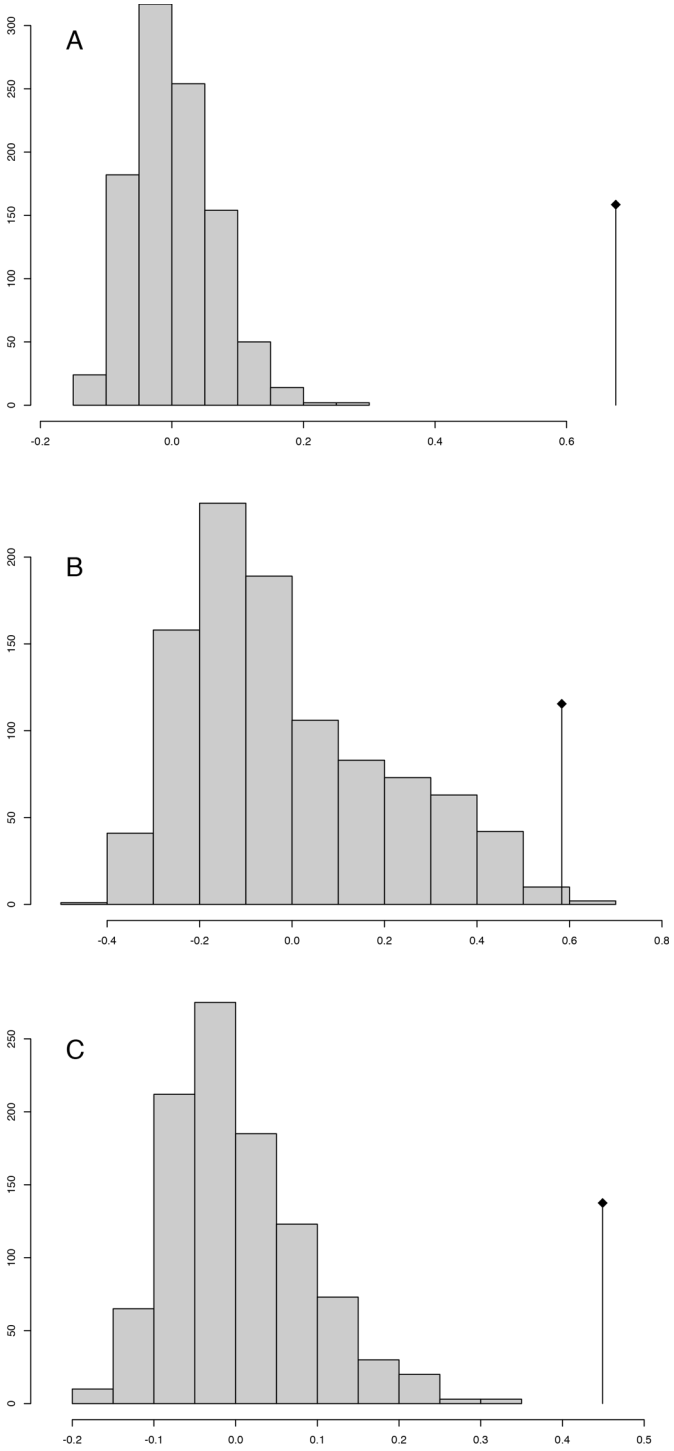


**Figure 40**: Mantel tests of isolation by distance. Bars are simulation bins and line to right is the empirical estimate from 4,035 SNPs. A) test at individual level, B) test at population level, and C) test deephead clade only.

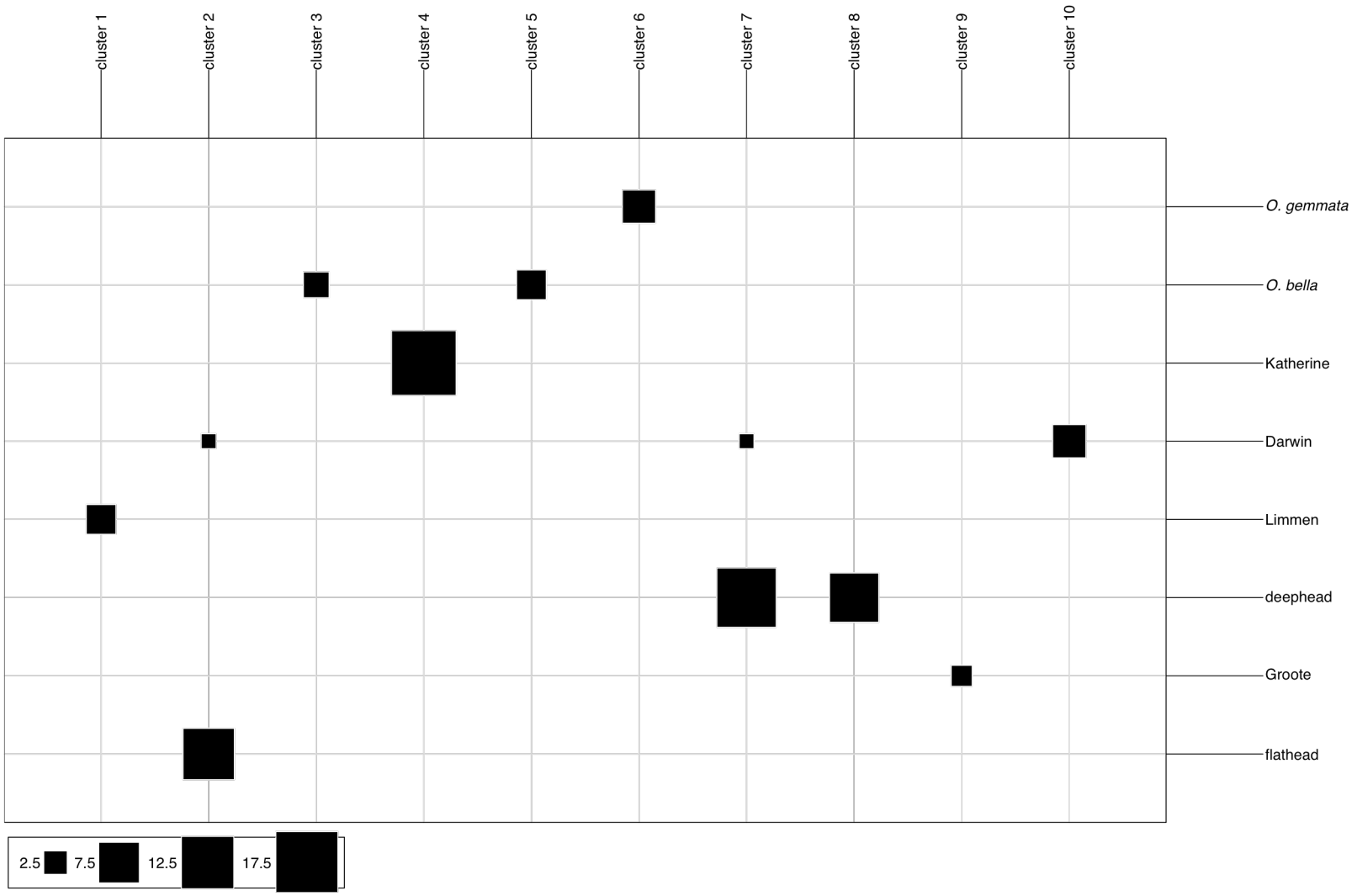


**Figure 41**: Kmeans plot of clusters for the Top End *O. marmorata* complex. Each square is proportional to the number of individuals from the 8 *a priori* populations assigned to each cluster. Squares at bottom left corner are scales for the number of individuals.

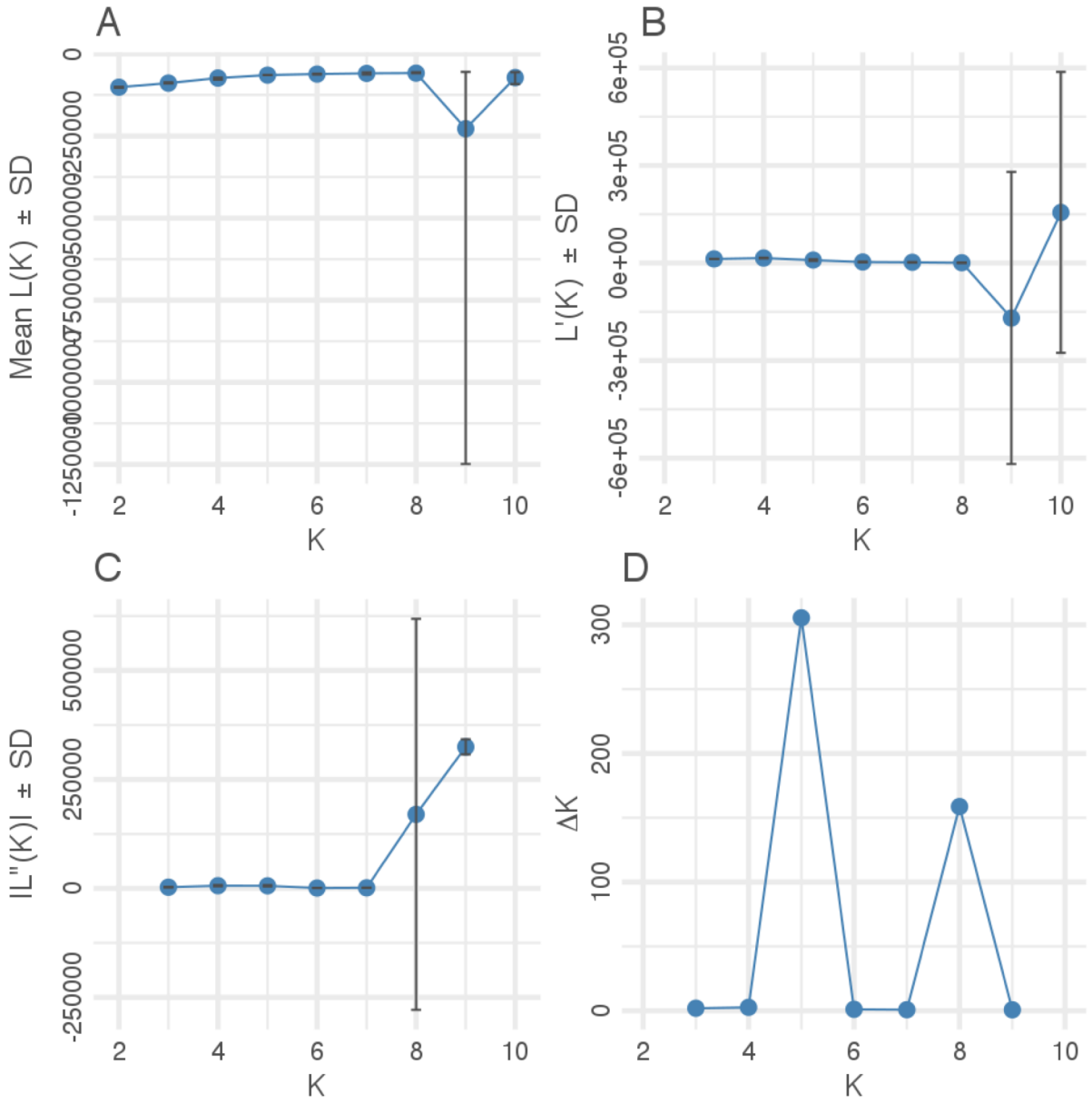


**Figure 42**: Results from STRUCTURE. A) Log probability (*K*) of each cluster. B) First order derivative of the Log probability (*K*) of each cluster. C) Second order derivative of the Log probability (*K*) of each cluster. D) Evanno's Δ*K*, with *K* = 5 being the optimal number of clusters.

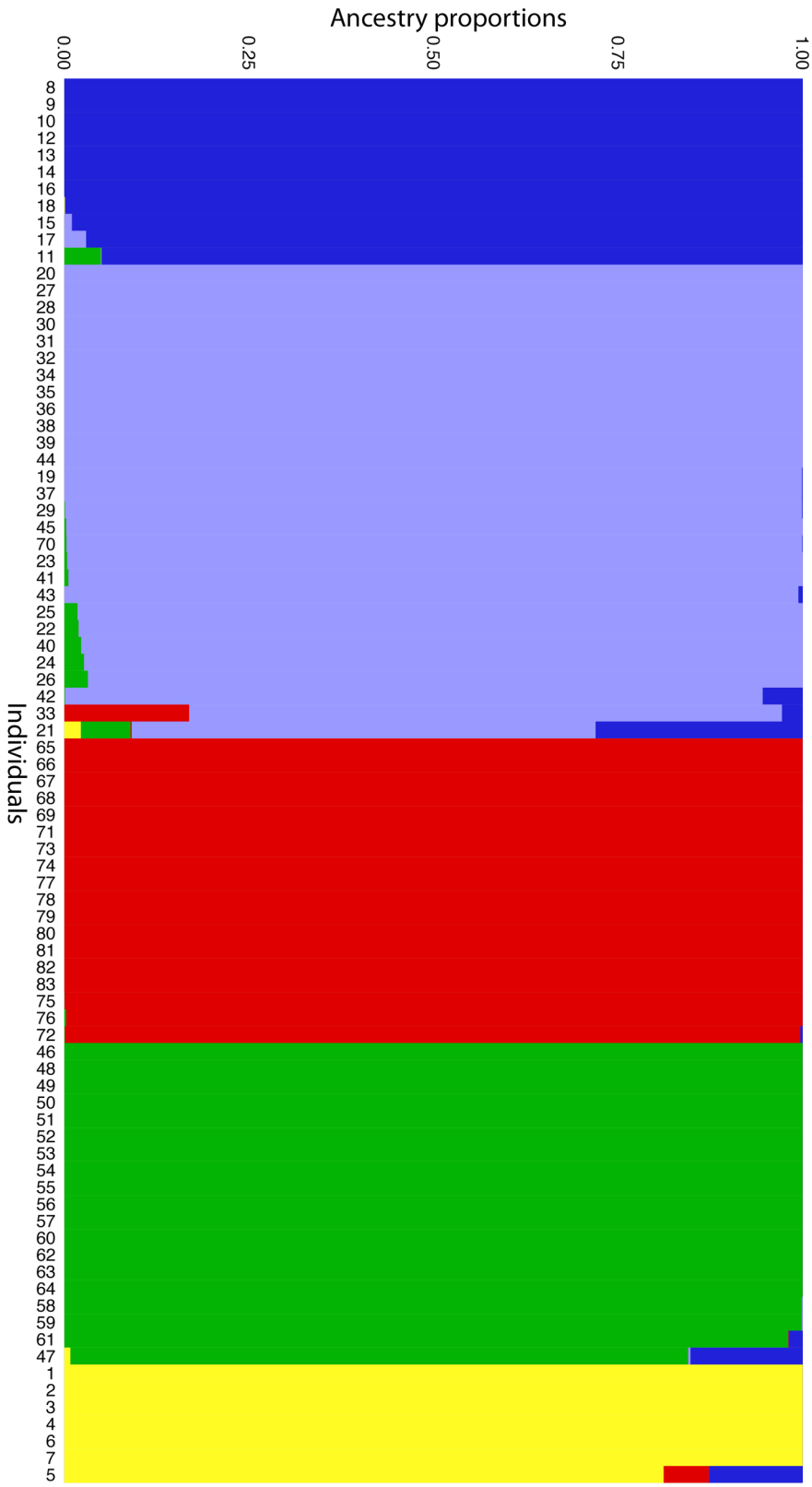


**Figure 43:** Results from STRUCTURE. Admixture plot of $K = 5$.

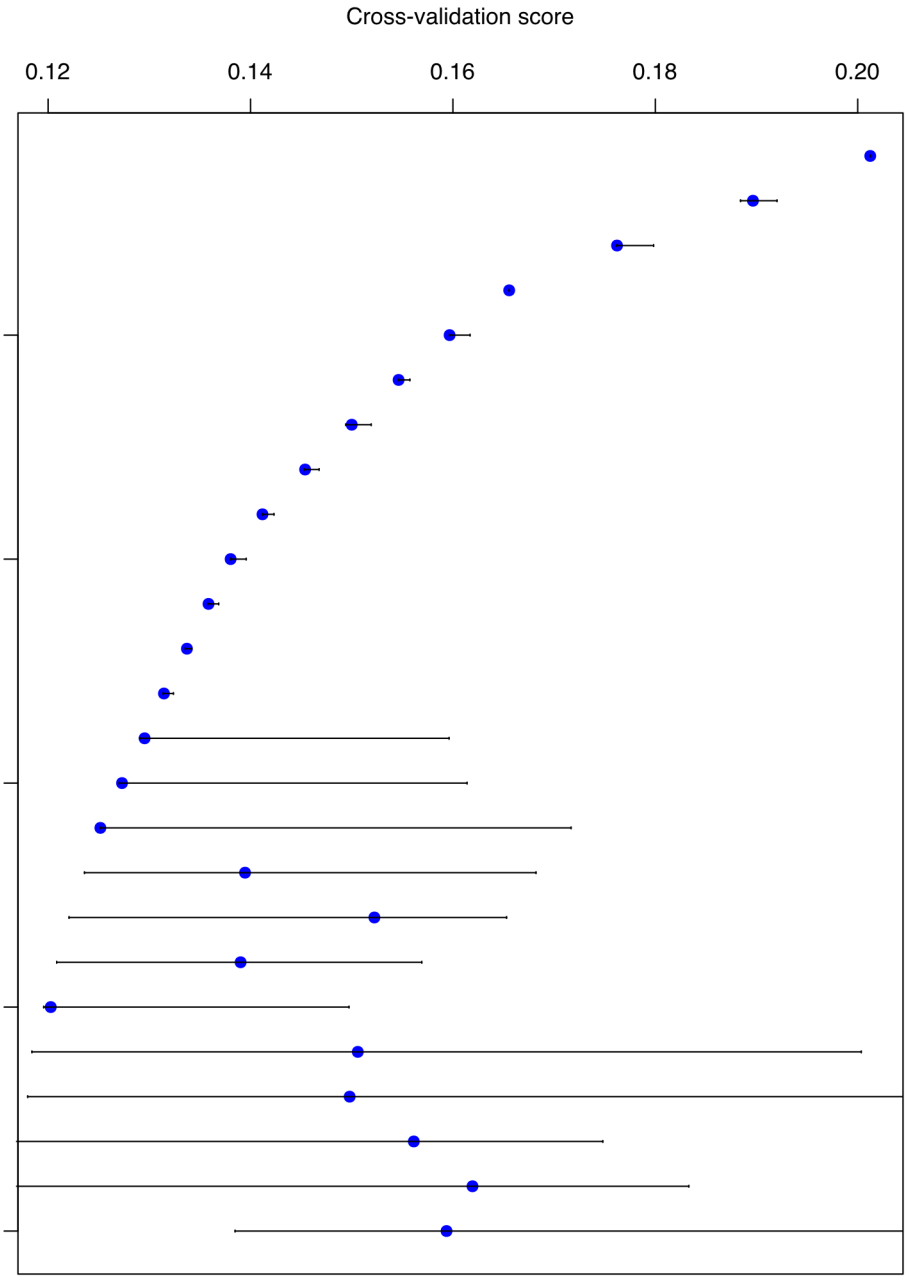


**Figure 44**: Cross validation scores from TESS3r for ancestral clusters. Error bars are standard error of the mean.

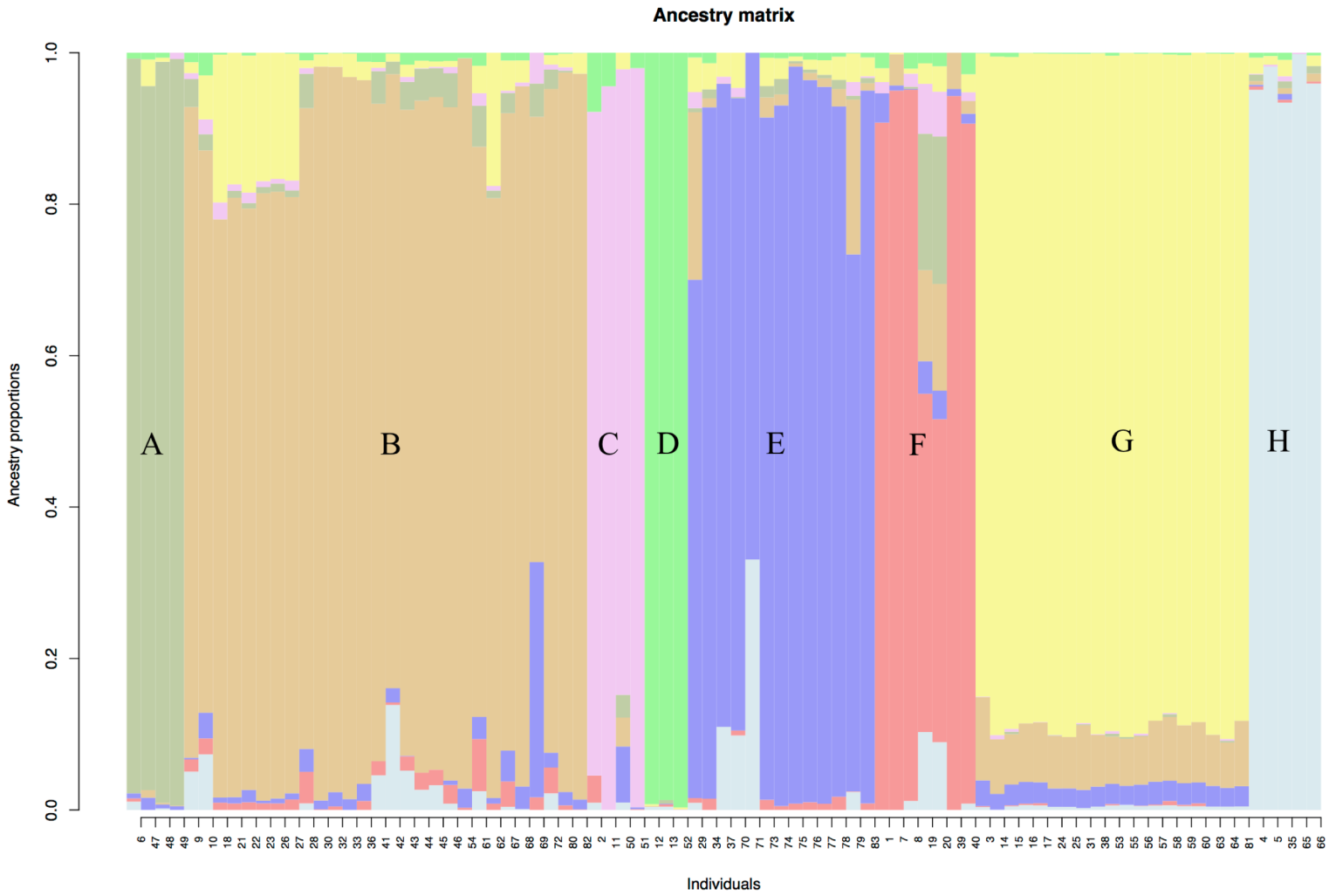


**Figure 45**: TESS3r ancestry coefficient plot for $K = 8$. A = Limmen, B = deephead, C = western *O. bella*, D = eastern *O. bella*, E = flathead, F = *O. gemmata*, G = Katherine, H = Darwin. See table 13.

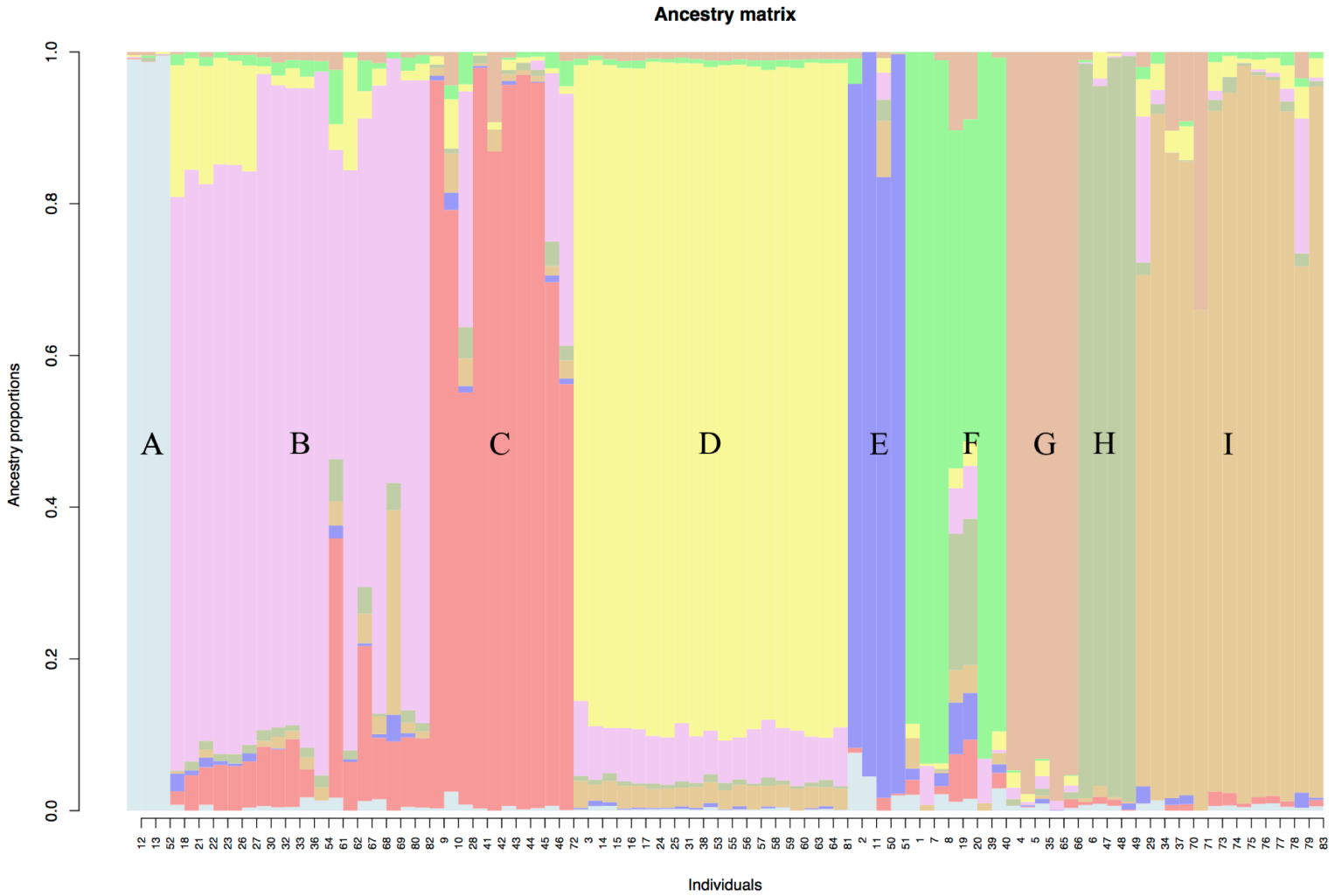


**Figure 46**: TESS3r ancestry coefficient plot for $K = 9$. A = eastern *O. bella*, B = western deephead, C = eastern deephead, D = Katherine, E = western *O. bella*, F = *O. gemmata*, G = Darwin, H = western *O. bella*, I = flathead. See table 13.

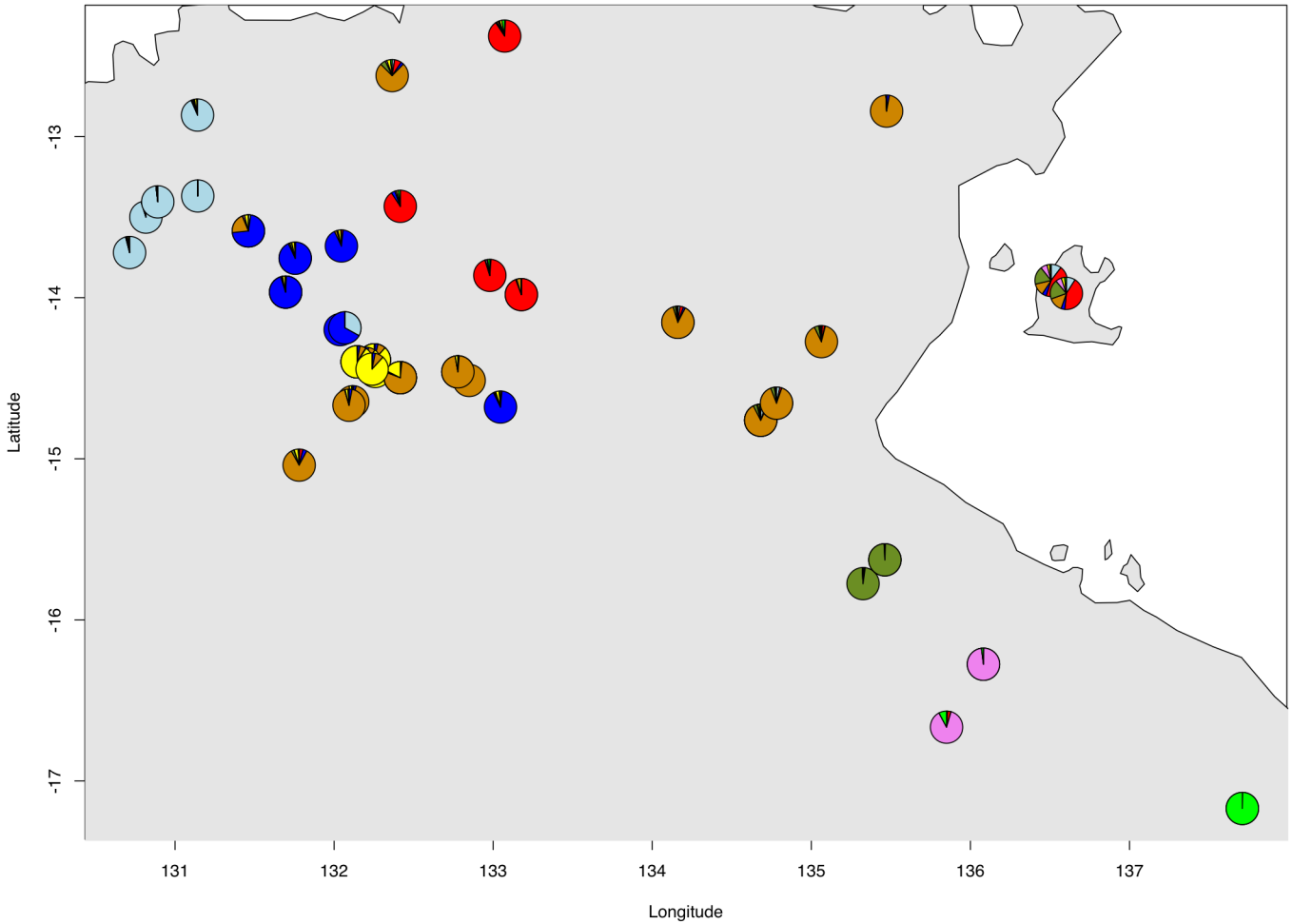


**Figure 47**: Map of TESS3r ancestry coefficients for $K = 8$. Pie chart proportions correspond to $Q$ matrix. See figure 45.

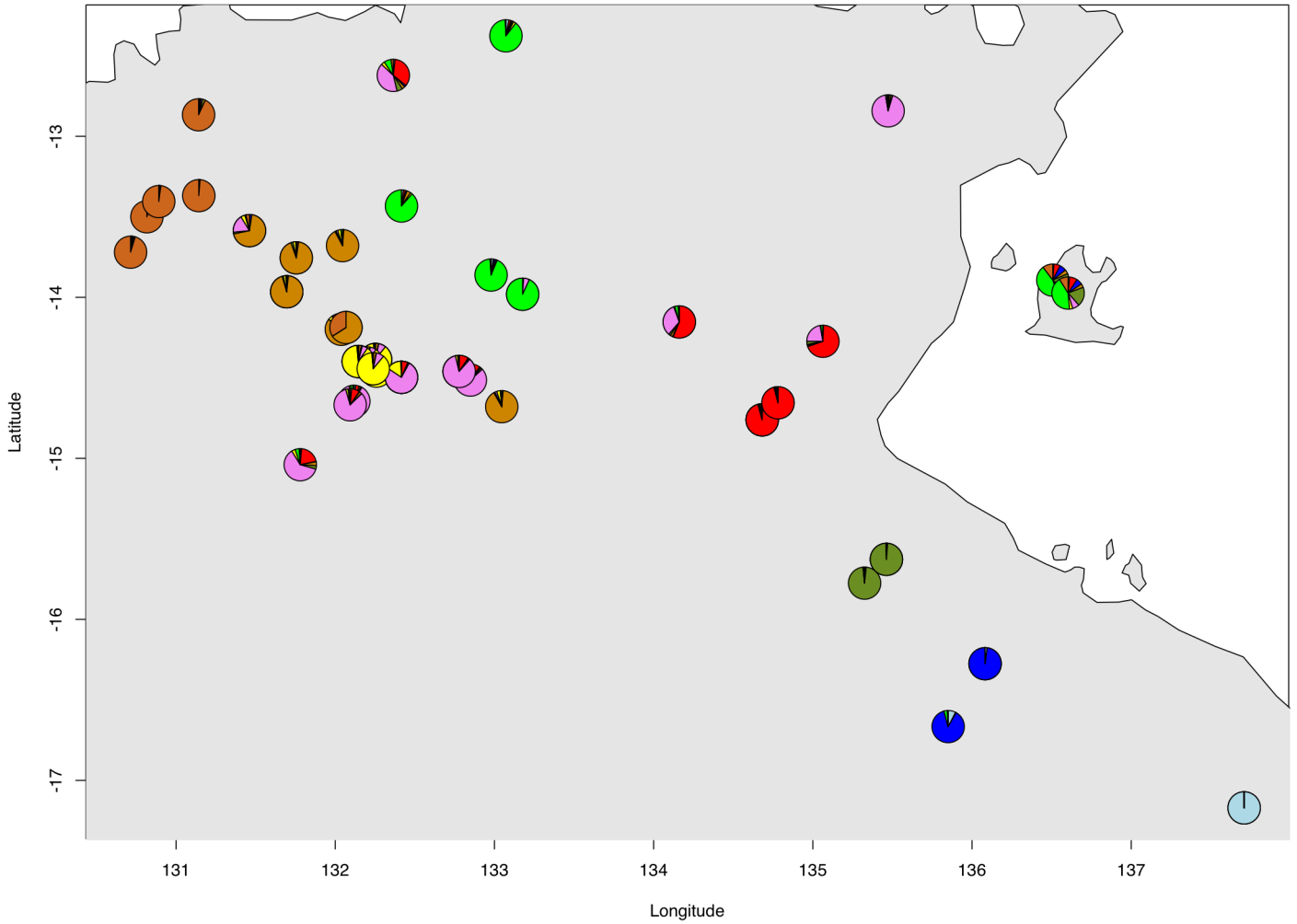


**Figure 48**: Map of TESS3r ancestry coefficients for $K = 9$. Pie chart proportions correspond to $Q$ matrix. See figure 46.

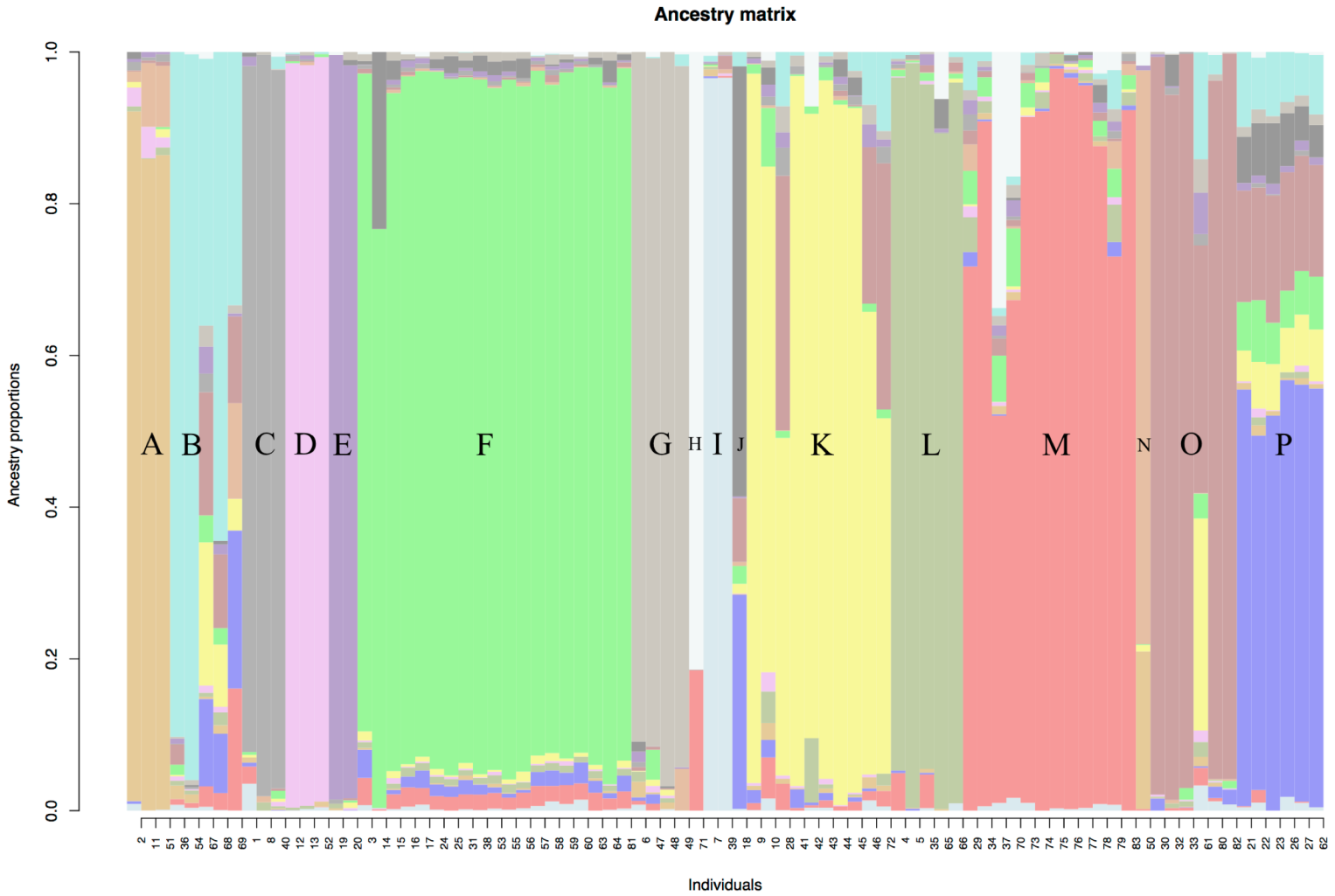


**Figure 49**: TESS3r ancestry coefficient plot for $K = 9$. A = western *O. bella*, B = southwestern/Arnhem Coast deephead, C = *O. gemmata*, D = eastern *O. bella*, E = Groote, F = Katherine, G = Limmen, H = Katherine flathead, I = southeastern *O. gemmata*, J = Katherine deephead, K = eastern deephead, L = Darwin, M = flathead, N = *O. bella*, O = central deephead, P = east Katherine deephead. See table 13.

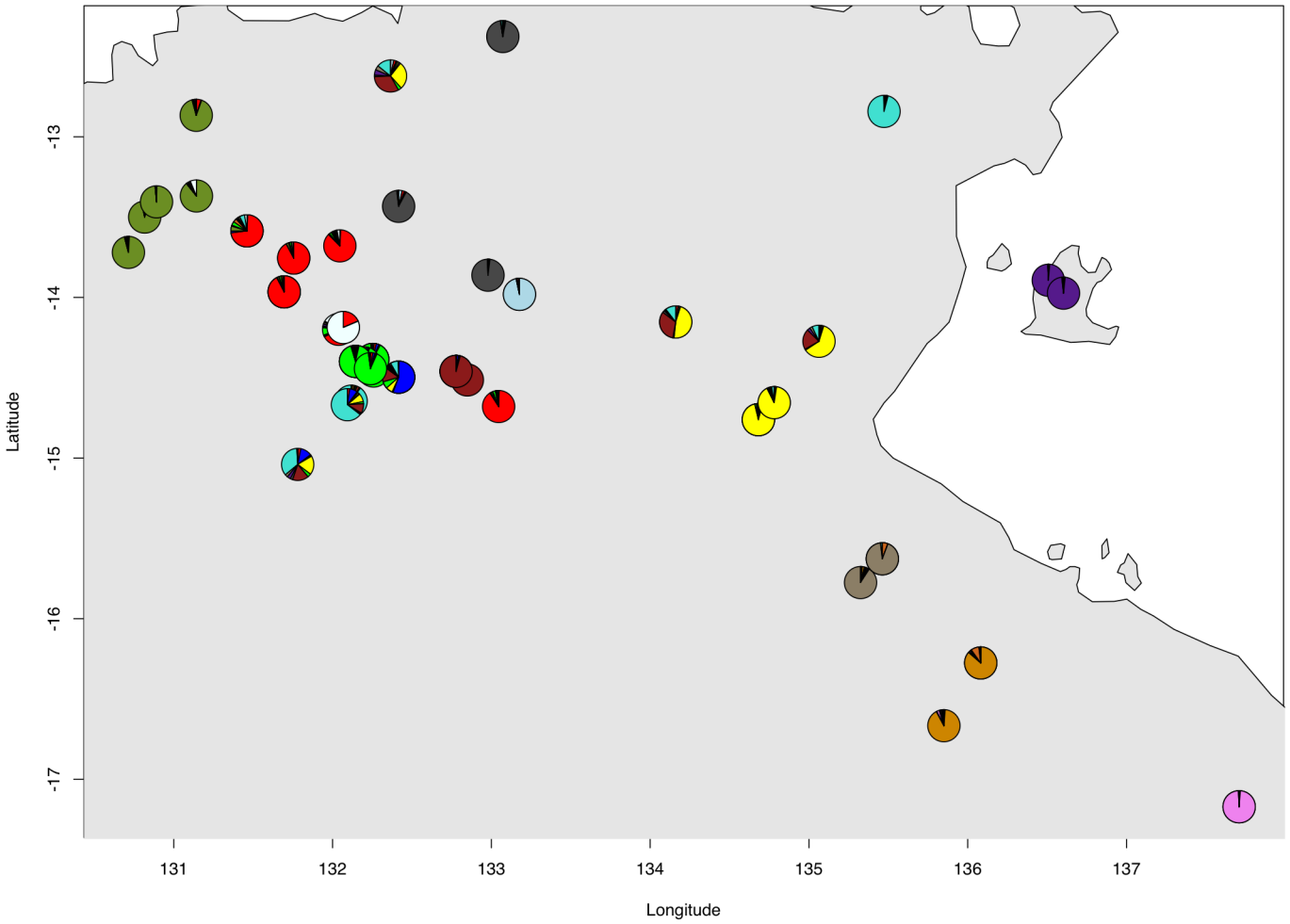


**Figure 50**: Map of TESS3r ancestry coefficients for $K = 16$. Pie chart proportions correspond to $Q$ matrix. See figure 49.

**Table 13**: All Top End *Oedura* used in this study. The first column corresponds to the individual numbers shown in the STRUCTURE and TESS3r ancestry coefficient plots. Clade corresponds to the mitochondrial and UCE phylogenies.

| # | Sample ID | Clade |
|---|---|---|
| 1 | JMPS001_GE1 | O. gemmata |
| 2 | JMPS001_GU1 | O. bella |
| 3 | JMPS001_N2 | Katherine |
| 4 | JMPS001_N7 | Darwin |
| 5 | JMPS001_N8 | Darwin |
| 6 | JMPS001_N9 | Limmen |
| 7 | JMPS001_RL183 | O. gemmata |
| 8 | JMPS001_RL184 | O. gemmata |
| 9 | JMPS002_CCM2203_Oedura_marmorata_S73 | deephead |
| 10 | JMPS002_CCM2214_Oedura_marmorata_S67 | deephead |
| 11 | JMPS002_CCM2667_Oedura_marmorata_S62 | O. bella |
| 12 | JMPS002_CCM2710_Oedura_marmorata_S72 | O. bella |
| 13 | JMPS002_CCM2711_Oedura_marmorata_S82 | O. bella |
| 14 | JMPS002_CCM3135_Oedura_marmorata_S57 | Katherine |
| 15 | JMPS002_CCM3136_Oedura_marmorata_S58 | Katherine |
| 16 | JMPS002_CCM3149_Oedura_marmorata_S59 | Katherine |
| 17 | JMPS002_CCM3151_Oedura_marmorata_S68 | Katherine |
| 18 | JMPS002_CCM3188_Oedura_marmorata_S63 | deephead |
| 19 | JMPS002_CCM4191_Oedura_marmorata_S89 | Groote |
| 20 | JMPS002_CCM4195_Oedura_marmorata_S88 | Groote |
| 21 | JMPS002_CCM4935_Oedura_marmorata_S69 | deephead |
| 22 | JMPS002_CCM4936_Oedura_marmorata_S70 | deephead |
| 23 | JMPS002_CCM4937_Oedura_marmorata_S74 | deephead |
| 24 | JMPS002_CCM4939_Oedura_marmorata_S71 | Katherine |
| 25 | JMPS002_CCM4941_Oedura_marmorata_S66 | Katherine |
| 26 | JMPS002_CCM4943_Oedura_marmorata_S54 | deephead |
| 27 | JMPS002_CCM4944_Oedura_marmorata_S64 | deephead |
| 28 | JMPS002_R36729_Oedura_marmorata_S84 | deephead |
| 29 | JMPS002_R36862_Oedura_marmorata_S61 | flathead |
| 30 | JMPS002_R36880_Oedura_marmorata_S60 | deephead |
| 31 | JMPS002_R36891_Oedura_marmorata_S80 | Katherine |
| 32 | JMPS002_R36894_Oedura_marmorata_S65 | deephead |

| | | |
|---|---|---|
| 33 | JMPS002_R36895_Oedura_marmorata_S75 | deephead |
| 34 | JMPS002_R36899_Oedura_marmorata_S79 | flathead |
| 35 | JMPS002_R36910_Oedura_marmorata_S78 | Darwin |
| 36 | JMPS002_R37070_Oedura_marmorata_S76 | deephead |
| 37 | JMPS002_R37081_Oedura_marmorata_S85 | flathead |
| 38 | JMPS002_R37147_Oedura_marmorata_S77 | Katherine |
| 39 | Oedura_gemmata_R34986_S135 | O. gemmata |
| 40 | Oedura_gemmata_R35753_S86 | O. gemmata |
| 41 | Oedura_marmorata_CCM2202_S123 | deephead |
| 42 | Oedura_marmorata_CCM2204_S83 | deephead |
| 43 | Oedura_marmorata_CCM2223_S110 | deephead |
| 44 | Oedura_marmorata_CCM2245_S141 | deephead |
| 45 | Oedura_marmorata_CCM2412_S127 | deephead |
| 46 | Oedura_marmorata_CCM2477_S128 | deephead |
| 47 | Oedura_marmorata_CCM2589_S78 | Limmen |
| 48 | Oedura_marmorata_CCM2590_S80 | Limmen |
| 49 | Oedura_marmorata_CCM2614_S104 | Limmen |
| 50 | Oedura_marmorata_CCM2655_S77 | O. bella |
| 51 | Oedura_marmorata_CCM2666_S132 | O. bella |
| 52 | Oedura_marmorata_CCM2696_S133 | O. bella |
| 53 | Oedura_marmorata_CCM3132_S85 | Katherine |
| 54 | Oedura_marmorata_CCM3133_S112 | deephead |
| 55 | Oedura_marmorata_CCM3134_S124 | Katherine |
| 56 | Oedura_marmorata_CCM3137_S84 | Katherine |
| 57 | Oedura_marmorata_CCM3150_S129 | Katherine |
| 58 | Oedura_marmorata_CCM3162_S121 | Katherine |
| 59 | Oedura_marmorata_CCM3163_S79 | Katherine |
| 60 | Oedura_marmorata_CCM3164_S81 | Katherine |
| 61 | Oedura_marmorata_CCM3844_S107 | deephead |
| 62 | Oedura_marmorata_CCM4934_S108 | deephead |
| 63 | Oedura_marmorata_CCM4940_S122 | Katherine |
| 64 | Oedura_marmorata_NTMR36801_S109 | Katherine |
| 65 | Oedura_marmorata_NTMR37058_S93 | Darwin |
| 66 | Oedura_marmorata_NTMR37059_S130 | Darwin |
| 67 | Oedura_marmorata_NTMR37061_S103 | deephead |
| 68 | Oedura_marmorata_NTMR37067_S125 | deephead |
| 69 | Oedura_marmorata_NTMR37069_S102 | deephead |
| 70 | Oedura_marmorata_NTMR37074_S105 | flathead |
| 71 | Oedura_marmorata_NTMR37091_S101 | Darwin |
| 72 | Oedura_marmorata_R36731_S95 | deephead |

| | | |
|---|---|---|
| 73 | Oedura_marmorata_R36830_S92 | flathead |
| 74 | Oedura_marmorata_R36831_S99 | flathead |
| 75 | Oedura_marmorata_R36837_S154 | flathead |
| 76 | Oedura_marmorata_R36838_S118 | flathead |
| 77 | Oedura_marmorata_R36839_S164 | flathead |
| 78 | Oedura_marmorata_R36858_S116 | flathead |
| 79 | Oedura_marmorata_R36863_S96 | flathead |
| 80 | Oedura_marmorata_R36890_S143 | deephead |
| 81 | Oedura_marmorata_R36892_S115 | Katherine |
| 82 | Oedura_marmorata_R36893_S94 | deephead |
| 83 | Oedura_marmorata_R36897_S137 | flathead |

**Table 14**: Mean Nei's non-Euclidean mean pairwise distance for mtDNA for all clade comparisons.

| | *O. bella* | *O. gemmata* | Groote | Limmen | deephead | Katherine | Darwin |
|---|---|---|---|---|---|---|---|
| *O. gemmata* | 0.19 | — | — | — | — | — | — |
| Groote | 0.21 | 0.12 | — | — | — | — | — |
| Limmen | 0.22 | 0.11 | 0.15 | — | — | — | — |
| deephead | 0.25 | 0.08 | 0.16 | 0.15 | — | — | — |
| Katherine | 0.25 | 0.13 | 0.17 | 0.16 | 0.17 | — | — |
| Darwin | 0.22 | 0.11 | 0.18 | 0.15 | 0.15 | 0.17 | — |
| flathead | 0.25 | 0.07 | 0.16 | 0.16 | 0.16 | 0.20 | 0.16 |

**Table 15**: Mean Nei's non-Euclidean mean pairwise distance for 4,035 UCE SNPs for all clade comparisons.

| | *O. gemmata* | *O. bella* | Katherine | Darwin | Limmen | deephead | Groote |
|---|---|---|---|---|---|---|---|
| *O. bella* | 0.11 | — | — | — | — | — | — |
| Katherine | 0.08 | 0.15 | — | — | — | — | — |
| Darwin | 0.07 | 0.14 | 0.06 | — | — | — | — |
| Limmen | 0.08 | 0.15 | 0.08 | 0.07 | — | — | — |
| deephead | 0.06 | 0.13 | 0.05 | 0.04 | 0.06 | — | — |
| Groote | 0.07 | 0.14 | 0.09 | 0.08 | 0.09 | 0.07 | — |
| flathead | 0.07 | 0.14 | 0.05 | 0.03 | 0.07 | 0.05 | 0.08 |

**Table 16**: $F_{ST}$ measures for all clade comparisons. Bold numbers are likely unreliable estimates due to the small sample size of the insular Groote clade (n = 2).

| | *O. gemmata* | *O. bella* | Katherine | Darwin | Limmen | deephead | Groote |
|---|---|---|---|---|---|---|---|
| *O. bella* | 0.45 | — | — | — | — | — | — |
| Katherine | 0.38 | 0.52 | — | — | — | — | — |
| Darwin | 0.40 | 0.51 | 0.34 | — | — | — | — |
| Limmen | 0.49 | 0.52 | 0.36 | 0.43 | — | — | — |
| deephead | 0.22 | 0.39 | 0.34 | 0.21 | 0.20 | — | — |
| Groote | **0.39** | **0.41** | **0.28** | **0.35** | **0.56** | **0.13** | **—** |
| flathead | 0.40 | 0.52 | 0.37 | 0.24 | 0.40 | 0.28 | 0.32 |